

Finite element analysis of a buried pipeline

A dissertation submitted to The University of Manchester for the degree of Master of

Science by Research

In the Faculty of Engineering and Physical Science

2010

Hyuk Lee

School of Mechanical, Aerospace and Civil Engineering

Table of Contents

TABLE OF CONTENTS	1
TABLE OF FIGURES.....	3
LIST OF TABLES.....	5
ABSTRACT	6
DECLARATION.....	7
COPYRIGHT STATEMENT.....	8
ACKNOWLEDGEMENT.....	9
PREFACE.....	10
DEDICATION.....	11
1. INTRODUCTION.....	12
1.1. BURIED PIPELINE.....	13
1.1.1. Two representative buried pipes.....	14
1.1.2. Buried pipeline for water supply	14
1.1.3. Performance of pipeline in earthquake.....	15
1.2. GROUND CONDITIONS	16
1.2.1. Two representative types of soil.....	16
1.2.2. Mechanical behaviour of geomaterial	17
1.2.3. Water effect of soil	17
1.2.4. Conclusion for ground condition.....	18
1.3. TYPES OF LOADS ON PIPELINE	22
1.3.1. Static loads.....	23
1.3.2. Seismic load.....	24
1.3.3. Conclusion for loads.....	26
1.4. CONCLUSION.....	27
2. RESEARCH OBJECTIVES	29
2.1. AIMS.....	30
2.2. OBJECTIVES	30
3. FINITE ELEMENT ANALYSIS (FEM) – ABAQUS	32
3.1. 3D-FINITE ELEMENT (FE) MODELLING.....	34
3.2. KEY TECHNOLOGIES TREATMENTS.....	37
3.2.1. Determination of stress models	37
3.2.2. Definition of constraint type.....	38
3.3. BOUNDARY CONDITIONS	38
3.3.1. Boundary condition of soil’s 3D-FE model	39
3.3.2. Boundary condition of pipeline’s 3D-FE model	40
3.4. ADAPTIVE MESHING FOR FINITE ELEMENT ANALYSIS (FEA).....	42

3.4.1.	THE TYPE OF ELEMENT	43
3.4.2.	The size of element.....	45
3.4.3.	Results and discussion.....	49
3.4.4.	Conclusion for adaptable mesh.....	59
3.5.	STATIC AND SEISMIC ANALYSIS.....	59
4.	NUMERICAL RESULTS AND DISCUSSION.....	61
4.1.	STATIC ANALYSIS	61
4.1.1.	Displacement of soil	62
4.1.2.	Displacement of buried pipeline.....	64
4.1.3.	Stress of soil.....	68
4.1.4.	Stress of buried pipeline	70
4.2.	BOUNDARY CONDITION EFFECT OF PIPELINE ENDS	73
4.2.1.	Displacement of soil	74
4.2.2.	Displacement of buried pipeline.....	76
4.2.3.	Stress of soil.....	78
4.2.4.	Stress of buried pipeline	80
4.3.	SEISMIC ANALYSIS	83
4.3.1.	General moist sandy soil with hinge boundary at pipeline ends	86
4.3.2.	General moist sandy soil with roller boundary at pipeline ends.....	87
4.3.3.	Fully saturated sandy soil with hinge boundary at pipeline ends	88
4.3.4.	Fully saturated sandy soil with roller boundary at pipeline ends	89
4.3.5.	General moist cohesive soil with hinge boundary at pipeline ends.....	90
4.3.6.	General moist cohesive soil with roller boundary at pipeline ends.....	91
4.3.7.	Fully saturated cohesive soil with hinge boundary at pipeline ends	92
4.3.8.	Fully saturated cohesive soil with roller boundary at pipeline ends.....	93
5.	CONCLUSIONS	94
	REFERENCES	99
	APPENDIX A – SEISMIC VERTICAL ACCELERATION DATA OF EL CENTRO EARTHQUAKE.....	102
	APPENDIX B – APPLIED MESHES ACCORDING TO THE DIFFERENT APPROXIMATE GLOBAL SIZES	115
	APPENDIX C – CALCULATED DATA FOR MESH STUDY	127
	APPENDIX D – THE GRAPHS FOR MESH STUDY	139
	APPENDIX E – THE CALCULATED DATA FOR STATIC ANALYSIS	145
	APPENDIX F – THE CALCULATED DATA FOR BOUNDARY CONDITION EFFECT....	153
	APPENDIX G – THE ENLARGED GRAPHS FOR SEISMIC ANALYSIS	169
	APPENDIX H – TUTORIAL.....	177

Table of Figures

Figure 1. 1	Dimensions of pipeline model - DN 1500	19
Figure 1. 2	Dimensions of soil model	21
Figure 1. 3	The eccelerogram of El Centro Earthquake in May, 1940	25
Figure 3. 1	3D-FE models under the FE software environment of ABAQUS	34
Figure 3. 2	3D-FE assembled models with soil and pipeline according to the each buried depth-- -----	35
Figure 3. 3	Three representative 3D-FE models of soil and pipeline according to the lengths--	36
Figure 3. 4	Basic 3D-FE model of pipeline and soil	38
Figure 3. 5	Boundary conditions of 3D-FE soil model	39
Figure 3. 6	Boundary conditions of 3D-FE pipeline model	40
Figure 3. 7	Two typical case of buried pipeline for pipeline end's boundaries	41
Figure 3. 8	Computed 100m model results according to different type and number of element-	51
Figure 3. 9	Computed 50m model results according to different type and number of element -	53
Figure 3. 10	Computed 15m model data according to different type and number of element---	55
Figure 3. 11	Involved error in meshed element expressed by 2D (Zienkiewicz and Zhu, 1987)	57
Figure 4. 1	Typical soil settlement under static loads	63
Figure 4. 2	Maximum settlement of soil under static loads.....	63
Figure 4. 3	Typical pipeline settlement under static loads	66
Figure 4. 4	Maximum settlement of buried pipeline under static loads	66
Figure 4. 5	Typical soil's stress under static loads	69
Figure 4. 6	Maximum stress of soil under static loads	70
Figure 4. 7	Typical pipeline's stress under static loads	71
Figure 4. 8	Maximum stress of soil under static loads	72
Figure 4. 9	Different soil settlement according to two boundary conditions of pipeline ends.....	75
Figure 4. 10	Maximum settlement of soil under static loads.....	75
Figure 4. 11	Different pipeline settlement according to two boundary conditions of pipeline ends	76
Figure 4. 12	Maximum settlement of buried pipeline under static loads	77
Figure 4. 13	Different soil's stress according to two boundary conditions of pipeline ends	79
Figure 4. 14	Maximum stress of soil under static loads	80
Figure 4. 15	different pipeline's stress according to two boundary conditions of pipeline ends .	81
Figure 4. 16	Maximum stress of buried pipeline under static loads.....	82
Figure 4. 17	Target path for checking displacement and stress under dynamic load.....	85
Figure 4. 18	Diagrams for general moist sandy soil with hinge boundary at pipeline ends.....	86
Figure 4. 19	Diagrams for general moist sandy soil with roller boundary at pipeline ends.....	87
Figure 4. 20	Diagrams for fully saturated sandy soil with hinge boundary at pipeline ends	88
Figure 4. 21	Diagrams for fully saturated sandy soil with roller boundary at pipeline ends	89

Figure 4. 22 Diagrams for general moist cohesive soil with hinge boundary at pipeline ends90
Figure 4. 23 Diagrams for general moist cohesive soil with roller boundary at pipeline ends91
Figure 4. 24 Diagrams for fully saturated cohesive soil with hinge boundary at pipeline ends...92
Figure 4. 25 Diagrams for fully saturated cohesive soil with roller boundary at pipeline ends...93

List of Tables

Table 1. 1	Material properties of pipeline	18
Table 1. 2	Material properties of soil	20
Table 1. 3	Static and dynamic loads	26
Table 3. 1	Selected element type for soil and pipeline's 3D-FE models.....	44
Table 3. 2	The number of meshed elements in 100 m model.....	46
Table 3. 3	The number of meshed elements in 50 m model.....	47
Table 3. 4	The number of meshed elements in 15 m model.....	48

Abstract

Nowadays, pipelines have various uses; water and energy supply systems, communication services and so on. Furthermore, the pipelines are affected by many types of load in various parts of the world.

In the case of a buried pipeline, forces are statically indeterminate because the characteristic of soil is not uniform (Watkins and Anderson, 2000). It is impossible to estimate accurately the seismic behaviour of a pipeline due to the uncertainty of both soil characteristic and seismic load. Thus, it is necessary to assess both the static and seismic pipeline behaviour for likely of buried pipeline behaviour.

This dissertation examines the typical pipeline behaviour caused by static and seismic load in accordance with soil types and a degree of saturation in considered soil. The finite element method (FEM) is selected as the examination method for the buried pipeline. The most challenging part of this dissertation is the static and seismic calibration stage which is executed by ABAQUS FEM package. Assessments about how a buried pipeline behaves in accordance with soil types, degree of saturation in soil and load types are made throughout this work.

Declaration

No portion of the work referred to in the dissertation has been submitted in support of an application for another degree or qualification of this or any other university or other institute of learning.

Copyright Statement

- i. The author of this dissertation (including any appendices and/or schedules to this dissertation) owns any copyright in it (the “Copyright”) and s/he has given The University of Manchester the right to use such Copyright for any administrative, promotional, educational and/or teaching purposes.
- ii. Copies of this dissertation, either in full or in extracts, may be made **only** in accordance with the regulations of the John Rylands University Library of Manchester. Details of these regulations may be obtained from the Librarian. This page must form part of any such copies made.
- iii. The ownership of any patents, designs, trade marks and any and all other intellectual property rights except for the Copyright (the “Intellectual Property Rights”) and any reproductions of copyright works, for example graphs and tables (“Reproductions”), which may be described in this dissertation, may not be owned by the author and may be owned by third parties. Such Intellectual property Rights and Reproductions cannot and must not be made available for use without the prior written permission of the owner(s) of the relevant Intellectual Property Rights and/or Reproductions.
- iv. Further information on the conditions under which disclosure, publication and exploitation of this dissertation, the Copyright and any Intellectual Property Right and/or Reproductions described in it may take place is available from the Head of School of Mechanical, Aerospace and Civil Engineering.

Acknowledgement

I wish to express my sincere gratitude to Dr. William Craig for his supervision throughout this dissertation and who was there whenever I needed his support and help. He is one of the greatest assets a student can ever have. I thank him for suggesting this subject to me and giving me the opportunity to work on such an interesting topic.

Last but not the least, I would like to thank my parents for their continuous support since I was born until this day. No words can express how I grateful I am to them.

It is no use saying, 'We are doing our best.'

You have got to succeed in doing what is necessary.

- *Winston Churchill*

Preface

A CD containing all the ABAQUS results the author has provided accompanies this work and is placed at the back end of the dissertation.

Dedication

To my parents

1. Introduction

It is acknowledged that underground structures suffer less damage from earthquakes than structures on the ground surface. Recent earthquakes have damaged many lifeline structures (Bulson, 1985). Buried gas and water pipelines are also no exceptions. The damage or disruption of buried pipelines due to earthquakes may severely affect civil lifeline structures since it may cause fires, economic losses, and disable of lifeline networks.

Subsequently, the seismic analysis and behaviour of buried pipelines have been investigated by many researchers. Most of the studies mainly deal with the numerical modelling of buried pipelines, soil-pipeline interaction, and earthquake induced pipeline stress. The seismic response analysis of buried pipelines is somewhat complex since it considers the three-dimensional dynamic analysis of the soil-pipeline interaction under multipoint earthquake excitation (Wang and Raymond, 1979). Therefore, a rigorous analysis is impossible. For these reasons, it is necessary to use elaborate and state-of-the-art test devices in order to estimate failure aspects of buried pipeline. However, Finite Element Methods (FEM) are also helpful for executing rigorous analysis for seismic response analysis of buried pipelines.

Investigating geotechnical problems using FEM has been widely used in this research area for many years even though there are limitations for analysing such problems accurately. However, linear and nonlinear problems such as prediction of settlement and deformation between buried pipelines and soil is highly amenable to solution by FEM. For this reason, ABAQUS, which is used for general Finite Element Analysis (FEA), was chosen in order to estimate failure aspects of buried pipelines.

The main purpose of this study is to understand failure aspects of buried flexible pipeline caused by earthquake through FEA. However, it is necessary to execute static analysis initially without considering seismic effects before computing dynamic analysis with the seismic effects

because it is possible to understand seismic effects more easily by comparing static and seismic analysis. Therefore, in this dissertation, static and seismic analysis for buried pipeline caused by earthquakes will be reported simultaneously and compared with each other.

1.1. Buried pipeline

Pipelines are used for a number of purposes in the development of urban systems such as water, power and communication lifeline systems. According to Robert (1977), urban areas with most of the population nowadays rely on a regular inflow materials and services that support life. But these lifelines providing essential services into urban areas are relatively vulnerable to forces which threaten the population. Among these forces the one of most dreadful can be an earthquake, due to the extensive synchronous crash of all of lifelines.

From the historical point of view, the relatively serious problems caused by earthquakes have been associated with the corruption of water and sewage lifeline systems. Epidemics have arisen from the pollution of portable water supply. Moreover, the loss of water supply system is caused by unrespectable and uncontrollable fires due to breakout of earthquake.

To prevent these disasters and protect lifeline systems which maintain life in urban areas, it is essential to study buried pipelines affected by earthquakes. The suitable expectation related to the buried pipelines' behaviour caused earthquakes, from this study, will suggest some diverse approaches for reducing destructive disaster.

1.1.1. Two representative buried pipes

According to Young and Trott (1984), pipelines are typically divided into two types which are rigid pipes and flexible pipes. Although the rigid pipe is similar to a beam because rigid pipes support loads in the ground by virtue of the resistance of the pipe as a ring to bending, a flexible pipe is analogous to an arch because flexible pipes rely on horizontal thrust from the soil at the sides to enable them to resist vertical loads without excessive deformation. Moreover, rigid pipes, such as clay pipes and unreinforced concrete pipes, do not deform sufficiently under maximum load and produce a significant restraint at the side from the soil in which it is laid because of rigid material characteristics. On the other hand, flexible pipes, such as thin-walled steel pipes, must be capable of deforming to a considerable extent under maximum load.

Thus, when the study related to the buried pipeline is executed, it is necessary to consider these different characteristics from rigid and flexible pipes.

1.1.2. Buried pipeline for water supply

Whereas, nowadays, concrete pipelines, which are considered as rigid, are normally used for drainage systems, there are many thousands of kilometres of steel pipeline, which are considered as flexible, in service for supplying water into urban areas. However, these steel pipelines confront some problems that it is difficult to monitor from a failure from corrosion of steel pipelines which tends to pollute water inside the pipe.

Furthermore, there is a growing tendency for the size of major steel pipelines, which supply water into the urban area, to increasing in size as demand for water increases. For this reason, lots of cities are replacing old small conduits used as water supply by large diameter water supply pipeline in order to improve quality of water and satisfy the increased demands.

It is certain that the steel pipelines of increased size are more vulnerable to diverse forces such as traffic load and earthquake load, etc. Therefore, the study of large diameter steel lifeline under earthquake load is required in order to estimate wholly damage of lifeline.

1.1.3. Performance of pipeline in earthquake

According to mention of Jeremy (1978), there are a lot of factors, which influence the effect of seismic action on underground water pipelines, such as conditions of soil, severity of ground shaking, surges in internal pressure, design dimensions including diameter and wall thickness and material strength of pipelines. Each of these factors has to be considered in pipeline design and analysis in order to evaluate and reduce possible damage because each of these factors exerts different influence in different situations. In the case of Puget Sound Earthquake, in 1965, a lot of leakages were caused by corrosion of pipelines because of severe ground shaking. In other case of Santa Rose Earthquake, in 1969, there were mainly lateral breaks of pipelines because the wall thickness of lateral pipelines had become thin caused by some corrosion before appearing earthquake. Like above examples, it is impossible to execute accurate study for seismic behaviour of pipelines, which considers all of factors from seismic action and pipelines because different failures of pipelines will be shown due to diverse factors. This means that it is necessary to chose limited variable associated factors for assessing damages of pipelines.

Leon and Wang (1978) reported that the movement of buried pipelines is closely linked to the ground in both lateral and longitudinal directions as verified by most field data. It is rare for the inertia force caused by the motion of the buried pipelines to influence the response of buried structure itself. It is concluded that the ground displacement characteristics caused by an earthquake affect mainly the response of buried pipelines. Therefore, examining the relative seismic displacements between buried pipelines and ground are suitable for estimating failure

aspects of buried pipelines caused by earthquake because the behaviour of buried pipelines is mostly governed by relative ground movement from earthquake.

1.2. Ground conditions

It is necessary to determine ground properties for studying interaction between soil and a buried structure when considering the design of the structure, because there is considerable difference in the failure aspects of a buried structure and the interaction between soil and buried structure depending on the ground properties. According to Thorley and Atkinson (1994), ideally before commencing detailed design of a buried structure or construction, the ground condition at the area which will be constructed should be clarified and assessed in order to estimate behaviour of both soil and buried structure.

1.2.1. Two representative types of soil

It is possible to divide soils into two groups, which are sandy soils and cohesive soils. Sandy soil is often called frictional soil or drained soil and cohesive soil is normally classified as undrained soil. These two groups of soils have different characteristics and can cause different failure modes for buried structures. For example, according to Thorley and Atkinson (1994), the size of a thrust block is decided by the location of ground water table because the behaviour of buried structure in drained soil is considerably influenced by the elevation of the water table under the ground. For example, if the water table in drained soil rises from the bottom of a thrust block to above buried pipeline, the size of thrust block should be increased because of decreasing the capacity of the block as much as half of original capacity. While on the other, undrained soil is not much influenced on the capacity of the thrust block in accordance with the height of

groundwater table. Therefore, it is acceptable to consider two types of soil for studying failure aspects of buried structure and interaction between soil and buried structure because a wide difference between sandy soil and cohesive soil is shown when the behaviour of buried structure is estimated like above example.

1.2.2. Mechanical behaviour of geomaterial

The stress and strain behaviour of soils is not linearly elastic for the entire range of loading of practical interest but is considerably complicated and they show a great variety of behaviour when subjected to different mechanical behaviour of geomaterial. A lot of approaches and theories have been developed in order to provide a better prediction of complicated material behaviour of soil. However, although the results obtained by more other sophisticated stress-strain criteria are more accurate in estimating actual soil behaviour, coulomb theory related to soil's mechanical properties is a more straightforward method than others for dealing with mechanical behaviour of soil.

Therefore, it is the best way is to create a soil model using the Mohr-Coulomb theory in order to execute a study will give a benefit for understanding interaction between soil and buried structure straightforwardly.

1.2.3. Water effect of soil

It is necessary to consider water effects saturated in soil because there is a wide difference between moist and fully saturated soil. According to Richart et al (1970), the influence of boundary between the saturated soils and the dry or partially saturated soil shall be discussed

when estimating wave-propagation of soil caused by dynamic soil behaviour. This is because of a change in the wave-propagation velocity in the soil is also caused in accordance with the effect which causes a change in effective stress of soil. That is, the aspects of any load propagation are influenced by the water effect in the soil.

Thus, it is recommended that the evaluation according to fully saturated and moist ground condition should be conducted by both static and seismic load, because the load effect to buried structure is changed in accordance with the effect of saturated condition of soil. However, the effect of pore pressure according to the change of water level in soil should be ignored in order to make the analysis simplified and to examine only fully saturated soil and normal moist soil, which is called partially saturated soil.

1.2.4. Conclusion for ground condition

In order to accomplish the specific study for failure aspects of buried pipelines caused by earthquake, the relative large diameter steel pipeline which is used for water supply has been chosen, and an elastic, perfectly plastic and isotropic analysis for pipeline has been conducted on this study as following below table 1.1.

Table 1. 1 Material properties of pipeline (BSI., 2002b, Liu et al., 2010)

Mechanical property	Term	Value
Elastic property	Density (kg/m ³)	7850
	Young's modulus (MPa)	210.7×10^3
	Poisson's ratio	0.3
Plastic property	Yield strength (MPa)	490
	Tensile strength (MPa)	690 to 840

Furthermore, the size of pipeline, which is DN 1500, has been selected from BS EN 10224:2002 in order to execute study for the largest diameter steel pipeline which is used for water supply lifeline. The chosen thickness of wall (t) is 20 mm and outer diameter (OD) is 60 inches (= 1524 mm) also selected by following design criterion of DN 1500 (BSI., 2002a). For the finite element study, the length of pipeline (L') was selected as 15, 50, 100 metres for understanding the effect of pipeline's length in accordance with the different considered lengths of pipeline. The considered pipeline can be seen in Figure 1.1.

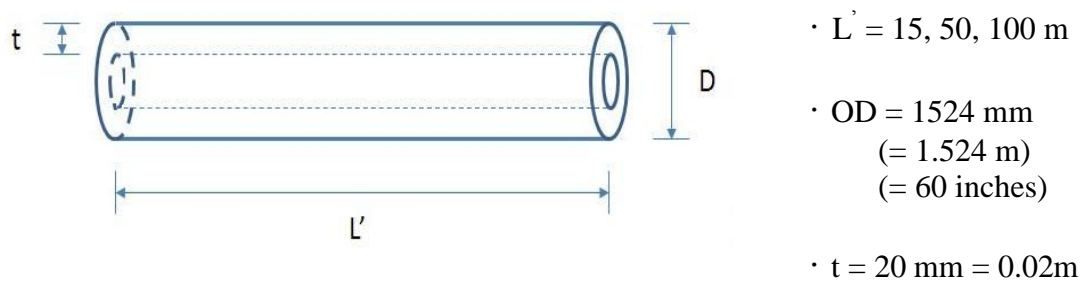


Figure 1. 1 Dimensions of pipeline model - DN 1500 (BSI., 2002a)

Secondly, in order to execute the study for interaction between soil and buried structure caused by earthquake, two typical types of soil (sandy soil and cohesive soil) were considered. Elasto-plastic analysis by Mohr-Coulomb theory has been conducted as mechanical properties of soil. Additionally, water effect in soil has been studied by considering representative elastic property values of both moist and saturated soil. For plastic property of soil, the representative maximum value of two types' soil has been used for study as in Table 1.2.

Table 1. 2 Material properties of soil (Liu et al., 2010, Raymond and James, 1985, Nixon and Child, 1989, <http://www.finesoftware.en/geotechnical-sodtware/help/fem>, 2010)

Type of soil	Mechanical properties	Term	Value	
Sandy soil	Elastic property	Density (kg/m^3)	Moist	Saturated
			1850	2160
		Young's modulus (MPa)	Moist	Saturated
			24	96
		Poisson's ratio	Moist	Saturated
			0.2	0.25
	Plastic property	Cohesive strength (C - kPa)	0 to 17	
		Friction angle (ϕ - deg)	35 to 40	
		Dilation angle (ψ - deg)	2	
Cohesive soil	Elastic property	Density (kg/m^3)	Moist	Saturated
			1700	2000
		Young's modulus (MPa)	Moist	Saturated
			19	48
		Poisson's ratio	Moist	Saturated
			0.25	0.45
	Plastic property	Cohesive strength (C - kPa)	17 to 252	
		Friction angle (ϕ - deg)	20 to 29	
		Dilation angle (ψ - deg)	2	

The scale of soil was created as a cuboid with buried pipeline on one centre line. For the same reason related to the length of pipeline, the soil's length (L) will also be considered as 15, 50 and 100 metres. The width (W) and height (H) of soil were created as 10 metres and 15 metres in order to ensure the affordable space in which the pipeline with soil is failed when finite element analysis is executed. The effects of buried depth of pipeline from the pipe's crown (h) were also considered in conformity to each buried depths of pipeline such as 0.5, 1, 1.5, 2, 2.5, 3, 4, 5 and 6 metres from the top surface of soil to crest of pipeline as shown in Figure 1.2.

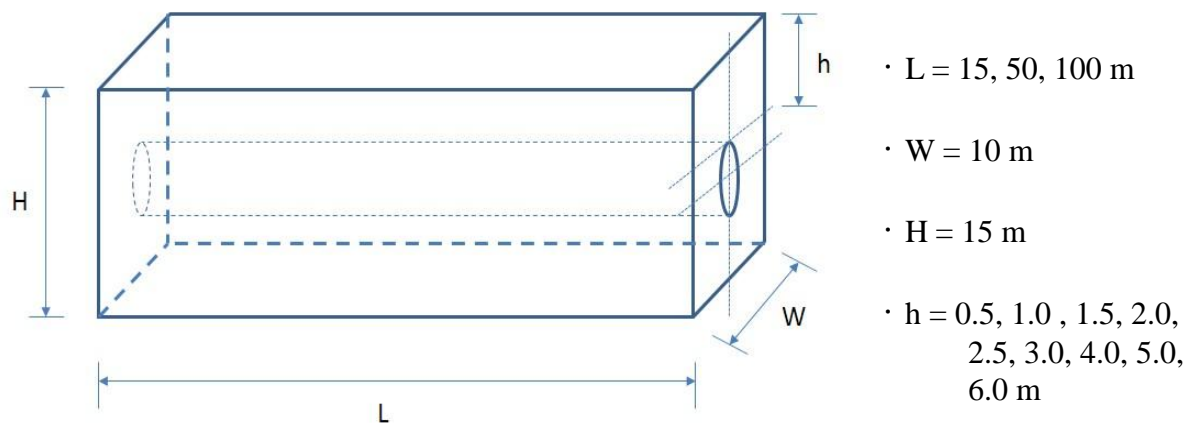


Figure 1. 2 Dimensions of soil model (BSI., 2010)

The limit depth of 6 m related to the buried pipeline is chosen, because, in the case of deeply buried pipeline, the live loads become negligible compared to the dead loads. It is of interest to note that for a pipeline, which is constructed at more than 6 metres depth, the live load becomes asymptotic to zero, so that further increase for buried depth of pipeline imposes negligible additional live load on the pipeline (Young and Trott, 1984). Although the minimum buried depth of pipeline is regulated at 0.9 metres or 1.2 metres in a construction field of pipeline, it is possible to examine the behaviour of pipeline more conspicuously by studying the measuring with buried depth, which is less than 0.9 m or 1.2 m.

1.3. Types of loads on pipeline

In general, several loads and load combinations affect buried structures. The buried pipeline is no exception. Thus, the effect of these loads has to be considered in pipeline structure design and analysis. According to Yong (2001), loads can be fractionalized as functional loads, environmental loads and accidental loads; functional loads are the operated loads usually in normal condition, environmental loads are loads influenced by environments and accidental loads are rarely loads influencing the structure. Whereas the functional loads and environmental loads are correlated to the pipeline system, accidental loads are related to critical loads to the local components. In this study, the functional loads can be expressed as weights of soil and pipeline and internal pressure of pipeline. Environmental loads can be introduced to traffic load and water effect, which is considered by material properties. Finally, accidental loads can be manifested by seismic load.

The loads can be also divided into two types; static and dynamic loads. This criterion, which demarcates types of load, is related to the method of analysis. Static analysis might be executed by using some passive loads, which can be expressed as static loads such as gravity of soil and pipeline, internal pressure of pipeline and typical traffic pressure on road. On the other hand, seismic analysis is practiced by using active loads, which can be expressed by seismic loads such as earthquake wave propagation in the ground.

The buried pipeline's deformability is determined by the structural response to load, which is caused by the effects of soil overburden, traffic and other accidental load. Under such loads, a thin-walled pipeline, which can be delineated as flexible pipeline, acts as flexible rings and is deformed like oval horizontally. These responses under loads give rise to two crucial effects. Passive pressures are mobilized in the backfill by the movement at the sides of pipeline and the inward movement at the crown and invert of pipeline causes the vertical pressure to reduce.

These responses of buried flexible pipeline under loads should be reflected in the design criteria so that their deformation, expressed as the extension of the horizontal diameter, do not exceed a specific limit, which is normally taken to be five percents.

1.3.1. Static loads

The static design and analysis of buried flexible pipeline are carried out for the total loads, comprising the effects of the dead load exerted by soil and the live load caused by traffic. Both the dead and live load influence the plane directly above the pipeline and the resultant vertical load will be the total static load on the pipeline.

Firstly, the weights of soil, which is generally called dead load, can be calculated by several factors such as width of excavated trench, cover depth and water table in the depth. But, in this study by finite element method, the consideration of width of excavated trench will be ignored in order to consider the effects of typical two soil types, which are sandy soil and cohesive soil, without deliberation of the backfill effects to the buried pipeline. Additionally, internal pressure of pipeline will be taken into account in this study. Even though the internal pressure caused by water flow in the buried pipeline does not much influence the deformability of the buried pipeline, the internal pressure in buried pipeline might play small role for preventing deformation of buried pipeline because the stiffness of buried pipeline may be increased due to the extension effect caused by water steady flow in the buried pipeline. Classically, water pressure in pipelines is operated between about 276 kPa, 40 psi, and 414 kPa, 60 psi. Therefore, 414 kPa, which is maximum water pressure in pipeline, will be considered in this study in order to examine critical state of buried pipeline.

Finally, the dead load on the buried pipeline is normally substantially greater than the live load because the effects of live load, which can be expressed as traffic, diminish rapidly with depth of soil. But, in the case of shallow buried depth pipeline, the live load becomes more critical load than dead load (Nath, 1994). In order to examine the critical deformation of pipeline, in this study, the heaviest vehicle load will be used. As following the documents such as BS 5400-2:2006 (BSI., 2006) and BS 9295:2010 (BSI., 2010), the eight wheel HB load in main road is the one of the heaviest loads for all public highways and bridges in the UK. The load on each wheel is 112.5 kN and spread over an contact area to the road of 0.102 m², to specified contact pressure of 1100kPa. However, an assumption is required for applying the eight wheel HB load in this study. The study for examining failure aspects of buried pipeline will be performed with considering short-term serviceability issue of structural behaviour. Thus, if the eight wheel HB load on the road is passed in large numbers, it is possible to think that there is a uniform surface load onto the ground as much as 1100 kPa. That is, the short-term structural serviceability issue of buried pipeline can be inspected by considering a uniform surface load onto the soil, 1100 kPa.

1.3.2. Seismic load

Stress waves in the ground are produced by earthquakes and various directions of the earthquake movement are instigated. These waves make the movement of ground more complex by reflecting and refracting waves. That is, the ground motion parameters such as amplitude of motion, frequency content and duration of the ground motion change because the seismic waves propagate through overlying soil and are refracted until reaching the ground surface (Wang, 1994).

Prasa (2004) mentioned that the predominant frequency of most of earthquakes, which cause fatal damage, is within the range 1 to 2 Hz and the peak average amplitude of acceleration has been found around 0.5 g. However, according to Wu (1971), the mechanism of earthquakes and the nature of the movements would not be changed radically from the past earthquakes because the crust of the earth does not change rapidly. For this reason, one specific source of time history ground motion, which is the El-Centro Earthquake in 1940 at Imperial Valley with magnitude 7.1 on the Richter Scale or 0.3 g of ground acceleration, has been used in this study for understanding the effects of specific earthquake impact to the buried structure. In order to apply seismic load in this study, the accelerogram dealing with amplitude of earthquake load, peak acceleration and time history has been used as in Figure 1.3 because the behaviour between soil and buried structure under earthquake motion can be analyzed by the ground acceleration as a series of harmonic components.

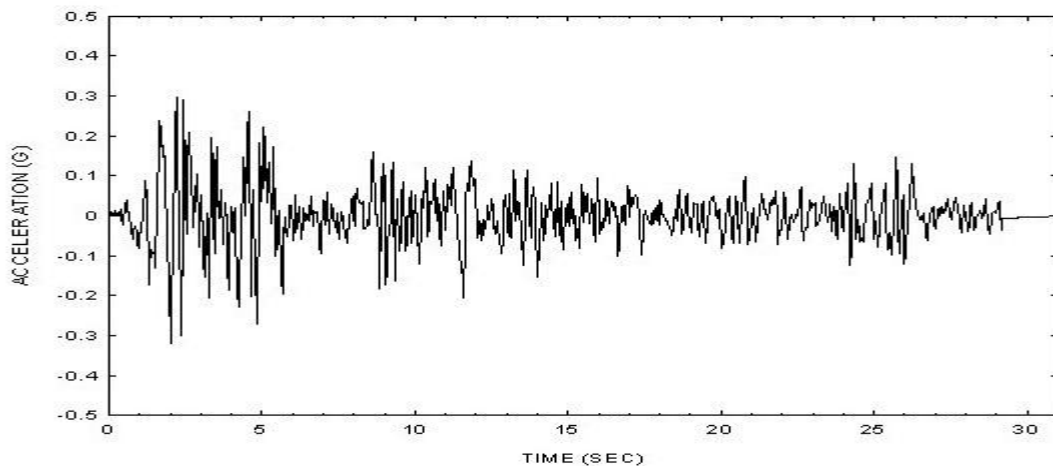


Figure 1.3 The eccelerogram of El Centro Earthquake in May, 1940
(<http://www.vibrationdata.com/elcentro.htm>, 2010)

Actual numerical data based on above seismic accelerogram of El Centro Earthquake are attached in Appendix A.

1.3.3. Conclusion for loads

The loads for non-seismic loads are internal operating pressure for water flow, gravity load from earth and the impact of traffic. Based on the plane stress and strain assumption, these loads produce ring tension caused by internal pressure for water flow in the pipeline and ring bending caused by the uniformly distributed gravity load to the buried pipeline. On the other hand, the buried pipeline may follow the movement of ground in both longitudinal and lateral directions during seismic shaking of the ground. This means that seismic analysis for buried pipeline needs to consider the effects of combined stress and strain in both hoop and longitudinal directions because the seismic analysis does not confine only hoop stress and strain direction.

In order to study for buried flexible pipeline considering different effects between static and seismic condition, the typical static and dynamic loads are determined as in Table 1.3.

Table 1.3 Static and dynamic loads

(BSI., 2006, BSI., 2010, <http://www.vibrationdata.com/elcentro.htm>, 2010)

Static loads	Gravity (N)	9.81
	Traffic load onto ground (kPa)	1100
	Internal water pressure in pipeline (kPa)	276 to 414
Seismic load	Peak acceleration of earthquake (g)	0.3
	History time (sec)	31.18

1.4. Conclusion

It is necessary to take two requirements into account for the analysis of the behaviour of flexible buried pipeline: the need to know the vertical deflections caused by both static and seismic load, and the need to know the ultimate strength of the pipelines caused by the above two loads. By examining above two requirements for study, it will be possible to make an observation related to diverse effects causing buried flexible pipeline to be deformed or failed.

First of all, there are several types of ground conditions: clays, sands, rocks, undistributed granular soils, placed granular soils and a compacted backfill ground around buried structure placed in an excavated ground or the ground involving diverse layers, which is involved in different types of soils. In fact, if the various ground conditions mentioned in this study related to the expectations of buried flexible pipeline's behaviour when these diverse properties of soils under seismic as well as static load are considered, the analysis would be too complicated. Thus the two representative material properties are determined such as typical sandy soil and cohesive soil for the purpose of investigating the effects of ground condition to the buried flexible pipeline.

Additionally, for assessing the effects of water saturated in the typical soils, the material properties related to two representative types, general moist and fully saturated soils, are also considered. Even though it is impossible to examine the effect of water saturated in the soil in accordance with a variation of water table under the ground, the anticipation for the effect of changeable water table below ground will be possible. This is because the ultimate range of the water effect will be calculated between normal and fully saturated soils.

Finally, in order to examine the effect of loads to the buried flexible pipeline, the loads are divided into two types; static and seismic loads. Even if various loads might exert an influence on buried pipeline, the two loads considered will be the typical and ideal loads in this study. The

effect of seismic load to the buried pipeline might be clearly explained by comparing with analysis of static loads.

2. Research objectives

There is a vast range of water and gas distribution systems in the world. Thirty years ago, according to Pocock et al (1980), about 500,000 km of buried pipelines involving large proportion located at shallow depth under highways in urban area was constituted in United Kingdom. This means that more than 500,000 km of buried pipelines has been constructed in proportion to increased demands of water and gas in the urban area of United Kingdom.

These buried pipelines are mainly located at shallow depth and were made in various types of materials, which can generally make the type of buried pipe divided into rigid pipes and flexible pipe in accordance with type of service. The failures of these buried pipelines are influenced by traffic, different ground condition and differential ground movement, etc. For that reason, the conventional design methods usually are founded on static analysis (Bulent, 1985).

It had been generally acknowledged that the buried structures such as subway stations and buried pipelines were safe during earthquakes until the 1995 Hyogoken-Nanbu Earthquake if they were not located near fault zones. However, Hyogoken-Nanbu Earthquake proved the buried structures to be vulnerable to earthquake ground motion as an example of Daikai Subway Station. Furthermore, there is another example which revealed that buried structure were also flimsy to earthquake ground motion. 76 metres of 2.4 m diameter buried pipeline collapsed and 23 metres of buried pipeline were deformed by the Northridge Earthquake in the northern San Fernando Valley in Southern California (Bardet and Davis, 1997). These examples demonstrate that it is necessary to study failure aspects of buried structures caused by severe earthquake in order to protect lifelines from earthquake.

2.1. Aims

Following the discussion of G. Madabhushi (2009), the proper understanding of soil-structure interaction caused by earthquakes will be helpful to supply a key to studying some of the failures. For the purpose of proper study of failure aspects of buried structures caused by severe earthquakes, it is recommended that a relatively large steel buried pipeline, used as domestic water supply pipeline will be suitable for studies using the Finite Element Methods (FEM).

The main aim of this study is to understand the seismic interaction between ground and buried pipelines when an earthquake occurs with comparing static interaction. The second aim of the study is to examine the variation of buried depth of pipeline affected by both earthquake load and static load in order to present the safest buried depth of pipeline.

2.2. Objectives

Seismic interaction related to both soil and buried structure during seismic events is a relatively complex problem because soil and embedded structure might undergo a series of complicated interactions during an earthquake. Moreover, if the study for failure aspects between soil and buried structure is considered as a three dimensional problem, this study will give rise to difficulties in examining failure aspects caused by the earthquake because three dimensional analysis involves more variables than will be considered in a two dimensional analysis.

The finite element software package, ABAQUS, is employed in order to analyse three dimensional element models because this method has the benefits that a detailed failure mode and effective analysis can be carried out to study failure aspects more easily than any other methods. According to Hugel (2008), the features related to soil mechanics can be dealt by

ABAQUS and several user subroutines make the specialized analysis for soil treated in ABAQUS.

The static state of a buried structure without considering the influence of the earthquake should be evaluated at first in order to assess the safety of the structure against an earthquake. With this measurement, the seismic state of the buried structure when considering the influence of the earthquake would be estimated by adding other earthquake factors. After modelling a buried structure and ground including a vibration model, seismic interpretation is to be executed by inputting the data of earthquake movement, waveform or response spectrum. The seismic analysis can be used to precisely measure actual movement of both the soil and the buried structure. By comparing these two analyses, which are static and seismic, the different failure aspects of buried pipelines according to the considerations between static and seismic state can be understood thoroughly.

3. Finite Element Analysis (FEM) – ABAQUS

In the finite element method, the actual continuum or body of solid is represented by an assemblage of subdivisions called finite elements. These elements are regarded as interconnected at specified joints called nodes or nodal points. The nodes are usually placed on the boundaries where adjacent elements are considered to be connected. It is necessary to assume that the variation of field variable inside a finite element can be approximated by a simple function because the actual variation of the field variable, such as displacement, stress, pressure or velocity, inside a continuum is not known. These approximated functions, which are also called interpolation models, are characterised as the values of the field variables at the nodes. When field equations, such as equilibrium equations, for the whole continuum are created, the new unknowns become the nodal values of the field variables. However, the nodal values of the field variable can become known values by solving the field equations, which are generally composed of matrix equations. Once these are known, the field variable throughout the assemblage of elements is clarified by the approximated functions. This orderly step-by-step process is always followed for the solution of a general continuum problem by the finite element method in the same manner as ABAQUS (Rao, 1999).

In this study, finite element models of the pipeline and soil are established using the package ABAQUS to carry out failure analysis of buried pipeline caused by static and seismic loads. In order to perform this analysis for a buried steel pipeline, it is necessary to accept three basic assumptions as below.

- (a) The welding between pipeline segments is not considered.
- (b) The soil is elasto-plastic characterised by Mohr Coulomb theory and the pipeline is isotropic, elastic and perfectly plastic.

- (c) Pipeline and soil are fully bonded each other and the interface between pipeline and soil is perfect without defects.

There are limitations above three assumptions; it is difficult to depict actual pipeline performance by considering the disregard of welding points between pipeline segments, application of fully bonded contact area between pipeline and soil and adaptation of simplified material properties of both soil and pipeline. This is because above three assumptions does not reflect actual pipeline performance. However, these assumptions make the analysis straightforward because typical pipeline performance can be depicted by disregarding ignorable small effects on pipeline performance.

3.1. 3D-Finite Element (FE) modelling

Based on the platform of ABAQUS, reasonable and practical 3D-FE models were established. Whereas the pipeline model was created as a 3D deformable shell model due to the thin thickness of the pipeline, the soil model was defined as a 3D deformable solid body as in Figure 3.1.

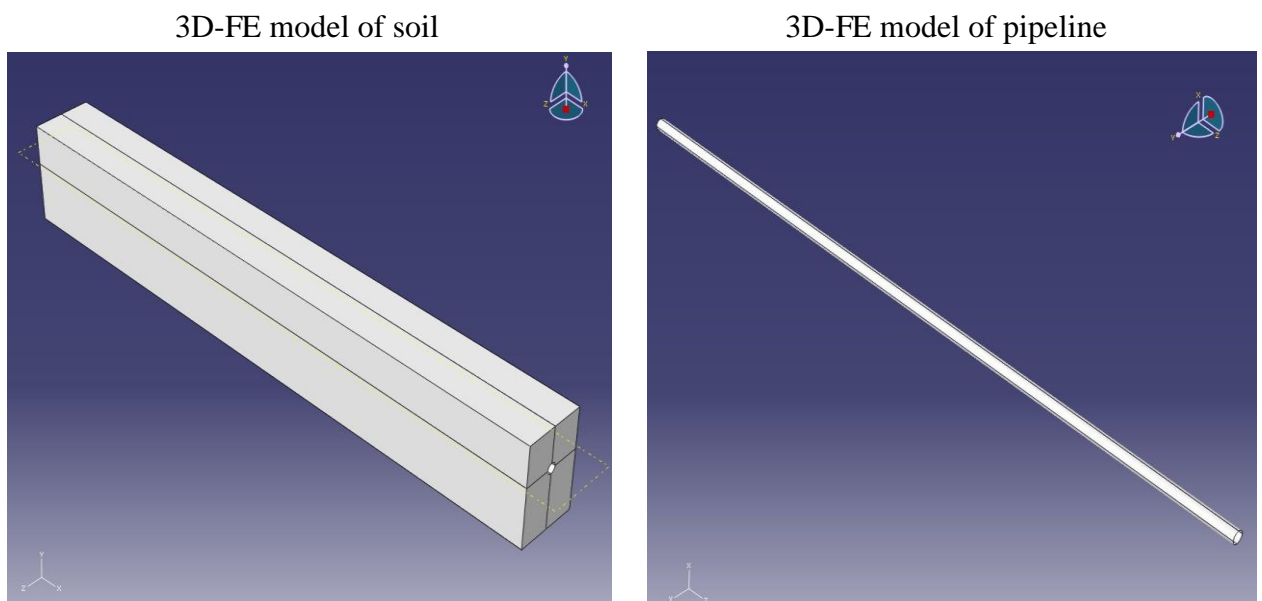
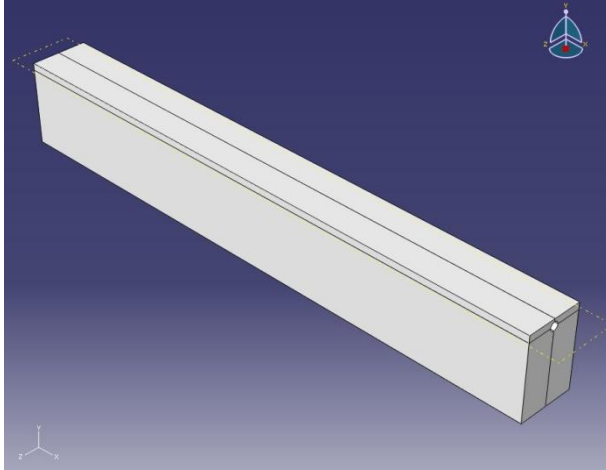


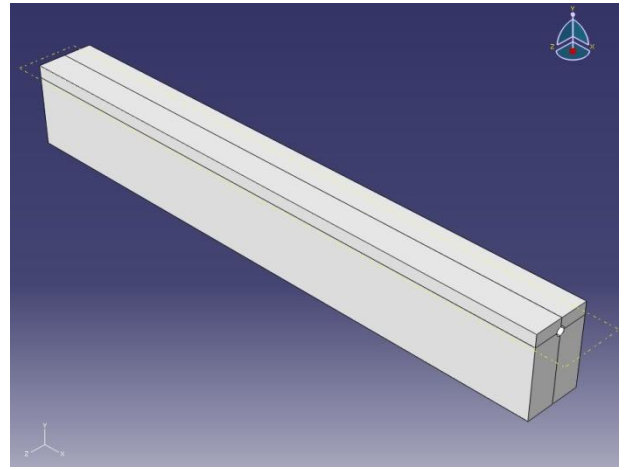
Figure 3. 1 3D-FE models under the FE software environment of ABAQUS

These two models were designed following the scale which was illustrated in section 1.2.4. In order to define the contacts between above two models and position them relative to each other, the contact surface between circumferential surface of pipeline and inside surface of soil is established as a fully tied surface so as to satisfy the third basic assumption that pipeline and soil are fully bonded each other and the interface between pipeline and soil is perfect without defects. The pipeline model was aligned with soil model in the centre of soil model's width according to the buried depths of pipeline from the top surface of soil to the crest of pipeline such as 0.5, 1, 1.5, 2, 2.5, 3, 4, 5 and 6 metres. The assembled models with soil and pipeline according to some of these buried depths can be seen in Figure 3.2.

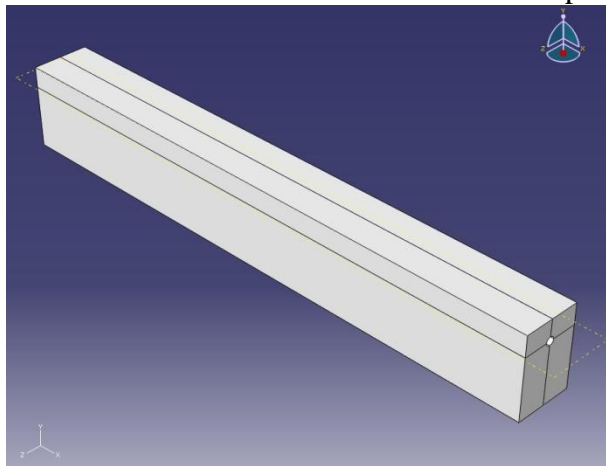
3D-FE assembled model of 0.5 m buried depth



3D-FE assembled model of 1.5 m buried depth



3D-FE assembled model of 3.0 m buried depth



3D-FE assembled model of 6.0 m buried depth

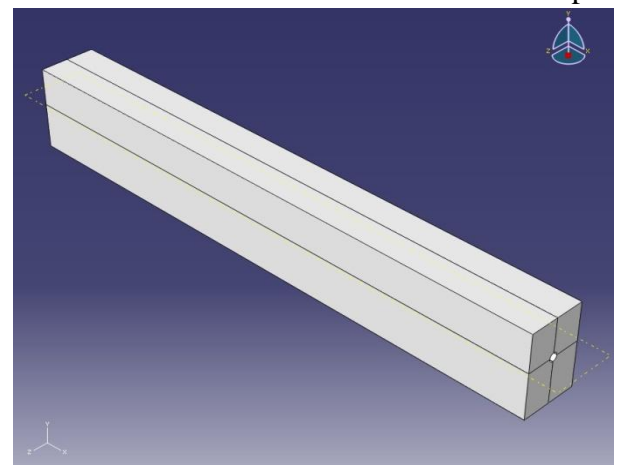


Figure 3. 2 3D-FE assembled models with soil and pipeline according to the each buried depth

Furthermore, lengths of 15m, 50m and 100m of were considered for verifying the effect of the length on modelled performance. The 15m and 50m models of soil and pipeline are reflected in short and middle length of models and 100m models is represented in infinite length or long length of models. These three discriminated models will prove that the length of pipeline is another factor which affects with failure of pipeline caused by considered loads. These three discriminated models can be seen in Figure 3.3.

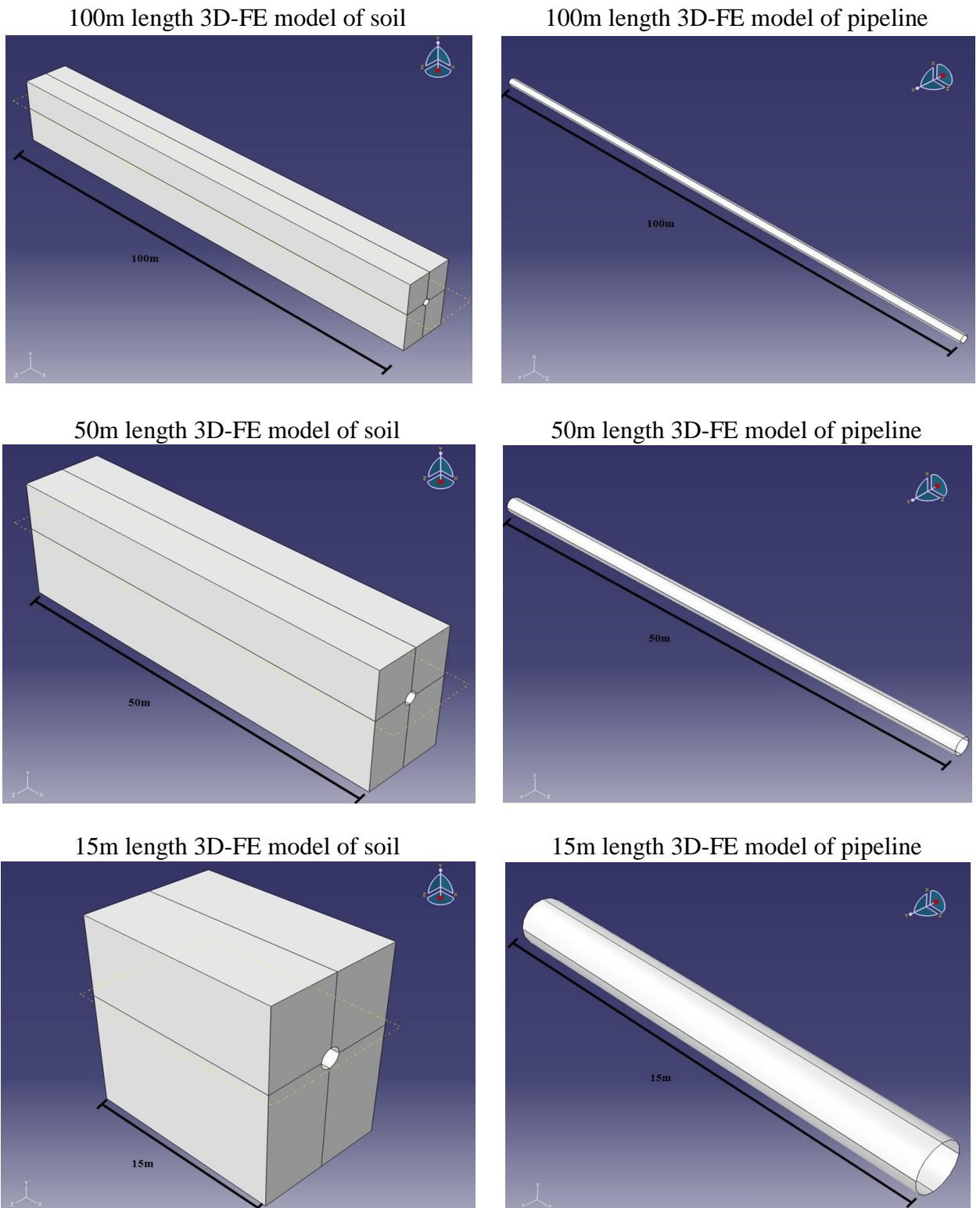


Figure 3.3 Three representative 3D-FE models of soil and pipeline according to the lengths

3.2. Key technologies treatments

3.2.1. Determination of stress models

First of all, for the static analysis in this study, the choice of a general static stress model is one key factor which controls the simulation results of buried pipeline failure caused by typical static loads. In ABAQUS, the general static stress model can be controlled as constitutive equations of material, defined as the relationship between plastic strain increment and stress increment during constituting process (Simulia, 2009). The following assumptions are needed.

- (a) Selected material of pipeline is perfectly elastic-plastic and chosen material of soil is elasto-plastic material according to Mohr-Coulomb theory.
- (b) The yield criterion of Von Mises is computed within the program for the plastic forming actions related to the stress in pipeline and soil.
- (c) In case of strain-hardening material, the reloading yield stress after loadoff is the unloading yield stress, and more than initial yield stress.

Thus the general static stress model performs the strain-hardening during application of static loads and determines the calculated figure, area and position of the resulting yield surface.

Additionally, for the choice of FE dynamic arithmetic, a dynamic implicit algorithm in simulation of earthquake exciting was selected. The choice can accept dynamic stress model caused by dynamic load with the characteristic of constringency which dynamic explicit algorithm does not make the model allow but dynamic implicit makes the model allow (Huang et al., 2008). By the evaluation of 3D-FE model considering a dynamic implicit algorithm, the variations of the dynamic force, stress field and strain field with time are investigated.

3.2.2. Definition of constraint type

Constraint between pipeline and soil may cause elastic and plastic deformation during loading process. In ABAQUS, the types of constraints include tie, rigid body, display body, coupling shell-to-solid coupling, embedded region and equation (Simulia, 2009). One constraint called Tie is adopted for simplicity to connect pipeline with soil, satisfying the third assumptions in section 3 that pipeline and soil are fully bonded each other and the interface between pipeline and soil is perfect without defects. Tie can combine pipeline with soil as a whole and provide them with different meshing methods, especially three-dimensional meshing.

3.3. Boundary conditions

In 3D-FE models related to soil and pipeline, two boundary conditions of 3D-FE soil model need to be considered; bottom surface and four beside surfaces of 3D-FE soil model and it is also necessary to consider two boundary conditions of 3D-FE pipeline model; two end surfaces of pipeline and circumferential pipeline surface which comes into contact with soil. The basic 3D-FE model of pipeline and soil can be delineated as in Figure 3.4.

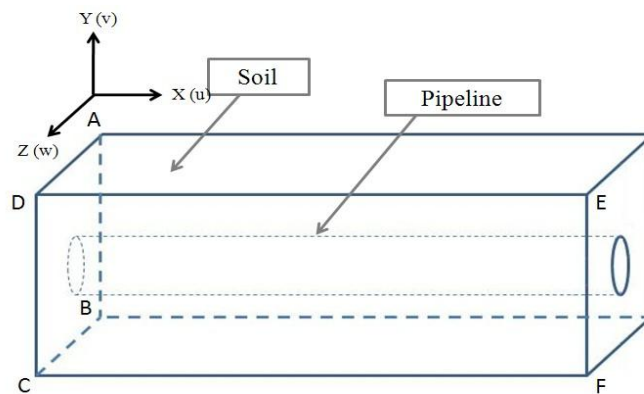


Figure 3.4 Basic 3D-FE model of pipeline and soil

3.3.1. Boundary condition of soil's 3D-FE model

The two assumed boundary conditions of 3D-FE soil model are expressed as in Figure 3.5 based on Figure 3.4; bottom surface and four beside surfaces of 3D-FE soil model.

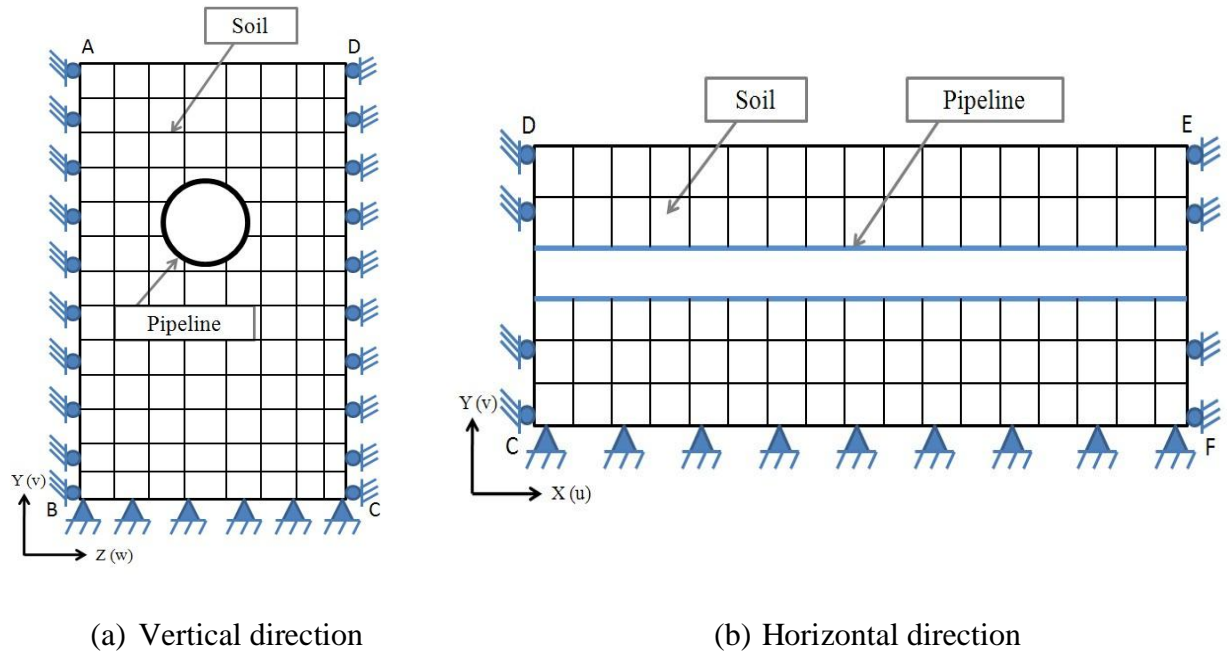


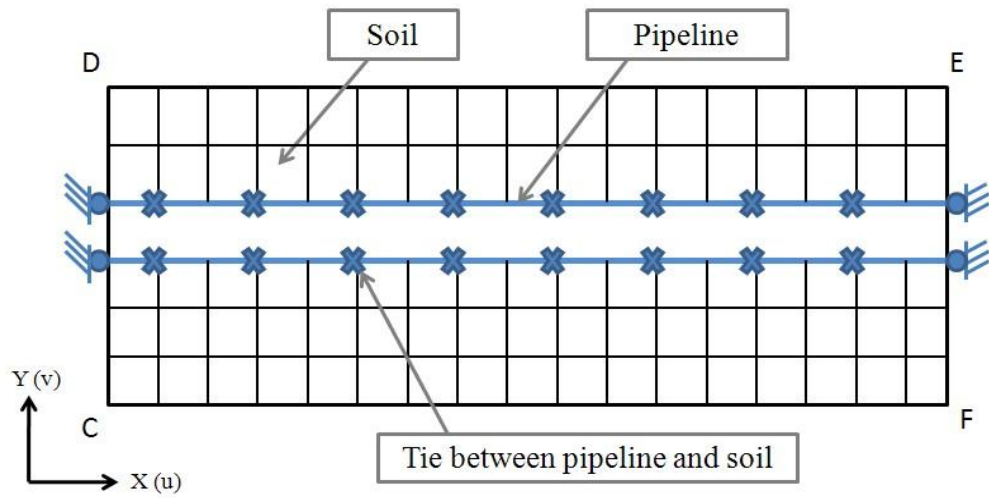
Figure 3. 5 Boundary conditions of 3D-FE soil model

Firstly, four beside surfaces of 3D-FE soil model are supposed to be on rollers as shown in Figure 3.5 since these sides for AB, CD and EF restrain only the horizontal movement (i.e. $u = w = 0$). Besides, it is adaptable to accept rollers for boundary of sides AB, CD and EF because infinite or semi infinite medium of soil can be assumed to move vertical direction by considering significant extent of the soil body (Rao, 1999).

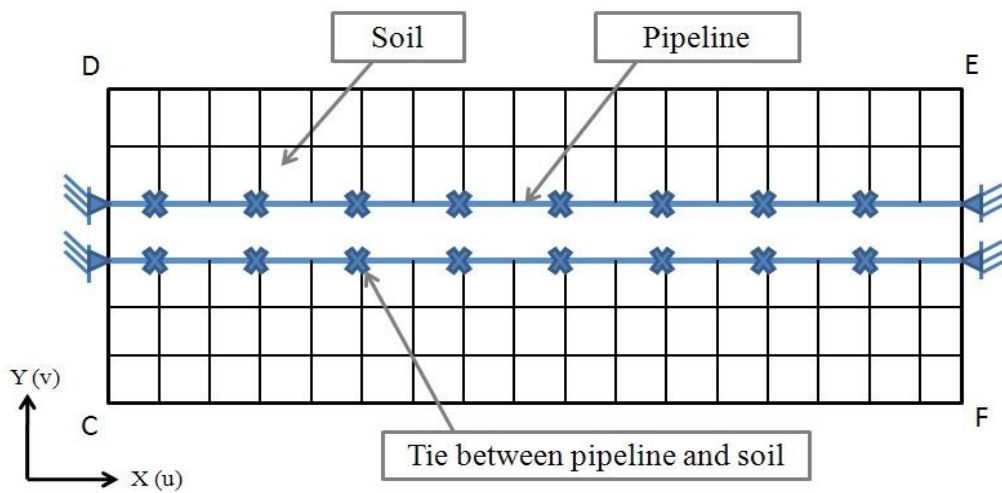
Additionally, the bottom surface of 3D-FE soil model is proposed to be completely fixed (i.e. $u = v = w = 0$ along BC and CF) in order to restrain horizontal (i.e. $u = w = 0$) and vertical movement (i.e. $v = 0$). This is because the bottom boundary is selected at the known location of a bedrock surface.

3.3.2. Boundary condition of pipeline's 3D-FE model

Two proposed boundary conditions of 3D-FE pipeline model are shown in Figure 3.6 based on Figure 3.4; two end surfaces of pipeline and surrounding pipeline surface which come into touch with soil.



(a) Roller boundaries for two end surfaces of pipeline

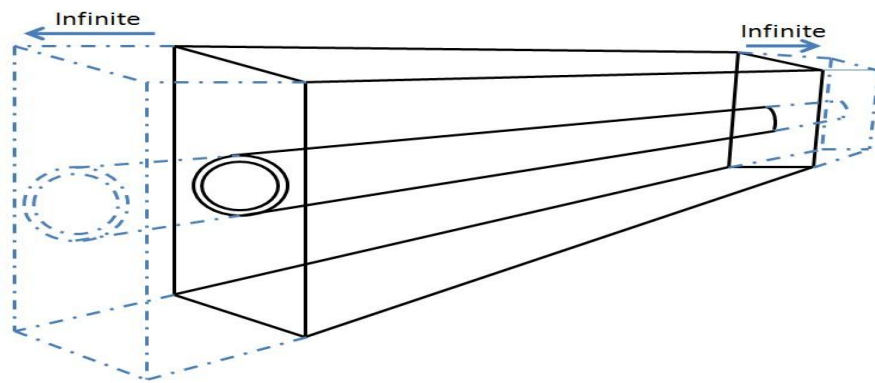


(b) Hinge boundaries for two end surfaces of pipeline

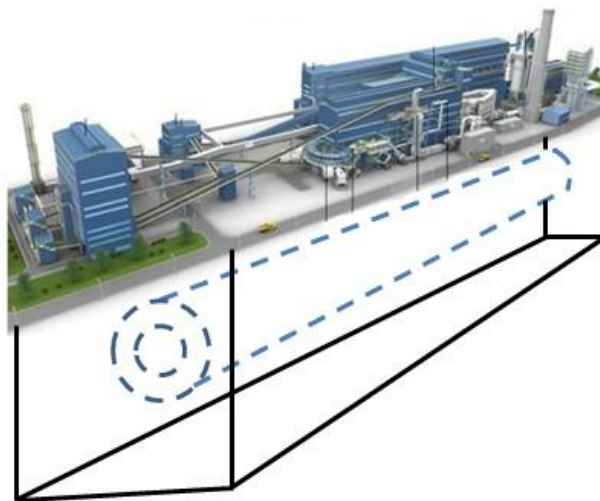
Figure 3. 6 Boundary conditions of 3D-FE pipeline model

The displacement and stress of pipeline are affected by the soil. The types of soil, such as sandy soil and cohesive soil, make the act of pipeline different (Liu et al., 2010). This means that buried pipeline is moved relatively with soil. Therefore, the circumferential surface of pipeline is assumed to be bonded with soil in order to simulate this behaviour of pipeline shown in Figure 3.6.

In the case of the pipeline end boundaries, it is necessary to consider two typical cases; infinite length of buried pipeline and finite length of buried pipeline as between two buildings see Figure 3.7.



(a) Infinite length of buried pipeline



(b) Finite length of buried pipeline between two buildings

Figure 3.7 Two typical case of buried pipeline for pipeline end's boundaries

If an infinite length of buried pipeline is taken into account, it is acceptable to consider roller as the boundary of the ends of pipeline because the buried pipeline may be moved with soil relatively. On the contrary, if finite length of buried pipeline is defined due to the existence of buildings at the ends of buried pipeline, it is suitable to consider hinge as the boundary of the ends of pipeline since the ends of buried pipeline will be restrained by connection between two buildings. Thus, the restrained ends of buried pipeline may be completely fixed in all directions (i.e. $u = v = w = 0$). To be honest, built-in infinite elements can simulate infinite boundary condition in ABAQUS. But, unknown errors occurred when the models were made in ABAQUS for this research. Therefore, considering roller boundary condition was presented in this research as an alternative method for considering infinite boundary condition.

3.4. Adaptive Meshing for Finite Element Analysis (FEA)

For Finite Element Analysis (FEA), it is very important to determine the type of element, the shape of element and the number of elements in order to obtain the more accurate results based on the available computational capacity, which is Intel Core Central Processing Unit (CPU) as the main configuration with two processors (the main frequency of each processor is 2.99 GHz) and 3.25 GB memory. The technology of adaptive meshing in 3D-FE model is a good to implement as it makes it possible to support a high-quality mesh throughout the analysis, especially when large deformation or stress of material occurs, by permitting the meshed element to move independently in material. The topology of the mesh is not changed by adaptive meshing technology in ABAQUS and is involved in the characteristics of pure Lagrangian analysis and pure Eulerian analysis simultaneously. This adaptive meshing type is called Arbitrary Lagrangian-Eulerian (ALE) analysis (Huang et al., 2008).

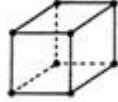
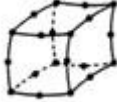


It is necessary to determine the representative 3D-FE models and loads in order to select the adaptive mesh. Firstly, the material properties of soil and pipeline based on the Tables 1.1 and 1.2 were used. Especially, in the case of soil's material properties, it is possible to examine available mesh by considering all cases of soil's material properties such as general moist or fully saturated sandy soils and general moist or fully saturated cohesive soils. Moreover, searching the adaptive mesh is available in accordance with the size of 3D-FE model by considering the three typical horizontal lengths which were already mentioned in Figure 3.3, while only 6 metres buried depth of pipeline under the ground was selected. Secondly, the static loads involving the self-weight of pipeline and soil, traffic load onto ground and internal pressure of pipeline were selected, based on Table 1.3. This is because it is difficult to examine the adaptive mesh due to changeable results depending on the passage of time when dynamic loads are chosen. On the contrary, it is possible to examine adaptive mesh more easily by choosing static loads because there is only one result based on static loads for one selected model without considering time dependence. Finally, all mentioned boundary conditions based on Figure 3.5 and 3.6 were chosen with considering only hinge boundary condition at the pipeline's ends. Therefore, selecting above representative factors of 3D-FE models makes the determination for adaptive mesh related to the type and number of elements available by checking the results of four different soil cases and three different lengths of 3D-FE models under same static loads and boundary conditions of 3D-FE models.

3.4.1. The type of element

In ABAQUS related to the 3D-FE modelling process, elements exist not only with appreciable rigidity called anti-distorting ability, but also with appreciable flexibility called good forming ability. Under the comprehensive consideration of the buried pipeline, whereas the 3D

reduced integration continuum element with eight nodes as a first-order (or linear) interpolation, C3D8R, and with twenty nodes as a second-order (or quadratic) interpolation, C3D20R were selected for the soil's 3D element, the 3D reduced shell continuum element with four nodes as a first-order (or linear) interpolation, S4R, and with eight nodes as a second-order (or quadratic) interpolation, S8R were chosen as shown in Table 3.1.

Table 3. 1 Selected element type for soil and pipeline's 3D-FE models

Material	Element type	First-order (or linear) interpolation		Second-order (or quadratic) interpolation	
Soil	Reduced integration continuum element	C3D8R		C3D20R	
Pipeline	Reduced shell element	S4R		S8R	

The reason why these two different orders of element are considered is to examine that which types of element related to different orders give a more precise analysis. This mesh refinement method is called 'p-refinement' by changing to higher order polynomial interpolations (Gago et al., 1982). However, it is concluded that second-order elements provide higher accuracy than first-order elements before executing the p-refinement method. The reason is that the stress and strain operator of first-order elements provides only constant volumetric stress and strain throughout the whole elements while second-order elements solve smooth problem due to existence of stress and strain operators between two edge stress and strain operators. In other words, second-order elements are more effective than first-order elements because the second-order elements can deal with bending dominant problems which cannot be performed by first-order elements.

3.4.2. The size of element

Increasing the density of the meshed elements also provides the accuracy of analysis because the number of elements in 3D-FE models is one of the most important factors for the quality of analysis as well as the selection of the adaptive element type. Mesh refinement for selecting the optimal number of elements is a difficult issue. This is because there is no regulation which number of meshed elements is an optimum number for the accuracy of analysis. Thus, in order to examine the best adaptable number of elements, it is necessary to investigate all the cases of each number of elements from a coarse mesh to a fine mesh within the range based on available computational capacity. This method for finding the adaptive mesh size of elements is called ‘h-refinement’ by subdividing the elements into smaller ones (Lo et al., 2010).

For accomplishing h-refinement mesh method, the considered approximate global size of meshed element, which is the average length of a meshed element in ABAQUS, was ranged from ten metres as a coarse mesh to zero point six metres as a fine mesh. These ranged mesh size was applied in each three typical lengths of 3D-FE models, which is 100, 50 and 15 metres as following Tables 3.2, 3.3 and 3.4. The applied meshes according to the different approximate global sizes of elements are shown in detail in Appendix B.

Convergence test for finding adaptable mesh size is the most efficient method to verify the error involving calculated displacement and stress results because fine mesh of model makes calculation became more accurate than coarse mesh. It is anticipated that there is a convergent point for calculated displacement and stress caused by designated static loads because the error with an increasing number of elements in designed models must converge nearly to zero, hence the results related to displacement and stress of model become accurate with increase of element numbers of model (Weck and Nottebaum, 1993).

Table 3. 2 The number of meshed elements in 100 m model

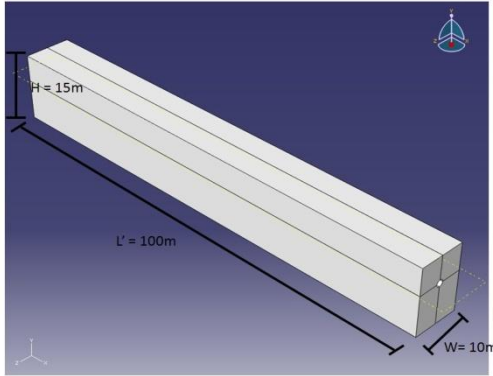
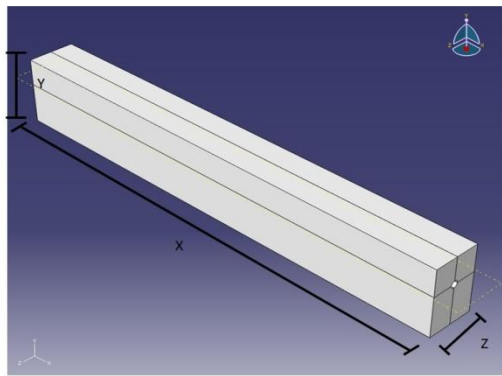
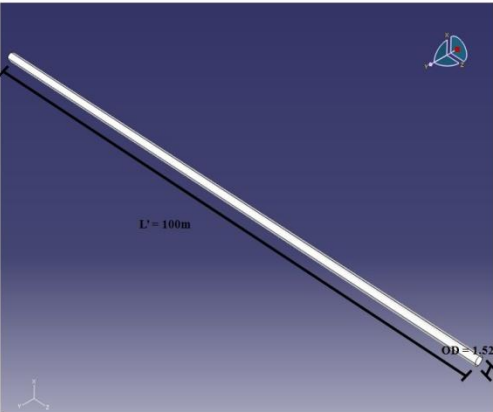
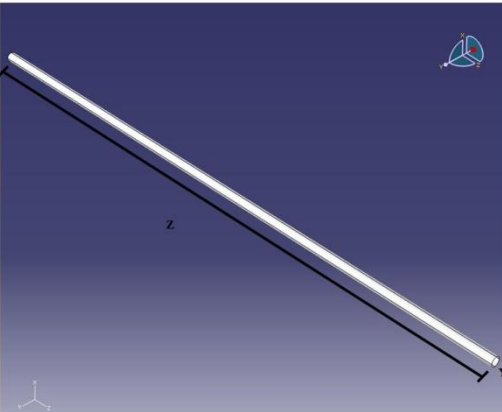
Type of model	Size of model		Number of element in model					
Soil								
								
			Soil			Pipeline		
Approximate global size of meshed elements	Total number of meshed elements in model	X	Y	Z	Number of meshed elements	Y	Z	Number of meshed elements
10	240	10	4	4	200	10	4	40
9	264	11	4	4	220	11	4	44
8	364	13	4	4	260	13	8	104
7	392	14	4	4	280	14	8	112
6	476	17	4	4	340	17	8	136
5	560	20	4	4	400	20	8	160
4	700	25	4	4	500	25	8	200
3	1056	33	5	4	792	33	8	264
2	3000	50	4	6	2600	50	8	400
1	16200	100	15	10	15400	100	8	800
0.9	23976	111	17	12	23088	111	8	888
0.8	30000	125	19	12	29000	125	8	1000
0.7	43758	143	21	14	42614	143	8	1144
0.6	68822	167	25	16	67486	167	8	1336

Table 3.3 The number of meshed elements in 50 m model

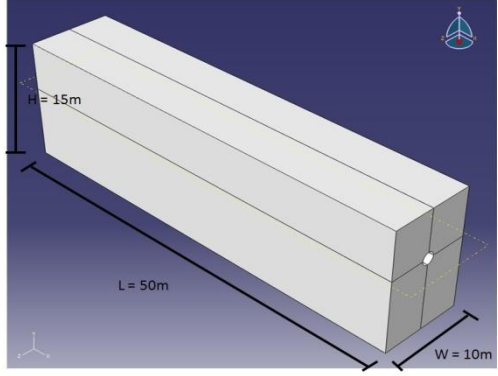
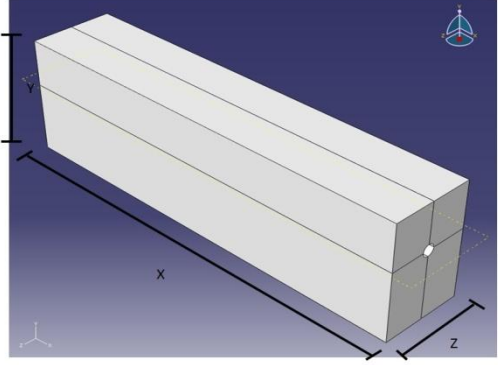
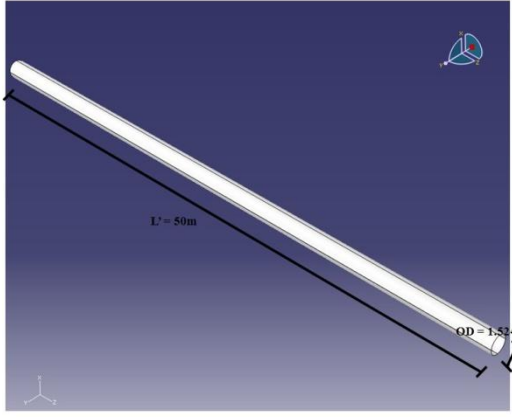
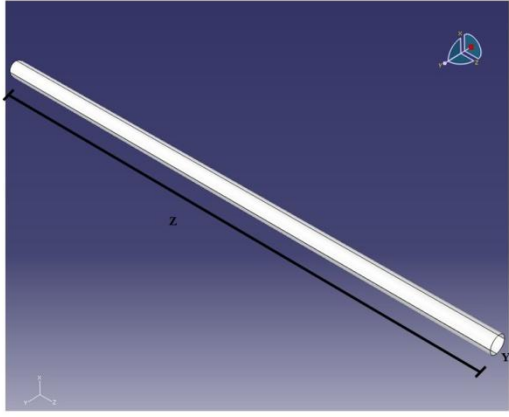
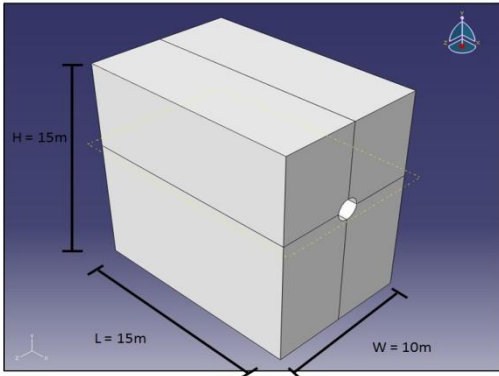
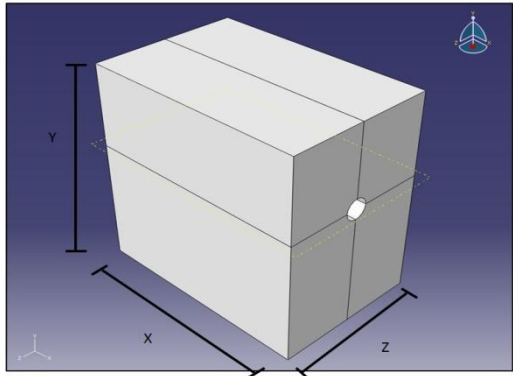
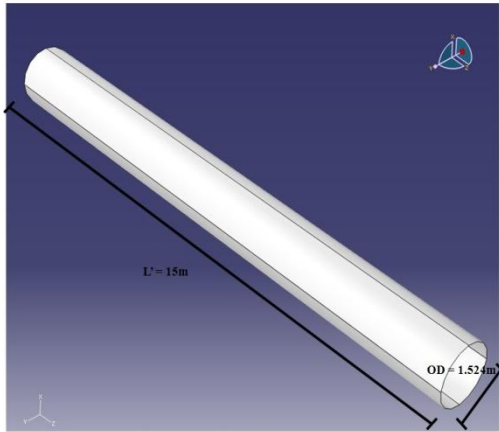
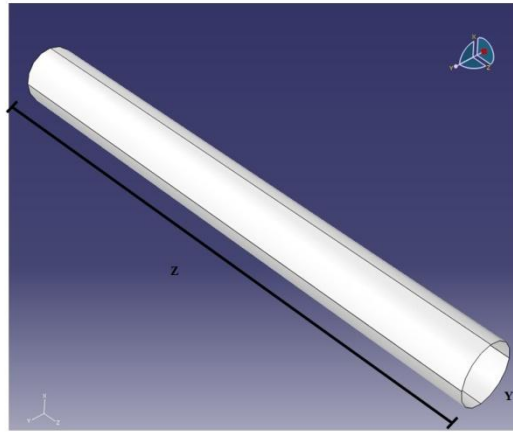
Type of model	Size of model	Number of element in model						
Soil								
								
		Soil		Pipeline				
Approximate global size of meshed elements	Total number of meshed elements in model	X	Y	Z	Number of meshed elements	Y	Z	Number of meshed elements
10	120	5	4	4	100	5	4	20
9	144	6	4	4	120	6	4	24
8	168	6	4	4	120	6	8	48
7	196	7	4	4	140	7	8	56
6	224	8	4	4	160	8	8	64
5	280	10	4	4	200	10	8	80
4	364	13	4	4	260	13	8	104
3	544	17	5	4	408	17	8	136
2	1500	25	8	6	1300	25	8	200
1	8100	50	15	10	7700	50	8	400
0.9	12096	56	17	12	11648	56	8	448
0.8	15120	63	19	12	14616	63	8	504
0.7	21726	71	21	14	21158	71	8	568
0.6	34196	83	25	16	33532	83	8	664

Table 3. 4 The number of meshed elements in 15 m model

Type of model	Size of model	Number of element in model						
Soil								
Pipeline								
		Soil		Pipeline				
Approximate global size of meshed elements	Total number of meshed elements in model	X	Y	Z	Number of meshed elements	Y	Z	Number of meshed elements
10	48	2	4	4	40	2	4	8
9	48	2	4	4	40	2	4	8
8	56	2	4	4	40	2	8	16
7	56	2	4	4	40	2	8	16
6	64	2	4	4	40	3	8	24
5	84	3	4	4	60	3	8	24
4	112	4	4	4	80	4	8	32
3	160	5	5	4	120	5	8	40
2	428	7	8	6	364	8	8	64
1	2430	15	15	10	2310	15	8	120
0.9	3672	17	17	12	3536	17	8	136
0.8	4560	19	19	12	4408	19	8	152
0.7	6426	21	21	14	6258	21	8	168
0.6	10300	25	25	16	10100	25	8	200

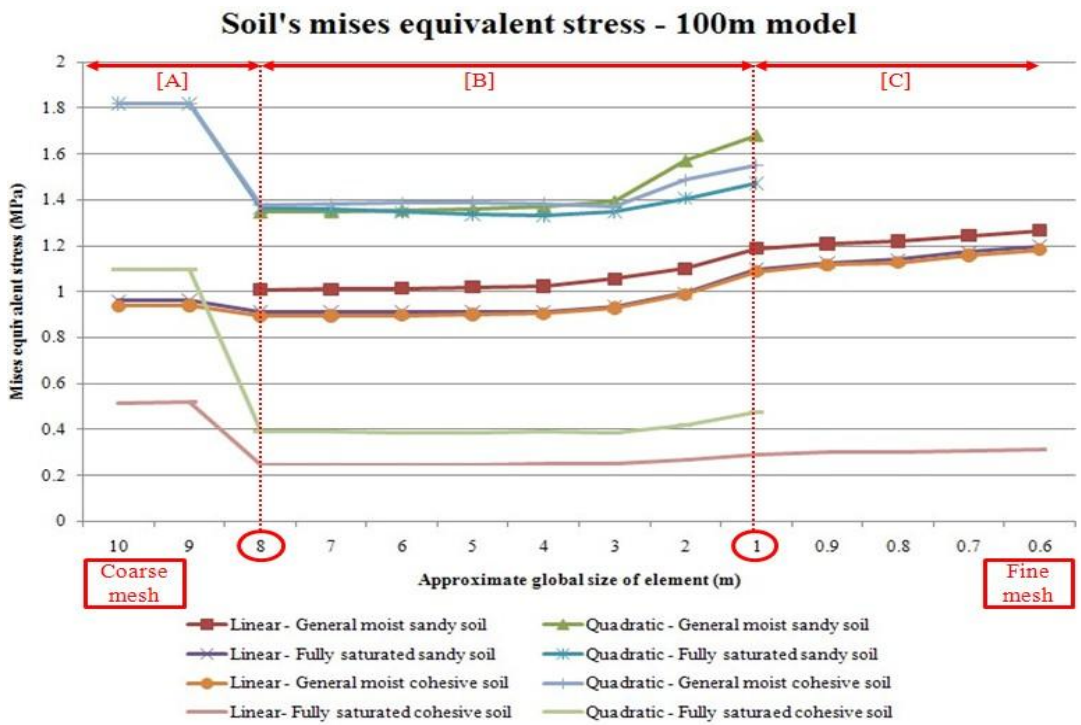
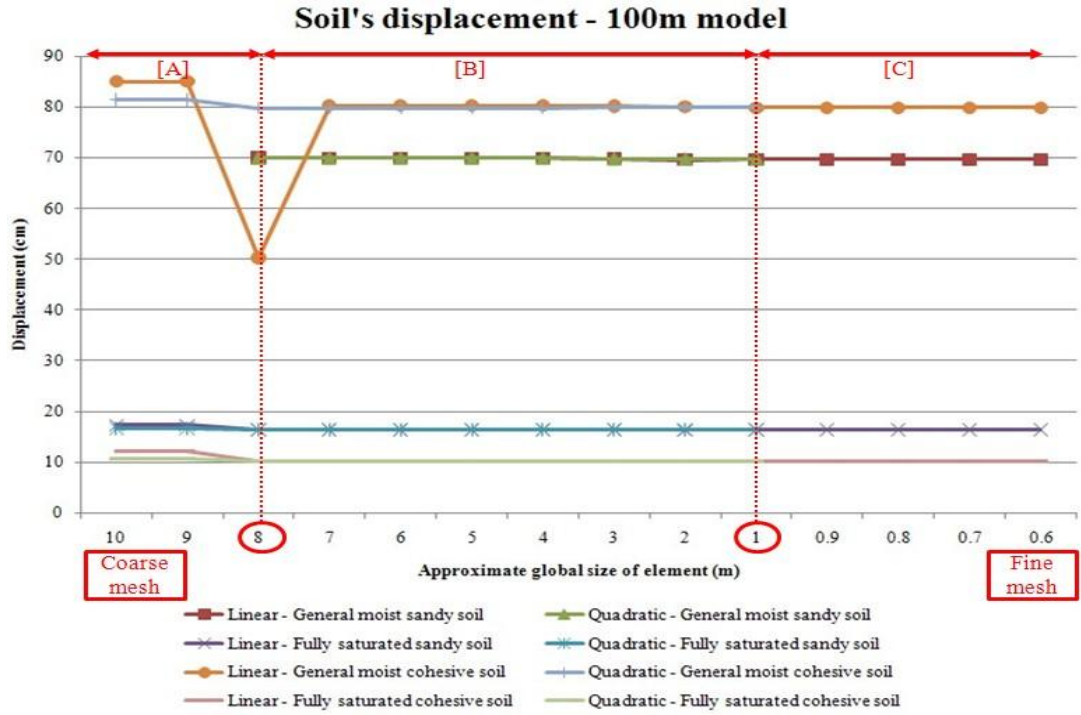
3.4.3. Results and discussion

The mesh adaptation provides the benefit of improving the accuracy of computed finite element analysis. Two mesh refinement methods were accomplished in order to assess the optimization of mesh; p-refinement which is the method by changing the element size and h-refinement which is the method by changing to higher order polynomial interpolations. However, choosing only one of the above two mesh refinement methods is not sufficient to expect accurate results of computed finite element analysis. Thus, the combination of h and p refinement method is requested because it is judged that benefit from above two mesh refinement methods can be offered for enhancing the quality of finite element analysis. This method is called 'hp-refinement'. The hp-refinement method is carried out by increasing the density of elements in the designed model and the polynomial order of elements. According to Georges & Shephard (1990), this hp-refinement is the most attainable method to achieve good quality of finite element analysis due to the reason that adapting each specific advantage causes the anticipated errors of results to converge nearly at zero. For these reasons, the hp-refinement method was adopted and this method expects to find the optimized mesh which should satisfy efficiency of computation and accuracy of results. The calculated results by ABAQUS are applied to Appendix C.

The effort in searching adaptive mesh involving h-refinement and p-refinement method was accomplished by examining maximum displacement and equivalent stress. The computed data by ABAQUS was classified into three different length models such as 15m, 50, 100m length model and was plotted as following Figures 3.8, 3.9 and 3.10. The graphs in Figure 3.8, 3.9 and 3.10 are attached again in Appendix D.

100 m model

Soil



100 m model

Pipeline

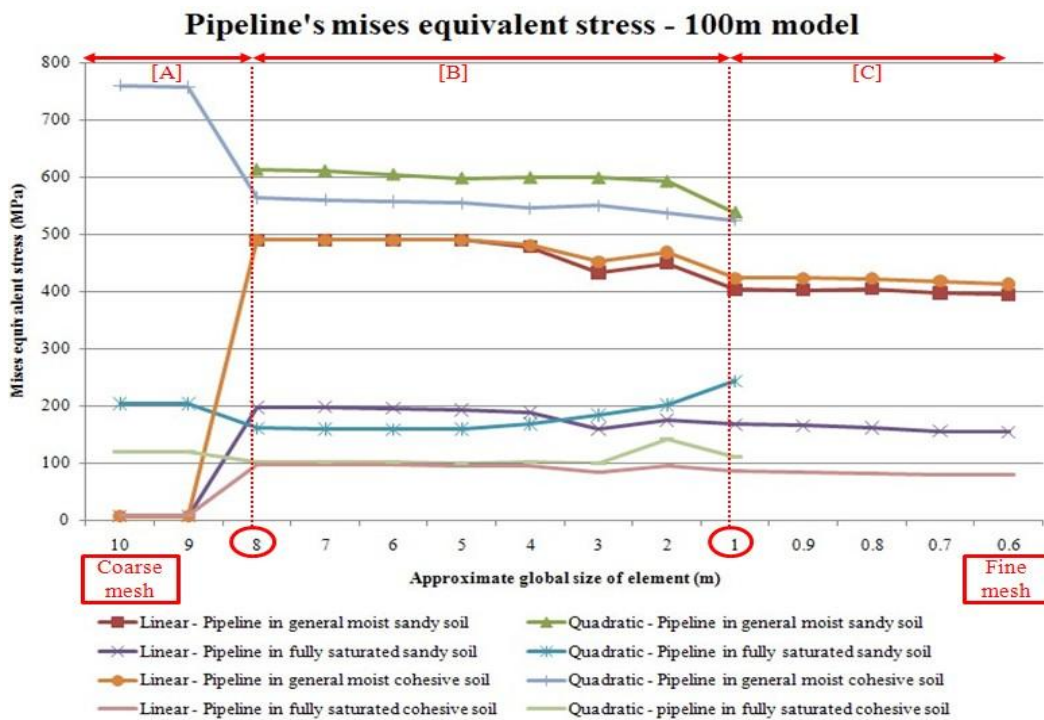
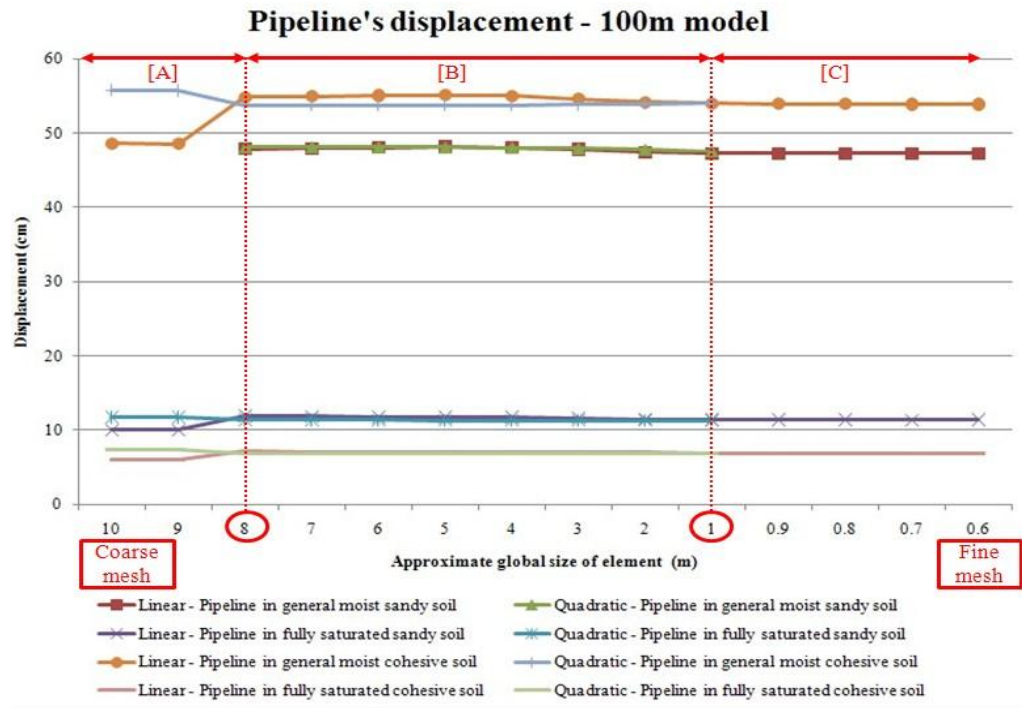
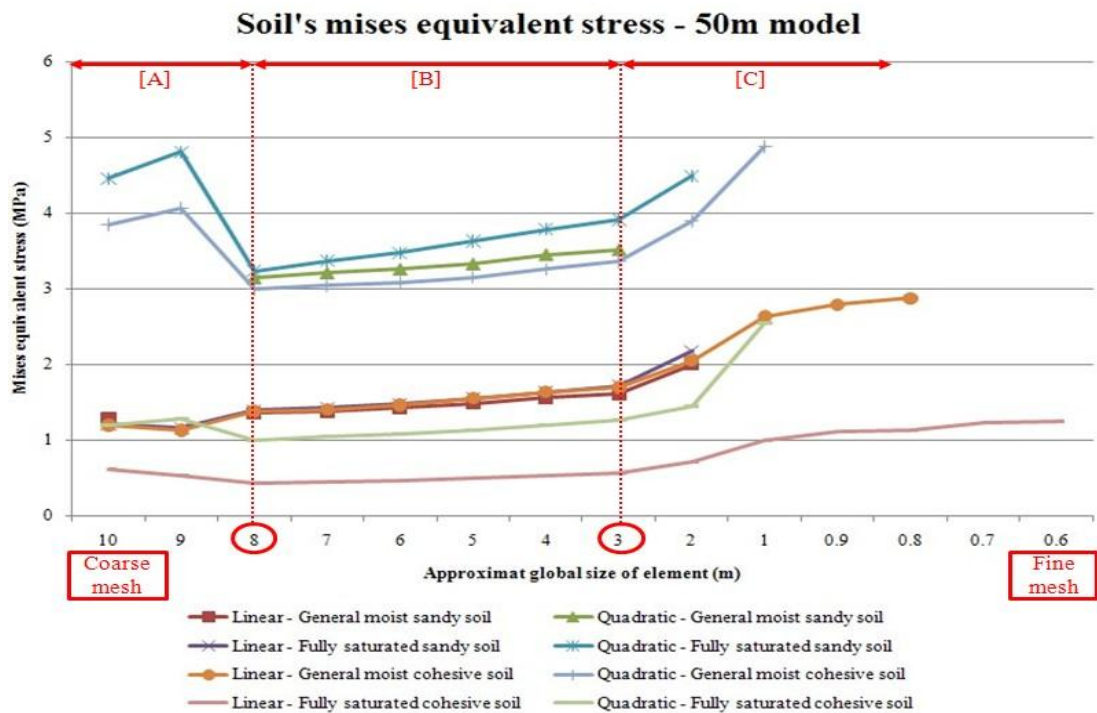
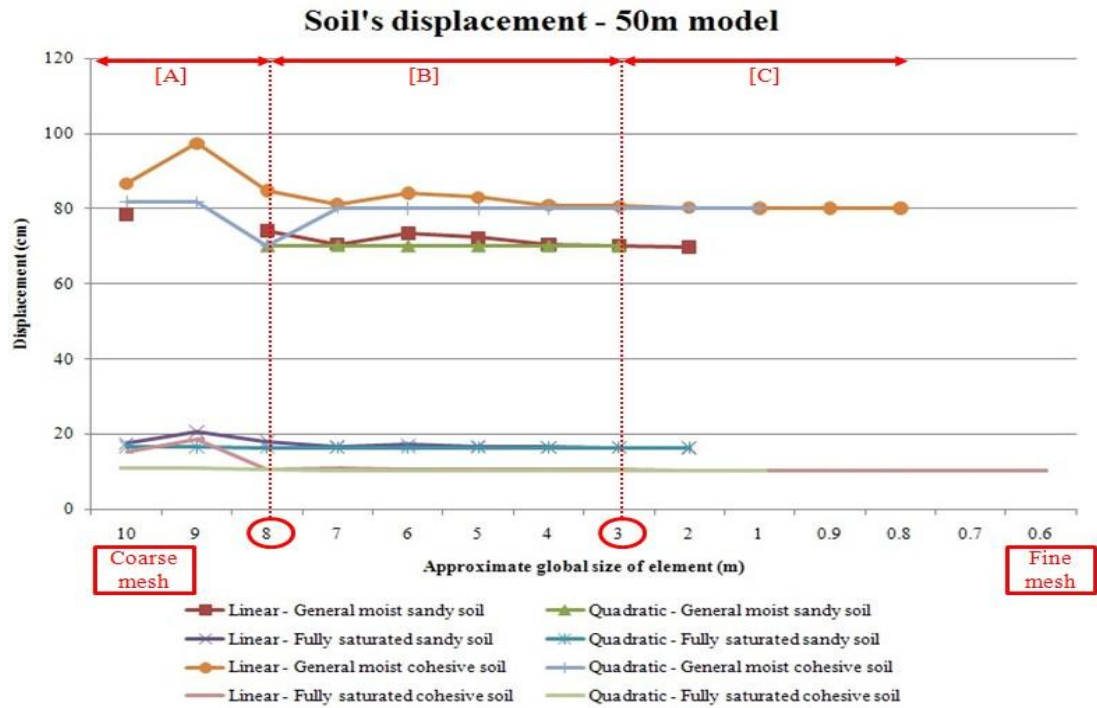


Figure 3.8 Computed 100m model results according to different type and number of element

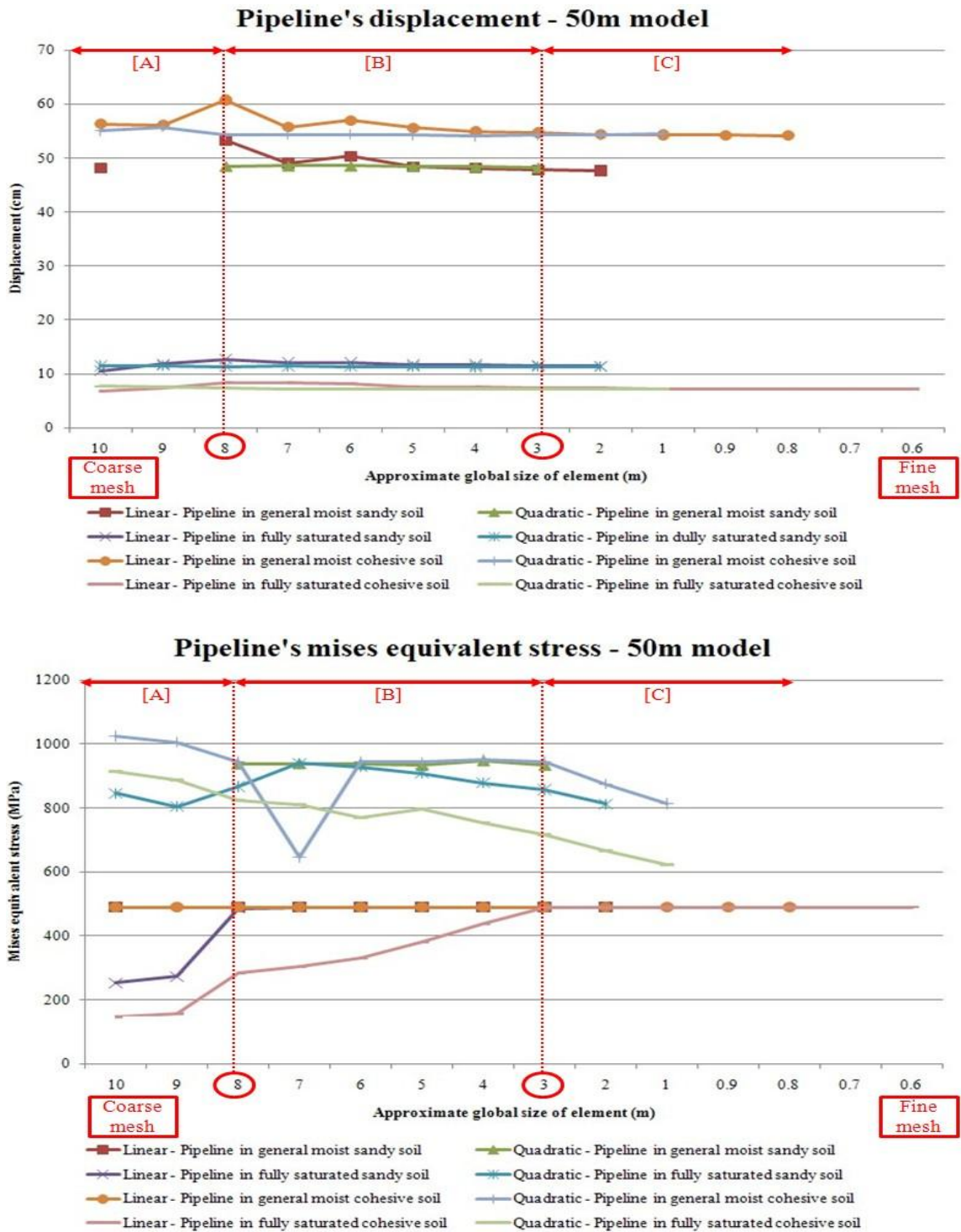
50 m model

Soil



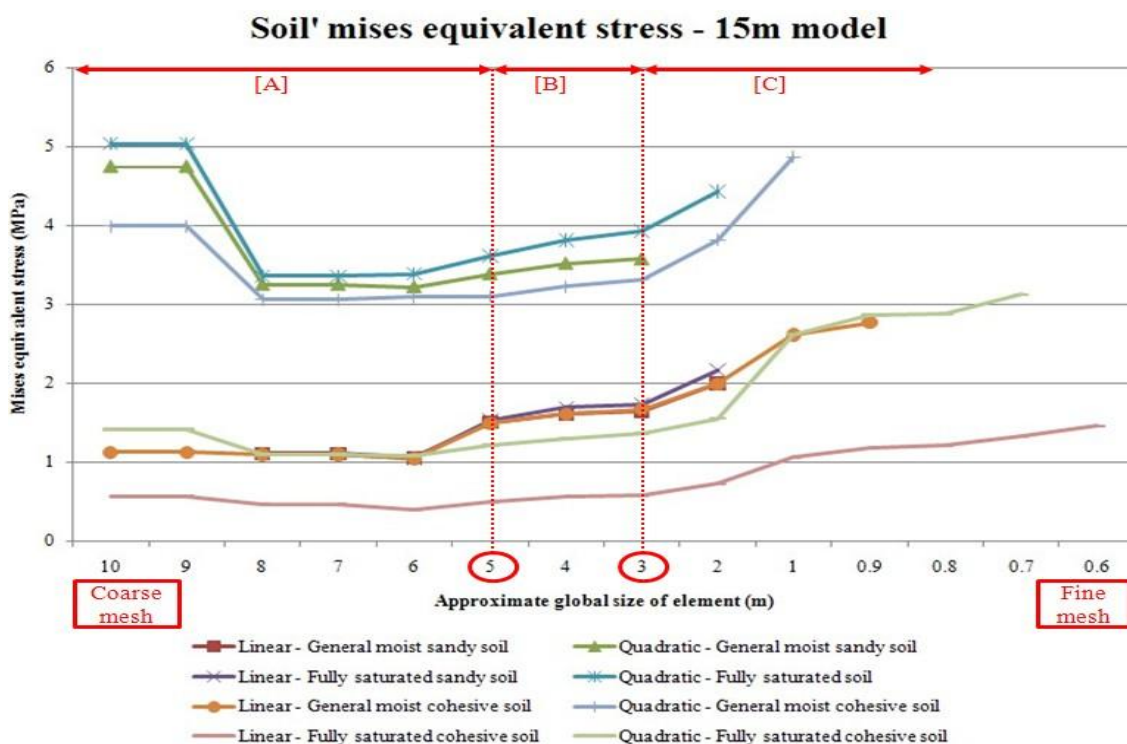
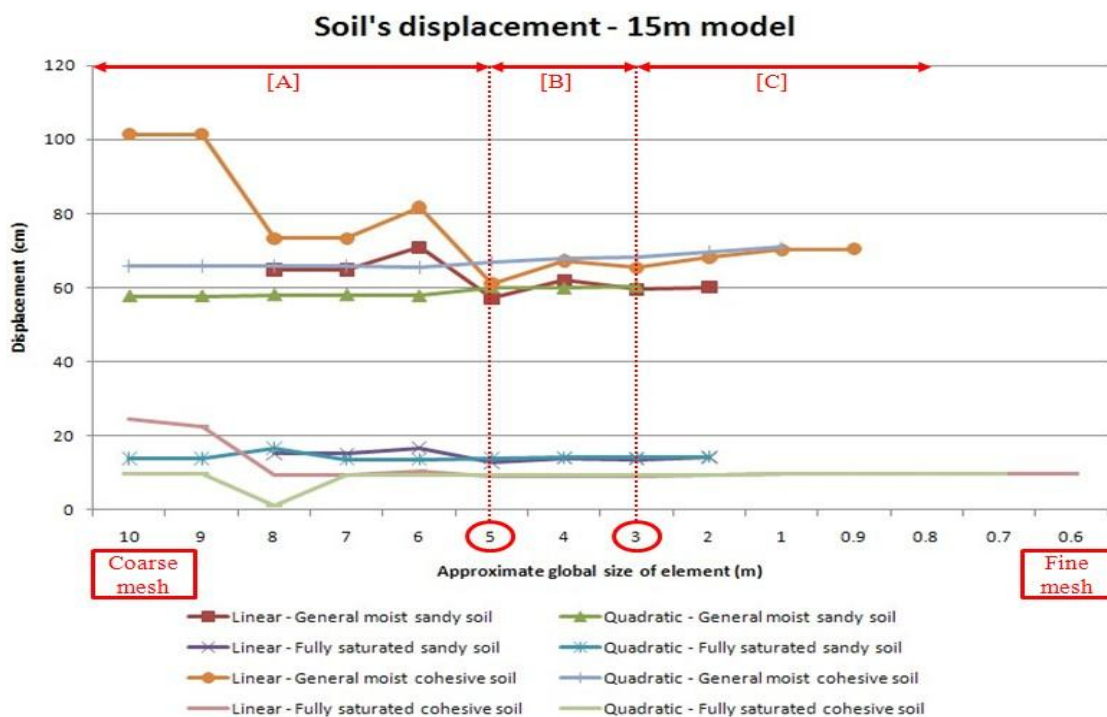
50 m model

Pipeline



15 m model

Soil



15 m model

Pipeline

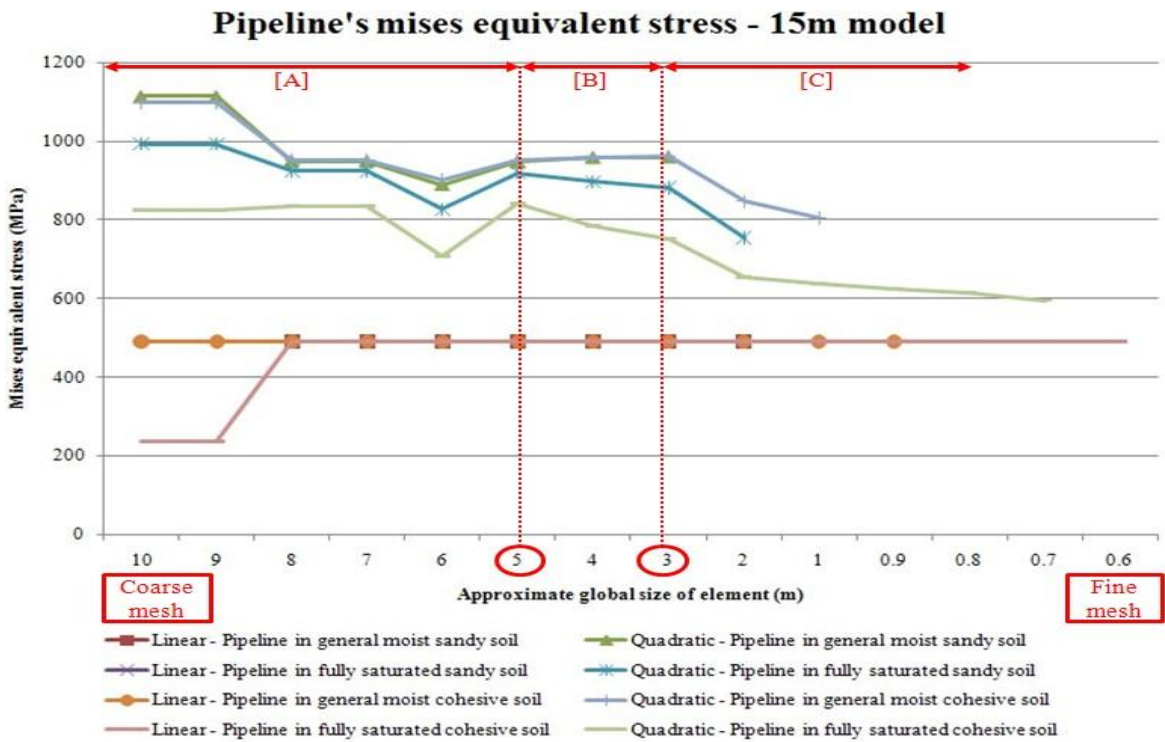
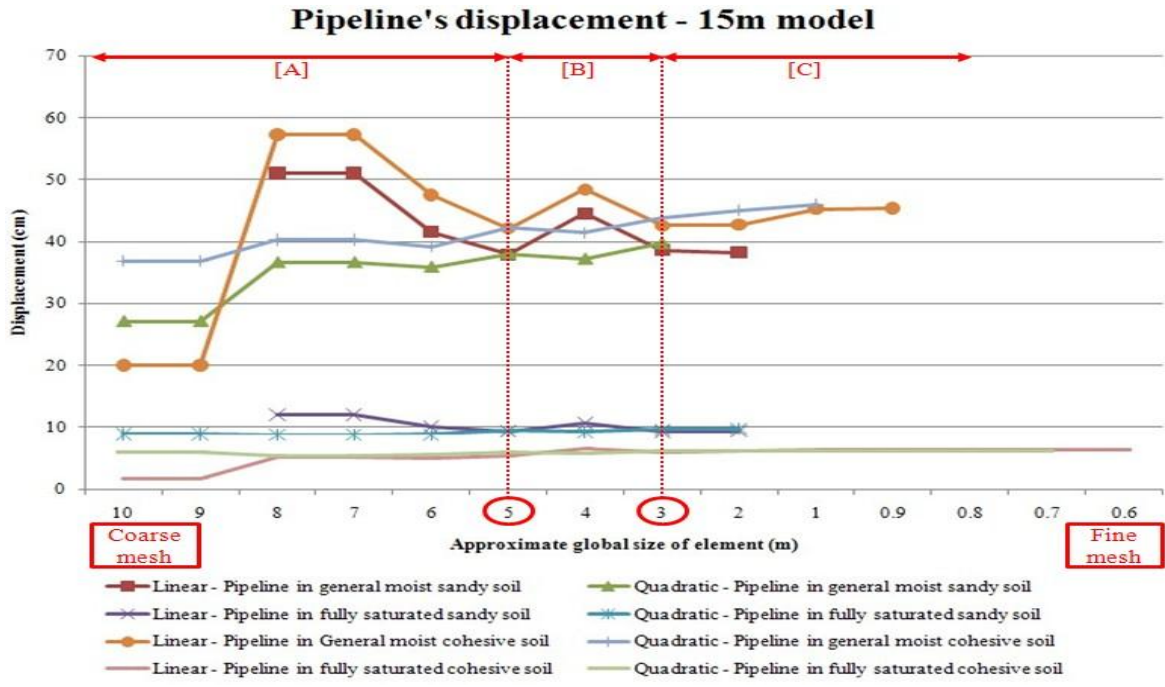


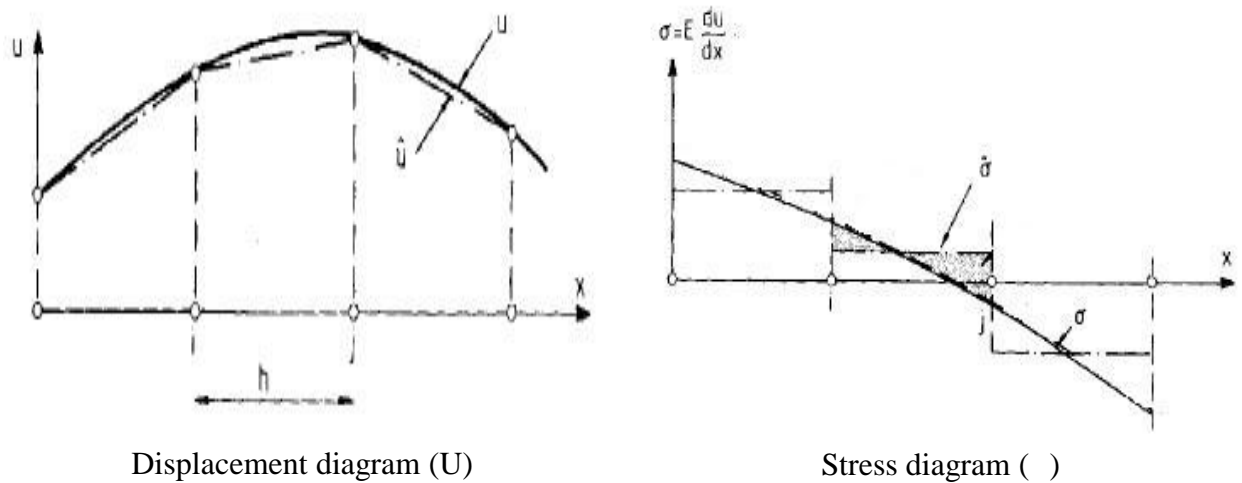
Figure 3. 10 Computed 15m model data according to different type and number of element

The approximated global sizes of element, which means the average length of meshed element, are located in x-axis and the calculated results regarding to maximum displacement and equivalent stress of each model are situated at y-axis. The x-axis reflected the h-refinement method because the size of meshed element is changed from coarse mesh to fine mesh when the approximated global size of element becomes small. On the contrary, eight plotted lines in each graph reflected p-refinement method considering four typical soil material properties and two calculation categories; linear and quadratic interpolation element lines. Three sections are demarcated in each graph; section A indicating magnificent calculated error, section B which signifies convergence to an accurate result and section C which purports that it is possible to get the most precise result because of fine mesh or to obtain result beyond accuracy because of the finest mesh. Even though an increment in the number of elements normally implies more precise results, there might be a certain number of elements beyond which the accuracy cannot be improved any more (Rao, 1999). Therefore, the results calculated by fine mesh including section C are not believable because it is possible to be overestimated by the finest mesh. Otherwise, if there is no change about the accuracy of results calculated by the finest mesh, it is better to accept adaptable mesh including section B due to the reason of efficiency because the finest mesh requires magnificent calculation time for analysis.

Since the true numerical solution for the problem is not given by the finite element method, ABAQUS, it is difficult to estimate the calculated error involved in results. However, it is possible to anticipate whether or not the given results from finite element method are accurate by checking the section of calculated results which keep regular when the considered element size becomes small, and which converge some point between linear and quadratic interpolation element. This section was included in section B above plotted Figures 3.8, 3.9 and 3.10.

In the range of section A which reflects coarse mesh, big variation of results was usually shown before approaching section B in Figures 3.8, 3.9 and 3.10 because an error is produced

due to big size of meshed elements. The cause of computed error by big size of meshed elements can be explained by Figure 3.11.



- U : Actual displacement
- : Calculated displacement by meshed element
- h : Approximate global size of meshed element
- i and j : A number of element's node
- : Actual stress
- : Calculated stress by meshed element

Figure 3.11 Involved error in meshed element expressed by 2D (Zienkiewicz and Zhu, 1987)

In the case of displacement, the displacement () calculated for the coarse mesh will be involved in some error due to rough meshed element as compared with actual displacement (U). However, if a fine mesh is used for solution, the computed displacement () will come close to actual displacement (U) because lots of meshed elements help calculated displacement () to be approached nearly at actual displacement (U). The case of stress will come to the same thing.

It is possible to clearly observe the constant computed maximum displacement results in section C after meeting convergent point between linear and quadratic interpolation element at the end of section B through the Figures 3.8, 3.9, 3.10. However, the calculated maximum equivalent stress results for fine meshed elements in section C usually deviated from the

maintained constant results. This is because the use of a large number of elements can cause the calculated results to be overestimated, even though the fine mesh generally improves the quality of computed results. Besides, some of the results by fine meshed elements, located in section C, were not calculated by ABAQUS. The reason is that the finite element analysis by fine meshed elements requested considerable computation time. For this reason, the finite element analysis, which needed considerable computation time such as one day or more, was aborted by own judgement for the reason of the efficiency because there was not much improvement of result's accuracy in accordance with fine meshes which needed magnificent calculation time. Therefore, it is possible to conclude that there is a limitation related to adaptable mesh size for accurate and efficient analysis and the optimum adaptable mesh size is located within section B for compromising both the accuracy and efficiency of analysis.

There is an obvious fact that the best calculated results yielded by higher order meshed model (Rao, 1999). Although a big variation between linear and quadratic interpolation element was observed in maximum equivalent stress results of each model without any convergence through Figures 3.8, 3.9 and 3.10, it is concluded that the results by quadratic interpolation element are more believable than those by linear interpolation element. Therefore, choosing the quadratic interpolation element is the most adaptable.

Finally, it is possible to recognize that the range among the three sections changed in accordance with the size of 3D-FE model; 100 m model's division criterion is eight to one, 50 m model's division criterion is eight to three and 15 m model's division criterion is five to three of approximate global element size. It is inevitable to regulate selection of adaptable mesh size because adaptable mesh size is changed in accordance with the size of 3D-FE models. Furthermore, the absolute consideration related to choosing the adaptable mesh size should be practiced within the range of section B and of near section C due to the reason of both accuracy of result and efficiency of calculation. Thus, 3m of approximate global size of element for 100m

and 4m of approximate global size of element for both 50m and 15m model are selected for accurate and efficient analysis.

3.4.4. Conclusion for adaptable mesh

Based on the above discussion, the following decisions were taken for choosing the adaptable mesh size of element and type of element.

- (a) Quadratic interpolation element will be used for the analysis of a buried pipeline.
- (b) For the consideration of the element size, 3 m of approximate global element size will be employed for the finite element analysis of 100m model and 4 m of approximate global element size will be applied for the finite element analysis of 50m and 15m model.
- (c) 100 m model will be mainly analysed because of convergence of calculated results for the two interpolation elements and constant maintained results after convergence of calculated results without relative big variation. But the 50 m model and 15 m model will be used for the comparison data with 100 m model.

3.5. Static and seismic analysis

The type of analysis can be divided into two according to the type of loads based on the chapter 1.3; static analysis and seismic analysis. The static analysis will be calculated by applying self-weights of soil and pipeline, eight wheel HB load and internal water pressure in the pipeline. The seismic analysis will be computed by adding seismic load, based on the El-Centro

Earthquake in 1940 at Imperial Valley with magnitude 7.1 on the Richter Scale or 0.3 g of ground acceleration, to the three static loads.

4. Numerical results and Discussion

Analysis is dealt with three sections for the purpose of understanding (i) static behaviour regarding to both soil and buried pipeline under static loads, (ii) the effect of boundary condition regarding to two pipeline ends and (iii) seismic pipeline's behaviour with soil under seismic load.

4.1. Static Analysis

Static analysis was executed by using the 100m model under static loads as outlined on section 1.3.1. The static loads involved were the self-weight of pipeline and soil, traffic load onto ground and internal pressure of pipeline. Among these loads, traffic load onto ground and internal pressure of pipeline were considered as maximum magnitude load in order to examine the critical statement of pipeline in the moment of the most danger. The self-weight of both pipeline and soil was considered by adding gravity, 9.81 N, to the created ABAQUS models. The traffic load onto ground was considered as a uniform contact pressure, 1100 kPa, on the top surface of soil model. The internal pressure of pipeline, 414 kPa, was applied to the internal surface of pipeline model.

This section does not mention all detailed calculated values of displacement and stress because both soil and pipeline behave similarly for different buried depths of pipeline. Therefore, typical behaviour of both soil and pipeline under static loads are only mentioned and calculated maximum displacement and stress are shown graphically in order to examine the behaviour of both soil and buried pipeline at different buried depths straightforwardly. The results involving all calculated data by ABAQUS for the various scenarios are attached in Appendix E.

4.1.1. Displacement of soil

The calculated soil subsidence was considered as a short-term serviceability issue because the present soil model created by ABAQUS considered only immediate settlement under static loads without considering drainage of water situated in the soil and the soil's consolidation depending on passage of time.

The pictures in Figure 4.1 are example results considering both hinge boundary condition at pipeline ends and 6m pipeline buried depth. The height of shown models in Figure 4.1 is not initial height, 15m, suggested in Figure 1.2 in section 1.2.4 because the pictures shown in Figure 4.1 are soil models deformed by considered static loads. The deformed meshes are also involved in all pictures shown in Figure 4.1. Figure 4.1-a is an isometric view involving subsiding soil with pipeline under static loads. Figure 4.1-b is a side view based on the Figure 4.1-a. Figure 4.1-c is a vertically sliced side view at the centreline of pipeline.

Even though the magnitude of 'soil settlement' in the vertical varied in accordance with different soil types such as sandy soil and cohesive soil, the soil settlement affected by static loads typically behaved vertically. All calculated scenarios considering each buried depth of pipeline and each soil type were shown by ABAQUS to yield results like those pictures in Figure 4.1 below. Whereas the red painted part of soil meant the part occurring maximum vertical soil settlement, the blue painted part of soil meant non-settlement area. This meant that static loads caused top soil's area to allow maximum settlement and caused the magnitude of soil's settlement to decrease gradually as the depth of soil becomes deeply. The inside deformed soil shape, shown in Figure 4.1-c, surrounding pipeline was affected by pipeline's deformation shape influencing static loads. Thus, this soil deformation tendency affected by pipeline deformation will be explained in 4.1.2 section, dealing displacement of buried pipeline.

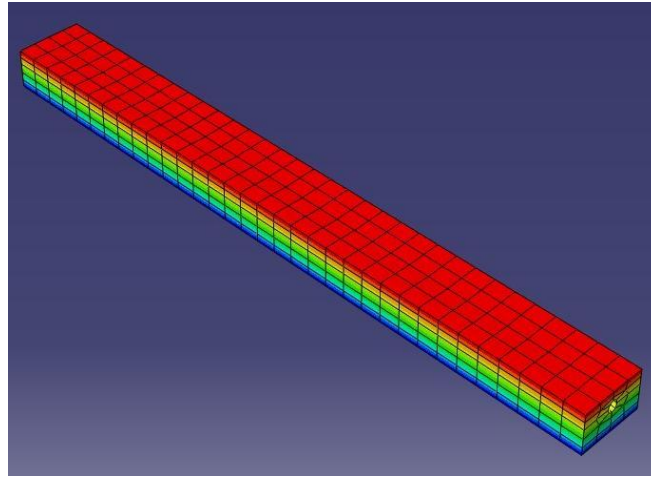


Figure 4.1-a

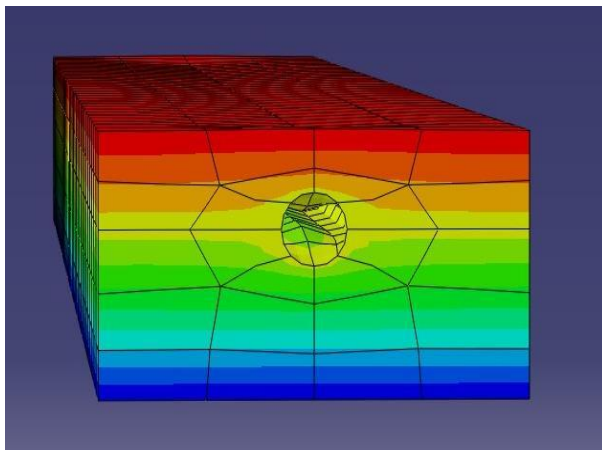


Figure 4.1-b

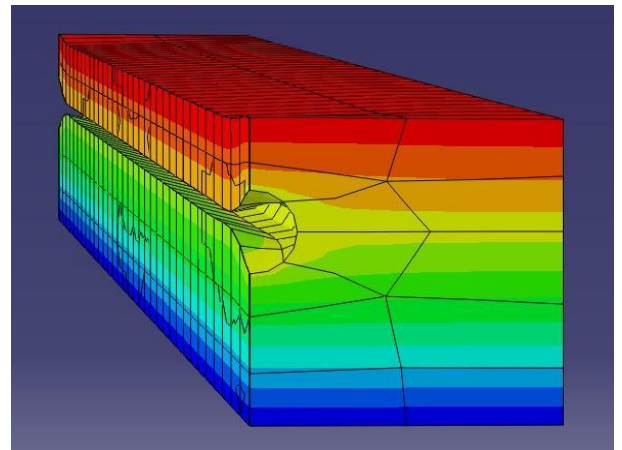
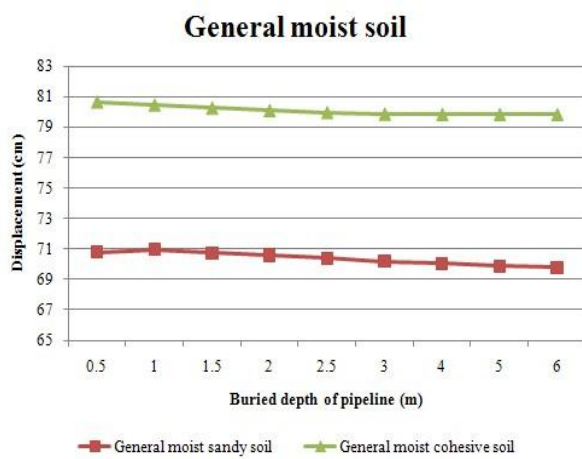
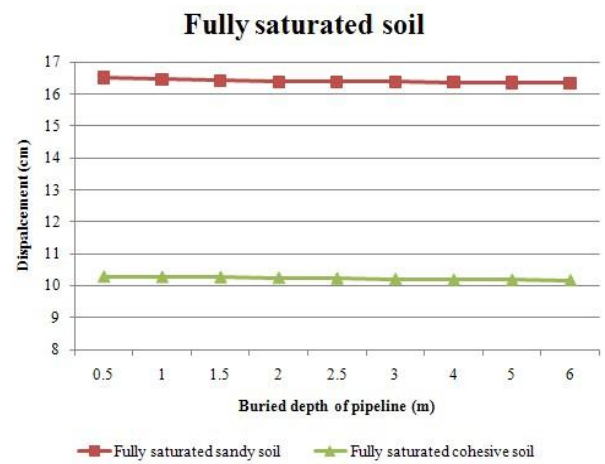


Figure 4.1-c

Figure 4. 1 Typical soil settlement under static loads



[Maximum settlement of general moist soil]



[Maximum settlement of fully saturated soil]

Figure 4. 2 Maximum settlement of soil under static loads

It is possible to examine the effect of both buried depth of pipeline and soil type on soil settlement as in Figure 4.2, which shows only maximum soil settlement located in top centreline of soil model in accordance with the buried depths of pipeline from 0.5m to 6.0m.

Firstly, different behaviour of soil was examined in accordance with a degree of saturation in soil; while the maximum settlement of general moist soil was calculated between 70cm and 80cm, the maximum settlement of fully saturated soil was computed between 10cm and 17cm. This meant that the immediate settlement of fully saturated soil is less than the immediate settlement of general moist soil when only considering short-term serviceability issue. Secondly, the different behaviour of soil was assessed in accordance with the type of soil; the maximum settlement of cohesive soil was lower than sandy soil when especially considering fully saturated soil. This meant that whereas the water in saturated sandy soil is allowed to move easily due to the effect of big grain of sandy soil and non-cohesion when adding static loads, it is impossible for the water in saturated cohesive soil to move easily because minute particles and cohesion of cohesive soil interrupt the movement of saturated water. Finally, there was little variation of soil settlement with the buried depth of pipeline whatever soil type was considered, although the shallow buried pipeline, which is between 0m and 1.5m, gave settlement of soil slightly bigger than that for a deeply buried pipeline, 1.5m to 6m. The variation of soil settlement is quite small a few millimetres. Thus, it is possible to assume that burial depth of pipeline hardly affects the settlement of the soil surface but the type of soil is more important factor influencing the soil settlement.

4.1.2. Displacement of buried pipeline

The pipeline was deformed like an oval shape along the whole length under the subsiding soil involved in short-term serviceability issue. Typical deformation of pipeline under static

loads is shown in Figure 4.3. Figure 4.3-a is an isometric view of pipeline and Figure 4.3-b is a side view of pipeline based on Figure 4.3-a. Figure 4.3-c is an inclined side view of pipeline. As following the results by ABAQUS, the maximum pipeline settlement with soil occurred at the crest of pipeline and is marked as red, the minimum pipeline settlement with soil occurred at the invert, which is marked as blue.

The calculated pipeline settlement did not mean own displacement of pipeline without considering movement with the soil settlement because the calculated results by ABAQUS demonstrated that the computed pipeline settlement meant relative settlement with soil movement. The computed results by ABAQUS presented different magnitude of settlements between at crest and invert of pipeline as a proof of that the calculated results were based on relative settlement of pipeline with soil movement. If the calculated results considered only own displacement of pipeline without considering the movement with soil settlement, the invert settlement of pipeline might be identical with the crest settlement of pipeline. This is because the same magnitude of displacement at both crest and invert of pipeline might be affected by static loads causing oval shape deformation of pipeline. Furthermore, the deformed shape of pipeline affected the inside deformed soil shape, shown in Figure 4.1-c, surrounding pipeline because buried pipeline deformed with soil simultaneously. It is possible for pipeline to examine strange deformation shape. While the shape of pipeline ends preserved the initial circle shape under static loads, the middle part was deformed like oval shape. This is because the boundary condition of pipeline ends influenced the behaviour of pipeline under static loads. When 100m models in ABAQUS were created, the boundary condition of pipeline ends was selected as hinge in order to delineate connected parts between two buildings. Thus, whereas there was no deformation at pipeline ends contrary to the oval shape deformation in the middle part of pipeline, the soil reaction acting on invert of pipeline caused by static load forces created oval shape deformation in the middle part of pipeline.

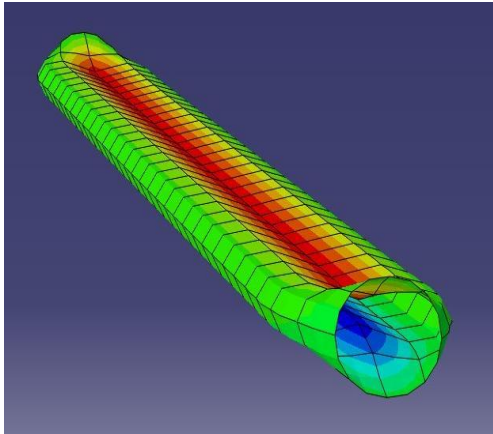


Figure 4.3-a

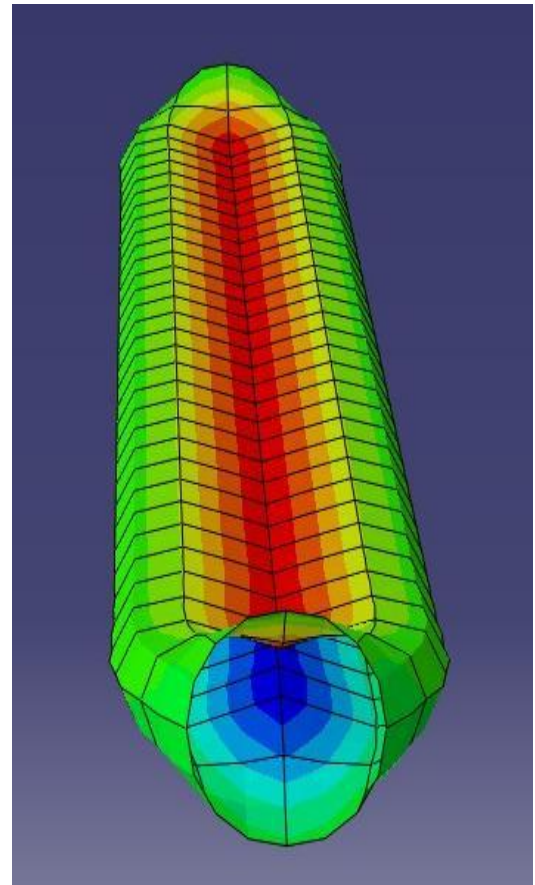


Figure 4.3-c

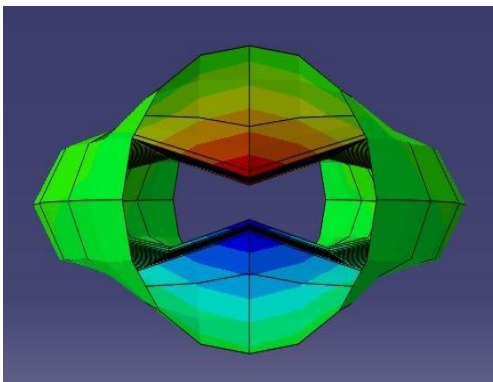


Figure 4.3-b

Figure 4.3 Typical pipeline settlement under static loads

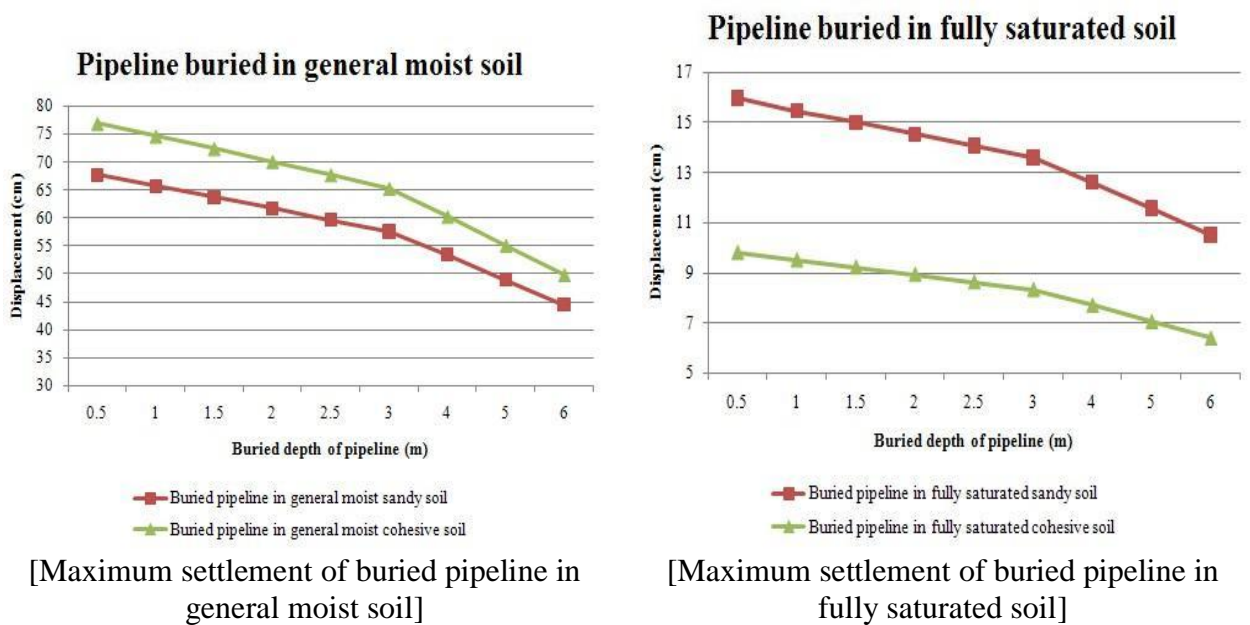


Figure 4.4 Maximum settlement of buried pipeline under static loads

Although the pipeline was moved with soil under static loads, it is possible to examine that the magnitude of pipeline settlement was less than the soil settlement by comparing Figure 4.2 meaning soil maximum settlement with Figure 4.4 meaning pipeline's maximum settlement.

Similar tendency of pipeline movement was assessed with soil behaviour in accordance with a degree of saturation in soil; whereas pipeline settlement in cohesive soil was higher than in sandy soil when considering pipeline settlement in general moist soil, pipeline settlement in cohesive soil was lower than in sandy soil when considering pipeline in fully saturated soil. This meant obviously that the pipeline moves with the soil surrounding pipeline because the pipeline buried in considered soil type moved and deformed with soil simultaneously. On the contrary, different tendency of pipeline settlement was examined to the tendency of soil settlement according to the extent of buried pipeline's depth. The pipeline settlement became decreased when buried depth of pipeline became deep. This meant that deep buried pipeline is more recommendable for the pipeline design than shallow buried pipeline under static loads in the point of view regarding only serviceability issue when constructing pipeline under the ground. Especially, if the pipeline is constructed under 6m in the general moist sandy ground, this buried pipeline is safer than the pipeline constructed under 0.5m in the general moist sandy ground because the pipeline buried under 6m is less moved down vertically as much as about 25cm than the pipeline buried under 0.5m. However, it is necessary to consider stress statement, economic problem and so on when considering buried depth of pipeline in actual construction field because it is impossible to conclude that the deepest buried pipeline is the safest and to construct all of pipeline deeply for the only purpose of safety.

4.1.3. Stress of soil

The Von Mises equivalent stress has been used for the plastic forming action related to pipeline and soil because the yield principle of Von Mises was adopted during creating models and assigning material properties involving pipeline and soil model. The term ‘stress’ for the used below analysis generally means the Mises equivalent stress.

Typical soil stress generated by static loads is shown in Figure 4.5. Figure 4.5-a is an isometric view of soil stress and Figure 4.5-b is an enlarged view for seeing the model’s end. Figure 4.5-c is a vertically sliced view at the centreline of pipeline, based on Figure 4.5-b. Figure 4.5-d is a side view based on Figure 4.5-b and Figure 4.5-e is a vertically sliced view at the centreline of pipeline, based on Figure 4.5-c.

The stress of soil occurred uniformly through whole length and depth of soil. However, the only soil’s part surrounding pipeline ends was different from whole parts of soil. Whereas the soil’s parts surrounding the both crest and invert of pipeline ends generated maximum stress of soil, the minimum stress of soil occurred at the soil’s parts surrounding spring-line of pipeline ends. This meant that the stress of soil is uniformly affected by static loads but the only connection parts of pipeline, which can be delineated as connected sections between two buildings, cause maximum stress and minimum stress.

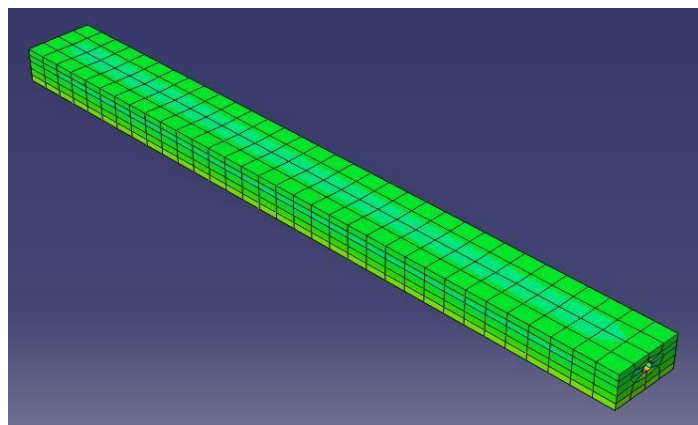


Figure 4.5-a

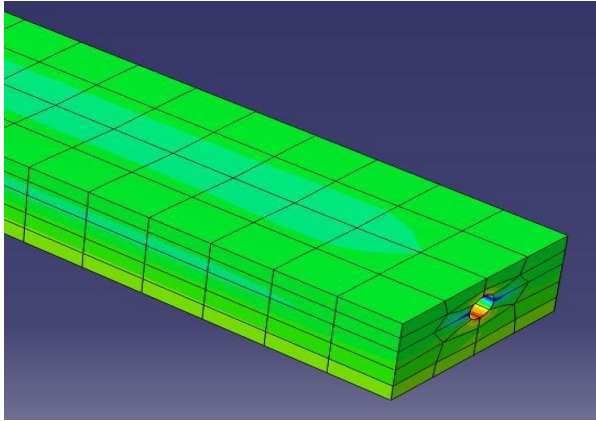


Figure 4.5-b

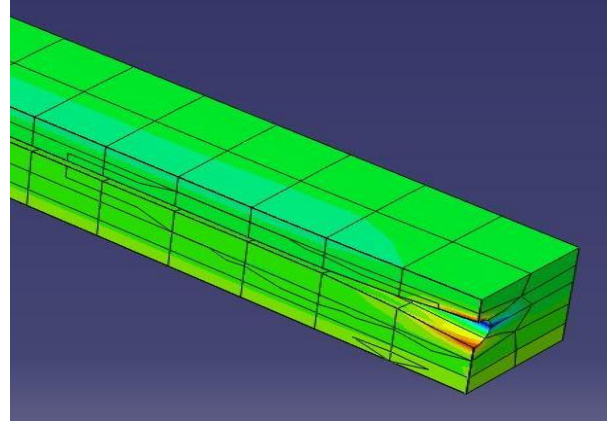


Figure 4.5-c

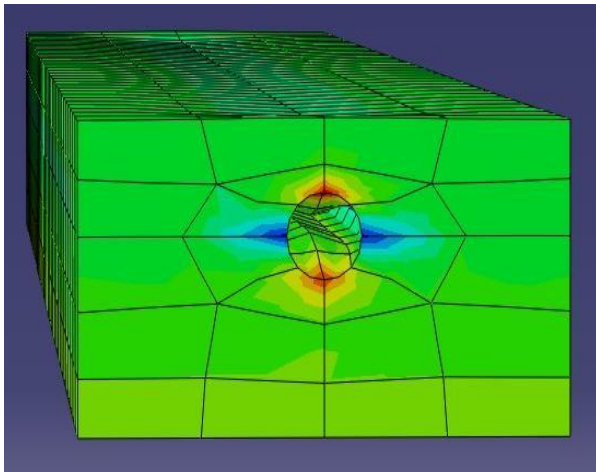


Figure 4.5-d

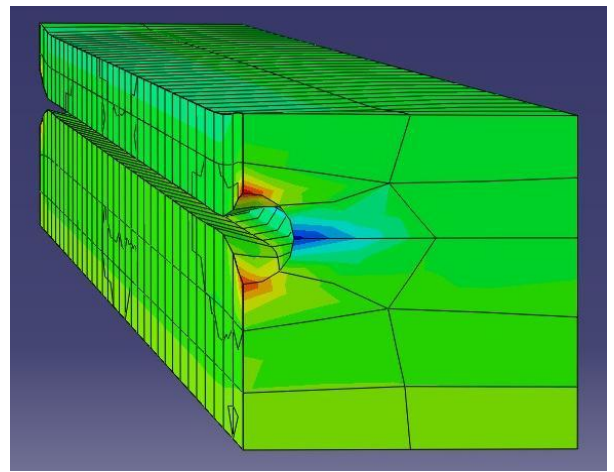


Figure 4.5-e

Figure 4.5 Typical soil's stress under static loads

The maximum stress in the soil at the both crest and invert at the pipeline ends was due to the effects of both compression force caused by static loads and binding force caused by restricted connection parts at two pipeline ends. Otherwise, the minimum stress of soil at spring line of pipeline ends was caused due to expansive force, which was created by deformation of pipeline as oval shape. The reason why the maximum and minimum stress of soil did not occur in the middle part of soil model is that the generated soil's stress under static loads was allowed to disperse uniformly through the whole length of pipeline without any restrictions.

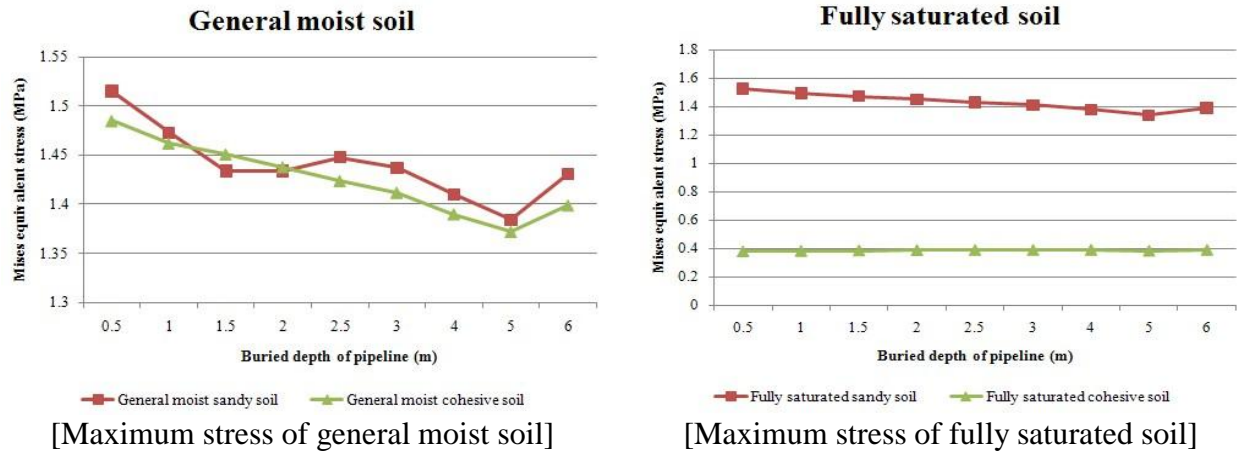


Figure 4.6 Maximum stress of soil under static loads

It is possible to examine that there was no much big variation of the soil's stress according to the buried depth of pipeline and soil's type as seen in Figure 4.6. However, it is possible to estimate that the soil stress involving shallowly buried pipeline is relatively less than the soil stress involving deeply buried pipeline.

Moreover, the stress of sandy soil was relatively bigger than the stress of cohesive soil with considering both general moist soil and fully saturated soil. This phenomenon confirmed that the soil stress was affected by the soil's material physical properties based on Table 1.2 located in section 1.2.4 because denser density and higher friction angle of sandy soil influenced higher sandy soil stress than cohesive soil stress.

4.1.4. Stress of buried pipeline

The static loads, which are operated vertically, caused the pipeline to be deformed as an oval shape and allowed the maximum stress of buried pipeline to occur at both the crest and invert of pipeline as in Figure 4.7. High stress of pipeline, which comes close to the maximum stress of pipeline, was also examined at the spring-line of pipeline. While the maximum stress was

generated by compression force caused by static loads acting vertically, the high stress which comes close to the maximum stress was caused by expansion force acting horizontally at spring-line of pipeline. Figure 4.7-a is an isometric view of pipeline. Figure 4.7-b is a side view of pipeline based on Figure 4.7-a and Figure 4.7-c is an inclined view of pipeline.

It is possible to estimate that the generated maximum stress of pipeline at both crest and invert of pipeline makes the flexible pipeline buckled at these positions of pipeline. This meant that if there is no enough strength of pipeline for resisting static loads, the buckling will be generated at both the crest and invert of pipeline and the flexible pipeline will be totally collapsed when the bucking reaches critical statement caused by maximum stress of pipeline.

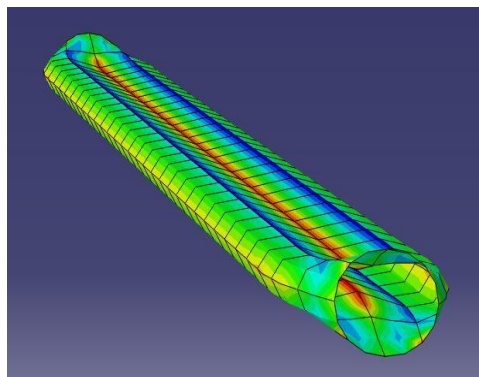


Figure 4.7-a

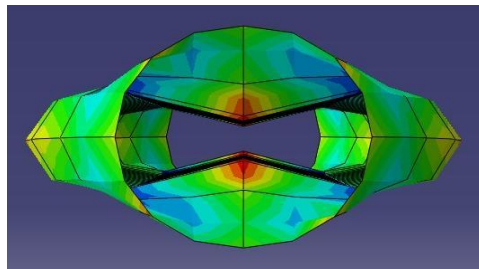


Figure 4.7-b

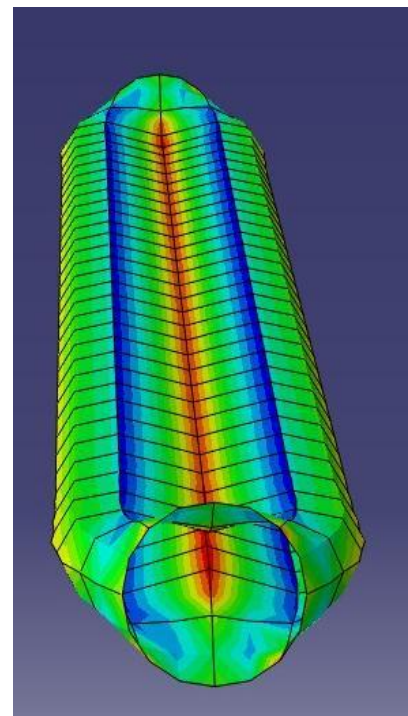


Figure 4.7-c

Figure 4.7 Typical pipeline's stress under static loads

Increase of pipeline's maximum stress was generally examined according as the buried depth of pipeline became deep without only the case of general moist cohesive soil as in Figure 4.8. This meant that deep burying of pipeline affects the pipeline to generate high stress and

makes the pipeline possible buckled more easily. Therefore, it is unreasonable to make a decision regarding that deeply buried pipeline is the safest for the only consideration of serviceability issue. On other words, it is adaptable to consider both settlement and stress of pipeline for making a decision regarding to the safest buried depth. Even though it is impossible to make a decision for choosing the exact safest buried depth, it is possible to make an assumption that the medium buried depth, such as between 1.5m and 3m of buried depth, is a safe range of buried pipeline's depth.

The higher stress of pipeline buried in sandy soil than the stress of pipeline buried in cohesive soil was examined with considering both general moist soil and fully saturated soil. This phenomenon occurred similarly to the tendency of soil stress and had the same reason. For example, when both general moist soil and fully saturated soil were considered simultaneously, higher sandy soil stress was generated by denser density and higher friction angle of sandy soil's physical material properties than of cohesive soil's physical material properties. As a basis on the same tendency of stress considering soil and pipeline, it is possible to conclude that the stress of both soil and pipeline was mainly influenced by soil type.

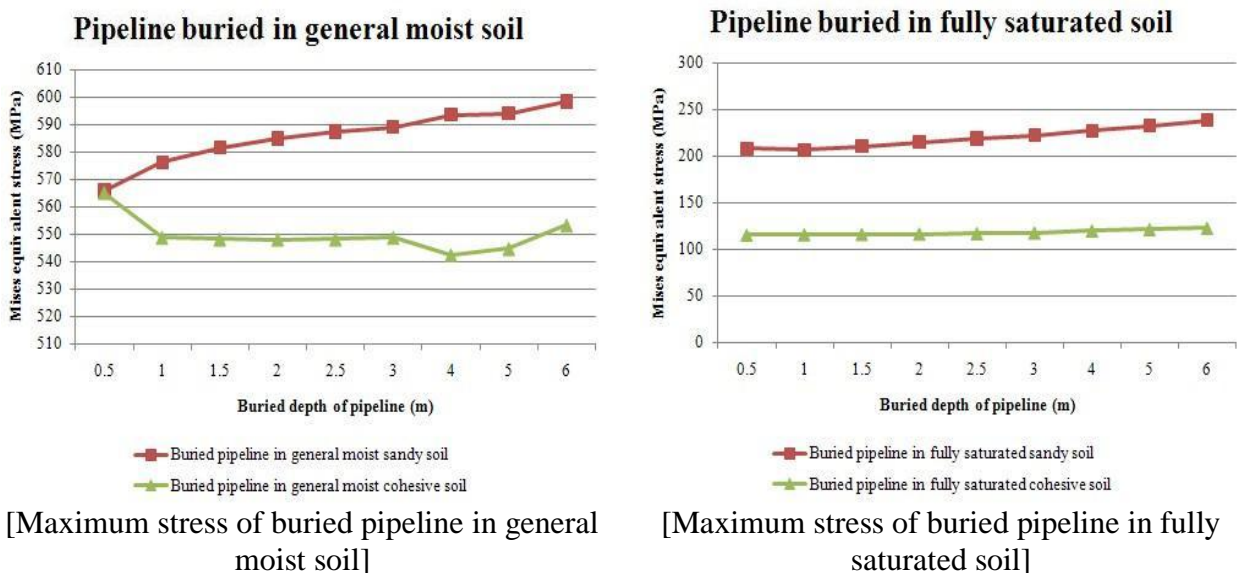


Figure 4. 8 Maximum stress of soil under static loads

4.2. Boundary condition effect of pipeline ends

Two boundary conditions were assumed in section 3.3.2 for examining the effect of boundary condition at pipeline ends; hinge and roller. On this assumption, two suppositions were involved in the two typical boundary conditions; whereas the hinge boundary condition represents that a pipeline between two buildings what are forced, the roller boundary condition represents an infinitely long pipeline. The different soil and pipeline behaviour will be examined in accordance with the two different boundary conditions.

It is necessary to use 50m model for examining the boundary condition effect. The longer, 100m model, might not show different behaviour clearly under static loads in accordance with two different boundary conditions of pipeline ends. The reason is that the consideration of longer model does not allow easy comparison in ABAQUS due to relatively long model length to the model width and height.

Moreover, the calculations by ABAQUS proved disadvantage of 100m model usage by presenting same calculated results without any difference between two boundary conditions at pipeline ends when analysis using 100m model was executed by ABAQUS in accordance with two different considerations about pipeline ends' boundary condition; hinge and roller. However, the static analysis by using 50m model provides different behaviour of both soil and pipeline clearly in accordance with the two different boundary conditions at pipeline ends due to the scale effect between 100m and 50m model. However, it is impossible to say that long pipeline, 100m model, appears less affected by boundary condition, even if long pipeline seem to be less affected than shot pipeline in 3D visualised results. All results in this section are based on 50m model. The detailed ABAQUS results regarding to displacement and stress of 50m model are attached in Appendix F.

4.2.1. Displacement of soil

Two different behaviours related to soil's settlement were examined by comparing results considering each boundary condition as in Figure 4.9. Figure 4.9-a and 4.9-b are isometric views of each model. Figure 4.9-c and 4.9-d are sliced views at the centreline of pipeline through the whole length. Figure 4.9-e and 4.9-f are end views of soil model based on each Figure 4.9-a and 4.9-b.

Whereas the soil settlement considering roller boundary condition of pipeline ends was uniform along the whole length of model, there was only uniform settlement in the middle part of soil model when considering hinge boundary condition of pipeline ends. In other words, in the case of hinge boundary condition, the soil model appeared with two bulged parts at the ends of soil model because hinge boundary condition at pipeline ends did not allow the pipeline to move uniformly with soil.

[Hinge]

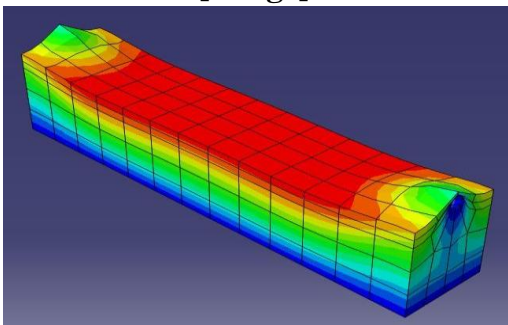


Figure 4.9-a

[Roller]

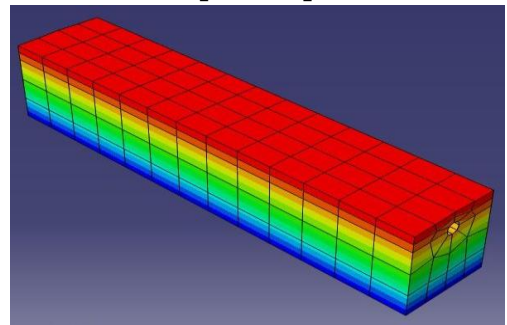


Figure 4.9-b

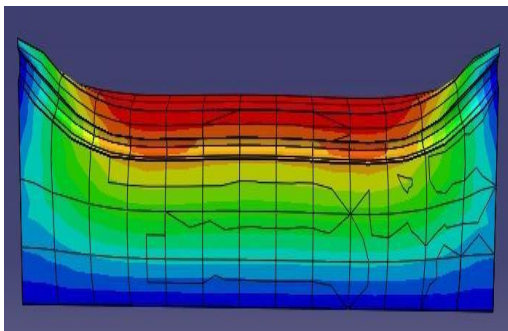


Figure 4.9-c

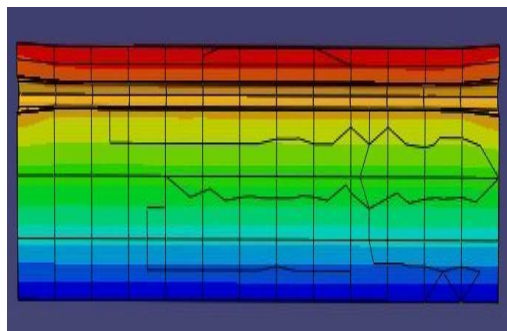


Figure 4.9-d

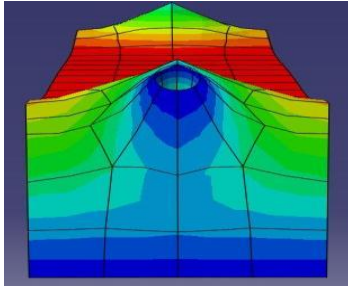


Figure 4.9-e

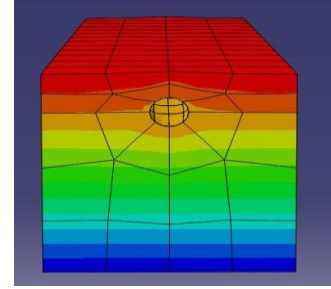


Figure 4.9-f

Figure 4.9 Different soil settlement according to two boundary conditions of pipeline ends

The magnitude of maximum soil settlement for the hinge boundary condition was almost identified to the roller boundary condition as in Figure 4.10. Moreover, it is possible to examine that the tendency of soil maximum settlement considering boundary condition of pipeline ends was also similar with the tendency of soil maximum settlement without considering boundary condition mentioned in section 4.1.1 in accordance with soil types. This meant that there is no big difference about the magnitude of soil settlement whether the boundary condition of pipeline ends is considered or not. However, only one difference discovered that the settlement shape of soil was different in accordance with the type of boundary condition of pipeline ends.

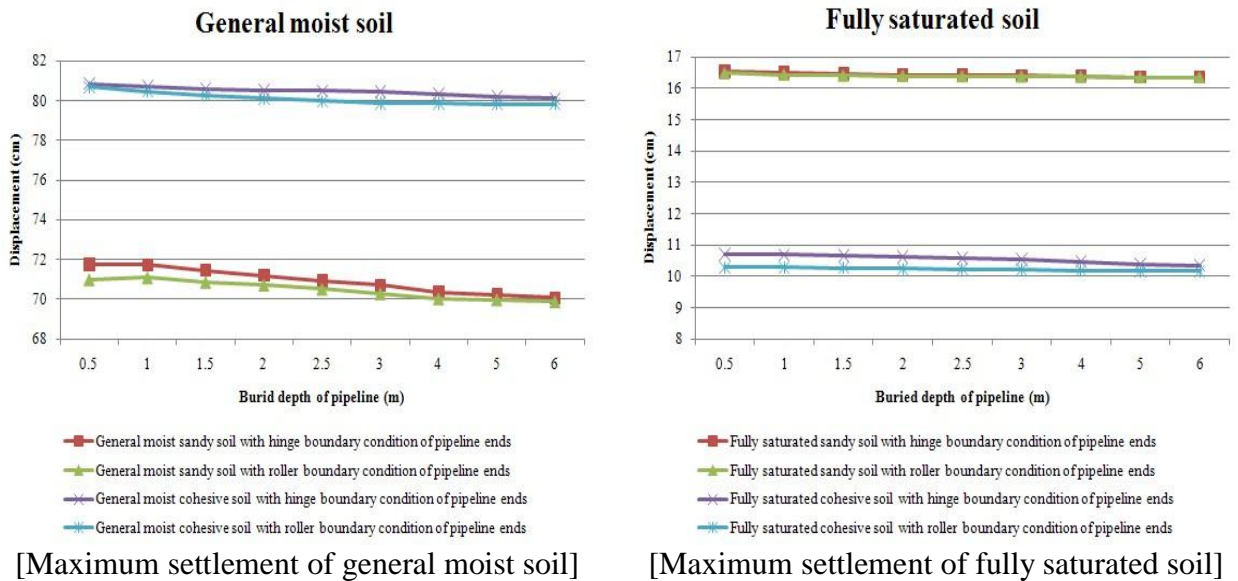


Figure 4.10 Maximum settlement of soil under static loads

4.2.2. Displacement of buried pipeline

Two different behaviours related to pipeline settlement were also examined by comparing results for each boundary condition of pipeline ends as shown in Figure 4.11. Figure 4.11-a and 4.11-b are isometric views of pipeline model. Figure 4.11-c and 4.11-d are side views of pipeline model.

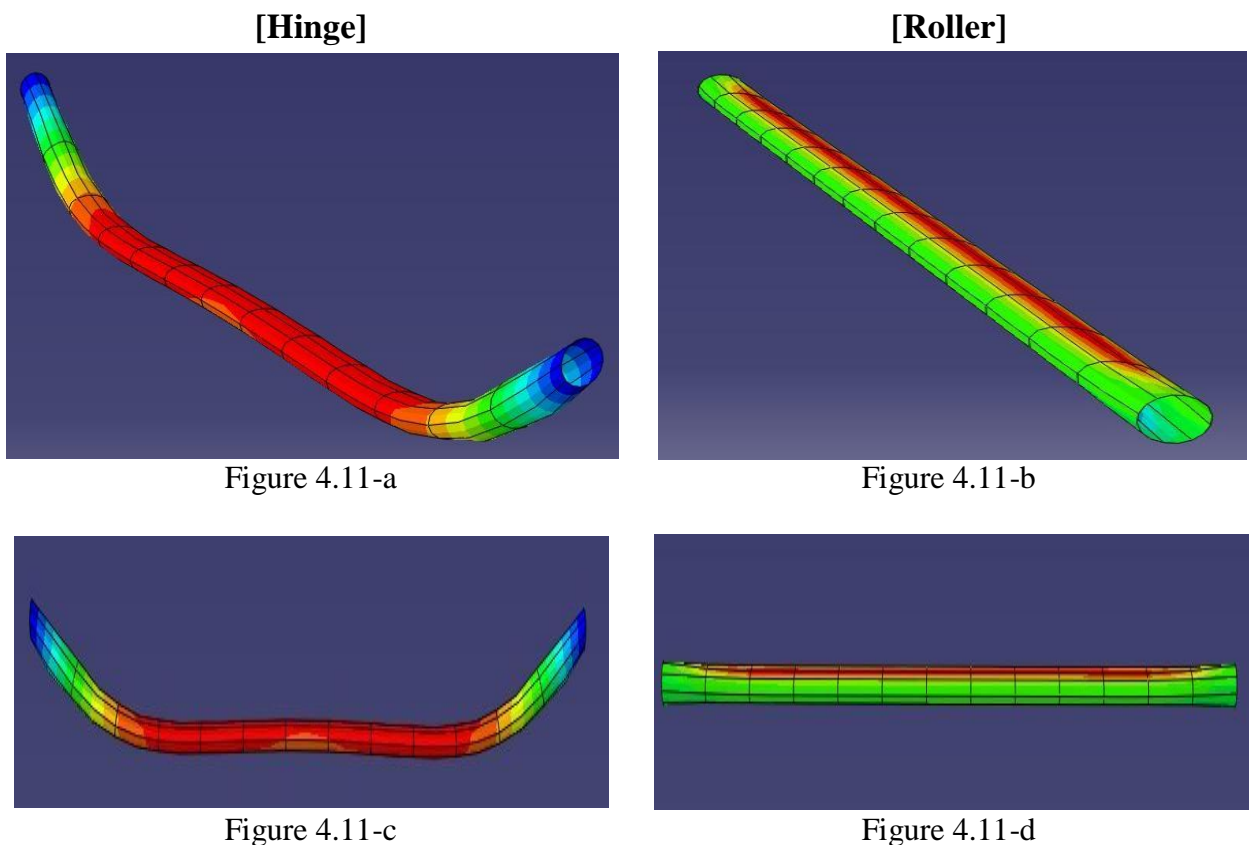


Figure 4. 11 Different pipeline settlement according to two boundary conditions of pipeline ends

Whereas the settlement of pipeline with roller boundary condition was formed almost uniformly through the whole length of pipeline model, a parabolic deformed shape of pipeline was observed when the hinge boundary condition was considered. The reason why the pipeline was deformed as a parabolic shape is that the restricted boundary condition did not allowed the pipe to move uniformly with soil movement. Thus, two restricted pipeline ends caused by hinge

boundary condition allowed the minimum displacement but permitted the maximum displacement at the middle pipeline area through the whole length. These different magnitudes of displacement according to two different locations in pipeline finally caused pipeline to be deformed as a deformed shape as a parabolic shape vertically.

It is possible to examine the pattern of pipeline maximum displacement considering the boundary condition through Figure 4.12. This was also similar to the tendency of pipeline maximum displacement mentioned in section 4.1.2 for the affected soil types. Furthermore, there was not much difference in maximum pipeline displacement when considering the boundary condition at the pipeline ends.

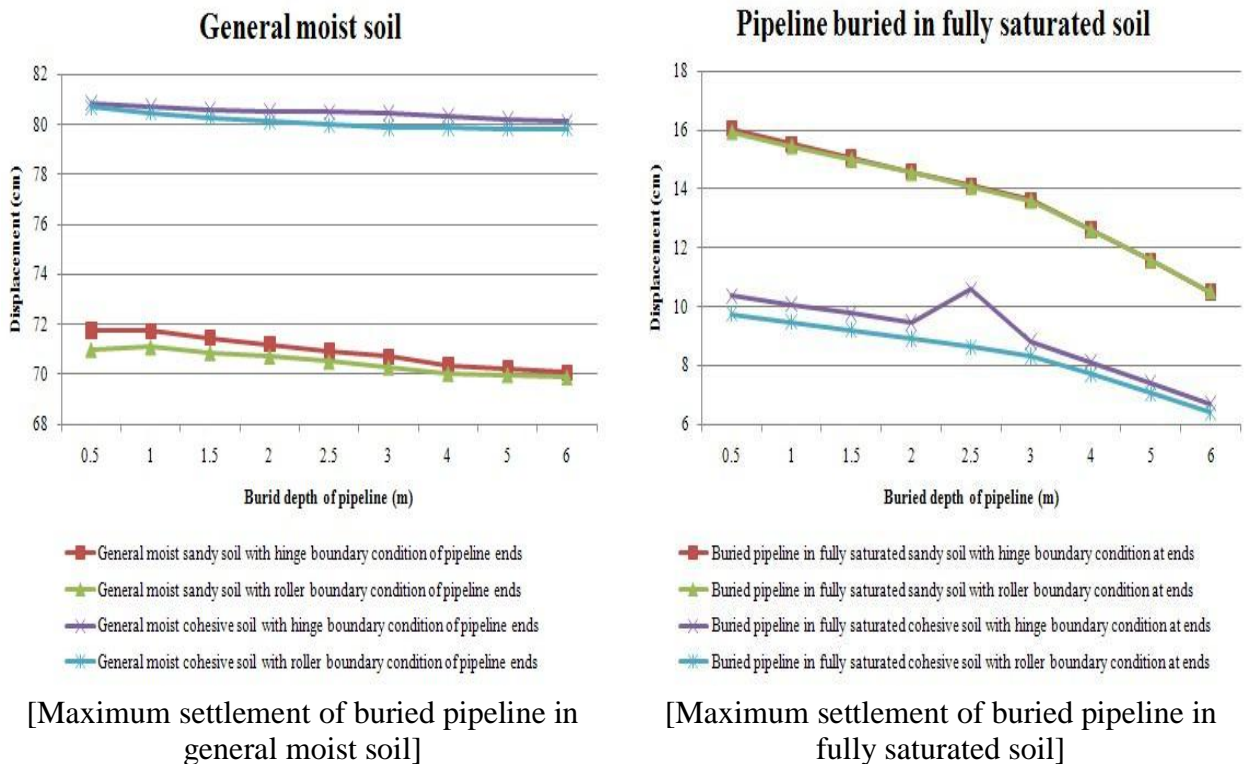


Figure 4. 12 Maximum settlement of buried pipeline under static loads

4.2.3. Stress of soil

While the maximum stress of soil occurred at the bulged part of soil surrounding pipeline ends due to binding force caused by hinge boundary condition when the hinge roller boundary condition was considered, the minimum stress of soil was observed through whole part of soil without only bulged parts of soil.

On the contrary, uniform stress condition was examined through whole model without only the soil parts surrounding spring-line of pipeline ends when the roller boundary condition was considered at pipeline ends. The reason why the minimum stress of soil was formed only at the part surrounding pipeline's spring-line is that compression force causing deformation of pipeline as an oval shape was generated by static loads acting vertically. On other words, the compression force caused both oval shape deformation of pipeline and compressed stress in soil. This compression force acting all soil parts was relatively bigger than the expansion force caused by pipeline horizontal deformation at spring-line of pipeline.

The generated soil stress can be shown as in Figure 4.13. Figure 4.13-a and 4.13-b are isometric views of each model. Figure 4.13-c and 4.13-d are sliced views at the centreline of pipeline through the whole length. Figure 4.13-e and 4.13-f are side views of soil model based on each Figure 4.13-a and 4.13-b.

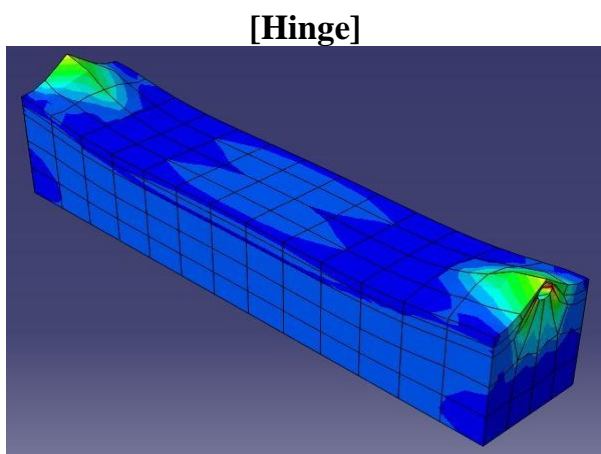


Figure 4.13-a

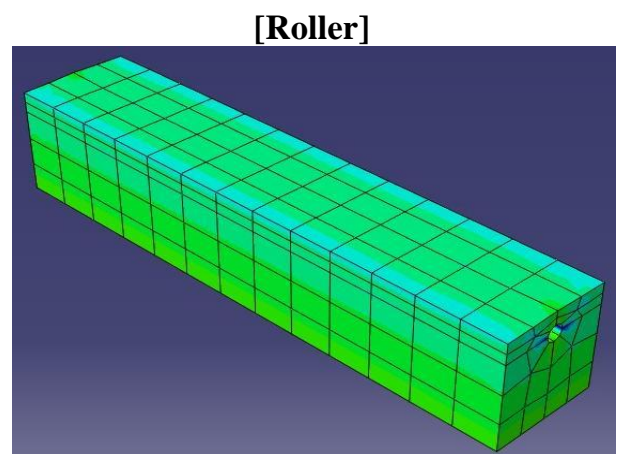


Figure 4.13-b

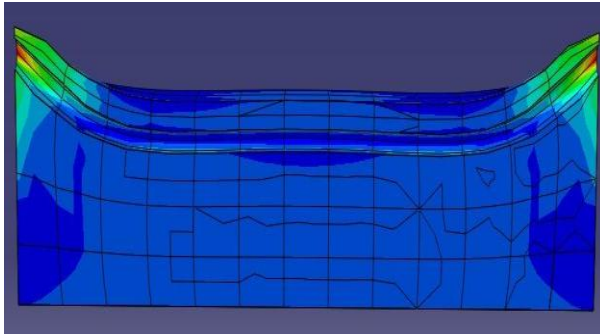


Figure 4.13-c

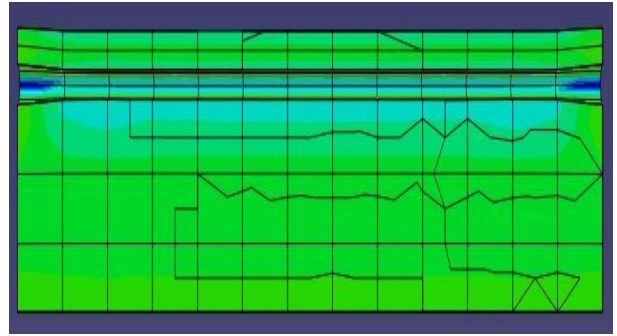


Figure 4.13-d

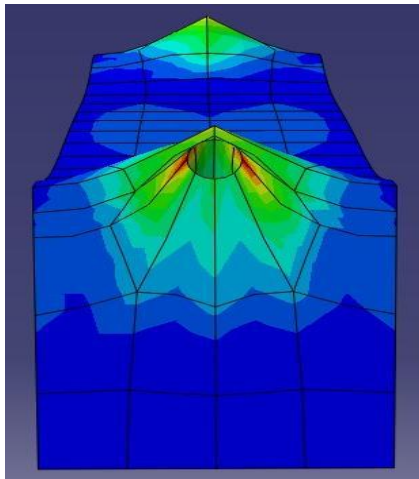


Figure 4.13-e

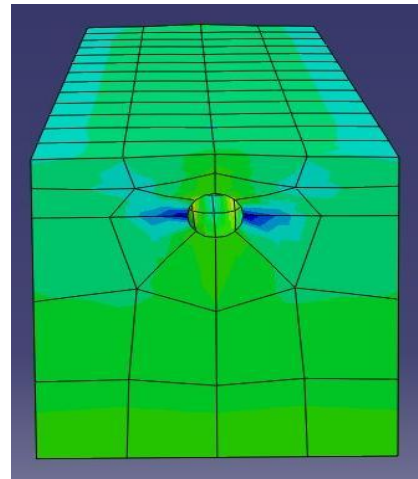


Figure 4.13-f

Figure 4. 13 Different soil's stress according to two boundary conditions of pipeline ends

Bigger maximum sandy soil stress was examined than maximum cohesive soil stress in accordance with the consideration of each boundary condition at the pipeline ends as in Figure 4.14. And bigger maximum soil stress considering hinge boundary condition at pipeline ends was assessed than maximum soil stress considering roller boundary condition at pipeline ends. This meant that cohesive soil stress was less affected by static loads than sandy soil stress and roller boundary condition was less influenced by static loads than hinge boundary condition.

Furthermore, when the buried depth of pipeline approached 1.5m, the maximum soil stress involving all of soil types and boundary condition decreased. This meant that the soil stress caused by static loads was less affected when the pipeline was buried at 1.5m under the ground.

If small variation of the pipeline stresses was examined in accordance with buried depths of pipeline, it is possible to say that 1.5m buried depth of pipeline is the best depth because the relatively smallest maximum soil stress was examined at this buried depth of pipeline and there was not much big variation of pipeline stress. It will possible to examine whether this assumption is correct or not after checking pipeline stress.

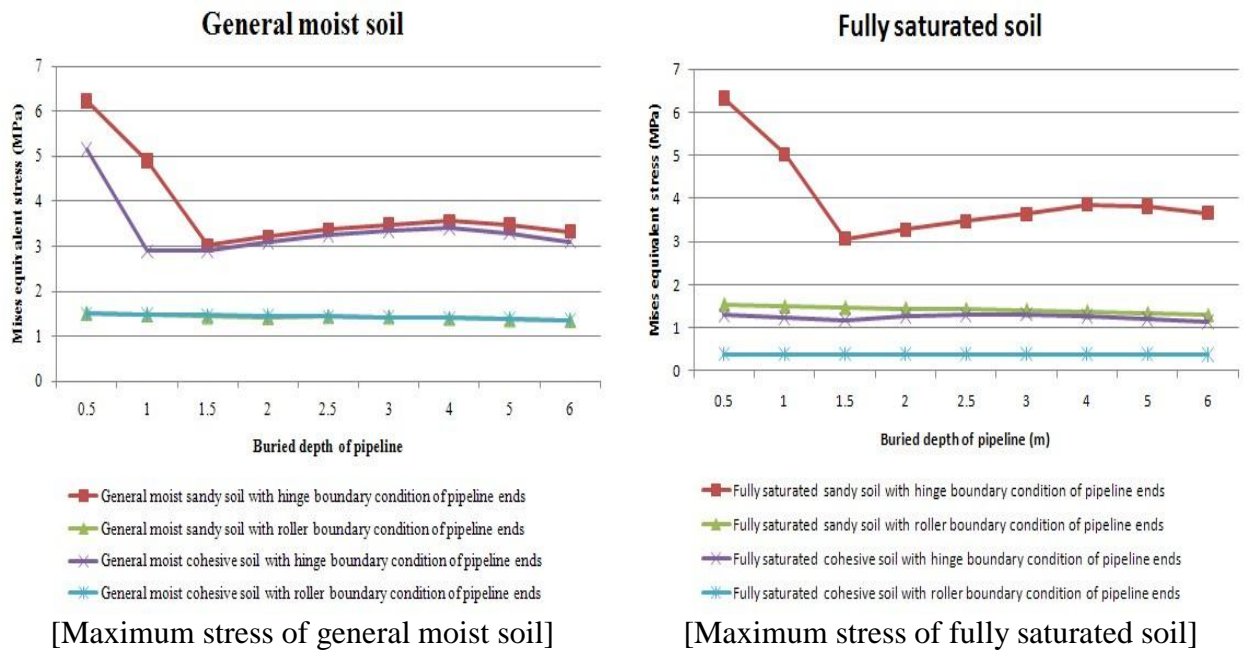


Figure 4. 14 Maximum stress of soil under static loads

4.2.4. Stress of buried pipeline

The maximum stress of pipeline was developed at the pipeline ends when considering hinge boundary condition because of binding force caused by hinge boundary condition. However, the maximum stress of pipeline was created at the spring-line of pipeline when considering roller boundary condition at pipeline ends due to pipeline's deformation as an oval shape. As basis on these different positions generating maximum pipeline stress according to boundary conditions at pipeline ends, two different suggestions for the pipeline design can be provided with examining

the different position of pipeline stress based on Figure 4.15 according to the consideration of pipeline's boundary condition at the ends. Figure 4.15-a and 4.15-b are isometric view of pipeline model and figure 4.15-c and 4.15-d are side view of pipeline along the length, based on Figure 4.15-a and 4.15-b.

The pipeline ends have to be critically designed when the pipeline is built between two buildings because the maximum pipeline stress was generated at pipeline ends when considering hinge boundary condition at pipeline ends. On the other hands, the pipeline should be designed for improving the strength at spring line of pipeline when quite long distance pipeline is constructed because the maximum pipeline stress was generated at spring-line of pipeline along the length when considering roller boundary condition at pipeline ends.

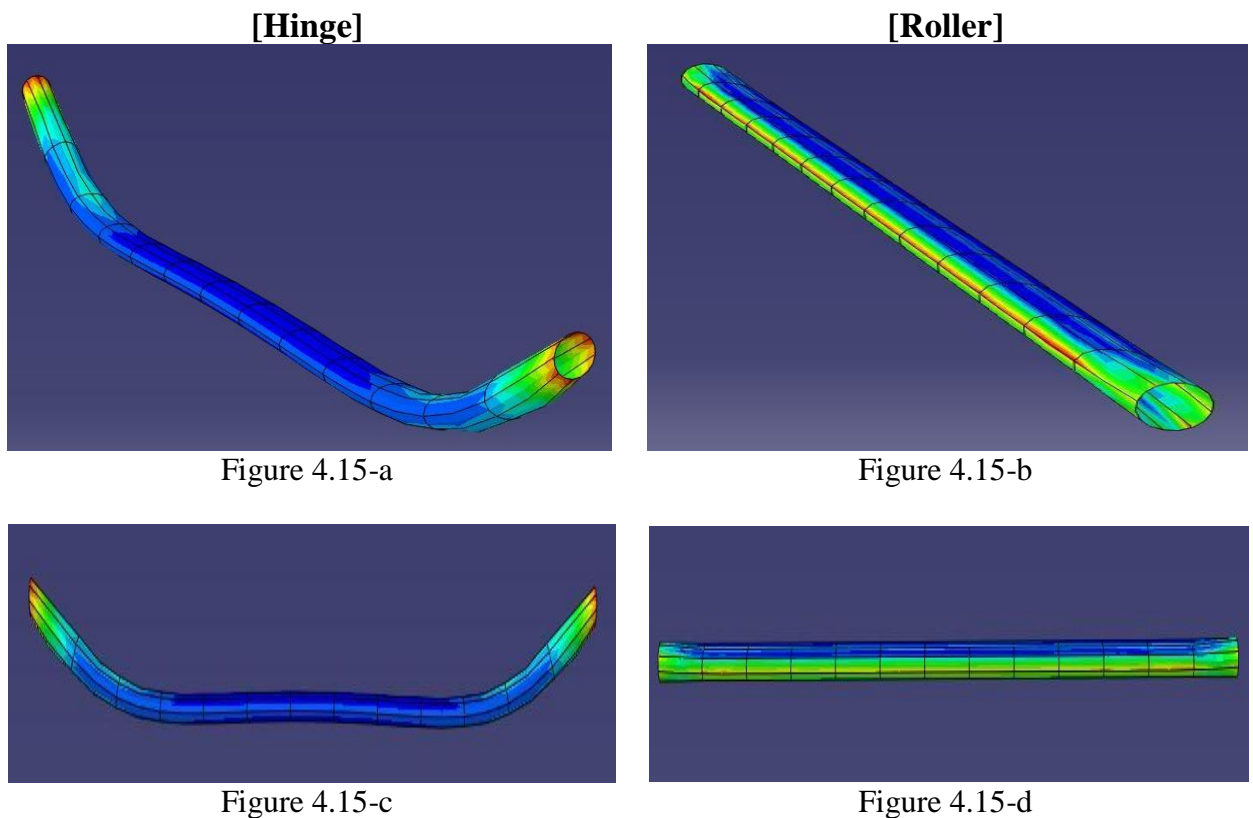


Figure 4. 15 different pipeline's stress according to two boundary conditions of pipeline ends

Moreover, when the pipeline is built in fully saturated sandy soil, the boundary condition at pipeline ends should be cautious for construction because big variation of stress was discovered between two boundary conditions, which are roller and hinge, in fully saturated sandy soil as in Figure 4.16.

Bigger maximum pipeline stresses considering hinge boundary condition at pipeline ends were assessed than maximum pipeline stress considering roller boundary condition at pipeline ends. This tendency of pipeline stress was also examined with the case of soil stress. Thus, it is possible to conclude that roller boundary condition at pipeline ends less influences the stress of both soil and pipeline than the hinge boundary condition at pipeline ends.

Not much big variation of the maximum pipeline stresses was examined in accordance with buried depths of pipeline. Thus, it is possible to conclude that 1.5m buried depth of pipeline is the safest buried depth of pipeline as basis on the previous assumption mentioned in section 4.2.3.

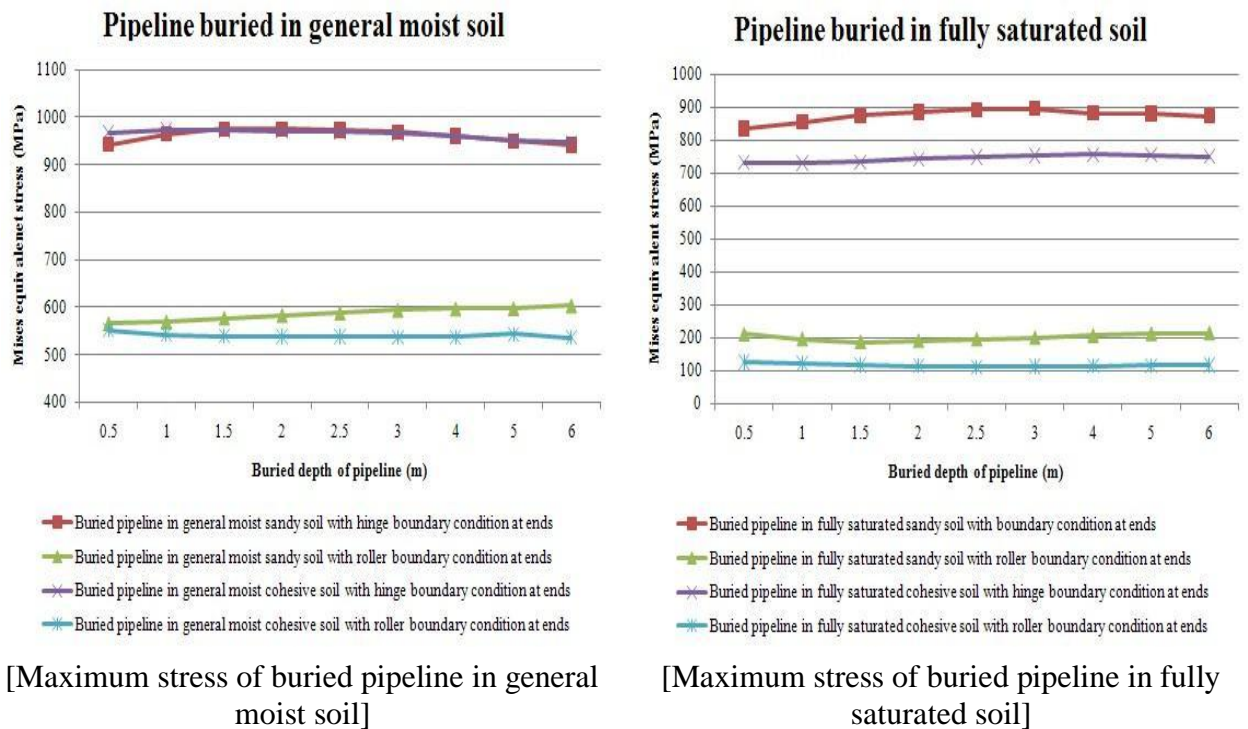


Figure 4. 16 Maximum stress of buried pipeline under static loads

4.3. Seismic analysis

Seismic analysis was executed by using the 100m model under seismic load described as El-Centro Earthquake as outlined on section 1.3.2 and Appendix A. The El-Centro Earthquake has about 0.3g of vertical ground acceleration with 7.1 magnitude on the Richter Scale and 31.18sec duration time history. In this section, seismic pipeline displacement and stress affected by a quasi-state 0.31882g of downward vertical ground acceleration at 2.02sec are analysed in order to examine critical statement of pipeline behaviour in the moment of the most danger because peak ground acceleration of seismic load causes the most considerable movement of the pipeline interacting with the soil.

The observed path for seismic analysis is the crown-line along the whole length of pipeline model interacting with soil model as in Figure 4.17. Figure 4.17-a is an isometric view sliced at the centreline of pipeline along the whole length. Figure 4.17-b is a side view based on Figure 4.17-a. Three divided parts in targeted path based on Figure 4.17-b are analysed in order to evaluate each different pipeline action according to three different locations of pipeline affected by seismic load; left part of targeted path which is from left ends of pipeline crest to 20m inside targeted path; right part of targeted path which is from right ends of pipeline crest to 20m inside targeted path; middle part of targeted path which is from left 20m inside targeted path to right 20m inside targeted path.

In plain words, the purpose in this section was to examine pipeline behaviour affected by considered seismic load in accordance with considerations of each soil type and buried depth of pipeline. But, it was possible to examine only typical seismic pipeline behaviour in accordance with soil types without assessing seismic pipeline behaviour in accordance with each buried depth of pipeline. That is, it was impossible to find a certain pattern of seismic pipeline behaviour in accordance with buried pipeline depth. This was because the incongruent time

choice, related to selecting exact 2.02sec involving 0.31882g vertical peak ground acceleration, was accomplished when the examination about seismic pipeline behaviour was executed by ABAQUS. When the ABAQUS models involving both seismic time history and vertical ground acceleration depending on each seismic time history were run, step times which make the calculated model analysed possibly at considered step time were automatically changed. This phenomenon made the examination for seismic pipeline behaviour according to each buried pipeline depths difficult because each ABAQUS model considering each buried depth of pipeline was created separately and the produced step time for analysis was different in every model. This fault for analysis caused incorrect seismic analysis because different step time for each analysis was considered in all calculated results considering the effect of pipeline burial depth. Thus, the explanation and comparison according to the considerations of each different pipeline burial depth is not mentioned. Moreover, the comparison with other researches was failed in my research because it was difficult to find any other similar research with mine.

However, not much different step time within the range from 1.98sec to 2.2sec, involving vertical peak ground acceleration, was selected for analysis. This alternative solution made the examination for typical seismic buried pipeline behaviour possible. Two types of graph are dealt in this section; displacement and stress graph versus true length of targeted path. These graphs also considered the two soil types, and two degrees of saturation and two boundary conditions at pipeline ends considered presently. The enlarged graphs in Figure 4.18 to 4.25 are attached again in Appendix G.

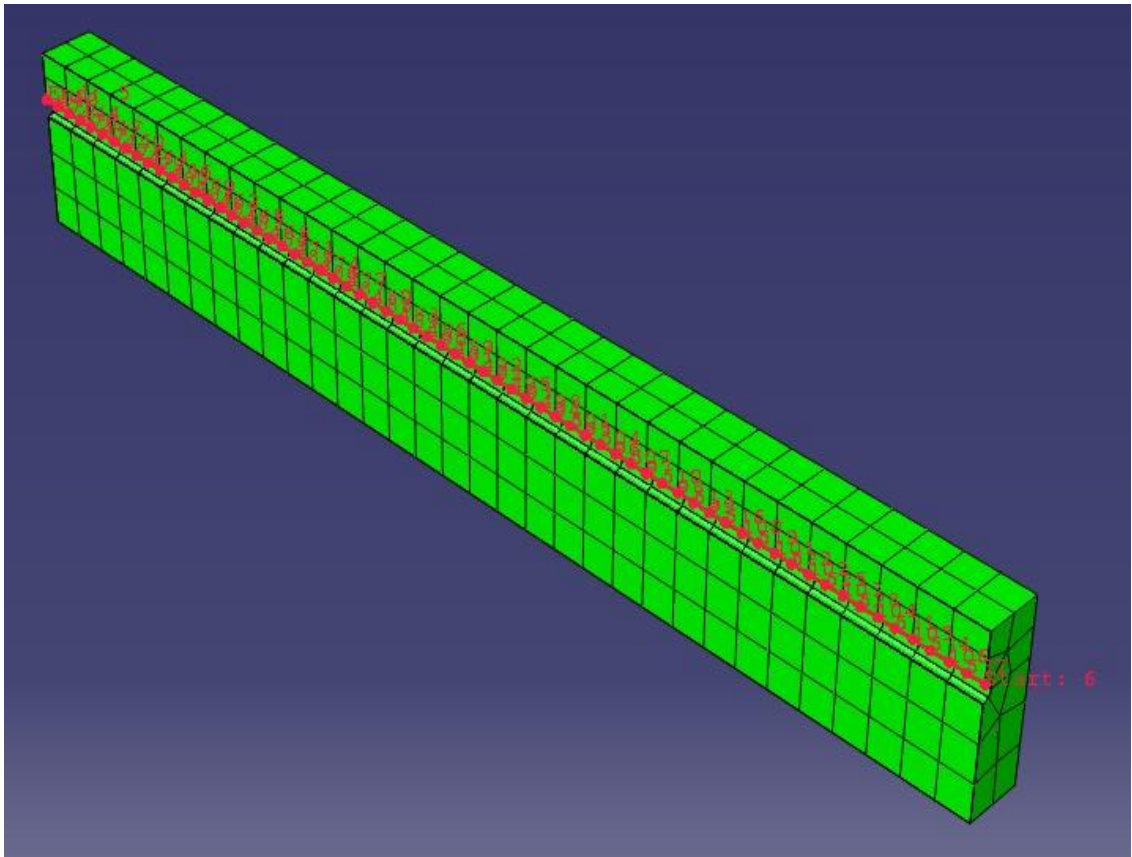


Figure 4.17-a

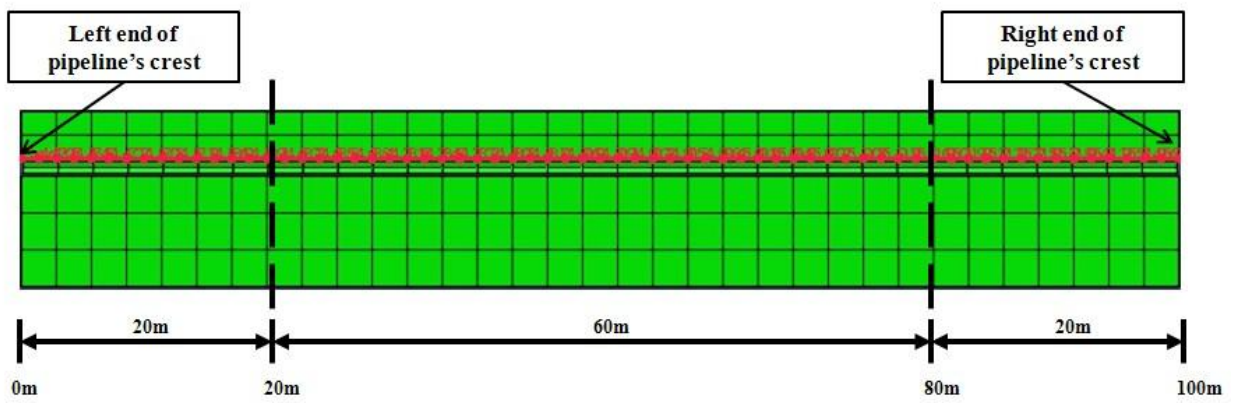


Figure 4.17-b

Figure 4.17 Target path for checking displacement and stress under dynamic load

4.3.1. General moist sandy soil with hinge boundary at pipeline ends

Displacement and stress along the whole length of pipeline, situated in moist sandy soil with the hinge boundary condition at both pipeline ends, are shown in Figure 4.18. Each line on the graph corresponding to each buried depth of pipeline considered.

First of all, rapidly downward bent deformation of pipeline was examined in both left and right parts of pipeline due to the effect of hinge boundary condition at pipeline ends. Through examining this deformation of pipeline, it is possible to assess the effect of boundary condition at pipeline ends when seismic load acts on pipeline. The hinge boundary condition at pipeline ends restricted them to move with soil and caused rapidly increased the stress of pipeline. In middle part of pipeline, there was upward bent deformation and increased stress of pipeline. This deformation tendency of pipeline meant that third mode of pipeline vibration was operated by the peak acceleration of seismic loads acting at about 2.02sec.

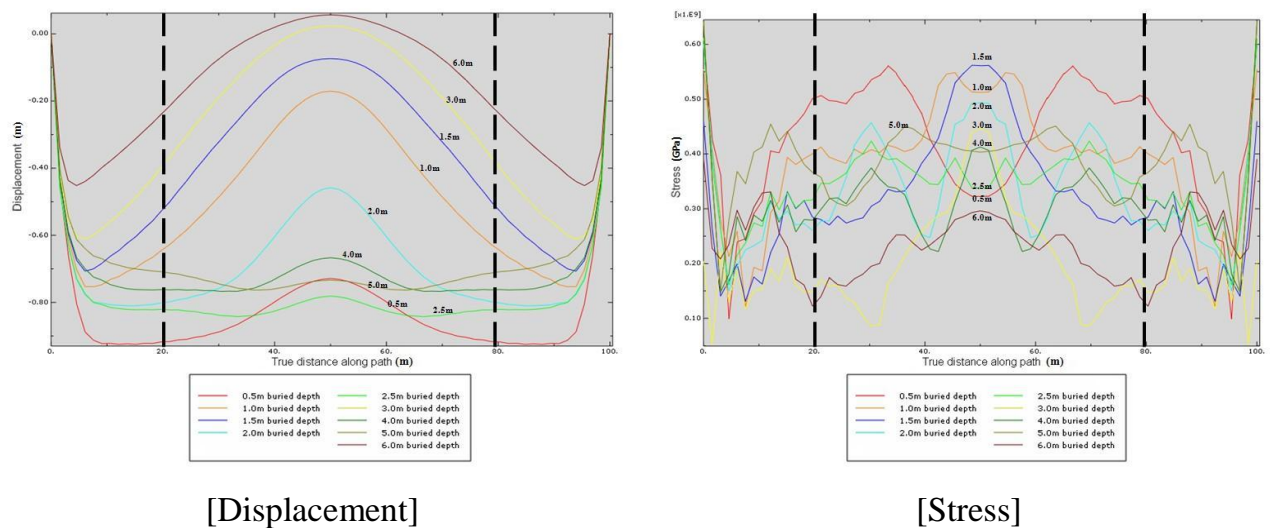


Figure 4. 18 Diagrams for general moist sandy soil with hinge boundary at pipeline ends

4.3.2. General moist sandy soil with roller boundary at pipeline ends

Displacement and stress along the whole length of pipeline, situated in moist sandy soil with the roller boundary condition at both pipeline ends, are shown in Figure 4.19. Each buried depth of pipeline is considered in graphs.

Firstly, relatively uniform displacement of pipeline buried in general moist sandy soil with roller boundary condition at pipeline ends was examined in accordance with each buried depth of pipeline. There was only increasing displacement of pipeline at both left and right part of pipeline and this increasing displacement of pipeline was maintained in the whole middle part of pipeline. This behaviour related to pipeline displacement under seismic load suggested that roller boundary condition at pipeline ends influence the pipeline movement and deformation. This is because roller boundary condition at pipeline ends allowed the pipeline not only to move with soil and but also to deform pipeline uniformly without any radical displacement. Relatively uniform displacement caused by roller boundary condition at pipeline ends gave rise to relatively uniform pipeline stress in middle part of pipeline.

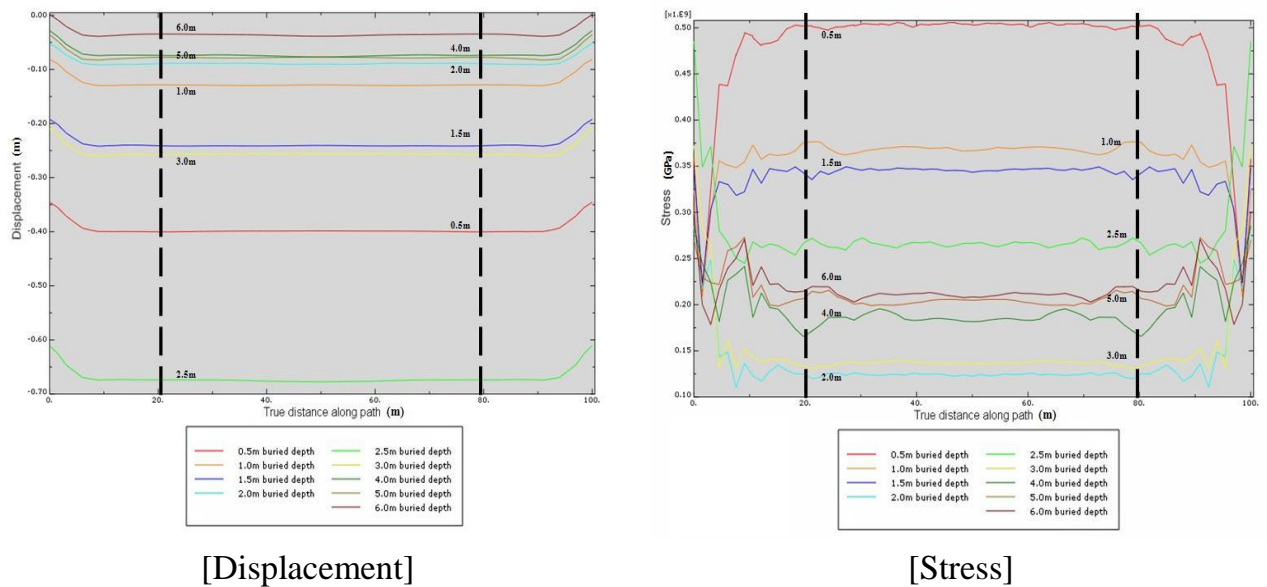


Figure 4. 19 Diagrams for general moist sandy soil with roller boundary at pipeline ends

4.3.3. Fully saturated sandy soil with hinge boundary at pipeline ends

Displacement and stresses along the whole length of pipeline, located in fully saturated sandy soil with the hinge boundary condition at both pipeline ends, are shown in Figure 4.20. Each buried depth of pipeline is considered in graphs.

Similar deformation behaviour with pipeline buried in general moist sandy soil with hinge boundary condition was examined in the case of pipeline located in fully saturated sandy soil with hinge boundary condition at pipeline ends. Left and right part of pipeline was rapidly deformed downward due to hinge boundary condition at pipeline ends and there was upward pipeline deformation in middle part of pipeline. By assessing these three rapidly bending formations of pipeline, it is possible to estimate that the buckling of pipeline might be caused at that position generating rapidly bending formation of pipeline because there was rapidly increasing pipeline stress when the pipeline was rapidly deformed. Additionally, This pipeline deformation tendency suggested clearly that third mode of pipeline vibration is normally generated in sandy soil with considering hinge boundary condition at pipeline ends because similar deformation tendency was also examined in the case of pipeline buried in general moist sandy soil.

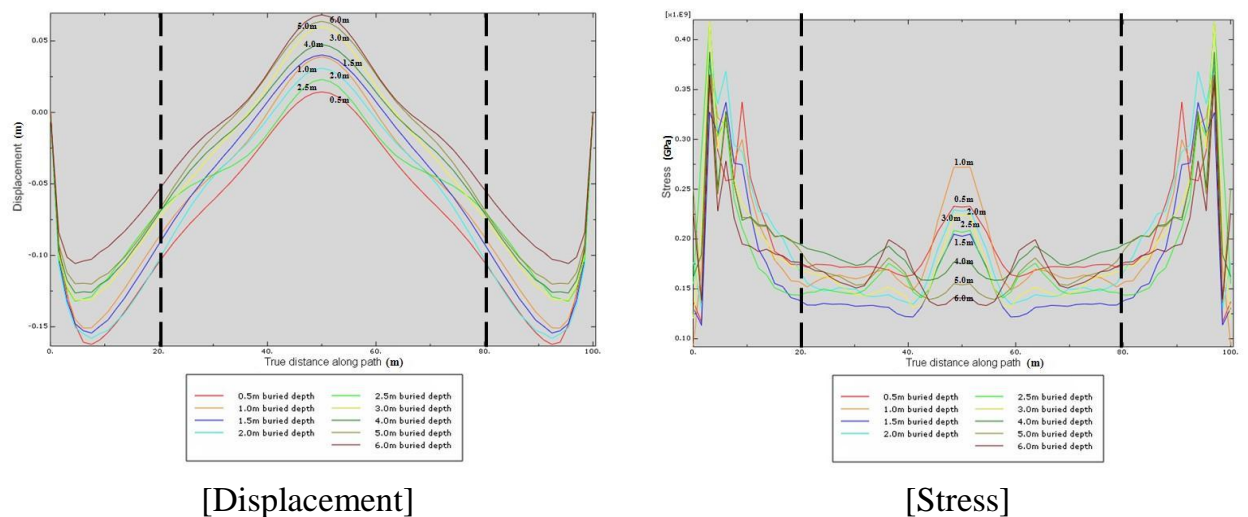


Figure 4. 20 Diagrams for fully saturated sandy soil with hinge boundary at pipeline ends

4.3.4. Fully saturated sandy soil with roller boundary at pipeline ends

Displacement and stress along the whole length of pipeline, located in fully saturated sandy soil with the roller boundary condition at both pipeline ends, were shown in Figure 4.21. Each buried depth of pipeline is drawn in graphs.

Similar deformation behaviour with pipeline buried in general moist sandy soil with roller boundary condition was examined in the case of pipeline buried in fully saturated sandy soil with roller boundary at pipeline ends. There was relatively uniform deformation in middle part of pipeline because roller boundary condition allowed the pipeline to move with soil. Moreover, increasing pipeline stress due to pipeline deformation caused by seismic load was also maintained uniformly in middle part of pipeline. This coincidence behaviour of pipeline, buried in both general moist sandy soil and fully saturated sandy soil, intimated that the consideration for the pipeline strength is more important than the pipeline ends because uniformly maintained stress of pipeline was existed almost along the whole length of pipeline when seismic load excited. Thus, pipeline's durability reinforcing pipeline strength should be reflected in the design of pipeline buried in sandy soil with roller boundary condition at pipeline ends.

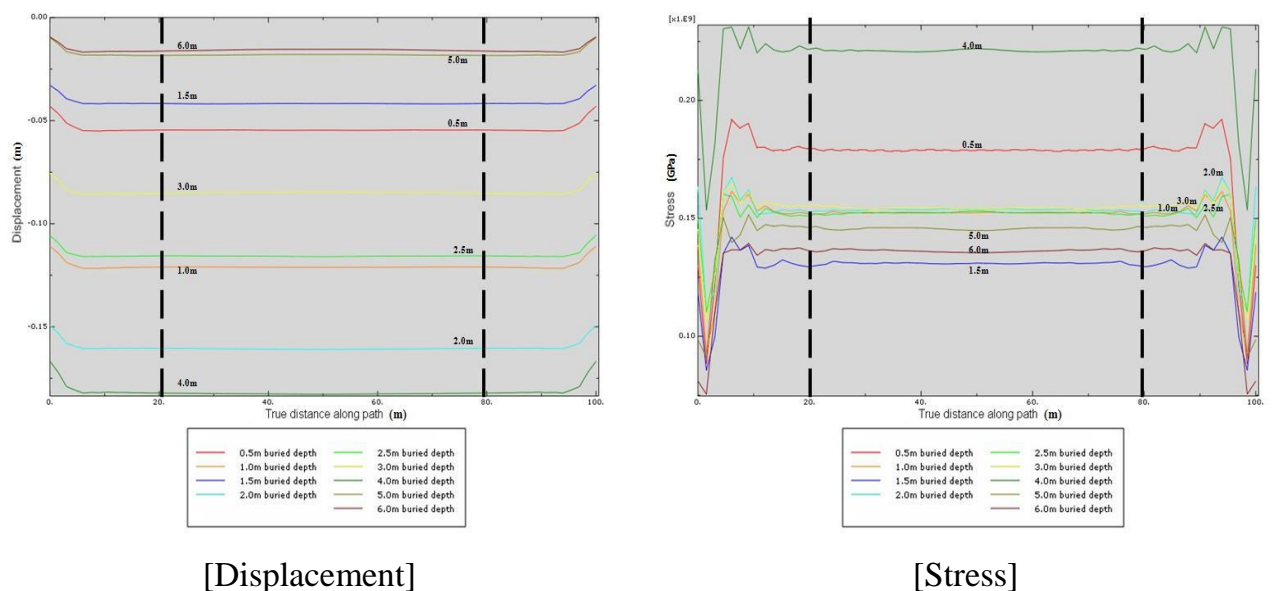


Figure 4. 21 Diagrams for fully saturated sandy soil with roller boundary at pipeline ends

4.3.5. General moist cohesive soil with hinge boundary at pipeline ends

Displacement and stress along the whole length of pipeline, buried in moist cohesive soil with hinge boundary condition at both pipeline ends, are shown in Figure 4.22. Each buried depth of pipeline is dealt in graphs.

By comparing the case of general moist sandy soil with consideration of hinge boundary condition at pipeline ends, based on Figure 4.18 in section 4.3.1, the almost same pipeline behaviour of both displacement and stress was examined. However, in the case of general moist cohesive soil with hinge boundary condition at pipeline ends, especially 4m buried depth of pipeline was much affected by peak seismic load excitation because big variation of both displacement and stress and fifth mode of pipeline vibration were observed contrary to the case of general moist sandy soil with hinge boundary condition at pipeline ends. Thus, it is possible to conclude that 4m buried depth is a critical buried depth of pipeline, when especially considering general moist cohesive soil with hinge boundary condition at pipeline ends.

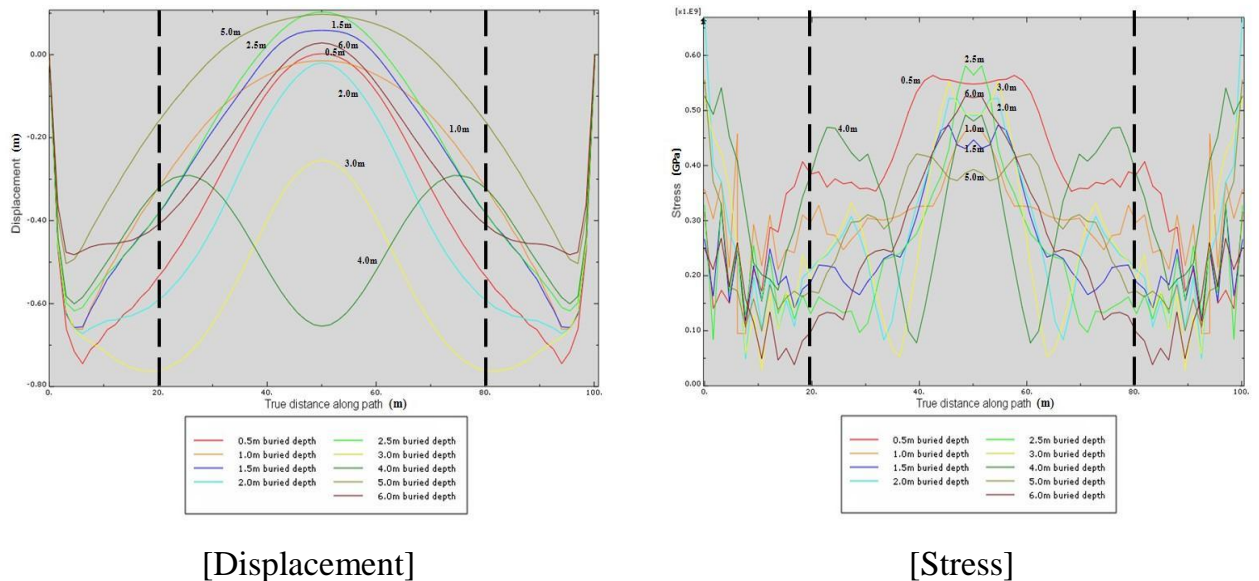


Figure 4. 22 Diagrams for general moist cohesive soil with hinge boundary at pipeline ends

4.3.6. General moist cohesive soil with roller boundary at pipeline ends

Displacement and stress along the whole length of pipeline, buried in moist cohesive soil with the roller boundary condition at pipeline ends, are shown in Figure 4.23. Each buried depth of pipeline is considered in graphs.

By comparing the case of general moist sandy soil with considering roller boundary condition at pipeline ends, based on the Figure 4.19 in section 4.3.2, it is possible to recognise that the displacement and stress pattern of general moist cohesive soil with roller boundary condition at pipeline ends was mostly similar to the patterns of general moist sandy soil with roller boundary condition at pipeline ends. However, in the case of general moist cohesive soil with roller boundary condition at pipeline ends, further pipeline settlement and smaller pipeline stress was examined than general moist sandy soil with roller boundary condition at pipeline ends. That is, whereas general moist sandy soil allowed lower pipeline settlement than general moist cohesive soil, bigger pipeline stress was generated than general moist cohesive soil. This meant that general moist sandy soil has bigger soil strength resisting settlement from seismic excitation than general moist cohesive soil and this bigger general moist sandy soil strength resisting settlement from seismic load brings about bigger stress of pipeline buried in general moist sandy soil than the stress of pipeline buried in general moist cohesive soil.

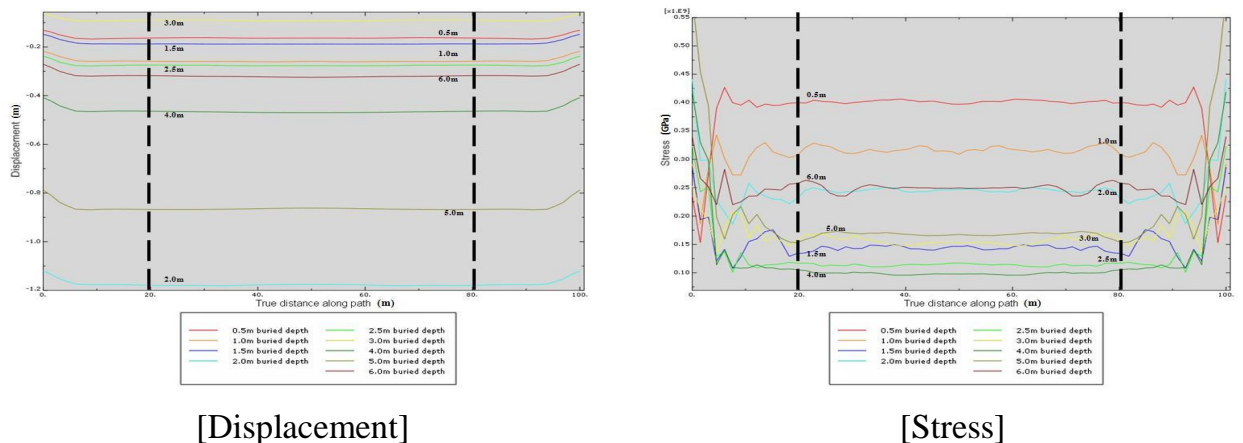


Figure 4. 23 Diagrams for general moist cohesive soil with roller boundary at pipeline ends

4.3.7. Fully saturated cohesive soil with hinge boundary at pipeline ends

Displacement and stress along the whole length of pipeline crest, buried in fully saturated cohesive soil with the hinge boundary condition at both pipeline ends, are shown in Figure 4.24. Each buried depth of pipeline is considered in graphs.

By comparing the case of fully saturated sandy soil with considering hinge boundary condition at pipeline ends, based on Figure 4.20 in section 4.3.3, multi mode of pipeline vibration mode was examined contrary to third mode of pipeline vibration, which was examined in the case of fully saturated sandy soil with considering hinge boundary condition at pipeline ends. This multi mode of pipeline vibration caused bended pipeline deformation at many places along the pipeline length and various magnitude of pipeline stress at places generating bended pipeline deformation without constant magnitude of pipeline stress along the pipeline length. The multi mode of pipeline vibration was observed in all cases of buried depth of pipeline. Therefore, it is possible to conclude that when the pipeline was constructed in fully saturated cohesive soil with hinge boundary condition at pipeline ends and seismic vibration is excited, all pipelines under each buried depth develop into the most critical statement from the seismic load excitation. That is, even though multi-mode of vibration is impossible in actual pipeline performance, it is possible to estimate that the pipeline will be buckled and failed when the multi mode of pipeline vibration is examined in FE results.

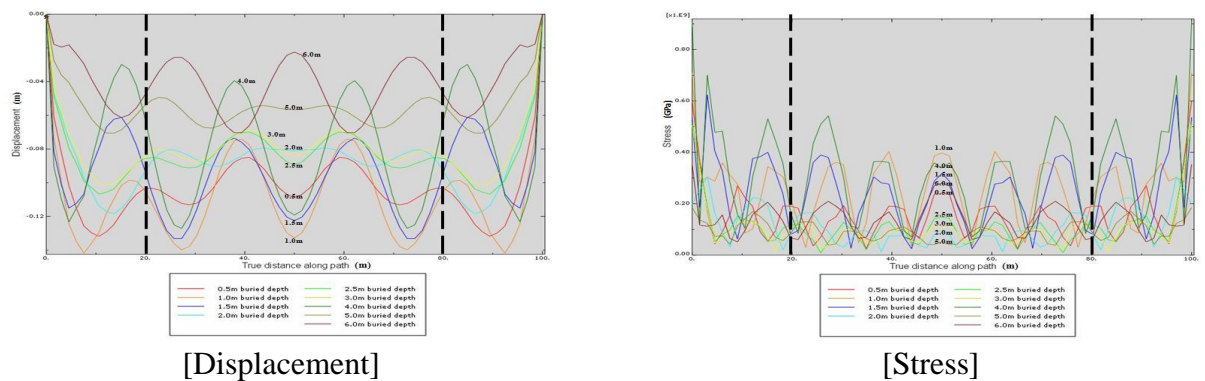


Figure 4. 24 Diagrams for fully saturated cohesive soil with hinge boundary at pipeline ends

4.3.8. Fully saturated cohesive soil with roller boundary at pipeline ends

Displacement and stress along the whole length of pipeline crest, buried in fully saturated cohesive soil with the roller boundary condition at both pipeline ends, are shown in Figure 4.25. Each line on the graph corresponding to buried depth of pipeline considered.

By comparing the case of fully saturated sandy soil with considering roller boundary condition at pipeline ends, based on Figure 4.21 in section 4.3.4, there was not much difference related to displacement of pipeline buried in fully saturated cohesive soil with roller boundary condition at pipeline ends. However, the pipeline stress considerably decreased as compared with the stress of pipeline buried in fully saturated sandy soil. This meant that fully saturated cohesive soil less influences pipeline to generate stress caused by seismic load excitation than fully saturated sandy soil.

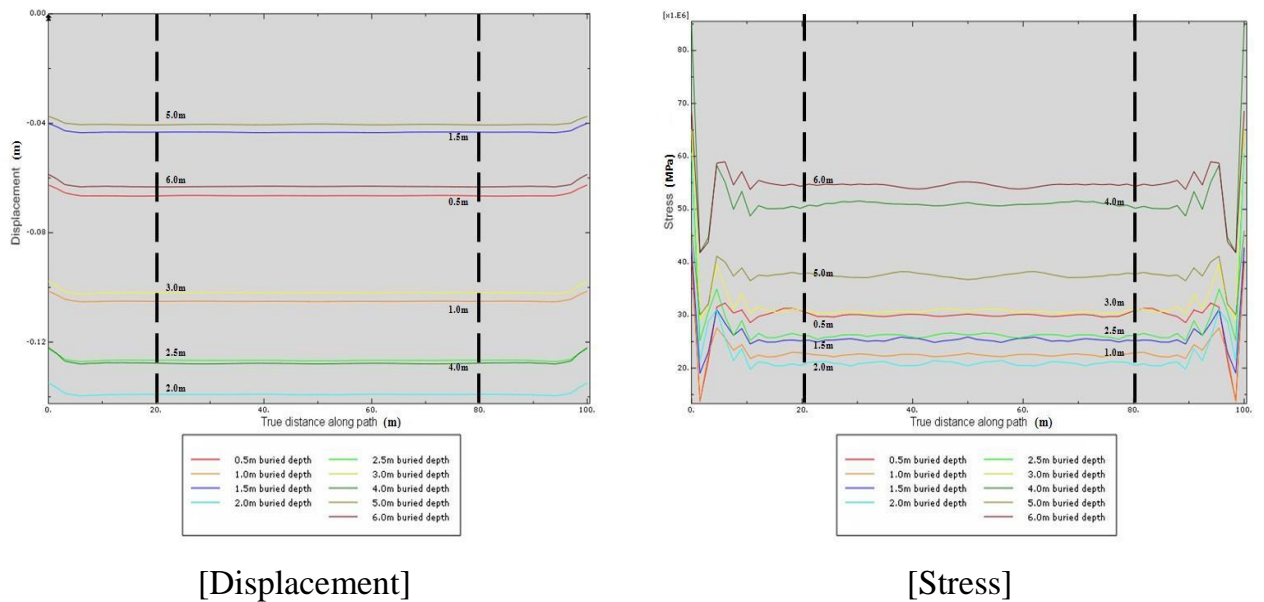


Figure 4. 25 Diagrams for fully saturated cohesive soil with roller boundary at pipeline ends

5. Conclusions

Initially, a mesh study was carried out in order to determine adaptive mesh types in the Finite Element Analysis for buried pipelines - for static analysis, the analysis for understanding boundary condition effects of pipeline ends and seismic analysis. For selecting an element type, a quadratic interpolation element was chosen in accordance with Rao (1999). In the case of element sizes, whereas 3m of approximate global element size was suitable for the static and seismic analysis with usage of 100m length models involving soil and pipeline model, 4m of approximate global element size was adopted for studying boundary condition effects of pipeline ends by using 50m length models involving soil and pipeline models. This is because there are limitations related to the mesh size for accurate and efficient analysis in accordance with different models.

Secondly, static loads were applied to the 100m models involving both soil and pipeline; 1100kPa uniform traffic surface load onto the top surface of the soil, 414kPa internal pipeline pressure on internal pipeline surface and self-weight of both pipeline and soil. Static loads generally cause oval shaped pipeline deformation and vertical soil settlement with pipeline. The behaviour of both soil and pipeline caused by static loads was considered in short-term serviceability issues because the permeability of water situated in soil and the consolidation of soil depending on passage of time were not considered. Different magnitudes of settlement comparing soil and pipeline were assessed because the pipeline settlement was relatively smaller than the settlement of the soil burying pipeline. This meant that even though the pipeline buried in the soil moves vertically under static loads, the pipeline movement is smaller than the movement of the soil. According to the soil types, different magnitudes of both soil and pipeline settlements was also examined. When the soil was general moist soil, the sandy soil caused lower pipeline and soil settlement than the case of cohesive soil due to the effect of higher

young's modulus of sandy soil than young's modulus of cohesive soil, based on Table 1.2 in section 1.2.4. On the contrary, when the soil was fully saturated soil, the cohesive soil caused lower pipeline and soil settlement than the case of sandy soil due to the effect of cohesion and low water permeability caused by minute particles of cohesive soil. Moreover, sandy soil caused higher stress of both pipeline and soil than the case of cohesive soil in all cases of soil types involving two different kinds of soil and two different degrees of saturation in soil. This phenomenon proved that the soil stress is affected by the soil's material physical properties based on Table 1.2 in section 1.2.4 and influences the stress of buried pipelines. This is because high density and friction angle of sandy soil generate higher stress than cohesive soil stress and this high stress of sandy soil also influences higher pipeline stress buried in sandy soil than pipeline stress buried in cohesive soil. Datta (1999) showed that the response of large diameter pipelines (or tunnels) in hard and soft soil is quite different because the two types of the soils have different stiffness affecting the response of buried pipelines crossing an interface between two types of soils due to different soil material properties. This proves that the examination by FEM (ABAQUS) related to the buried pipelines performance in different soil types is appropriate. According to the buried depths of pipelines, whereas big variation of soil settlement and stress was not examined, the pipeline settlement decreased when the buried depth of pipeline increased. This meant that deeply buried pipelines are the preferred under static loads with respect to only serviceability issue. However, Datta (1999) asserts that the embedment depth of pipelines has little effect on the stress because the pipe stresses are reduced by about 15% for shallow depths and become almost constant for embedment depth more than 30 times the radius of the pipeline. Thus, it is possible to say that there is adaptable pipeline burial depth and further research is needed for finding preferred pipeline burial depth compromising settlement and stress issue.

Thirdly, two boundary conditions at pipeline ends, hinge and roller, were assumed and 50m models involving soil and pipeline were used in order to examine the boundary condition effects on pipeline ends under static loads. Two different boundary conditions considered involve two different meanings; roller boundary condition at pipeline ends are consistent with infinitely long pipelines without any restriction at pipeline ends and hinge boundary condition with a pipeline between two buildings at pipeline ends. The same magnitudes of stress and displacement related to each soil and pipeline were examined with static analysis without considering boundary condition effects in all cases of soil types. However, the distinct difference related to soil and pipeline deformation shapes was examined in accordance with the consideration of each boundary condition at pipeline ends; hinge and roller. According to the soil settlement deformation shape, although uniform settlement along the whole length of soil model was assessed when considering roller boundary condition at pipeline ends, two less deformed parts appeared at two soil model ends as two bulged soil deformation shapes at the ends of the soil model with uniform settlement in the middle of soil model due to the restricted boundary condition effect when considering hinge boundary condition at pipeline ends. This meant that while roller boundary conditions at pipeline ends allowed the pipeline to move with soil uniformly, hinge boundary condition at pipeline ends restricted the pipeline ends to move with soil uniformly. Datta (1999) further adds that the axial and bending stresses at the fixed ends are about 10 and 54 times more than those in the middle. These boundary condition effects also influenced the pipeline deformation shape. The pipeline was deformed uniformly as an oval shape along the whole length of the pipeline model under static loads when considering roller boundary condition at pipeline ends. On the contrary, the pipeline was deformed as a parabolic shape with oval shaped deformation when considering hinge boundary condition at pipeline ends. Therefore, it is possible to conclude that infinitely long pipelines modelled by the roller boundary condition should improve the durability for resisting uniform vertical stress and the

pipeline located between two buildings should be designed well especially at the ends of the pipeline.

Finally, a seismic load was applied to the 100m models involving soil and pipeline; El-Centro earthquake was about 0.3g of vertical peak ground acceleration with 31.18sec seismic time history. Especially, the pipeline behaviour at 2.02sec involving -0.31882 peak ground acceleration was examined in order to assess critical movements of the pipeline interacting with soil. The observed path for seismic analysis was the crest-line of the pipeline along the whole length of the pipeline model interacting with the soil model. The observed path was divided into three parts in order to evaluate different pipeline actions according to three different locations of pipeline affected by the seismic load; the left and right parts of the targeted path which are from the left and right ends of pipeline crest to 20m inside targeted path and middle part of targeted path which is from the left 20m inside the targeted path to the right 20m inside the targeted path. The magnitude of both pipeline displacement and stress was different with respect to the soil types and boundary condition at pipeline ends. The observation of typical modes of pipeline vibration (or failure) makes designers establish performance criteria to develop a methodology that minimizes the probability of system failure (Datta, 1999). This means that the observation of the modes of pipeline vibration can guide assessment of likely failure modes of pipeline. According to the types of boundary condition at pipeline ends, the third mode of pipeline vibration caused by a seismic load excitation was generally examined in all cases of hinge boundary condition at pipeline ends; the left and right ends of the targeted path showed rapidly downward bending deformation and middle part of the targeted path was deformed as upward bending deformation in all soil types but fully saturated cohesive soil, caused the pipeline vibration mode to be multi mode. This meant that hinge boundary condition of pipeline ends causes big pipeline stress at three parts, these generated big stresses at each part resulting in critical buckling of the pipeline and the generated multi mode of pipeline vibration in fully

saturated cohesive soil is the most dangerous statement of pipeline. Thus, it is possible to conclude that the decrease of generated pipeline stress should be considered for pipeline design under seismic load when the pipeline is built between two buildings. In the case of roller boundary condition at pipeline ends, a relatively uniform deformation was examined and this uniform deformation caused uniform pipeline stresses along the whole length of the pipeline because roller boundary conditions at pipeline ends allowed the pipeline to move uniformly with the soil. Thus, it is possible to conclude that the increase of pipeline strength along the whole pipeline length should be considered when the pipeline, which will be constructed, is infinitely long.

However, in the seismic analysis for buried pipelines, there is something to be desired because the effect of each burial depth of pipeline caused by vertical peak ground acceleration was not examined due to the different step time selection for the analysis. If it is possible to solve this problem related to the selection of the exact step time, 2.02sec involving 0.31882g vertical peak ground acceleration, in every calculated model, it will be possible to accurately examine the effect of each burial depth of pipeline caused by the vertical peak ground acceleration and to search variable burial depths of pipelines in order to present accurate data for finding the safest buried depth of pipelines.

References

- BARDET, J. P. & DAVIS, C. A. (1997) Seismic analysis of flexible buried structures. IN PEDRO, S. S. (Ed.) *Seismic behaviour of ground and geotechnical structures*. Rotterdam, A.A. Balkema.
- BSI. (2002a) Nonalloy steel tubes and fittings for the conveyance of water and other aqueous liquid - Technical delivery conditions. IN CEN (Ed. *BS 10224:2002*. London, BSI.
- BSI. (2002b) Seamless steel tubes for pressure purpose - Technical delivery conditions - Part 2: Non-alloy and alloy tubes with specified elevated temperature properties. IN CEN (Ed. *BS EN 10216-2:2002*. London, BSI.
- BSI. (2006) Steel, concrete and composite bridges - Part 2: Specification for loads. IN CEN (Ed. *BS 5400-2:2006*. London, BSI.
- BSI. (2010) Guide to the structural design of buried pipelines. IN CEN (Ed. *BS 9295:2010*. London, BSI.
- BULENT, A. O. (1985) Dynamic response of buried pipelines. IN JEY, K. J. (Ed.) *Advances in underground pipelines engineering*. New York, American Society of Civil Engineers.
- BULSON, P. S. (1985) *Buried structures - Static and Dynamic Strength*, London, Chapman and Hall Ltd.
- DATTA, T. K. (1999) Seismic response of buried pipelines: a state-of-the-art review. *Nuclear Engineering and Design*, 192, 271-284.
- GAGO, J. P. D. S. R., KELLY, D. W. & ZIENKIEWICZ, O. C. (1982) A posteriori error analysis and adaptive processes in the finite element method: Part 2 - Adaptive mesh refinement. *International Journal for numerical methods in engineering*, 19, 1621-1656.
- GEORGES, M. K. & SHEPHARD, M. S. (1990) Automatic mesh generator for use in two-dimensional h-p analysis. *The Journal of Computing in Civil Engineering*, 4, 199-220.
- [HTTP://WWW.FINESOFTWARE.EN/GEOTECHNICAL-SODTWARE/HELP/FEM](http://www.finesoftware.en/geotechnical-sodtware/help/fem) (2010).
- [HTTP://WWW.VIBRATIONDATA.COM/ELCENTRO.HTM](http://www.vibrationdata.com/elcentro.htm) (2010).
- HUANG, L., YANG, H. & ZHAN, M. (2008) 3D-FE modeling method of splitting spinning. *Computational mechanics Science*, 42, 643-652.
- HUGEL, H. M., HENKE, S. & KINZLER, S. (2008) High-performance Abaqus simulations in soil mechanics. *Abaqus User's conference*.
- JEREMY, I. (1978) Underground pipeline behaviour under seismic loading. IN DIVISION, A. G. E. (Ed.) *Earthquake engineering and soil dynamics*. New York, American Society of Civil Engineers.

- LEON, R. L. & WANG, M. (1978) Performance of underground pipelines in earthquake. IN DIVISION, A. G. E. (Ed.) *Earthquake engineering and soil dynamics*. New York, American Society of Civil Engineers.
- LIU, P. F., ZHENG, J. Y., SHANG, B. J. & SHI, P. (2010) Failure analysis of natural gas buried X65 steel pipeline under deflection load using finite element method. *Material and Design*, 31, 1384-1391.
- LO, S. H., WU, D. & SZE, K. Y. (2010) Adaptive meshing and analysis using transitional quadrilateral and hexahedral elements. *Finite Element in Analysis and Design*, 46, 2-16.
- MADABHUSHI, S. P. G. (2009) Geotechnical aspects. IN BLAKEBOROUGH, A., MERRIMAN, P. A. & WILLIAMS, M. S. (Eds.) *The nothridge, california earthquake of 17 January 1994*. London, Earthquake Engineering Field Investigation Team.
- NATH, P. (1994) The effect of traffic loading on buried pipes. IN JOHN, W. B. (Ed.) *Soil-structure interaction: numerical analysis and modelling*. London, E & FN Spon.
- NIXON, I. K. & CHILD, G. H. (1989) Site investigation. IN BLAKE, L. S. (Ed.) *Civil Engineer's reference book*. 4 ed. Oxford, Elsevier.
- POCOCK, R. G., LAWRENCE, G. J. L. & TAYLOR, M. E. (1980) Behaviour of shallow buried pipeline under static and wheel loads. IN TRRL (Ed.) *Transport and road research laboratory*. Berkshire, Department of the environment and of the transport.
- PRASAD, S. K., TOWHATA, I., GHANDRADHARA, G. P. & NANJUNDASWAMY, P. (2004) Shaking table tests in earthquake geotechnical engineering. *Current Science*, 87.
- RAO, S. S. (1999) *The finite element method in engineering*, Boston, Butterworth-Heinemann.
- RAYMOND, B. S. & JAMES, M. D. (1985) Earth pressure and surface load effects on buried pipelines. IN JEY, K. J. (Ed.) *Advances in underground pipeline engineering*. New York, American Society of Civil Engineers.
- RICHART, F. E., WOODS, R. D. & HALL, J. R. (1970) *Vibration of soils and foundations*, New jersey, Prince-Hall, Inc.
- ROBERT, B. J. (1977) Earthquake protection of water and sewage lifelines. IN CALIFORNIA, U. O. (Ed.) *The current state of knowledge of lifeline earthquake engineering*. New York, American Society of Civil Engineers.
- SIMULIA (2009) ABAQUS analysis user's manual - version 6.9-2. USA.
- THORLEY, A. R. D. & ATKINSON, J. H. (1994) Guide to the design of thrust blocks for buried pressure pipelines. London, CIRIA.
- WANG, L. R. L. (1994) Numerical seismic analysis and modelling of buried pipelines. *Soil-structure interaction: numerical analysis and modelling*. London, E & FN Spon.

- WANG, L. R. L. & RAYMOND, C. Y. F. (1979) seismic design criteria for buried pipelines. IN CONFERENCE, A. P. D. S. (Ed.) *Pipelines in adverse environments - a state of the art*. New York, American Society of Civil Engineers.
- WATKINS, R. W. & ANDERSON, L. R. (2000) *Structural mechanics of buried pipes*, Boca Raton, CRC Press LLC.
- WECK, M. & NOTTEBAUM, T. (1993) Adaptive meshing - saving computational costs during the optimization of composite structures. *Structural Optimization*, 6, 108-115.
- WU, T. H. (1971) *Soil Dynamics*, Ohio, Allyn and Bacon, Inc.
- YONG, B. (2001) *Pipeline and editors*, Oxford, Elsevier.
- YOUNG, O. C. & TROTT, J. J. (1984) *Buried rigid pipes - Structural design of pipelines*, New York, Elsevier Applied Science Publishers.
- ZIENKIEWICZ, O. C. & ZHU, J. Z. (1987) A simple error estimator and adaptive procedure for practical engineering analysis. *International Journal for numerical methods in engineering*, 24, 337-357.

Appendix A – seismic vertical acceleration data of El Centro Earthquake

Time (sec)	Acceleration (G)	Time (sec)	Acceleration (G)	Time (sec)	Acceleration (G)
0	0.0063	0.76	-0.05723	1.52	-0.12902
0.02	0.00364	0.78	-0.04534	1.54	-0.07652
0.04	0.00099	0.8	-0.03346	1.56	-0.02401
0.06	0.00428	0.82	-0.03201	1.58	0.02849
0.08	0.00758	0.84	-0.03056	1.6	0.08099
0.1	0.01087	0.86	-0.02911	1.62	0.1335
0.12	0.00682	0.88	-0.02766	1.64	0.186
0.14	0.00277	0.9	-0.04116	1.66	0.2385
0.16	-0.00128	0.92	-0.05466	1.68	0.21993
0.18	0.00368	0.94	-0.06816	1.7	0.20135
0.2	0.00864	0.96	-0.08166	1.72	0.18277
0.22	0.0136	0.98	-0.06846	1.74	0.1642
0.24	0.00727	1	-0.05527	1.76	0.14562
0.26	0.00094	1.02	-0.04208	1.78	0.16143
0.28	0.0042	1.04	-0.04259	1.8	0.17725
0.3	0.00221	1.06	-0.04311	1.82	0.13215
0.32	0.00021	1.08	-0.02428	1.84	0.08705
0.34	0.00444	1.1	-0.00545	1.86	0.04196
0.36	0.00867	1.12	0.01338	1.88	-0.00314
0.38	0.0129	1.14	0.03221	1.9	-0.04824
0.4	0.01713	1.16	0.05104	1.92	-0.09334
0.42	-0.00343	1.18	0.06987	1.94	-0.13843
0.44	-0.024	1.2	0.0887	1.96	-0.18353
0.46	-0.00992	1.22	0.04524	1.98	-0.22863
0.48	0.00416	1.24	0.00179	2	0.004809
0.5	0.00528	1.26	-0.04167	2.02	-0.31882
0.52	0.01653	1.28	-0.08513	2.04	-0.25024
0.54	0.02779	1.3	-0.12858	2.06	-0.18166
0.56	0.03904	1.32	-0.17204	2.08	-0.11309
0.58	0.02449	1.34	-0.12908	2.1	-0.04451
0.6	0.00995	1.36	-0.08613	2.12	0.02407
0.62	0.00961	1.38	-0.08902	2.14	0.09265
0.64	0.00926	1.4	-0.09192	2.16	0.16123
0.66	0.00892	1.42	-0.09482	2.18	0.22981
0.68	-0.00486	1.44	-0.09324	2.2	0.29839
0.7	-0.01864	1.46	-0.09166	2.22	0.23197
0.72	-0.03242	1.48	-0.09478	2.24	0.16554
0.74	-0.03365	1.5	-0.09789	2.26	0.09912

Time (sec)	Acceleration (G)	Time (sec)	Acceleration (G)	Time (sec)	Acceleration (G)
2.28	0.0327	3.14	-0.11314	4	0.0228
2.3	-0.03372	3.16	-0.07304	4.02	-0.00996
2.32	-0.10014	3.18	-0.03294	4.04	-0.04272
2.34	-0.16656	3.2	0.00715	4.06	-0.02147
2.36	-0.23299	3.22	-0.0635	4.08	-0.00021
2.38	-0.29941	3.24	-0.13415	4.1	0.02104
2.4	-0.00421	3.26	-0.2048	4.12	-0.01459
2.42	0.29099	3.28	-0.12482	4.14	-0.05022
2.44	0.2238	3.3	-0.04485	4.16	-0.08585
2.46	0.15662	3.32	0.03513	4.18	-0.12148
2.48	0.08943	3.34	0.1151	4.2	-0.15711
2.5	0.02224	3.36	0.19508	4.22	-0.19274
2.52	-0.04495	3.38	0.12301	4.24	-0.22837
2.54	0.01834	3.4	0.05094	4.26	-0.18145
2.56	0.08163	3.42	-0.02113	4.28	-0.13453
2.58	0.14491	3.44	-0.0932	4.3	-0.08761
2.6	0.2082	3.46	-0.02663	4.32	-0.04069
2.62	0.18973	3.48	0.03995	4.34	0.00623
2.64	0.17125	3.5	0.10653	4.36	0.05316
2.66	0.13759	3.52	0.17311	4.38	0.10008
2.68	0.10393	3.54	0.11283	4.4	0.147
2.7	0.07027	3.56	0.05255	4.42	0.09754
2.72	0.03661	3.58	-0.00772	4.44	0.04808
2.74	0.00295	3.6	0.01064	4.46	-0.00138
2.76	-0.03071	3.62	0.029	4.48	0.05141
2.78	-0.00561	3.64	0.04737	4.5	0.1042
2.8	0.01948	3.66	0.06573	4.52	0.15699
2.82	0.04458	3.68	0.02021	4.54	0.20979
2.84	0.06468	3.7	-0.0253	4.56	0.26258
2.86	0.08478	3.72	-0.07081	4.58	0.16996
2.88	0.10487	3.74	-0.04107	4.6	0.07734
2.9	0.05895	3.76	-0.01133	4.62	-0.01527
2.92	0.01303	3.78	0.00288	4.64	-0.10789
2.94	-0.03289	3.8	0.01709	4.66	-0.20051
2.96	-0.07882	3.82	0.03131	4.68	-0.06786
2.98	-0.03556	3.84	-0.02278	4.7	0.06479
3	0.00771	3.86	-0.07686	4.72	0.01671
3.02	0.05097	3.88	-0.13095	4.74	-0.03137
3.04	0.01013	3.9	-0.18504	4.76	-0.07945
3.06	-0.03071	3.92	-0.14347	4.78	-0.12753
3.08	-0.07156	3.94	-0.1019	4.8	-0.17561
3.1	-0.1124	3.96	-0.06034	4.82	-0.22369
3.12	-0.15324	3.98	-0.01877	4.84	-0.27177

Time (sec)	Acceleration (G)	Time (sec)	Acceleration (G)	Time (sec)	Acceleration (G)
4.86	-0.15851	5.72	-0.05127	6.58	0.03365
4.88	-0.04525	5.74	-0.00298	6.6	0.04867
4.9	0.06802	5.76	-0.01952	6.62	0.0304
4.92	0.18128	5.78	-0.03605	6.64	0.01213
4.94	0.14464	5.8	-0.05259	6.66	-0.00614
4.96	0.108	5.82	-0.04182	6.68	-0.02441
4.98	0.07137	5.84	-0.03106	6.7	0.01375
5	0.03473	5.86	-0.02903	6.72	0.01099
5.02	0.09666	5.88	-0.02699	6.74	0.00823
5.04	0.1586	5.9	0.02515	6.76	0.00547
5.06	0.22053	5.92	0.0177	6.78	0.00812
5.08	0.18296	5.94	0.02213	6.8	0.01077
5.1	0.14538	5.96	0.02656	6.82	-0.00692
5.12	0.1078	5.98	0.00419	6.84	-0.02461
5.14	0.07023	6	-0.01819	6.86	-0.0423
5.16	0.03265	6.02	-0.04057	6.88	-0.05999
5.18	0.06649	6.04	-0.06294	6.9	-0.07768
5.2	0.10033	6.06	-0.02417	6.92	-0.09538
5.22	0.13417	6.08	0.0146	6.94	-0.06209
5.24	0.10337	6.1	0.05337	6.96	-0.0288
5.26	0.07257	6.12	0.02428	6.98	0.00448
5.28	0.04177	6.14	-0.0048	7	0.03777
5.3	0.01097	6.16	-0.03389	7.02	0.01773
5.32	-0.01983	6.18	-0.00557	7.04	-0.00231
5.34	0.04438	6.2	0.02274	7.06	-0.02235
5.36	0.1086	6.22	0.00679	7.08	0.01791
5.38	0.17281	6.24	-0.00915	7.1	0.05816
5.4	0.10416	6.26	-0.02509	7.12	0.03738
5.42	0.03551	6.28	-0.04103	7.14	0.0166
5.44	-0.03315	6.3	-0.05698	7.16	-0.00418
5.46	-0.1018	6.32	-0.01826	7.18	-0.02496
5.48	-0.07262	6.34	0.02046	7.2	-0.04574
5.5	-0.04344	6.36	0.00454	7.22	-0.02071
5.52	-0.01426	6.38	-0.01138	7.24	0.00432
5.54	0.01492	6.4	-0.00215	7.26	0.02935
5.56	-0.02025	6.42	0.00708	7.28	0.01526
5.58	-0.05543	6.44	0.00496	7.3	0.01806
5.6	-0.0906	6.46	0.00285	7.32	0.02086
5.62	-0.12578	6.48	0.00074	7.34	0.00793
5.64	-0.16095	6.5	-0.00534	7.36	-0.00501
5.66	-0.19613	6.52	-0.01141	7.38	-0.01795
5.68	-0.14784	6.54	0.00361	7.4	-0.03089
5.7	-0.09955	6.56	0.01863	7.42	-0.01841

Time (sec)	Acceleration (G)	Time (sec)	Acceleration (G)	Time (sec)	Acceleration (G)
7.44	-0.00593	8.3	0.01348	9.16	-0.03647
7.46	0.00655	8.32	-0.00942	9.18	-0.03984
7.48	-0.02519	8.34	-0.03231	9.2	-0.00517
7.5	-0.05693	8.36	-0.02997	9.22	0.0295
7.52	-0.04045	8.38	-0.03095	9.24	0.06417
7.54	-0.02398	8.4	-0.03192	9.26	0.09883
7.56	-0.0075	8.42	-0.02588	9.28	0.1335
7.58	0.00897	8.44	-0.01984	9.3	0.05924
7.6	0.00384	8.46	-0.01379	9.32	-0.01503
7.62	-0.00129	8.48	-0.00775	9.34	-0.08929
7.64	-0.00642	8.5	-0.01449	9.36	-0.16355
7.66	-0.01156	8.52	-0.02123	9.38	-0.06096
7.68	-0.02619	8.54	0.01523	9.4	0.04164
7.7	-0.04082	8.56	0.0517	9.42	0.01551
7.72	-0.05545	8.58	0.08816	9.44	-0.01061
7.74	-0.04366	8.6	0.12463	9.46	-0.03674
7.76	-0.03188	8.62	0.16109	9.48	-0.06287
7.78	-0.06964	8.64	0.12987	9.5	-0.08899
7.8	-0.05634	8.66	0.09864	9.52	-0.0543
7.82	-0.04303	8.68	0.06741	9.54	-0.01961
7.84	-0.02972	8.7	0.03618	9.56	0.01508
7.86	-0.01642	8.72	0.00495	9.58	0.04977
7.88	-0.00311	8.74	0.0042	9.6	0.08446
7.9	0.0102	8.76	0.00345	9.62	0.05023
7.92	0.0235	8.78	0.00269	9.64	0.016
7.94	0.03681	8.8	-0.05922	9.66	-0.01823
7.96	0.05011	8.82	-0.12112	9.68	-0.05246
7.98	0.02436	8.84	-0.18303	9.7	-0.08669
8	-0.00139	8.86	-0.12043	9.72	-0.06769
8.02	-0.02714	8.88	-0.05782	9.74	-0.0487
8.04	-0.00309	8.9	0.00479	9.76	-0.0297
8.06	0.02096	8.92	0.0674	9.78	-0.01071
8.08	0.04501	8.94	0.13001	9.8	0.00829
8.1	0.06906	8.96	0.08373	9.82	-0.00314
8.12	0.05773	8.98	0.03745	9.84	0.02966
8.14	0.0464	9	0.06979	9.86	0.06246
8.16	0.03507	9.02	0.10213	9.88	-0.00234
8.18	0.03357	9.04	-0.03517	9.9	-0.06714
8.2	0.03207	9.06	-0.17247	9.92	-0.04051
8.22	0.03057	9.08	-0.13763	9.94	-0.01388
8.24	0.0325	9.1	-0.10278	9.96	0.01274
8.26	0.03444	9.12	-0.06794	9.98	0.00805
8.28	0.03637	9.14	-0.0331	10	0.03024

Time (sec)	Acceleration (G)	Time (sec)	Acceleration (G)	Time (sec)	Acceleration (G)
10.02	0.05243	10.88	-0.00633	11.74	0.06906
10.04	0.02351	10.9	0.02724	11.76	0.06236
10.06	-0.00541	10.92	0.0608	11.78	0.08735
10.08	-0.03432	10.94	0.03669	11.8	0.11235
10.1	-0.06324	10.96	0.01258	11.82	0.13734
10.12	-0.09215	10.98	-0.01153	11.84	0.12175
10.14	-0.12107	11	-0.03564	11.86	0.10616
10.16	-0.0845	11.02	-0.00677	11.88	0.09057
10.18	-0.04794	11.04	0.0221	11.9	0.07498
10.2	-0.01137	11.06	0.05098	11.92	0.08011
10.22	0.0252	11.08	0.07985	11.94	0.08524
10.24	0.06177	11.1	0.06915	11.96	0.09037
10.26	0.04028	11.12	0.05845	11.98	0.06208
10.28	0.0188	11.14	0.04775	12	0.03378
10.3	0.04456	11.16	0.03706	12.02	0.00549
10.32	0.07032	11.18	0.02636	12.04	-0.02281
10.34	0.09608	11.2	0.05822	12.06	-0.05444
10.36	0.12184	11.22	0.09009	12.08	-0.0403
10.38	0.0635	11.24	0.12196	12.1	-0.02615
10.4	0.00517	11.26	0.10069	12.12	-0.01201
10.42	-0.05317	11.28	0.07943	12.14	-0.02028
10.44	-0.03124	11.3	0.05816	12.16	-0.02855
10.46	-0.0093	11.32	0.03689	12.18	-0.06243
10.48	0.01263	11.34	0.01563	12.2	-0.03524
10.5	0.03457	11.36	-0.00564	12.22	-0.00805
10.52	0.03283	11.38	-0.0269	12.24	-0.04948
10.54	0.03109	11.4	-0.04817	12.26	-0.03643
10.56	0.02935	11.42	-0.06944	12.28	-0.02337
10.58	0.04511	11.44	-0.0907	12.3	-0.03368
10.6	0.06087	11.46	-0.11197	12.32	-0.01879
10.62	0.07663	11.48	-0.11521	12.34	-0.00389
10.64	0.09239	11.5	-0.11846	12.36	0.011
10.66	0.05742	11.52	-0.1217	12.38	0.02589
10.68	0.02245	11.54	-0.12494	12.4	0.01446
10.7	-0.01252	11.56	-0.165	12.42	0.00303
10.72	0.0068	11.58	-0.20505	12.44	-0.0084
10.74	0.02611	11.6	-0.15713	12.46	0.00463
10.76	0.04543	11.62	-0.10921	12.48	0.01766
10.78	0.01571	11.64	-0.06129	12.5	0.03069
10.8	-0.01402	11.66	-0.01337	12.52	0.04372
10.82	-0.04374	11.68	0.03455	12.54	0.02165
10.84	-0.07347	11.7	0.08247	12.56	-0.00042
10.86	-0.0399	11.72	0.07576	12.58	-0.02249

Time (sec)	Acceleration (G)	Time (sec)	Acceleration (G)	Time (sec)	Acceleration (G)
12.6	-0.04456	13.46	-0.02181	14.32	-0.003
12.62	-0.03638	13.48	-0.04704	14.34	0.00335
12.64	-0.02819	13.5	-0.07227	14.36	0.0097
12.66	-0.02001	13.52	-0.0975	14.38	0.01605
12.68	-0.01182	13.54	-0.12273	14.4	0.02239
12.7	-0.02445	13.56	-0.08317	14.42	0.04215
12.72	-0.03707	13.58	-0.04362	14.44	0.06191
12.74	-0.04969	13.6	-0.00407	14.46	0.08167
12.76	-0.05882	13.62	0.03549	14.48	0.03477
12.78	-0.06795	13.64	0.07504	14.5	-0.01212
12.8	-0.07707	13.66	0.1146	14.52	-0.01309
12.82	-0.0862	13.68	0.07769	14.54	-0.01407
12.84	-0.09533	13.7	0.04078	14.56	-0.05274
12.86	-0.06276	13.72	0.00387	14.58	-0.02544
12.88	-0.03018	13.74	0.00284	14.6	0.00186
12.9	0.00239	13.76	0.00182	14.62	0.02916
12.92	0.03496	13.78	-0.05513	14.64	0.05646
12.94	0.04399	13.8	0.04732	14.66	0.08376
12.96	0.05301	13.82	0.05223	14.68	0.01754
12.98	0.03176	13.84	0.05715	14.7	-0.04869
13	0.01051	13.86	0.06206	14.72	-0.02074
13.02	-0.01073	13.88	0.06698	14.74	0.00722
13.04	-0.03198	13.9	0.07189	14.76	0.03517
13.06	-0.05323	13.92	0.02705	14.78	-0.00528
13.08	0.00186	13.94	-0.01779	14.8	-0.04572
13.1	0.05696	13.96	-0.06263	14.82	-0.08617
13.12	0.01985	13.98	-0.10747	14.84	-0.0696
13.14	-0.01726	14	-0.15232	14.86	-0.05303
13.16	-0.05438	14.02	-0.12591	14.88	-0.03646
13.18	-0.01204	14.04	-0.0995	14.9	-0.01989
13.2	0.03031	14.06	-0.07309	14.92	-0.00332
13.22	0.07265	14.08	-0.04668	14.94	0.01325
13.24	0.11499	14.1	-0.02027	14.96	0.02982
13.26	0.07237	14.12	0.00614	14.98	0.01101
13.28	0.02975	14.14	0.03255	15	-0.00781
13.3	-0.01288	14.16	0.00859	15.02	-0.02662
13.32	0.01212	14.18	-0.01537	15.04	-0.00563
13.34	0.03711	14.2	-0.03932	15.06	0.01536
13.36	0.03517	14.22	-0.06328	15.08	0.03635
13.38	0.03323	14.24	-0.03322	15.1	0.05734
13.4	0.01853	14.26	-0.00315	15.12	0.03159
13.42	0.00383	14.28	0.02691	15.14	0.00584
13.44	0.00342	14.3	0.01196	15.16	-0.01992

Time (sec)	Acceleration (G)	Time (sec)	Acceleration (G)	Time (sec)	Acceleration (G)
15.18	-0.00201	16.04	-0.0448	16.9	0.01656
15.2	0.01589	16.06	-0.01083	16.92	0.0359
15.22	-0.01024	16.08	-0.01869	16.94	0.05525
15.24	-0.03636	16.1	-0.02655	16.96	0.07459
15.26	-0.06249	16.12	-0.03441	16.98	0.06203
15.28	-0.0478	16.14	-0.02503	17	0.04948
15.3	-0.03311	16.16	-0.01564	17.02	0.03692
15.32	-0.04941	16.18	-0.00626	17.04	-0.00145
15.34	-0.0657	16.2	-0.01009	17.06	0.04599
15.36	-0.082	16.22	-0.01392	17.08	0.04079
15.38	-0.0498	16.24	0.0149	17.1	0.03558
15.4	-0.0176	16.26	0.04372	17.12	0.03037
15.42	0.0146	16.28	0.03463	17.14	0.03626
15.44	0.0468	16.3	0.02098	17.16	0.04215
15.46	0.079	16.32	0.00733	17.18	0.04803
15.48	0.0475	16.34	-0.00632	17.2	0.05392
15.5	0.016	16.36	-0.01997	17.22	0.04947
15.52	-0.0155	16.38	0.00767	17.24	0.04502
15.54	-0.00102	16.4	0.03532	17.26	0.04056
15.56	0.01347	16.42	0.03409	17.28	0.03611
15.58	0.02795	16.44	0.03287	17.3	0.03166
15.6	0.04244	16.46	0.03164	17.32	0.00614
15.62	0.05692	16.48	0.02403	17.34	-0.01937
15.64	0.03781	16.5	0.01642	17.36	-0.04489
15.66	0.0187	16.52	0.00982	17.38	-0.0704
15.68	-0.00041	16.54	0.00322	17.4	-0.09592
15.7	-0.01952	16.56	-0.00339	17.42	-0.07745
15.72	-0.00427	16.58	0.02202	17.44	-0.05899
15.74	0.01098	16.6	-0.01941	17.46	-0.04052
15.76	0.02623	16.62	-0.06085	17.48	-0.02206
15.78	0.04148	16.64	-0.10228	17.5	-0.00359
15.8	0.01821	16.66	-0.07847	17.52	0.01487
15.82	-0.00506	16.68	-0.05466	17.54	0.01005
15.84	-0.00874	16.7	-0.03084	17.56	0.00523
15.86	-0.03726	16.72	-0.00703	17.58	0.00041
15.88	-0.06579	16.74	0.01678	17.6	-0.00441
15.9	-0.026	16.76	0.01946	17.62	-0.00923
15.92	0.0138	16.78	0.02214	17.64	-0.01189
15.94	0.05359	16.8	0.02483	17.66	-0.01523
15.96	0.09338	16.82	0.01809	17.68	-0.01856
15.98	0.05883	16.84	-0.00202	17.7	-0.0219
16	0.02429	16.86	-0.02213	17.72	-0.00983
16.02	-0.01026	16.88	-0.00278	17.74	0.00224

Time (sec)	Acceleration (G)	Time (sec)	Acceleration (G)	Time (sec)	Acceleration (G)
17.76	0.01431	18.62	0.06708	19.48	-0.04117
17.78	0.00335	18.64	0.0482	19.5	-0.06699
17.8	-0.0076	18.66	0.02932	19.52	-0.05207
17.82	-0.01856	18.68	0.01043	19.54	-0.03715
17.84	-0.00737	18.7	-0.00845	19.56	-0.02222
17.86	0.00383	18.72	-0.02733	19.58	-0.0073
17.88	0.01502	18.74	-0.04621	19.6	0.00762
17.9	0.02622	18.76	-0.03155	19.62	0.02254
17.92	0.01016	18.78	-0.01688	19.64	0.03747
17.94	-0.0059	18.8	-0.00222	19.66	0.04001
17.96	-0.02196	18.82	0.01244	19.68	0.04256
17.98	-0.00121	18.84	0.02683	19.7	0.04507
18	0.01953	18.86	0.04121	19.72	0.04759
18.02	0.04027	18.88	0.05559	19.74	0.0501
18.04	0.02826	18.9	0.03253	19.76	0.04545
18.06	0.01625	18.92	0.00946	19.78	0.0408
18.08	0.00424	18.94	-0.0136	19.8	0.02876
18.1	0.00196	18.96	-0.01432	19.82	0.01671
18.12	-0.00031	18.98	-0.01504	19.84	0.00467
18.14	-0.00258	19	-0.01576	19.86	-0.00738
18.16	-0.00486	19.02	-0.04209	19.88	-0.00116
18.18	-0.00713	19.04	-0.02685	19.9	0.00506
18.2	-0.00941	19.06	-0.01161	19.92	0.01128
18.22	-0.01168	19.08	0.00363	19.94	0.0175
18.24	-0.01396	19.1	0.01887	19.96	-0.00211
18.26	-0.0175	19.12	0.03411	19.98	-0.02173
18.28	-0.02104	19.14	0.03115	20	-0.04135
18.3	-0.02458	19.16	0.02819	20.02	-0.06096
18.32	-0.02813	19.18	0.02917	20.04	-0.08058
18.34	-0.03167	19.2	0.03015	20.06	-0.06995
18.36	-0.03521	19.22	0.03113	20.08	-0.05931
18.38	-0.04205	19.24	0.00388	20.1	-0.04868
18.4	-0.04889	19.26	-0.02337	20.12	-0.03805
18.42	-0.03559	19.28	-0.05062	20.14	-0.02557
18.44	-0.02229	19.3	-0.0382	20.16	-0.0131
18.46	-0.00899	19.32	-0.02579	20.18	-0.00063
18.48	0.00431	19.34	-0.01337	20.2	0.01185
18.5	0.01762	19.36	-0.00095	20.22	0.02432
18.52	0.00714	19.38	0.01146	20.24	0.0368
18.54	-0.00334	19.4	0.02388	20.26	0.04927
18.56	-0.01383	19.42	0.03629	20.28	0.02974
18.58	0.01314	19.44	0.01047	20.3	0.01021
18.6	0.04011	19.46	-0.01535	20.32	-0.00932

Time (sec)	Acceleration (G)	Time (sec)	Acceleration (G)	Time (sec)	Acceleration (G)
20.34	-0.02884	21.2	-0.02272	22.06	0.03958
20.36	-0.04837	21.22	-0.00843	22.08	0.05866
20.38	-0.0679	21.24	0.00587	22.1	0.03556
20.4	-0.04862	21.26	0.02017	22.12	0.01245
20.42	-0.02934	21.28	0.02698	22.14	-0.01066
20.44	-0.01006	21.3	0.03379	22.16	-0.03376
20.46	0.00922	21.32	0.04061	22.18	-0.05687
20.48	0.02851	21.34	0.04742	22.2	-0.04502
20.5	0.04779	21.36	0.05423	22.22	-0.03317
20.52	0.02456	21.38	0.03535	22.24	-0.02131
20.54	0.00133	21.4	0.01647	22.26	-0.00946
20.56	-0.0219	21.42	0.01622	22.28	0.00239
20.58	-0.04513	21.44	0.01598	22.3	-0.00208
20.6	-0.06836	21.46	0.01574	22.32	-0.00654
20.62	-0.04978	21.48	0.00747	22.34	-0.01101
20.64	-0.0312	21.5	-0.0008	22.36	-0.01548
20.66	-0.01262	21.52	-0.00907	22.38	-0.012
20.68	0.00596	21.54	0.00072	22.4	-0.00851
20.7	0.02453	21.56	0.01051	22.42	-0.00503
20.72	0.04311	21.58	0.0203	22.44	-0.00154
20.74	0.06169	21.6	0.03009	22.46	0.00195
20.76	0.08027	21.62	0.03989	22.48	0.00051
20.78	0.09885	21.64	0.03478	22.5	-0.00092
20.8	0.06452	21.66	0.02967	22.52	0.01135
20.82	0.03019	21.68	0.02457	22.54	0.02363
20.84	-0.00414	21.7	0.03075	22.56	0.0359
20.86	-0.03848	21.72	0.03694	22.58	0.04818
20.88	-0.07281	21.74	0.04313	22.6	0.06045
20.9	-0.05999	21.76	0.04931	22.62	0.07273
20.92	-0.04717	21.78	0.0555	22.64	0.02847
20.94	-0.03435	21.8	0.06168	22.66	-0.01579
20.96	-0.03231	21.82	-0.00526	22.68	-0.06004
20.98	-0.03028	21.84	-0.0722	22.7	-0.05069
21	-0.02824	21.86	-0.06336	22.72	-0.04134
21.02	-0.00396	21.88	-0.05451	22.74	-0.03199
21.04	0.02032	21.9	-0.04566	22.76	-0.03135
21.06	0.00313	21.92	-0.03681	22.78	-0.03071
21.08	-0.01406	21.94	-0.03678	22.8	-0.03007
21.1	-0.03124	21.96	-0.03675	22.82	-0.01863
21.12	-0.04843	21.98	-0.03672	22.84	-0.00719
21.14	-0.06562	22	-0.01765	22.86	0.00425
21.16	-0.05132	22.02	0.00143	22.88	0.0157
21.18	-0.03702	22.04	0.02051	22.9	0.02714

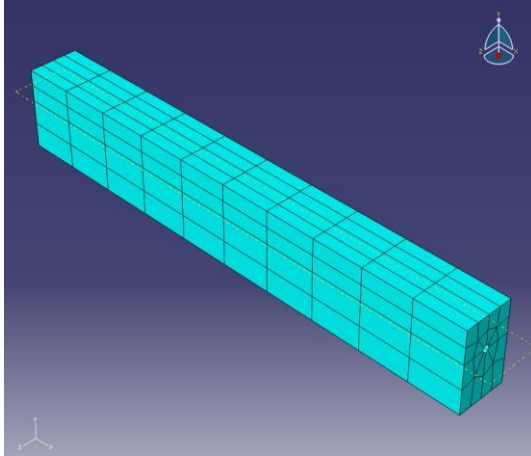
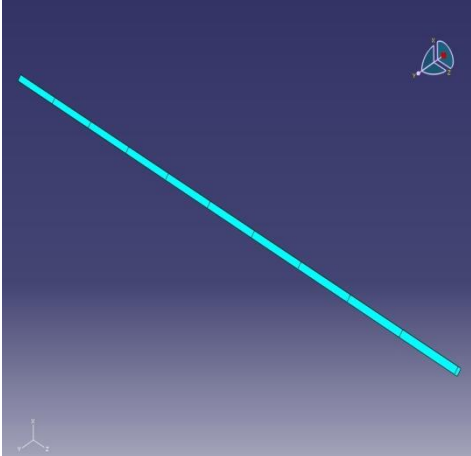
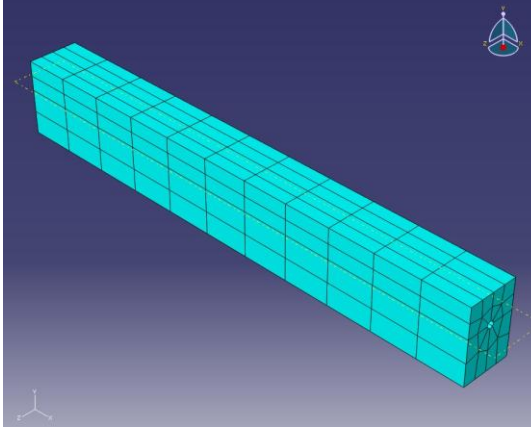
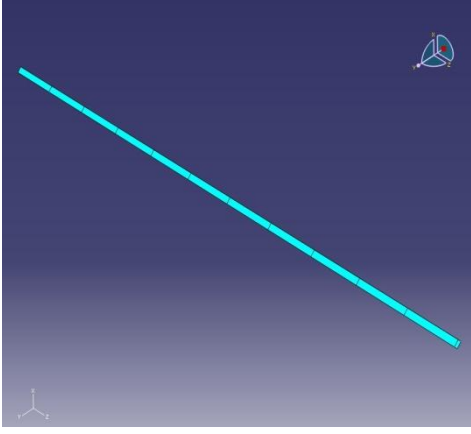
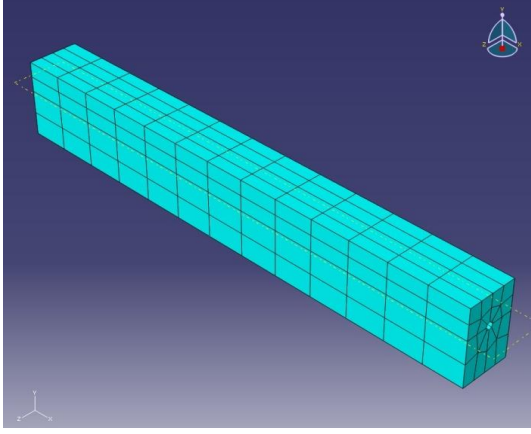
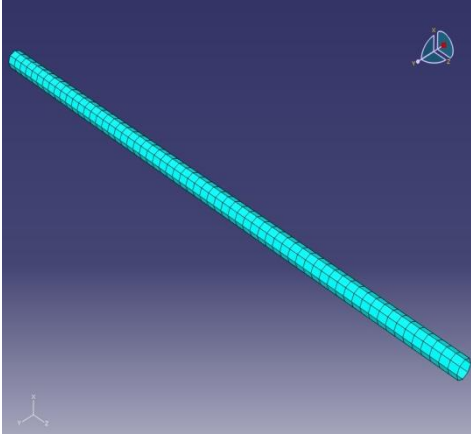
Time (sec)	Acceleration (G)	Time (sec)	Acceleration (G)	Time (sec)	Acceleration (G)
22.92	0.03858	23.78	-0.041	24.64	-0.06528
22.94	0.02975	23.8	-0.05703	24.66	-0.04628
22.96	0.02092	23.82	-0.0292	24.68	-0.02728
22.98	0.02334	23.84	-0.00137	24.7	-0.00829
23	0.02576	23.86	0.02645	24.72	0.01071
23.02	0.02819	23.88	0.05428	24.74	0.0297
23.04	0.03061	23.9	0.03587	24.76	0.03138
23.06	0.03304	23.92	0.01746	24.78	0.03306
23.08	0.01371	23.94	-0.00096	24.8	0.03474
23.1	-0.00561	23.96	-0.01937	24.82	0.03642
23.12	-0.02494	23.98	-0.03778	24.84	0.04574
23.14	-0.02208	24	-0.02281	24.86	0.05506
23.16	-0.01923	24.02	-0.00784	24.88	0.06439
23.18	-0.01638	24.04	0.00713	24.9	0.07371
23.2	-0.01353	24.06	0.0221	24.92	0.08303
23.22	-0.01261	24.08	0.03707	24.94	0.03605
23.24	-0.0117	24.1	0.05204	24.96	-0.01092
23.26	-0.00169	24.12	0.06701	24.98	-0.0579
23.28	0.00833	24.14	0.08198	25	-0.04696
23.3	0.01834	24.16	0.03085	25.02	-0.03602
23.32	0.02835	24.18	-0.02027	25.04	-0.02508
23.34	0.03836	24.2	-0.0714	25.06	-0.01414
23.36	0.04838	24.22	-0.12253	25.08	-0.03561
23.38	0.03749	24.24	-0.08644	25.1	-0.05708
23.4	0.0266	24.26	-0.05035	25.12	-0.07855
23.42	0.01571	24.28	-0.01426	25.14	-0.06304
23.44	0.00482	24.3	0.02183	25.16	-0.04753
23.46	-0.00607	24.32	0.05792	25.18	-0.03203
23.48	-0.01696	24.34	0.094	25.2	-0.01652
23.5	-0.0078	24.36	0.13009	25.22	-0.00102
23.52	0.00136	24.38	0.03611	25.24	0.00922
23.54	0.01052	24.4	-0.05787	25.26	0.01946
23.56	0.01968	24.42	-0.04802	25.28	0.0297
23.58	0.02884	24.44	-0.03817	25.3	0.03993
23.6	-0.00504	24.46	-0.02832	25.32	0.05017
23.62	-0.03893	24.48	-0.01846	25.34	0.06041
23.64	-0.02342	24.5	-0.00861	25.36	0.07065
23.66	-0.00791	24.52	-0.03652	25.38	0.08089
23.68	0.00759	24.54	-0.06444	25.4	-0.00192
23.7	0.0231	24.56	-0.06169	25.42	-0.08473
23.72	0.00707	24.58	-0.05894	25.44	-0.07032
23.74	-0.00895	24.6	-0.05618	25.46	-0.0559
23.76	-0.02498	24.62	-0.06073	25.48	-0.04148

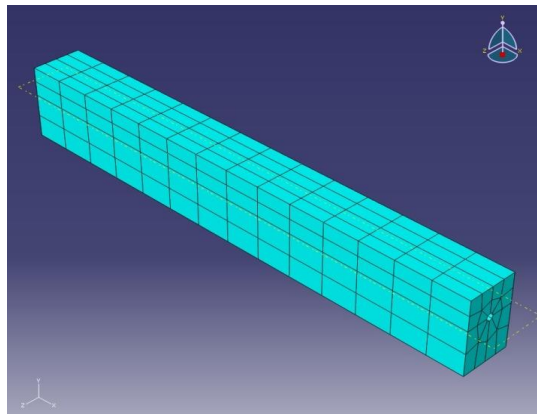
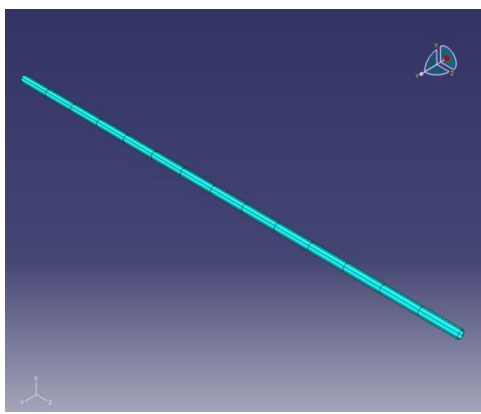
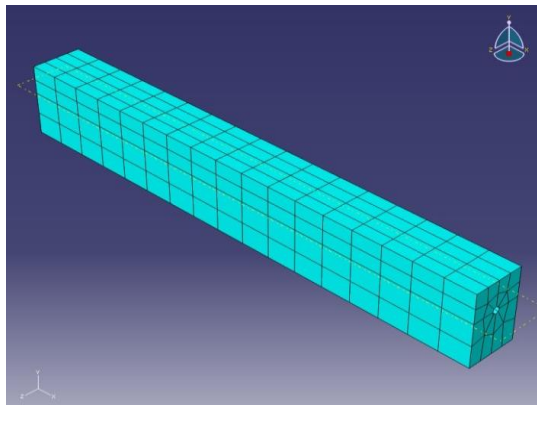
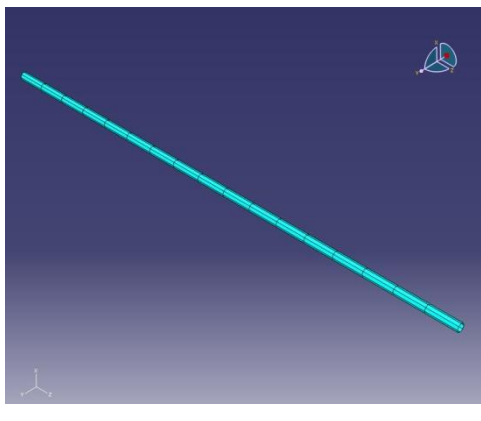
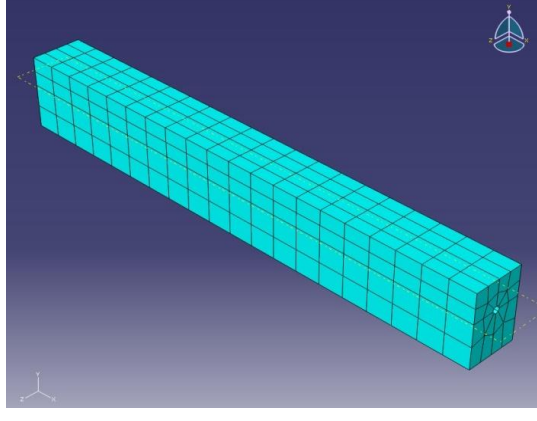
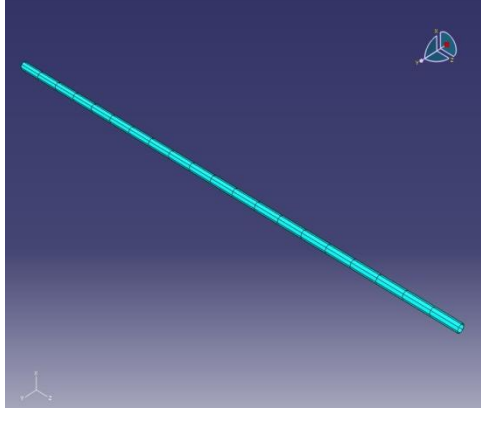
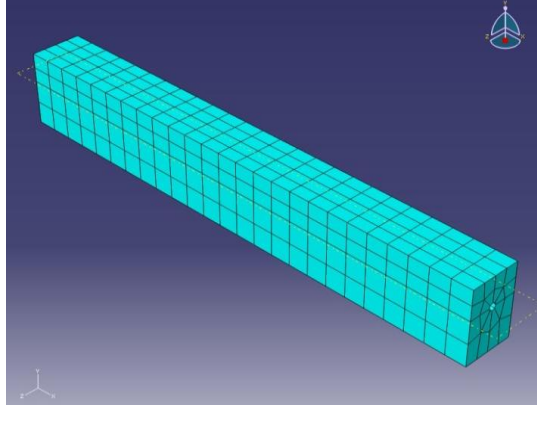
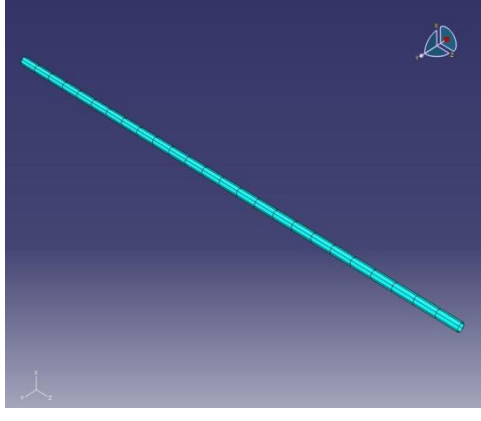
Time (sec)	Acceleration (G)	Time (sec)	Acceleration (G)	Time (sec)	Acceleration (G)
25.5	-0.05296	26.36	0.03056	27.22	0.01537
25.52	-0.06443	26.38	0.02107	27.24	0.02251
25.54	-0.0759	26.4	0.01158	27.26	0.01713
25.56	-0.08738	26.42	0.0078	27.28	0.01175
25.58	-0.09885	26.44	0.00402	27.3	0.00637
25.6	-0.06798	26.46	0.00024	27.32	0.01376
25.62	-0.0371	26.48	-0.00354	27.34	0.02114
25.64	-0.00623	26.5	-0.00732	27.36	0.02852
25.66	0.02465	26.52	-0.0111	27.38	0.03591
25.68	0.05553	26.54	-0.0078	27.4	0.04329
25.7	0.0864	26.56	-0.0045	27.42	0.03458
25.72	0.11728	26.58	-0.0012	27.44	0.02587
25.74	0.14815	26.6	0.0021	27.46	0.01715
25.76	0.08715	26.62	0.0054	27.48	0.00844
25.78	0.02615	26.64	-0.00831	27.5	-0.00027
25.8	-0.03485	26.66	-0.02203	27.52	-0.00898
25.82	-0.09584	26.68	-0.03575	27.54	-0.00126
25.84	-0.071	26.7	-0.04947	27.56	0.00645
25.86	-0.04616	26.72	-0.06319	27.58	0.01417
25.88	-0.02132	26.74	-0.05046	27.6	0.02039
25.9	0.00353	26.76	-0.03773	27.62	0.02661
25.92	0.02837	26.78	-0.025	27.64	0.03283
25.94	0.05321	26.8	-0.01227	27.66	0.03905
25.96	-0.00469	26.82	0.00046	27.68	0.04527
25.98	-0.06258	26.84	0.00482	27.7	0.03639
26	-0.12048	26.86	0.00919	27.72	0.0275
26.02	-0.0996	26.88	0.01355	27.74	0.01862
26.04	-0.07872	26.9	0.01791	27.76	0.00974
26.06	-0.05784	26.92	0.02228	27.78	0.00086
26.08	-0.03696	26.94	0.00883	27.8	-0.01333
26.1	-0.01608	26.96	-0.00462	27.82	-0.02752
26.12	0.0048	26.98	-0.01807	27.84	-0.04171
26.14	0.02568	27	-0.03152	27.86	-0.02812
26.16	0.04656	27.02	-0.02276	27.88	-0.01453
26.18	0.06744	27.04	-0.01401	27.9	-0.00094
26.2	0.08832	27.06	-0.00526	27.92	0.01264
26.22	0.1092	27.08	0.0035	27.94	0.02623
26.24	0.13008	27.1	0.01225	27.96	0.0169
26.26	0.10995	27.12	0.02101	27.98	0.00756
26.28	0.08982	27.14	0.01437	28	-0.00177
26.3	0.06969	27.16	0.00773	28.02	-0.01111
26.32	0.04955	27.18	0.0011	28.04	-0.02044
26.34	0.04006	27.2	0.00823	28.06	-0.02977

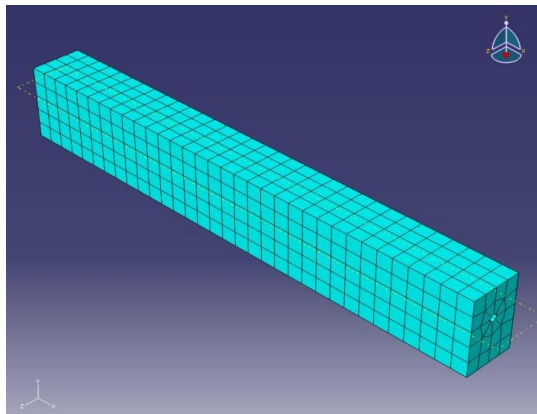
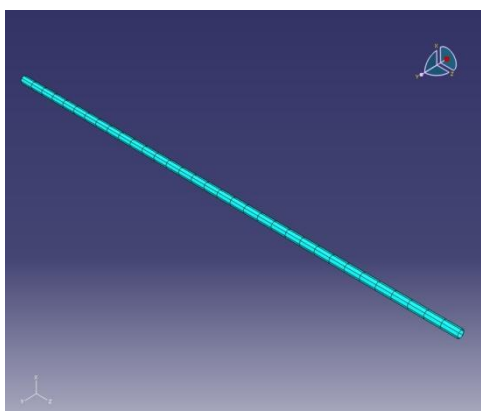
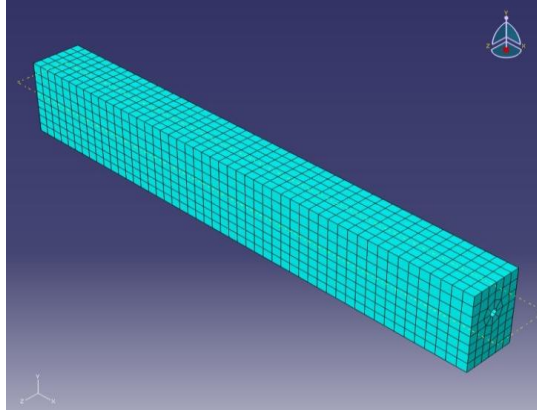
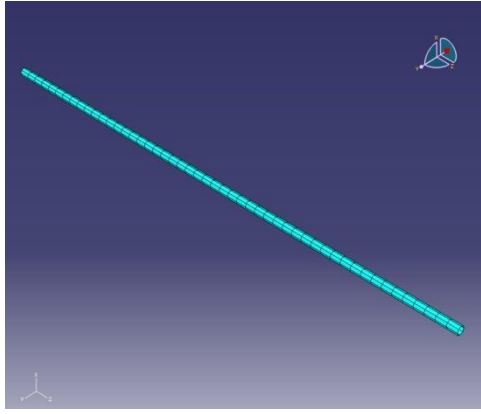
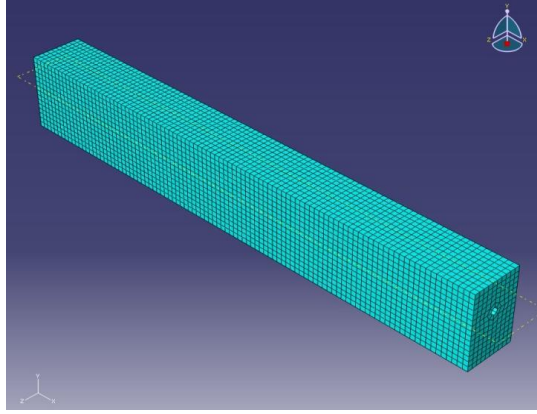
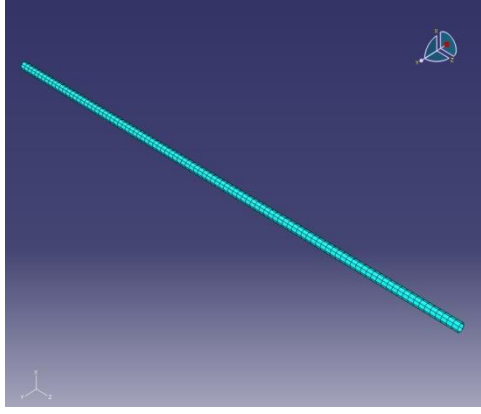
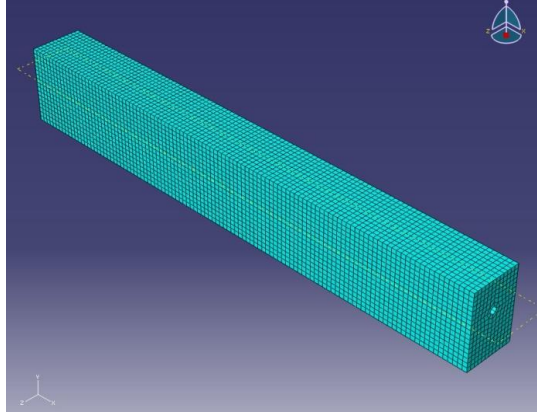
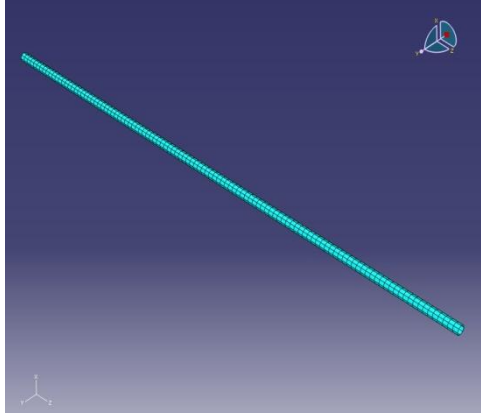
Time (sec)	Acceleration (G)	Time (sec)	Acceleration (G)	Time (sec)	Acceleration (G)
28.08	-0.03911	28.94	0.00876	29.8	-0.00431
28.1	-0.02442	28.96	0.00768	29.82	-0.00425
28.12	-0.00973	28.98	0.00661	29.84	-0.00418
28.14	0.00496	29	0.01234	29.86	-0.00412
28.16	0.01965	29.02	0.01807	29.88	-0.00406
28.18	0.03434	29.04	0.0238	29.9	-0.00399
28.2	0.02054	29.06	0.02953	29.92	-0.00393
28.22	0.00674	29.08	0.03526	29.94	-0.00387
28.24	-0.00706	29.1	0.02784	29.96	-0.0038
28.26	-0.02086	29.12	0.02042	29.98	-0.00374
28.28	-0.03466	29.14	0.013	30	-0.00368
28.3	-0.02663	29.16	-0.03415	30.02	-0.00361
28.32	-0.0186	29.18	-0.00628	30.04	-0.00355
28.34	-0.01057	29.2	-0.00621	30.06	-0.00349
28.36	-0.00254	29.22	-0.00615	30.08	-0.00342
28.38	-0.00063	29.24	-0.00609	30.1	-0.00336
28.4	0.00128	29.26	-0.00602	30.12	-0.0033
28.42	0.00319	29.28	-0.00596	30.14	-0.00323
28.44	0.0051	29.3	-0.0059	30.16	-0.00317
28.46	0.00999	29.32	-0.00583	30.18	-0.00311
28.48	0.01488	29.34	-0.00577	30.2	-0.00304
28.5	0.00791	29.36	-0.00571	30.22	-0.00298
28.52	0.00093	29.38	-0.00564	30.24	-0.00292
28.54	-0.00605	29.4	-0.00558	30.26	-0.00285
28.56	0.00342	29.42	-0.00552	30.28	-0.00279
28.58	0.01288	29.44	-0.00545	30.3	-0.00273
28.6	0.02235	29.46	-0.00539	30.32	-0.00266
28.62	0.03181	29.48	-0.00532	30.34	-0.0026
28.64	0.04128	29.5	-0.00526	30.36	-0.00254
28.66	0.02707	29.52	-0.0052	30.38	-0.00247
28.68	0.01287	29.54	-0.00513	30.4	-0.00241
28.7	-0.00134	29.56	-0.00507	30.42	-0.00235
28.72	-0.01554	29.58	-0.00501	30.44	-0.00228
28.74	-0.02975	29.6	-0.00494	30.46	-0.00222
28.76	-0.04395	29.62	-0.00488	30.48	-0.00216
28.78	-0.03612	29.64	-0.00482	30.5	-0.00209
28.8	-0.02828	29.66	-0.00475	30.52	-0.00203
28.82	-0.02044	29.68	-0.00469	30.54	-0.00197
28.84	-0.0126	29.7	-0.00463	30.56	-0.0019
28.86	-0.00476	29.72	-0.00456	30.58	-0.00184
28.88	0.00307	29.74	-0.0045	30.6	-0.00178
28.9	0.01091	29.76	-0.00444	30.62	-0.00171
28.92	0.00984	29.78	-0.00437	30.64	-0.00165

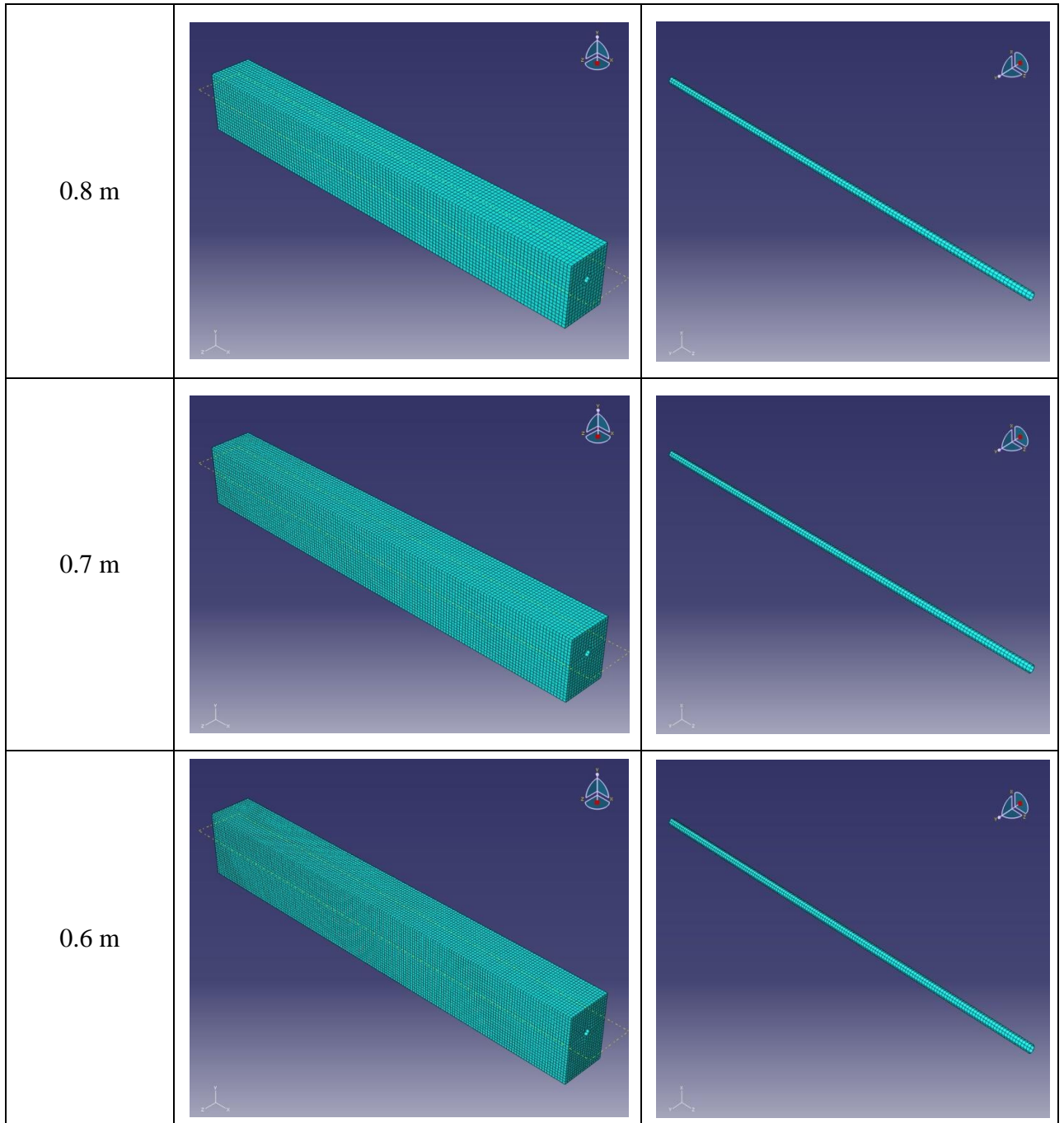
Time (sec)	Acceleration (G)	Time (sec)	Acceleration (G)	Time (sec)	Acceleration (G)
30.66	-0.00158				
30.68	-0.00152				
30.7	-0.00146				
30.72	-0.00139				
30.74	-0.00133				
30.76	-0.00127				
30.78	-0.0012				
30.8	-0.00114				
30.82	-0.00108				
30.84	-0.00101				
30.86	-0.00095				
30.88	-0.00089				
30.9	-0.00082				
30.92	-0.00076				
30.94	-0.0007				
30.96	-0.00063				
30.98	-0.00057				
31	-0.00051				
31.02	-0.00044				
31.04	-0.00038				
31.06	-0.00032				
31.08	-0.00025				
31.1	-0.00019				
31.12	-0.00013				
31.14	-0.00006				
31.16	0				
31.18	0				

Appendix B – applied meshes according to the different approximate global sizes

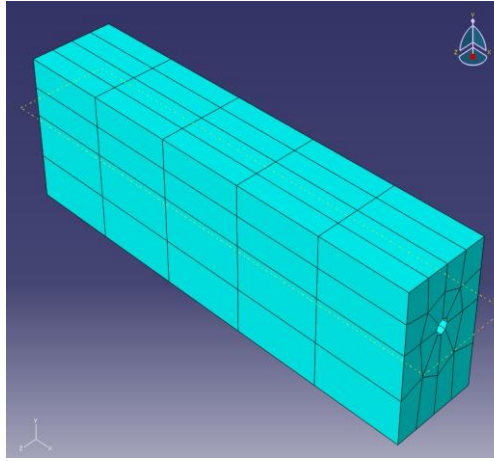
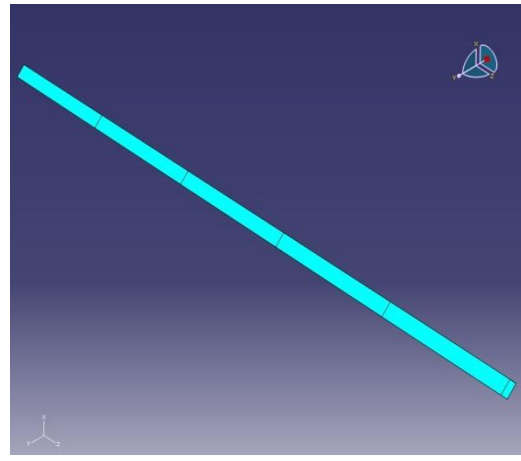
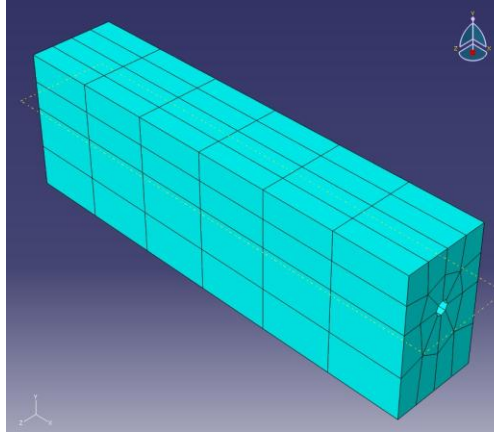
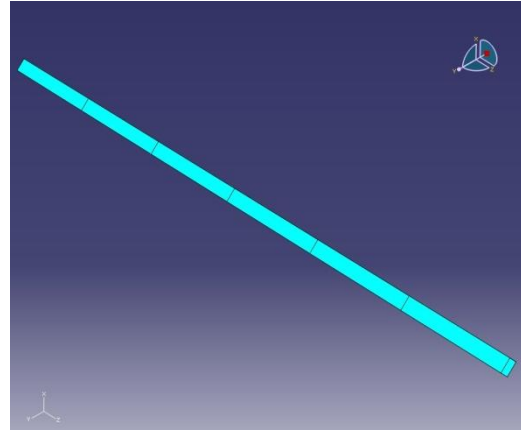
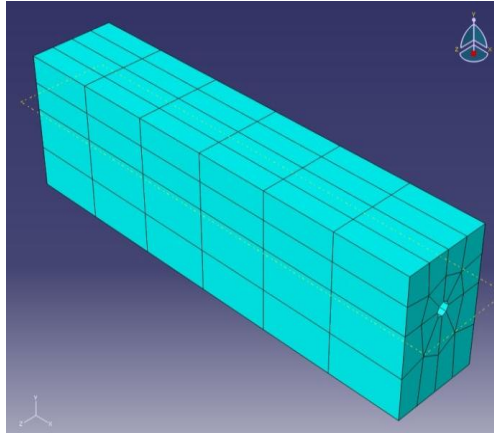
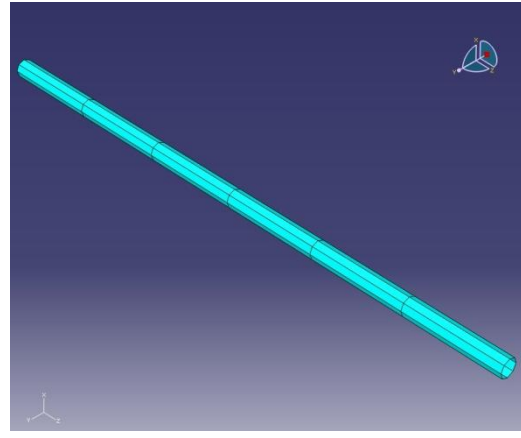
Approximate global size of meshed elements	Soil	Pipeline
10 m		
9 m		
8 m		

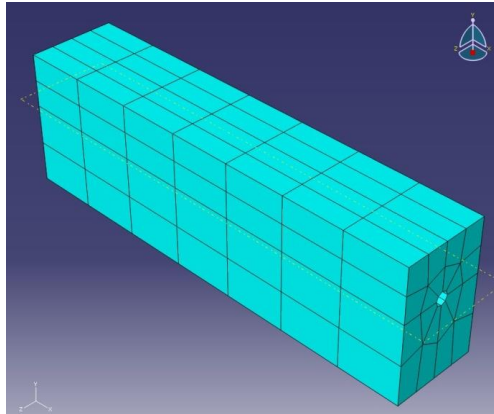
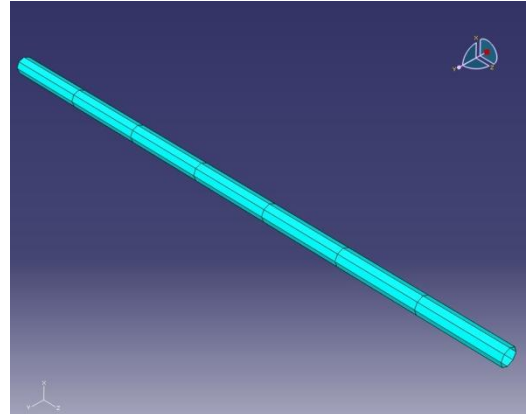
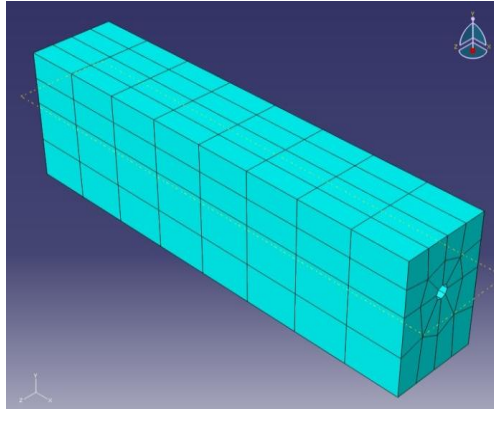
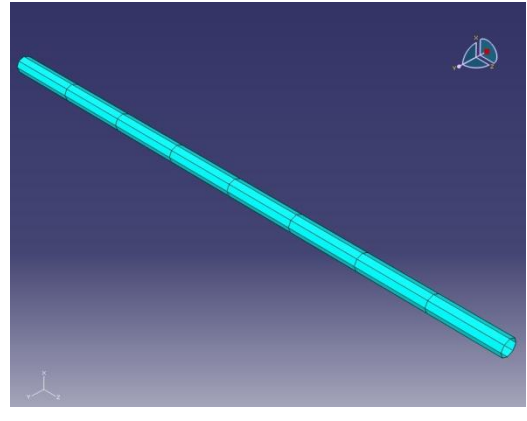
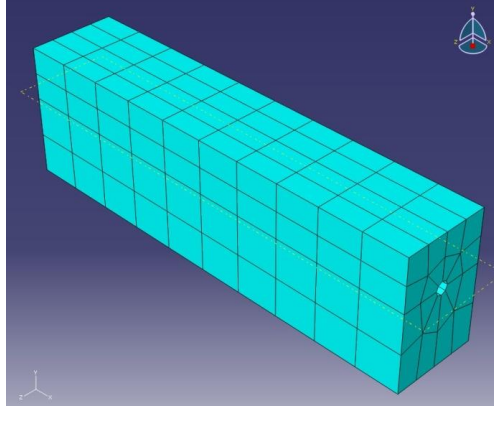
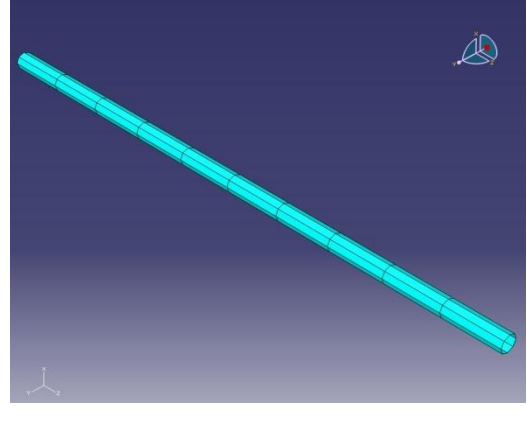
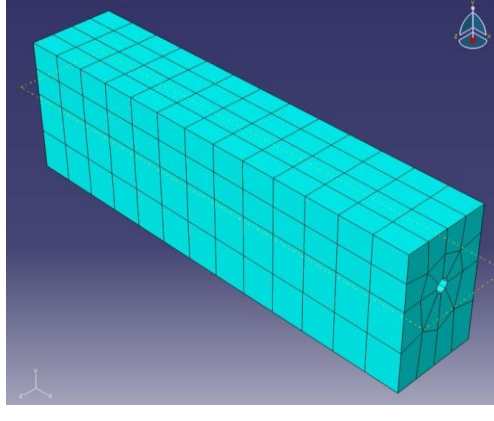
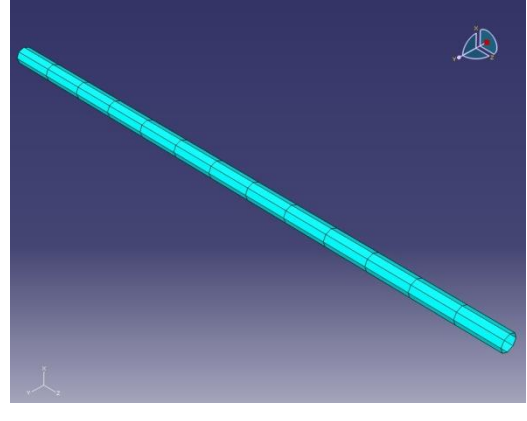
<p>7 m</p>		
<p>6 m</p>		
<p>5 m</p>		
<p>4 m</p>		

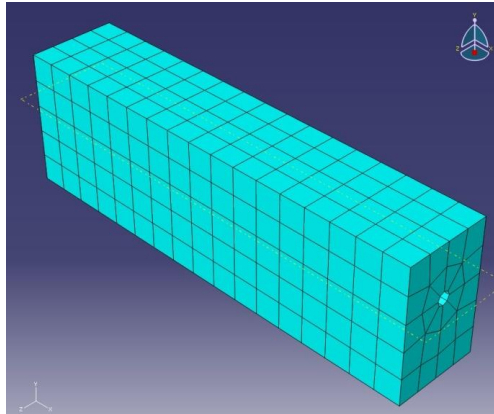
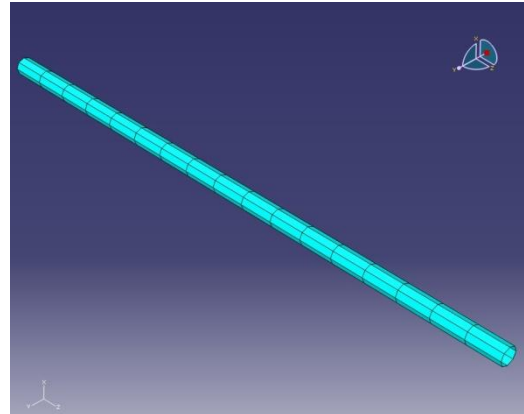
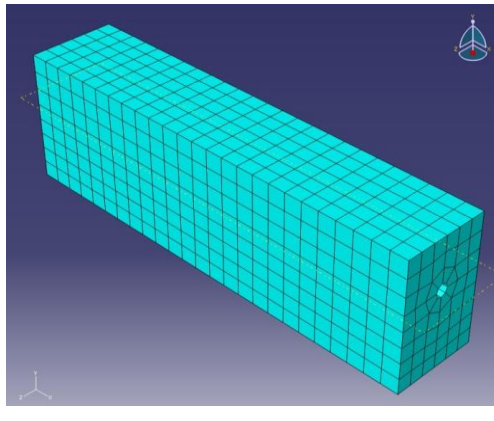
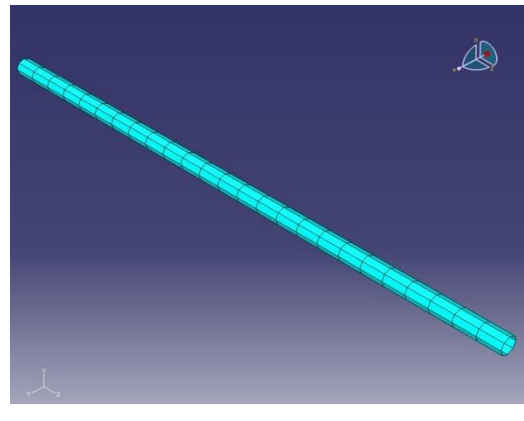
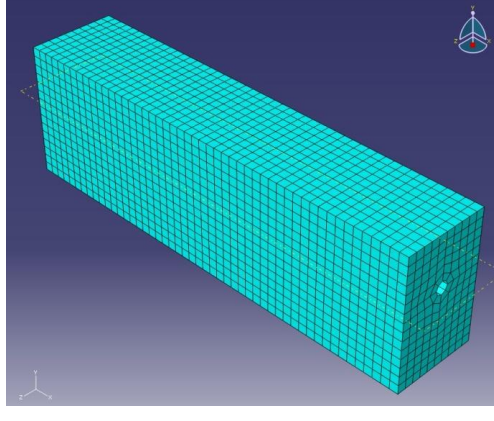
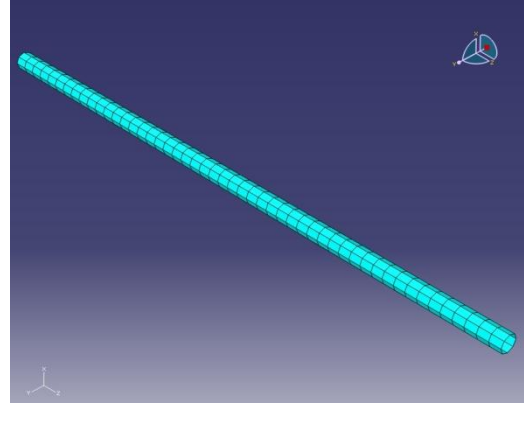
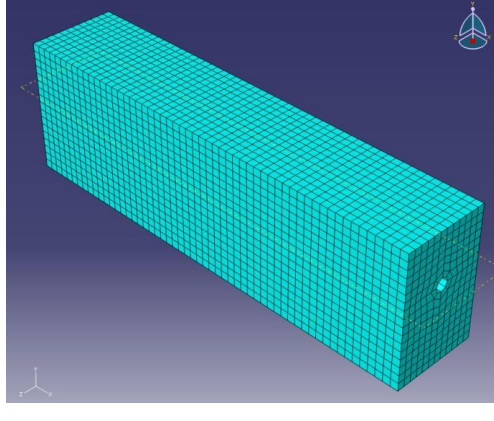
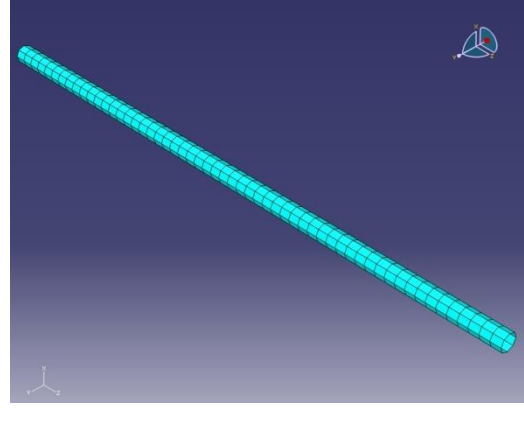
<p>3 m</p>		
<p>2 m</p>		
<p>1 m</p>		
<p>0.9 m</p>		

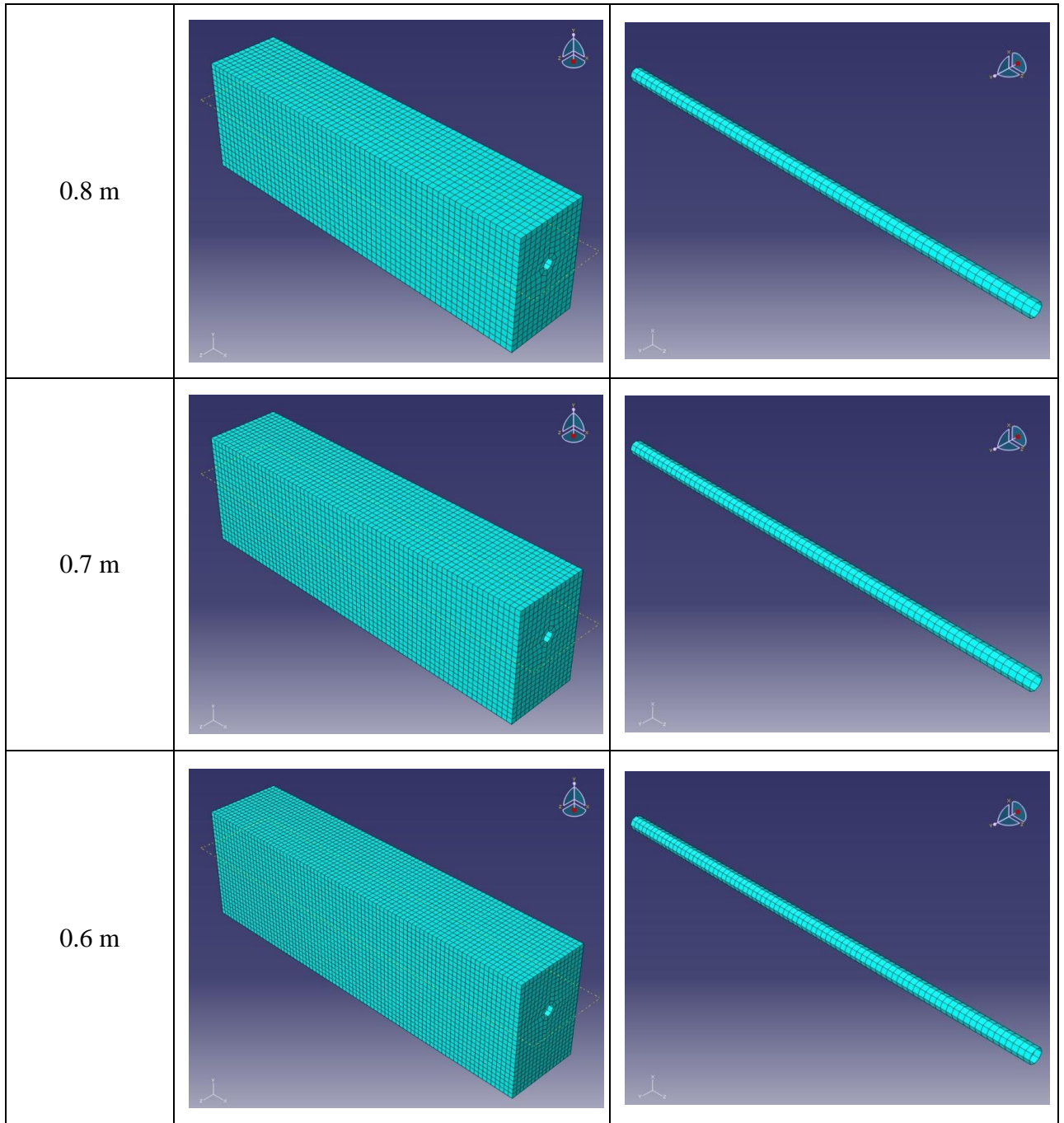


Appendix. B. 1. Applied meshes according to the different approximate global sizes of elements in 100 m models

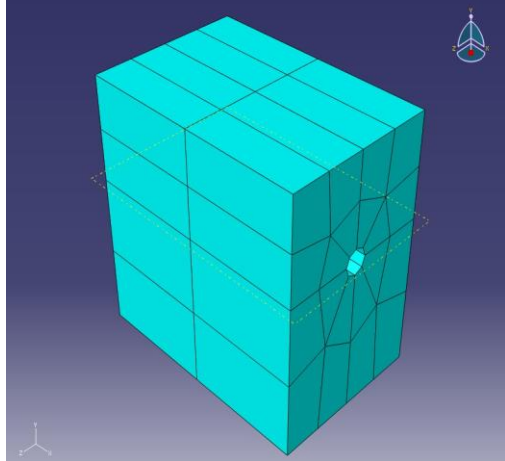
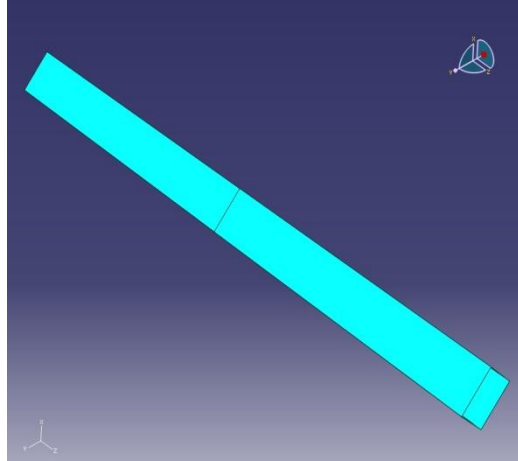
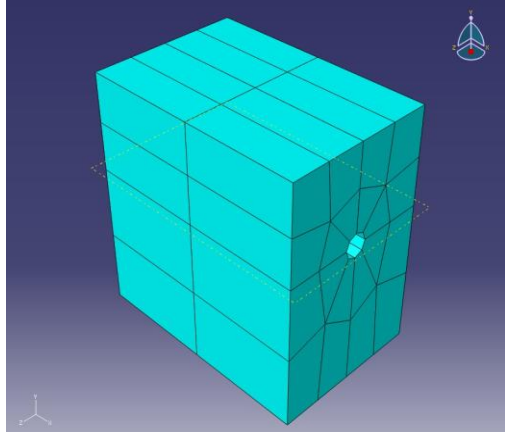
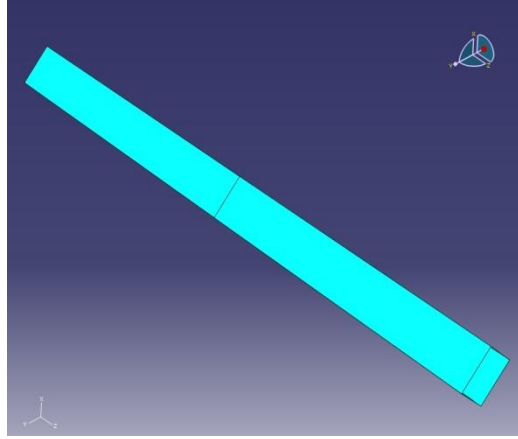
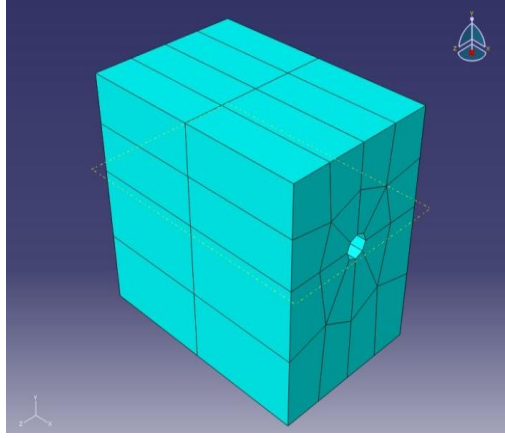
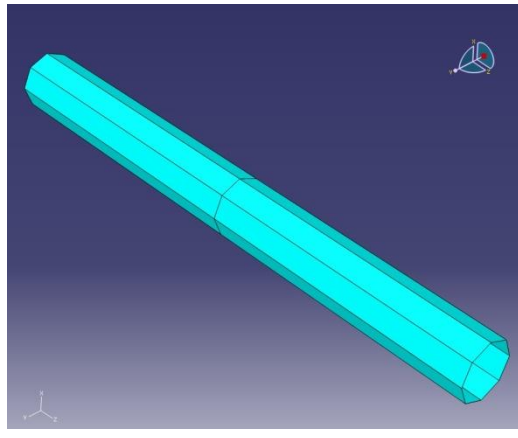
Approximate global size of meshed elements	Soil	Pipeline
10 m	 <p>A 3D perspective view of a rectangular soil block meshed with cyan elements. The mesh is composed of approximately 10x10x10 elements. A small 3D coordinate system icon is visible in the top right corner of the image.</p>	 <p>A 3D perspective view of a long, thin cylindrical pipeline meshed with cyan elements. The mesh consists of approximately 10 segments along the length. A small 3D coordinate system icon is visible in the top right corner of the image.</p>
9 m	 <p>A 3D perspective view of a rectangular soil block meshed with cyan elements. The mesh is composed of approximately 9x9x9 elements. A small 3D coordinate system icon is visible in the top right corner of the image.</p>	 <p>A 3D perspective view of a long, thin cylindrical pipeline meshed with cyan elements. The mesh consists of approximately 9 segments along the length. A small 3D coordinate system icon is visible in the top right corner of the image.</p>
8 m	 <p>A 3D perspective view of a rectangular soil block meshed with cyan elements. The mesh is composed of approximately 8x8x8 elements. A small 3D coordinate system icon is visible in the top right corner of the image.</p>	 <p>A 3D perspective view of a long, thin cylindrical pipeline meshed with cyan elements. The mesh consists of approximately 8 segments along the length. A small 3D coordinate system icon is visible in the top right corner of the image.</p>

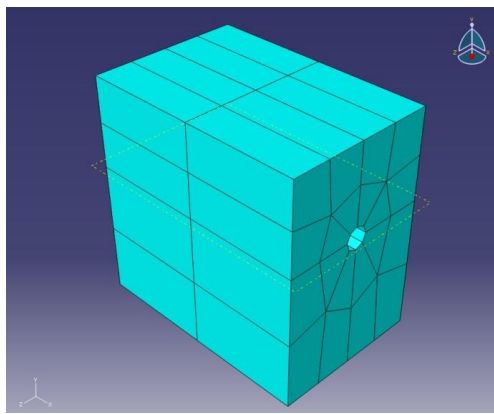
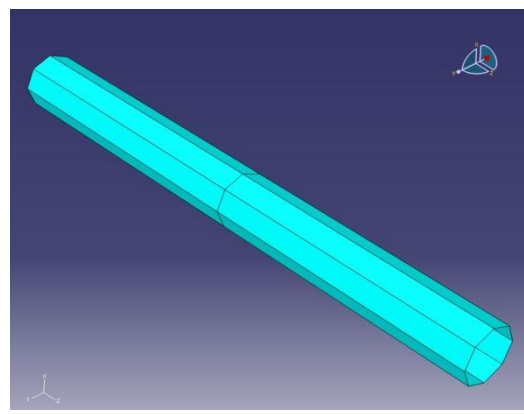
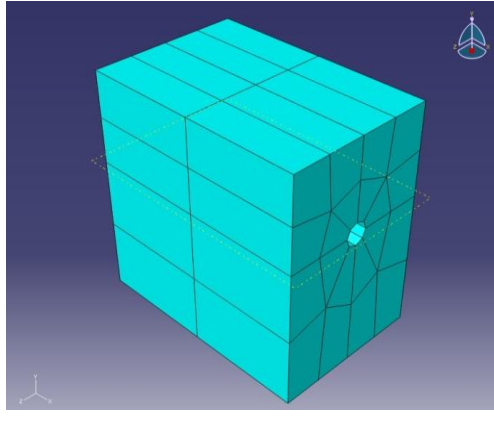
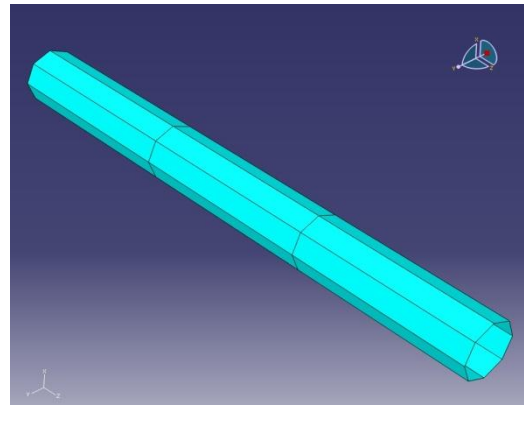
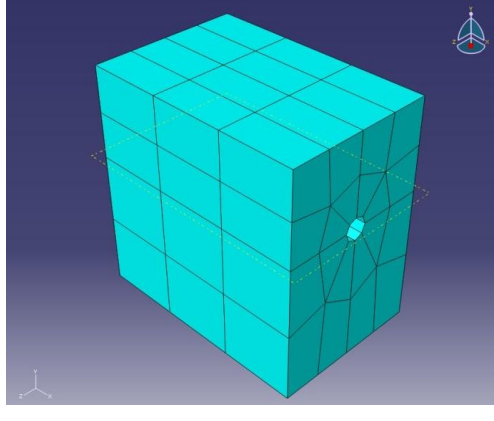
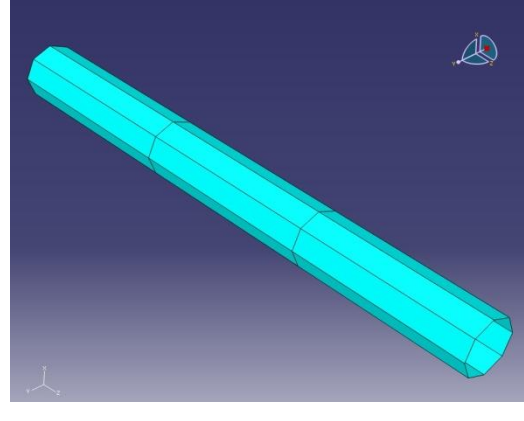
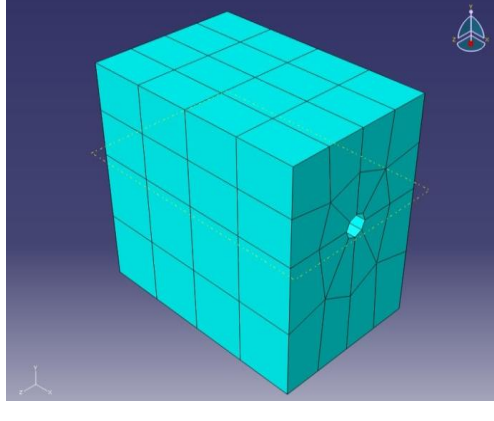
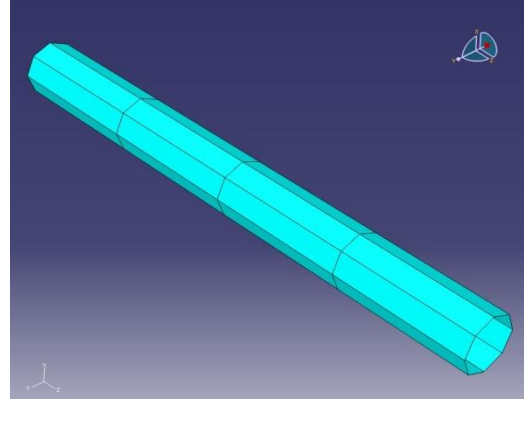
<p>7 m</p>		
<p>6 m</p>		
<p>5 m</p>		
<p>4 m</p>		

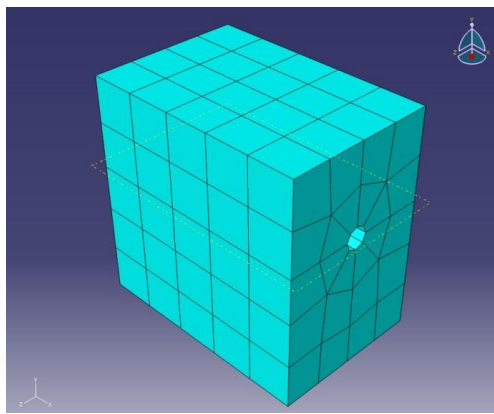
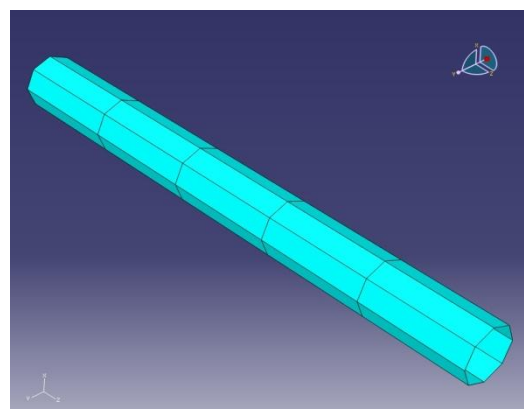
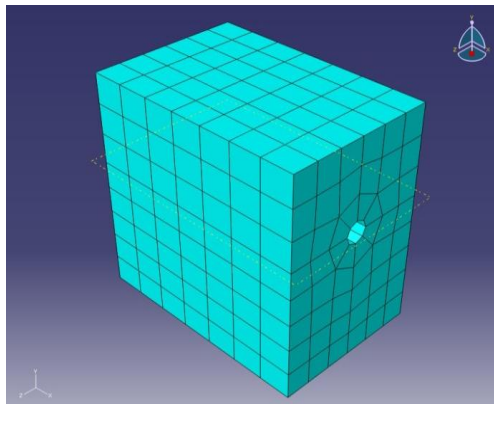
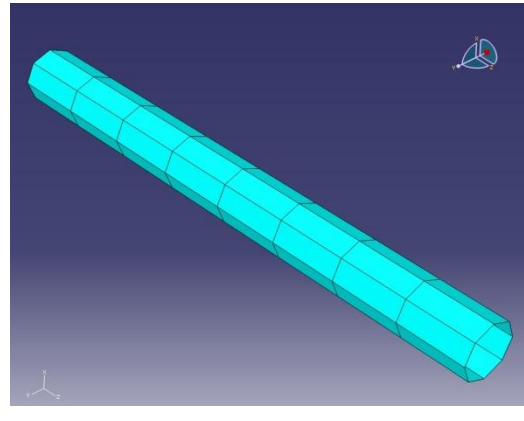
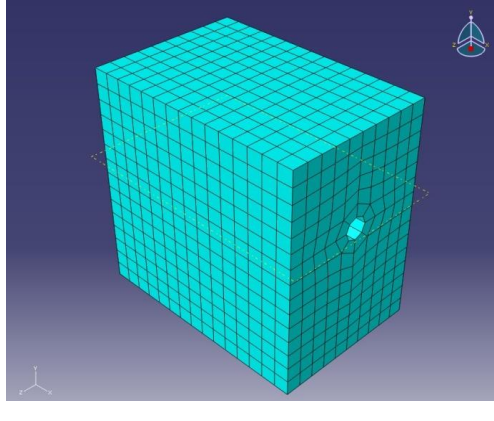
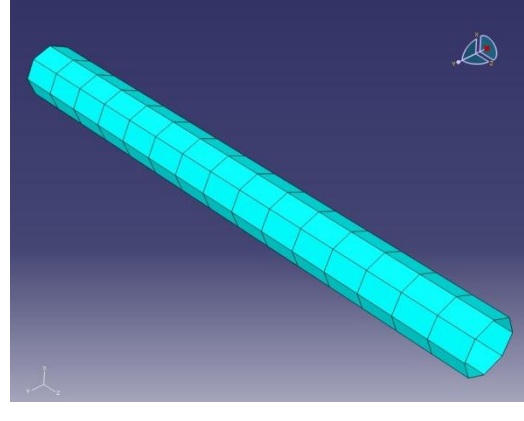
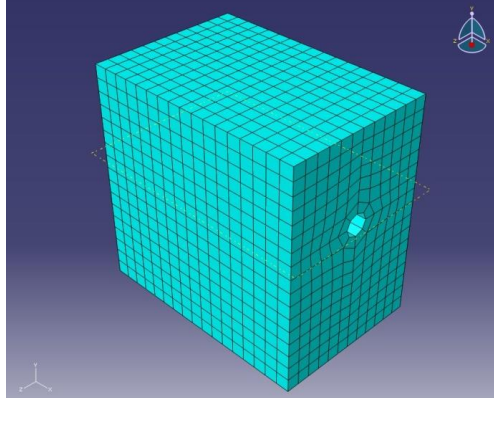
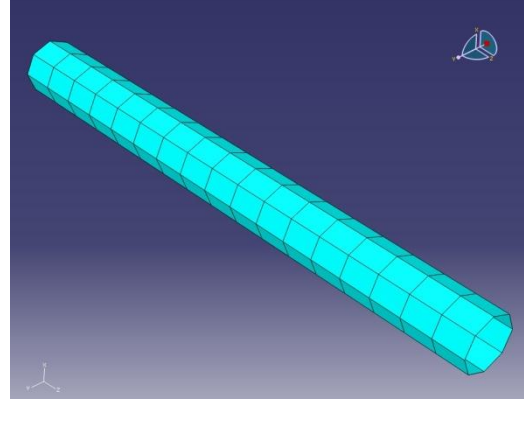
<p>3 m</p>		
<p>2 m</p>		
<p>1 m</p>		
<p>0.9 m</p>		

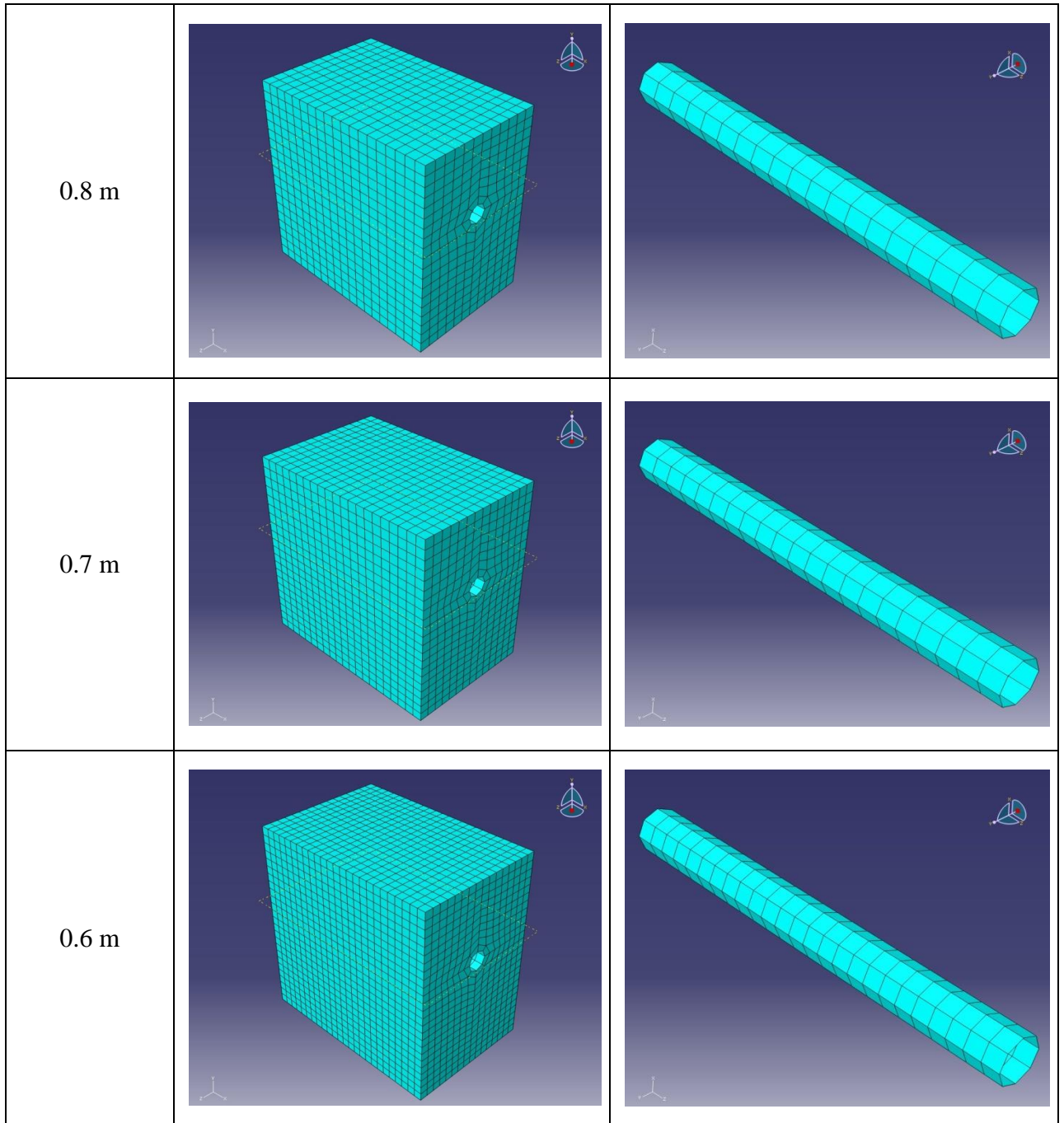


Appendix. B. 2. Applied meshes according to the different approximate global sizes of elements in 50 m models

Approximate global size of meshed elements	Soil	Pipeline
10 m		
9 m		
8 m		

<p>7 m</p>		
<p>6 m</p>		
<p>5 m</p>		
<p>4 m</p>		

<p>3 m</p>	 <p>A 3D visualization of a cube with a side length of 3 meters. The cube is discretized into a coarse mesh of approximately 3x3x3 elements. A circular hole is present on the front face, with a mesh refinement around its perimeter. A 3D coordinate system is shown in the bottom-left corner, and a rotation handle is in the top-right corner.</p>	 <p>A 3D visualization of a cylinder with a length of 3 meters. The cylinder is discretized into a coarse mesh of approximately 10 segments along its length. A 3D coordinate system is shown in the bottom-left corner, and a rotation handle is in the top-right corner.</p>
<p>2 m</p>	 <p>A 3D visualization of a cube with a side length of 2 meters. The cube is discretized into a medium mesh of approximately 4x4x4 elements. A circular hole is present on the front face, with a mesh refinement around its perimeter. A 3D coordinate system is shown in the bottom-left corner, and a rotation handle is in the top-right corner.</p>	 <p>A 3D visualization of a cylinder with a length of 2 meters. The cylinder is discretized into a medium mesh of approximately 15 segments along its length. A 3D coordinate system is shown in the bottom-left corner, and a rotation handle is in the top-right corner.</p>
<p>1 m</p>	 <p>A 3D visualization of a cube with a side length of 1 meter. The cube is discretized into a fine mesh of approximately 8x8x8 elements. A circular hole is present on the front face, with a mesh refinement around its perimeter. A 3D coordinate system is shown in the bottom-left corner, and a rotation handle is in the top-right corner.</p>	 <p>A 3D visualization of a cylinder with a length of 1 meter. The cylinder is discretized into a fine mesh of approximately 25 segments along its length. A 3D coordinate system is shown in the bottom-left corner, and a rotation handle is in the top-right corner.</p>
<p>0.9 m</p>	 <p>A 3D visualization of a cube with a side length of 0.9 meters. The cube is discretized into a very fine mesh of approximately 10x10x10 elements. A circular hole is present on the front face, with a mesh refinement around its perimeter. A 3D coordinate system is shown in the bottom-left corner, and a rotation handle is in the top-right corner.</p>	 <p>A 3D visualization of a cylinder with a length of 0.9 meters. The cylinder is discretized into a very fine mesh of approximately 30 segments along its length. A 3D coordinate system is shown in the bottom-left corner, and a rotation handle is in the top-right corner.</p>



Appendix. B. 3. Applied meshes according to the different approximate global sizes of elements in 15 m models

Appendix C – calculated data for mesh study

Approximate global size of element (m)	Number of element		Total number of Elements	Maximum displacement (U)		Mises equivalent stress	
	Soil (No)	Pipeline (No)		Soil (cm)	Pipeline (cm)	Soil (MPa)	Pipeline (MPa)
10	200	40	240	-	-	-	-
9	220	44	264	-	-	-	-
8	260	104	364	69.96	47.88	1.009	490
7	280	112	392	69.95	47.95	1.011	490
6	340	136	476	69.9	48.07	1.015	490
5	400	160	560	69.93	48.14	1.02	490
4	500	200	700	69.9	48.05	1.024	478.3
3	792	264	1056	69.86	47.8	1.056	432.5
2	2600	400	3000	69.57	47.43	1.1	449.3
1	15400	800	16200	69.63	47.29	1.188	402.9
0.9	23088	888	23976	69.7	47.25	1.209	402.7
0.8	29000	1000	30000	69.66	47.29	1.219	404.9
0.7	42614	1144	43758	69.67	47.25	1.244	396.9
0.6	67486	1336	68822	69.64	47.26	1.267	394.1

Appendix. C. 1. Calculated data for mesh study by ABAQUS
 - Linear interpolation element in 100 m model
 (General moist sandy soil: C3D8R + pipeline: S4R)

Approximate global size of element (m)	Number of element		Total number of Elements	Maximum displacement (U)		Mises equivalent stress	
	Soil (No)	Pipeline (No)		Soil (cm)	Pipeline (cm)	Soil (MPa)	Pipeline (MPa)
10	200	40	240	-	-	-	-
9	220	44	264	-	-	-	-
8	260	104	364	69.98	48.1	1.348	613.3
7	280	112	392	69.98	48.11	1.35	611.3
6	340	136	476	69.97	48.1	1.357	604.6
5	400	160	560	69.96	48.08	1.362	598.3
4	500	200	700	69.96	48.06	1.37	599
3	792	264	1056	69.86	47.92	1.394	598.5
2	2600	400	3000	69.78	47.75	1.571	592.7
1	15400	800	16200	69.76	47.52	1.682	538.3
0.9	23088	888	23976	-	-	-	-
0.8	29000	1000	30000	-	-	-	-
0.7	42614	1144	43758	-	-	-	-
0.6	67486	1336	68822	-	-	-	-

Appendix. C. 2. Calculated data for mesh study by ABAQUS
 - Quadratic interpolation element in 100 m model
 (General moist sandy soil: C3D20R + pipeline: S8R)

Approximate global size of element (m)	Number of element		Total number of Elements	Maximum displacement (U)		Mises equivalent stress	
	Soil (No)	Pipeline (No)		Soil (cm)	Pipeline (cm)	Soil (MPa)	Pipeline (MPa)
10	200	40	240	17.29	10.02	0.9608	6.722
9	220	44	264	17.3	10.01	0.9628	6.878
8	260	104	364	16.39	11.91	0.9124	197.4
7	280	112	392	16.38	11.84	0.9124	197.6
6	340	136	476	16.4	11.74	0.9125	195.4
5	400	160	560	16.4	11.73	0.9133	193.1
4	500	200	700	16.39	11.75	0.9143	188.5
3	792	264	1056	16.37	11.66	0.9363	159.4
2	2600	400	3000	16.33	11.45	0.9932	174.9
1	15400	800	16200	16.37	11.41	1.098	167.6
0.9	23088	888	23976	16.38	11.4	1.127	165
0.8	29000	1000	30000	16.38	11.41	1.139	161.4
0.7	42614	1144	43758	16.37	11.38	1.173	155.7
0.6	67486	1336	68822	16.37	11.4	1.199	154.4
Appendix. C. 3. Calculated data for mesh study by ABAQUS - Linear interpolation element in 100 m model (Fully saturated sandy soil: C3D8R + pipeline: S4R)							

Approximate global size of element (m)	Number of element		Total number of Elements	Maximum displacement (U)		Mises equivalent stress	
	Soil (No)	Pipeline (No)		Soil (cm)	Pipeline (cm)	Soil (MPa)	Pipeline (MPa)
10	200	40	240	16.64	11.75	1.819	203.6
9	220	44	264	16.64	11.74	1.82	204.2
8	260	104	364	16.37	11.42	1.364	161
7	280	112	392	16.36	11.41	1.36	159.6
6	340	136	476	16.35	11.36	1.347	158.4
5	400	160	560	16.35	11.33	1.336	159.1
4	500	200	700	16.35	11.32	1.332	168.1
3	792	264	1056	16.35	11.32	1.349	183.8
2	2600	400	3000	16.35	11.32	1.407	201.8
1	15400	800	16200	16.35	11.31	1.472	243.4
0.9	23088	888	23976	-	-	-	-
0.8	29000	1000	30000	-	-	-	-
0.7	42614	1144	43758	-	-	-	-
0.6	67486	1336	68822	-	-	-	-
Appendix. C. 4. Calculated data for mesh study by ABAQUS - Quadratic interpolation element in 100 m model (Fully saturated sandy soil: C3D20R + pipeline: S8R)							

Approximate global size of element (m)	Number of element		Total number of Elements	Maximum displacement (U)		Mises equivalent stress	
	Soil (No)	Pipeline (No)		Soil (cm)	Pipeline (cm)	Soil (MPa)	Pipeline (MPa)
10	200	40	240	85.01	48.59	0.9383	6.763
9	220	44	264	85.05	48.58	0.9403	6.898
8	260	104	364	50.29	54.84	0.8929	490
7	280	112	392	80.28	54.98	0.8943	490
6	340	136	476	80.31	55.09	0.8974	490
5	400	160	560	80.31	55.15	0.9008	490
4	500	200	700	80.27	55.02	0.9043	481.3
3	792	264	1056	80.24	54.63	0.9277	452.1
2	2600	400	3000	80.06	54.2	0.9879	468.7
1	15400	800	16200	79.91	53.99	1.088	423.4
0.9	23088	888	23976	79.88	53.94	1.117	423.4
0.8	29000	1000	30000	79.88	53.93	1.126	422.4
0.7	42614	1144	43758	79.88	53.92	1.158	417.7
0.6	67486	1336	68822	79.89	53.9	1.182	412.7

Appendix. C. 5. Calculated data for mesh study by ABAQUS
- Linear interpolation element in 100 m model
(General moist cohesive soil: C3D8R + pipeline: S4R)

Approximate global size of element (m)	Number of element		Total number of Elements	Maximum displacement (U)		Mises equivalent stress	
	Soil (No)	Pipeline (No)		Soil (cm)	Pipeline (cm)	Soil (MPa)	Pipeline (MPa)
10	200	40	240	81.46	55.81	1.821	760.1
9	220	44	264	81.44	55.75	1.82	757.6
8	260	104	364	79.84	53.76	1.378	564.2
7	280	112	392	79.84	53.78	1.381	560.1
6	340	136	476	79.84	53.8	1.387	557.6
5	400	160	560	79.84	53.8	1.388	554.1
4	500	200	700	79.84	53.78	1.383	545.7
3	792	264	1056	79.86	53.84	1.371	549.9
2	2600	400	3000	79.89	53.93	1.487	536.8
1	15400	800	16200	79.97	54.01	1.55	524.9
0.9	23088	888	23976	-	-	-	-
0.8	29000	1000	30000	-	-	-	-
0.7	42614	1144	43758	-	-	-	-
0.6	67486	1336	68822	-	-	-	-

Appendix. C. 6. Calculated data for mesh study by ABAQUS
- Quadratic interpolation element in 100 m model
(General moist cohesive soil: C3D20R + pipeline: S8R)

Approximate global size of element (m)	Number of element		Total number of Elements	Maximum displacement (U)		Mises equivalent stress	
	Soil (No)	Pipeline (No)		Soil (cm)	Pipeline (cm)	Soil (MPa)	Pipeline (MPa)
10	200	40	240	12.05	6.075	0.5131	7.936
9	220	44	264	12.08	6.06	0.5188	8.254
8	260	104	364	10.24	7.127	0.2461	98.27
7	280	112	392	10.23	7.098	0.2463	97.94
6	340	136	476	10.23	7.051	0.2468	97.23
5	400	160	560	10.23	7.079	0.2475	95.94
4	500	200	700	10.23	7.087	0.2481	93.87
3	792	264	1056	10.23	7.074	0.2529	84.57
2	2600	400	3000	10.21	6.987	0.2668	94.48
1	15400	800	16200	10.19	6.947	0.291	85.16
0.9	23088	888	23976	10.18	6.937	0.2985	82.88
0.8	29000	1000	30000	10.18	6.939	0.3003	82.25
0.7	42614	1144	43758	10.18	6.93	0.3076	80.51
0.6	67486	1336	68822	10.18	6.929	0.3131	78.9

Appendix. C. 7. Calculated data for mesh study by ABAQUS
- Linear interpolation element in 100 m model
(Fully saturated cohesive soil: C3D8R + pipeline: S4R)

Approximate global size of element (m)	Number of element		Total number of Elements	Maximum displacement (U)		Mises equivalent stress	
	Soil (No)	Pipeline (No)		Soil (cm)	Pipeline (cm)	Soil (MPa)	Pipeline (MPa)
10	200	40	240	10.62	7.317	1.099	120.2
9	220	44	264	10.62	7.31	1.096	119.7
8	260	104	364	10.19	6.943	0.3927	102.7
7	280	112	392	10.18	6.936	0.3903	102.5
6	340	136	476	10.18	6.914	0.3841	101.4
5	400	160	560	10.18	6.899	0.3866	100.3
4	500	200	700	10.18	6.896	0.3893	101.9
3	792	264	1056	10.18	6.906	0.3823	99.7
2	2600	400	3000	10.16	6.892	0.4202	141.1
1	15400	800	16200	10.16	6.875	0.4753	109.9
0.9	23088	888	23976	-	-	-	-
0.8	29000	1000	30000	-	-	-	-
0.7	42614	1144	43758	-	-	-	-
0.6	67486	1336	68822	-	-	-	-

Appendix. C. 8. Calculated data for mesh study by ABAQUS
- Quadratic element in 100 m model
(Fully saturated cohesive soil: C3D20R + pipeline: S8R)

Approximate global size of element (m)	Number of element		Total number of Elements	Maximum displacement (U)		Mises equivalent stress	
	Soil (No)	Pipeline (No)		Soil (cm)	Pipeline (cm)	Soil (MPa)	Pipeline (MPa)
10	100	20	120	78.5	48.16	1.281	490
9	120	24	144	-	-	-	-
8	120	48	168	74.17	53.32	1.356	490
7	140	56	196	70.58	49	1.371	490
6	160	64	224	73.45	50.35	1.426	490
5	200	80	280	72.38	48.36	1.484	490
4	260	104	364	70.47	48.1	1.559	490
3	408	136	544	70.24	47.8	1.614	490
2	1300	200	1500	69.74	47.63	2.002	490
1	7700	400	8100	-	-	-	-
0.9	11648	448	12096	-	-	-	-
0.8	14616	504	15120	-	-	-	-
0.7	21158	568	21726	-	-	-	-
0.6	33532	664	34196	-	-	-	-

Appendix. C. 9. Calculated data for mesh study by ABAQUS
- Linear interpolation element in 50 m model
(General moist sandy soil: C3D8R + pipeline: S4R)

Approximate global size of element (m)	Number of element		Total number of Elements	Maximum displacement (U)		Mises equivalent stress	
	Soil (No)	Pipeline (No)		Soil (cm)	Pipeline (cm)	Soil (MPa)	Pipeline (MPa)
10	100	20	120	-	-	-	-
9	120	24	144	-	-	-	-
8	120	48	168	70.24	48.52	3.143	938.5
7	140	56	196	70.27	48.55	3.209	938.8
6	160	64	224	70.2	48.55	3.258	938.3
5	200	80	280	70.18	48.48	3.327	934.7
4	260	104	364	70.21	48.35	3.45	948.3
3	408	136	544	70.09	48.25	3.513	933.9
2	1300	200	1500	-	-	-	-
1	7700	400	8100	-	-	-	-
0.9	11648	448	12096	-	-	-	-
0.8	14616	504	15120	-	-	-	-
0.7	21158	568	21726	-	-	-	-
0.6	33532	664	34196	-	-	-	-

Appendix. C. 10. Calculated data for mesh study by ABAQUS
- Quadratic interpolation element in 50 m model
(General moist sandy soil: C3D20R + pipeline: S8R)

Approximate global size of element (m)	Number of element		Total number of Elements	Maximum displacement (U)		Mises equivalent stress	
	Soil (No)	Pipeline (No)		Soil (cm)	Pipeline (cm)	Soil (MPa)	Pipeline (MPa)
10	100	20	120	17.53	10.55	1.207	252.8
9	120	24	144	20.62	11.8	1.157	272.4
8	120	48	168	18.11	12.75	1.39	486.1
7	140	56	196	16.6	12.12	1.424	490
6	160	64	224	17.16	12.04	1.475	490
5	200	80	280	16.69	11.69	1.549	490
4	260	104	364	16.5	11.66	1.631	490
3	408	136	544	16.44	11.53	1.716	490
2	1300	200	1500	16.34	11.42	2.176	490
1	7700	400	8100	-	-	-	-
0.9	11648	448	12096	-	-	-	-
0.8	14616	504	15120	-	-	-	-
0.7	21158	568	21726	-	-	-	-
0.6	33532	664	34196	-	-	-	-

Appendix. C. 11. Calculated data for mesh study by ABAQUS
- Linear interpolation element in 50 m model
(Fully saturated sandy soil: C3D8R + pipeline: S4R)

Approximate global size of element (m)	Number of element		Total number of Elements	Maximum displacement (U)		Mises equivalent stress	
	Soil (No)	Pipeline (No)		Soil (cm)	Pipeline (cm)	Soil (MPa)	Pipeline (MPa)
10	100	20	120	16.67	11.48	4.459	846.2
9	120	24	144	16.64	11.54	4.807	805.2
8	120	48	168	16.38	11.38	3.237	867
7	140	56	196	16.39	11.4	3.366	939.6
6	160	64	224	16.37	11.38	3.473	929.1
5	200	80	280	16.36	11.36	3.631	909.1
4	260	104	364	16.36	11.31	3.787	879
3	408	136	544	16.36	11.35	3.91	857.4
2	1300	200	1500	16.36	11.35	4.488	812.8
1	7700	400	8100	-	-	-	-
0.9	11648	448	12096	-	-	-	-
0.8	14616	504	15120	-	-	-	-
0.7	21158	568	21726	-	-	-	-
0.6	33532	664	34196	-	-	-	-

Appendix. C.12. Calculated data for mesh study by ABAQUS
- Quadratic interpolation element in 50 m model
(Fully saturated sandy soil: C3D20R + pipeline: S8R)

Approximate global size of element (m)	Number of element		Total number of Elements	Maximum displacement (U)		Mises equivalent stress	
	Soil (No)	Pipeline (No)		Soil (cm)	Pipeline (cm)	Soil (MPa)	Pipeline (MPa)
10	100	20	120	86.77	56.35	1.193	490
9	120	24	144	97.45	56.16	1.129	490
8	120	48	168	84.83	60.75	1.379	490
7	140	56	196	81.22	55.77	1.403	490
6	160	64	224	84.15	57.01	1.464	490
5	200	80	280	83.01	55.6	1.554	490
4	260	104	364	80.87	54.91	1.636	490
3	408	136	544	80.71	54.72	1.698	490
2	1300	200	1500	80.3	54.4	2.052	490
1	7700	400	8100	80.17	54.29	2.635	490
0.9	11648	448	12096	80.13	54.27	2.79	490
0.8	14616	504	15120	80.12	54.21	2.871	490
0.7	21158	568	21726	-	-	-	-
0.6	33532	664	34196	-	-	-	-

Appendix. C.13. Calculated data for mesh study by ABAQUS
- Linear interpolation element in 50 m model
(General moist cohesive soil: C3D8R + pipeline: S4R)

Approximate global size of element (m)	Number of element		Total number of Elements	Maximum displacement (U)		Mises equivalent stress	
	Soil (No)	Pipeline (No)		Soil (cm)	Pipeline (cm)	Soil (MPa)	Pipeline (MPa)
10	100	20	120	81.95	55.01	3.847	1025
9	120	24	144	81.73	55.75	4.06	1006
8	120	48	168	70.15	54.26	2.989	944.6
7	140	56	196	80.25	54.4	3.041	645.2
6	160	64	224	80.15	54.38	3.084	945.3
5	200	80	280	80.14	54.31	3.154	942.9
4	260	104	364	80.17	54.14	3.255	951.1
3	408	136	544	80.18	54.25	3.362	944.7
2	1300	200	1500	80.21	54.34	3.897	875.1
1	7700	400	8100	80.28	54.43	4.88	813.6
0.9	11648	448	12096	-	-	-	-
0.8	14616	504	15120	-	-	-	-
0.7	21158	568	21726	-	-	-	-
0.6	33532	664	34196	-	-	-	-

Appendix. C. 14. Calculated data for mesh study by ABAQUS
- Quadratic interpolation element in 50 m model
(General moist cohesive soil: C3D20R + pipeline: S8R)

Approximate global size of element (m)	Number of element		Total number of Elements	Maximum displacement (U)		Mises equivalent stress	
	Soil (No)	Pipeline (No)		Soil (cm)	Pipeline (cm)	Soil (MPa)	Pipeline (MPa)
10	100	20	120	15.19	6.878	0.6167	147.3
9	120	24	144	18.77	7.466	0.5268	155.8
8	120	48	168	10.72	8.357	0.4356	285.3
7	140	56	196	10.92	8.33	0.4471	304.8
6	160	64	224	10.71	8.137	0.4677	331.9
5	200	80	280	10.75	7.628	0.4959	381.5
4	260	104	364	10.52	7.59	0.5297	439.5
3	408	136	544	10.49	7.44	0.5633	490
2	1300	200	1500	10.43	7.387	0.7103	490
1	7700	400	8100	10.39	7.27	0.999	490
0.9	11648	448	12096	10.4	7.267	1.105	490
0.8	14616	504	15120	10.38	7.256	1.131	490
0.7	21158	568	21726	10.38	7.243	1.236	490
0.6	33532	664	34196	10.37	7.237	1.251	490

Appendix. C. 15. Calculated data for mesh study by ABAQUS
- Linear interpolation element in 50 m model
(Fully saturated cohesive soil: C3D8R + pipeline: S4R)

Approximate global size of element (m)	Number of element		Total number of Elements	Maximum displacement (U)		Mises equivalent stress	
	Soil (No)	Pipeline (No)		Soil (cm)	Pipeline (cm)	Soil (MPa)	Pipeline (MPa)
10	100	20	120	10.93	7.678	1.199	915.4
9	120	24	144	10.83	7.601	1.274	887.7
8	120	48	168	10.46	7.36	0.9937	822.9
7	140	56	196	10.39	7.192	1.039	809.4
6	160	64	224	10.42	7.275	1.076	770.1
5	200	80	280	10.39	7.276	1.131	796.2
4	260	104	364	10.39	7.247	1.194	754.9
3	408	136	544	10.39	7.231	1.263	715.8
2	1300	200	1500	10.37	7.215	1.442	667.5
1	7700	400	8100	10.36	7.184	2.539	622.5
0.9	11648	448	12096	-	-	-	-
0.8	14616	504	15120	-	-	-	-
0.7	21158	568	21726	-	-	-	-
0.6	33532	664	34196	-	-	-	-

Appendix. C. 16. Calculated data for mesh study by ABAQUS
- Quadratic element in 50 m model
(Fully saturated cohesive soil: C3D20R + pipeline: S8R)

Approximate global size of element (m)	Number of element		Total number of Elements	Maximum displacement (U)		Mises equivalent stress	
	Soil (No)	Pipeline (No)		Soil (cm)		Soil (No)	Pipeline (No)
10	40	8	48	-	10	40	8
9	40	8	48	-	9	40	8
8	40	16	56	64.83	8	40	16
7	40	16	56	64.83	7	40	16
6	40	24	64	70.87	6	40	24
5	60	24	84	57.16	5	60	24
4	80	32	112	61.95	4	80	32
3	120	40	160	59.54	3	120	40
2	364	64	428	60.14	2	364	64
1	2310	120	2430	-	1	2310	120
0.9	3536	136	3672	-	0.9	3536	136
0.8	4408	152	4560	-	0.8	4408	152
0.7	6258	168	6426	-	0.7	6258	168
0.6	10100	200	10300	-	0.6	10100	200

Appendix. C. 17. Calculated data for mesh study by ABAQUS
- Linear interpolation element in 15 m model
(General moist sandy soil: C3D8R + pipeline: S4R)

Approximate global size of element (m)	Number of element		Total number of Elements	Maximum displacement (U)		Mises equivalent stress	
	Soil (No)	Pipeline (No)		Soil (cm)	Pipeline (cm)	Soil (MPa)	Pipeline (MPa)
10	40	8	48	57.75	27.09	4.745	1114
9	40	8	48	57.75	27.09	4.745	1114
8	40	16	56	58.06	36.6	3.251	948.8
7	40	16	56	58.06	36.6	3.251	948.8
6	40	24	64	57.78	35.87	3.22	889.1
5	60	24	84	60.08	37.98	3.386	948
4	80	32	112	59.85	37.16	3.517	958.3
3	120	40	160	60.39	39.7	3.575	959.5
2	364	64	428	-	-	-	-
1	2310	120	2430	-	-	-	-
0.9	3536	136	3672	-	-	-	-
0.8	4408	152	4560	-	-	-	-
0.7	6258	168	6426	-	-	-	-
0.6	10100	200	10300	-	-	-	-

Appendix. C. 18. Calculated data for mesh study by ABAQUS
- Quadratic interpolation element in 15 m model
(General moist sandy soil: C3D20R + pipeline: S8R)

Approximate global size of element (m)	Number of element		Total number of Elements	Maximum displacement (U)		Mises equivalent stress	
	Soil (No)	Pipeline (No)		Soil (cm)	Pipeline (cm)	Soil (MPa)	Pipeline (MPa)
10	40	8	48	-	-	-	-
9	40	8	48	-	-	-	-
8	40	16	56	15.13	12.07	1.103	490
7	40	16	56	15.13	12.07	1.103	490
6	40	24	64	16.83	10.09	1.045	490
5	60	24	84	12.82	9.368	1.536	490
4	80	32	112	14.07	10.69	1.69	490
3	120	40	160	13.66	9.316	1.731	490
2	364	64	428	14.15	9.384	2.16	490
1	2310	120	2430	-	-	-	-
0.9	3536	136	3672	-	-	-	-
0.8	4408	152	4560	-	-	-	-
0.7	6258	168	6426	-	-	-	-
0.6	10100	200	10300	-	-	-	-
Appendix. C. 19. Calculated data for mesh study by ABAQUS - Linear interpolation element in 15 m model (Fully saturated sandy soil: C3D8R + pipeline: S4R)							

Approximate global size of element (m)	Number of element		Total number of Elements	Maximum displacement (U)		Mises equivalent stress	
	Soil (No)	Pipeline (No)		Soil (cm)	Pipeline (cm)	Soil (MPa)	Pipeline (MPa)
10	40	8	48	13.92	8.917	5.034	993.5
9	40	8	48	13.92	8.917	5.034	993.5
8	40	16	56	16.67	8.79	3.359	925.4
7	40	16	56	13.67	8.79	3.359	925.4
6	40	24	64	13.74	8.879	3.384	827.1
5	60	24	84	14.02	9.47	3.611	919.3
4	80	32	112	14.12	9.218	3.815	896.8
3	120	40	160	14.19	9.61	3.928	881.7
2	364	64	428	14.36	9.732	4.43	755
1	2310	120	2430	-	-	-	-
0.9	3536	136	3672	-	-	-	-
0.8	4408	152	4560	-	-	-	-
0.7	6258	168	6426	-	-	-	-
0.6	10100	200	10300	-	-	-	-
Appendix. C. 20. Calculated data for mesh study by ABAQUS - Quadratic interpolation element in 15 m model (Fully saturated sandy soil: C3D20R + pipeline: S8R)							

Approximate global size of element (m)	Number of element		Total number of Elements	Maximum displacement (U)		Mises equivalent stress	
	Soil (No)	Pipeline (No)		Soil (cm)	Pipeline (cm)	Soil (MPa)	Pipeline (MPa)
10	40	8	48	101.4	20.05	1.121	490
9	40	8	48	101.4	20.05	1.121	490
8	40	16	56	73.35	57.26	1.096	490
7	40	16	56	73.35	57.26	1.096	490
6	40	24	64	81.73	47.55	1.044	490
5	60	24	84	61.19	42.12	1.492	490
4	80	32	112	67.22	48.44	1.609	490
3	120	40	160	65.45	42.58	1.668	490
2	364	64	428	68.17	42.74	1.99	490
1	2310	120	2430	70.23	45.28	2.61	490
0.9	3536	136	3672	70.49	45.38	2.767	490
0.8	4408	152	4560	-	-	-	-
0.7	6258	168	6426	-	-	-	-
0.6	10100	200	10300	-	-	-	-

Appendix. C. 21. Calculated data for mesh study by ABAQUS
- Linear interpolation element in 15 m model
(General moist cohesive soil: C3D8R + pipeline: S4R)

Approximate global size of element (m)	Number of element		Total number of Elements	Maximum displacement (U)		Mises equivalent stress	
	Soil (No)	Pipeline (No)		Soil (cm)	Pipeline (cm)	Soil (MPa)	Pipeline (MPa)
10	40	8	48	65.81	36.87	3.988	1098
9	40	8	48	65.81	36.87	3.988	1098
8	40	16	56	65.91	40.3	3.059	952.1
7	40	16	56	65.91	40.3	3.059	952.1
6	40	24	64	65.46	39.2	3.093	902.3
5	60	24	84	67	42.32	3.099	952.1
4	80	32	112	67.8	41.41	3.226	957.7
3	120	40	160	68.3	43.81	3.313	960.7
2	364	64	428	69.67	45.05	3.816	846.8
1	2310	120	2430	70.9	46.02	4.867	804.8
0.9	3536	136	3672	-	-	-	-
0.8	4408	152	4560	-	-	-	-
0.7	6258	168	6426	-	-	-	-
0.6	10100	200	10300	-	-	-	-

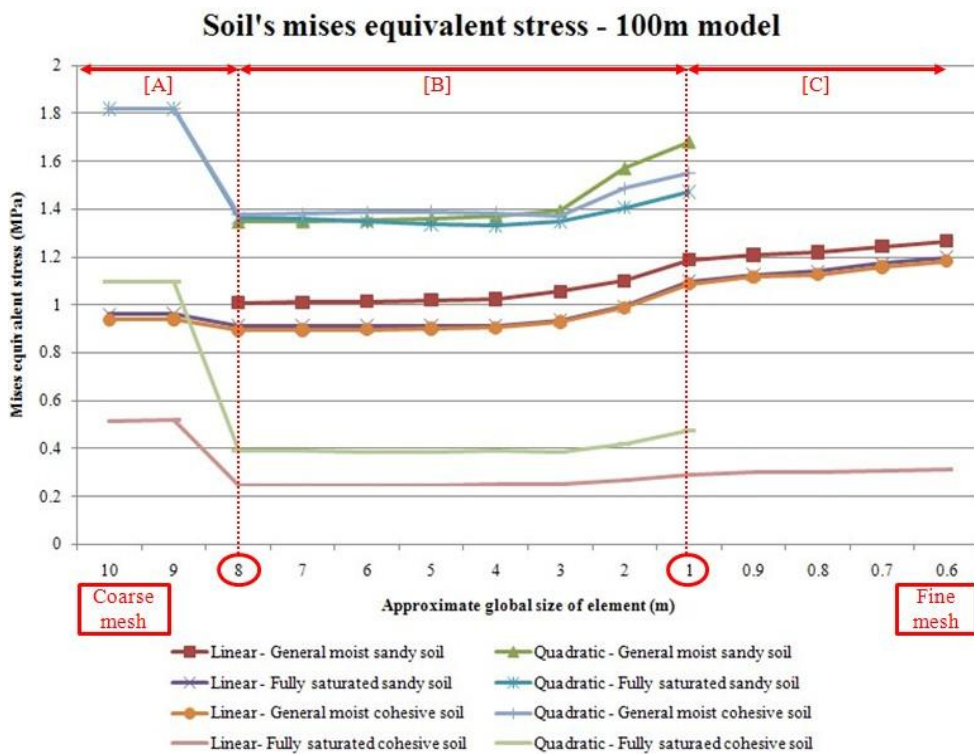
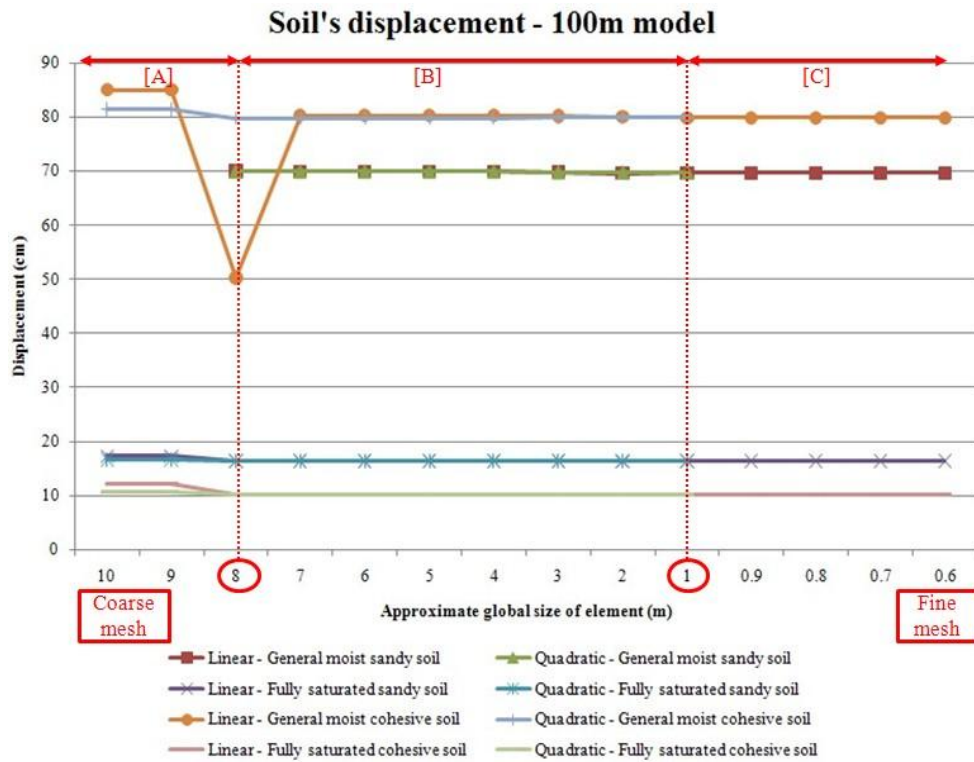
Appendix. C. 22. Calculated data for mesh study by ABAQUS
- Quadratic interpolation element in 15 m model
(General moist cohesive soil: C3D20R + pipeline: S8R)

Approximate global size of element (m)	Number of element		Total number of Elements	Maximum displacement (U)		Mises equivalent stress	
	Soil (No)	Pipeline (No)		Soil (cm)	Pipeline (cm)	Soil (MPa)	Pipeline (MPa)
10	40	8	48	24.43	1.789	0.5607	237.6
9	40	8	48	22.43	1.789	0.5607	237.6
8	40	16	56	9.324	5.212	0.4634	490
7	40	16	56	9.324	5.212	0.4634	490
6	40	24	64	10.38	4.933	0.3996	490
5	60	24	84	9.203	5.487	0.4981	490
4	80	32	112	9.072	6.593	0.5577	490
3	120	40	160	9.089	6.028	0.5811	490
2	364	64	428	9.48	6.24	0.7358	490
1	2310	120	2430	9.67	6.382	1.065	490
0.9	3536	136	3672	9.685	6.372	1.187	490
0.8	4408	152	4560	9.679	6.401	1.215	490
0.7	6258	168	6426	9.704	6.402	1.324	490
0.6	10100	200	10300	9.704	6.419	1.454	490
Appendix. C. 23. Calculated data for mesh study by ABAQUS - Linear interpolation element in 15 m model (Fully saturated cohesive soil: C3D8R + pipeline: S4R)							

Approximate global size of element (m)	Number of element		Total number of Elements	Maximum displacement (U)		Mises equivalent stress	
	Soil (No)	Pipeline (No)		Soil (cm)	Pipeline (cm)	Soil (MPa)	Pipeline (MPa)
10	40	8	48	9.706	6.009	1.418	825.4
9	40	8	48	9.706	6.009	1.418	825.4
8	40	16	56	1.294	5.447	1.098	835.4
7	40	16	56	9.294	5.447	1.098	835.4
6	40	24	64	9.393	5.556	1.072	708.5
5	60	24	84	9.493	5.972	1.207	840.7
4	80	32	112	9.493	5.806	1.298	785.8
3	120	40	160	9.567	6.168	1.366	752
2	364	64	428	9.617	6.217	1.553	654
1	2310	120	2430	9.67	6.236	2.62	638.8
0.9	3536	136	3672	9.676	6.249	2.867	623
0.8	4408	152	4560	9.68	6.257	2.876	613.3
0.7	6258	168	6426	9.684	6.268	3.121	595.7
0.6	10100	200	10300	-	-	-	-
Appendix. C. 24. Calculated data for mesh study by ABAQUS - Quadratic element in 15 m model (Fully saturated cohesive soil: C3D20R + pipeline: S8R)							

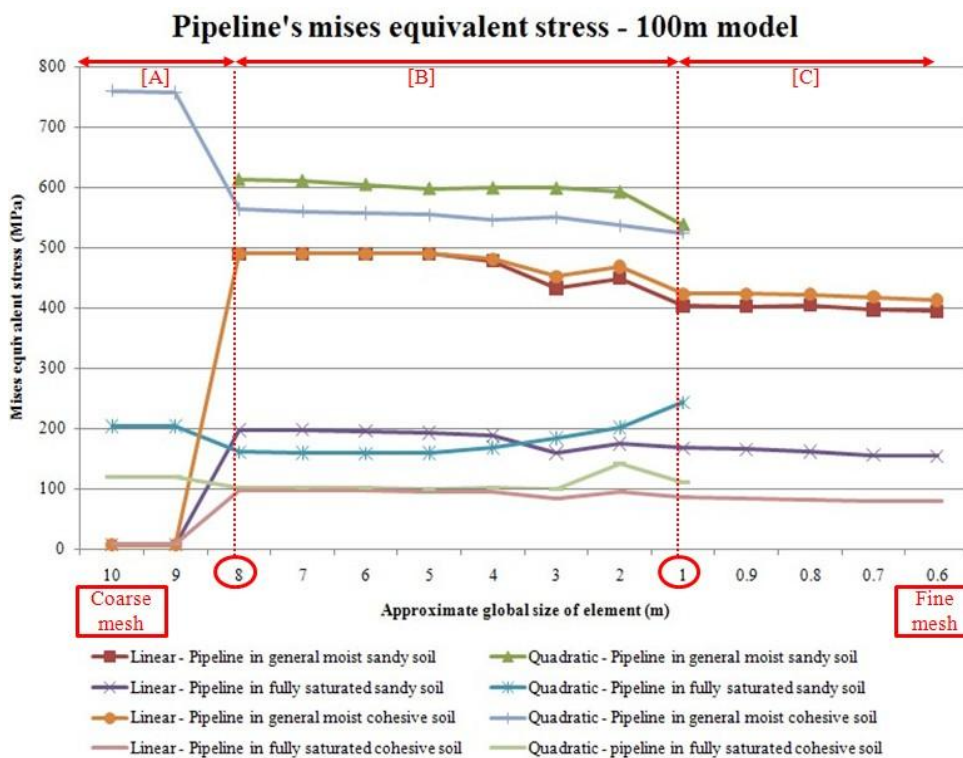
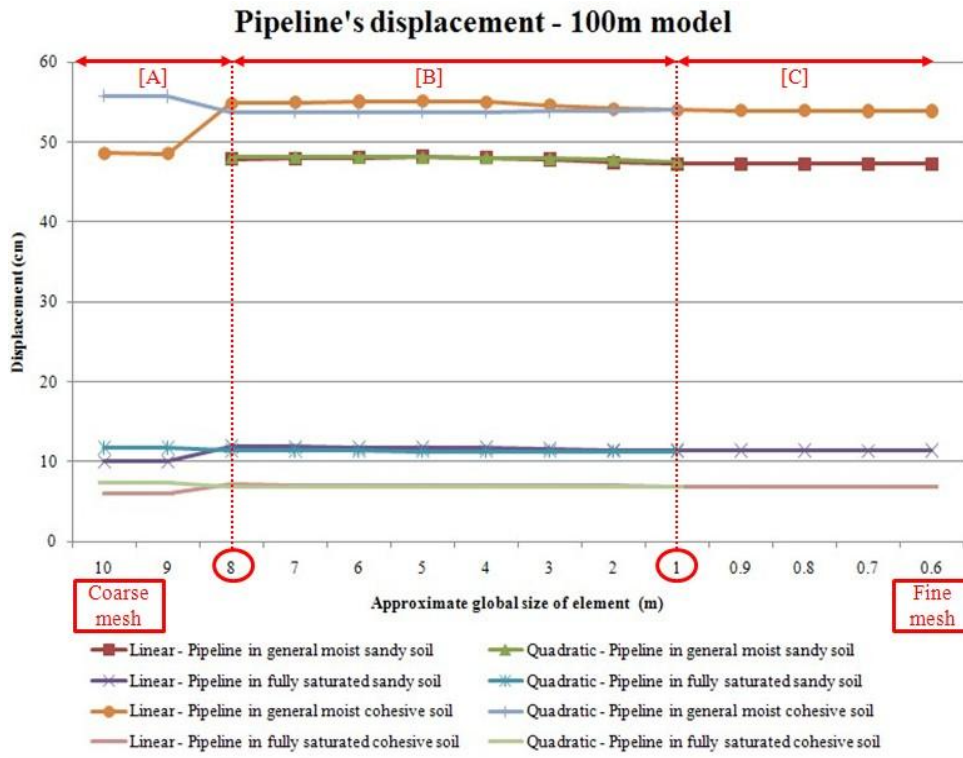
Appendix D – the graphs for mesh study

100 m model - soil



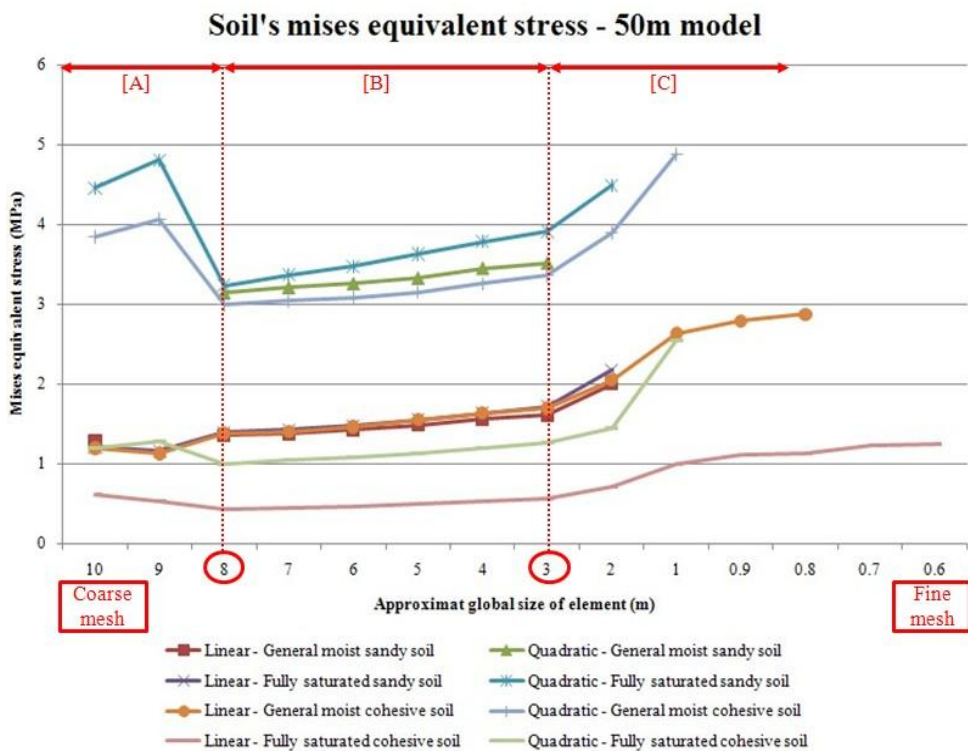
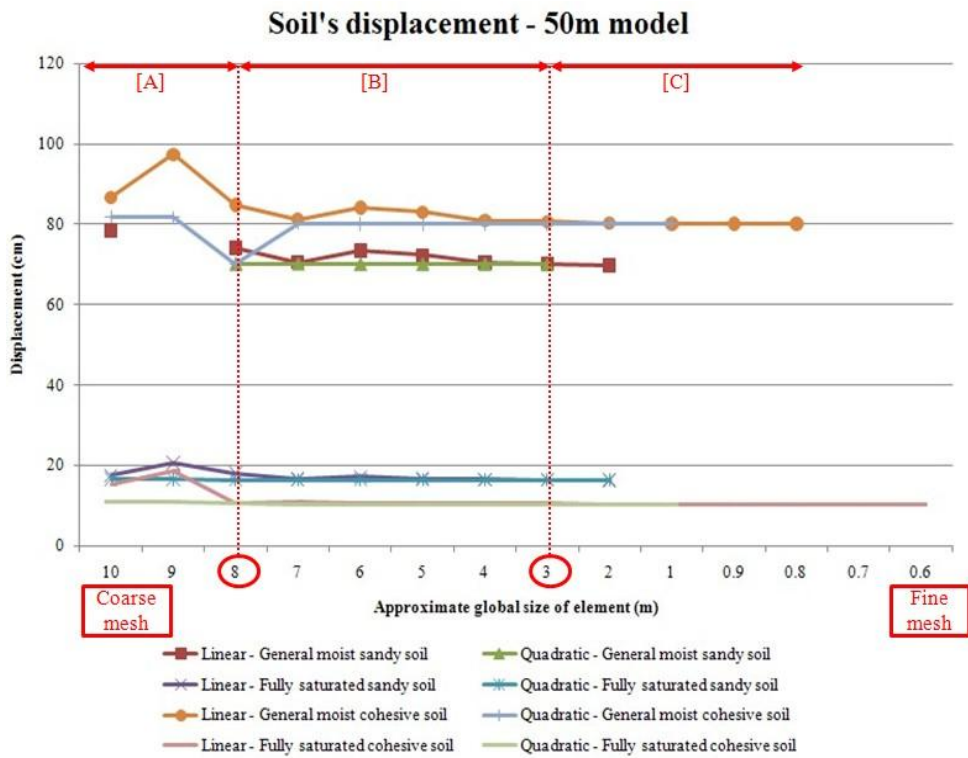
Appendix D. 1. Computed 100m soil model results according to different type and number of element

100 m model - pipeline



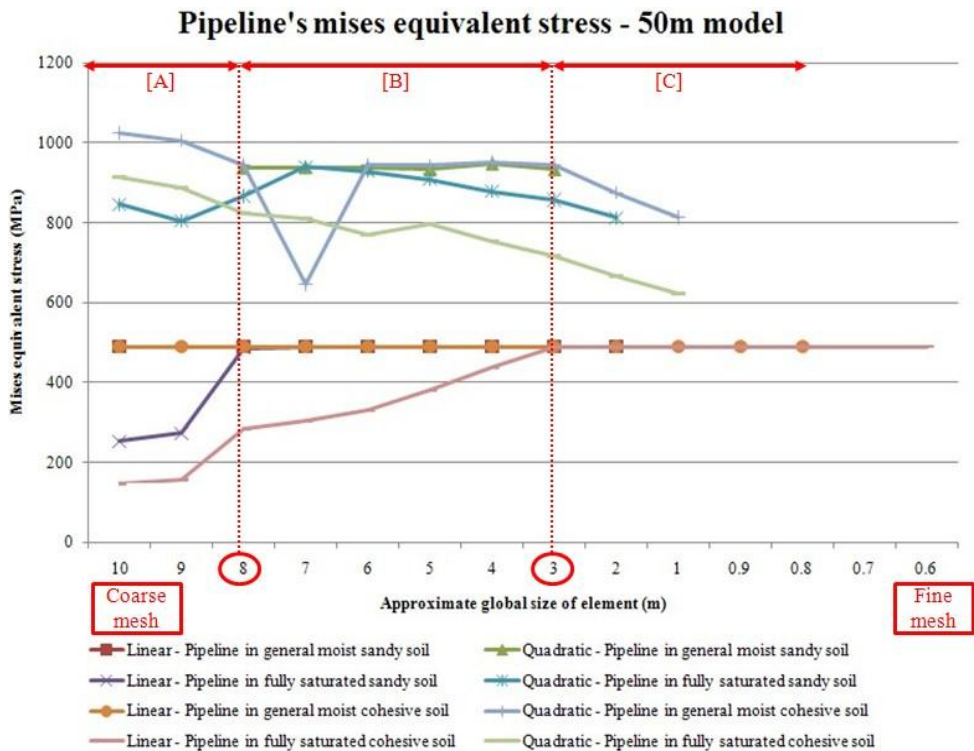
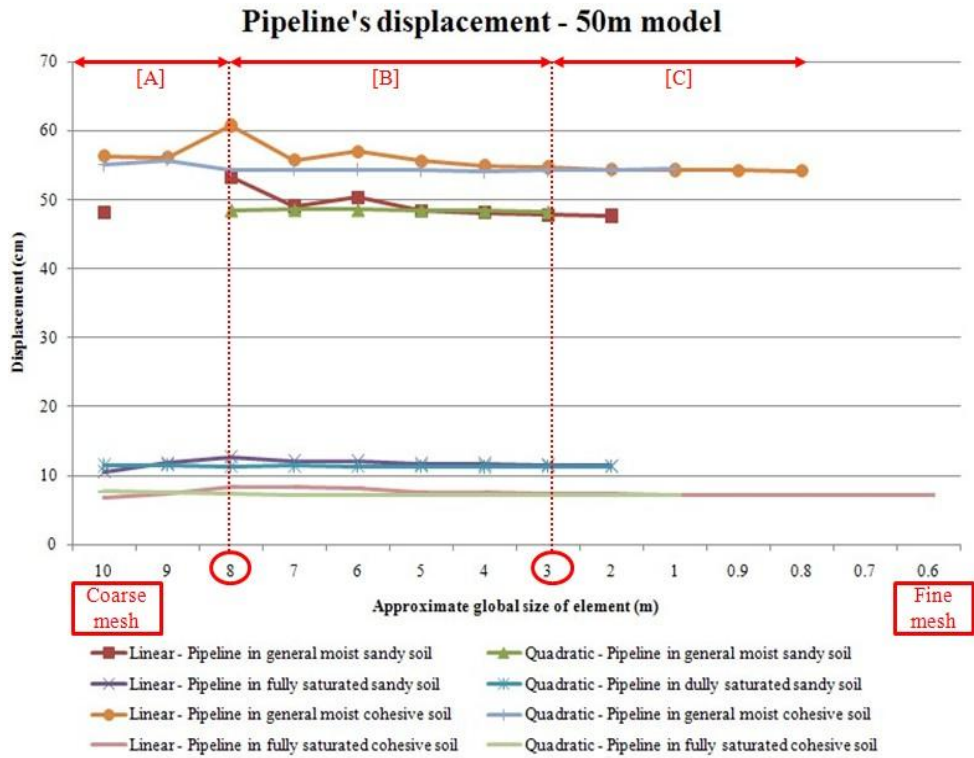
Appendix D. 2. Computed 100m pipeline model results according to different type and number of element

50 m model - soil



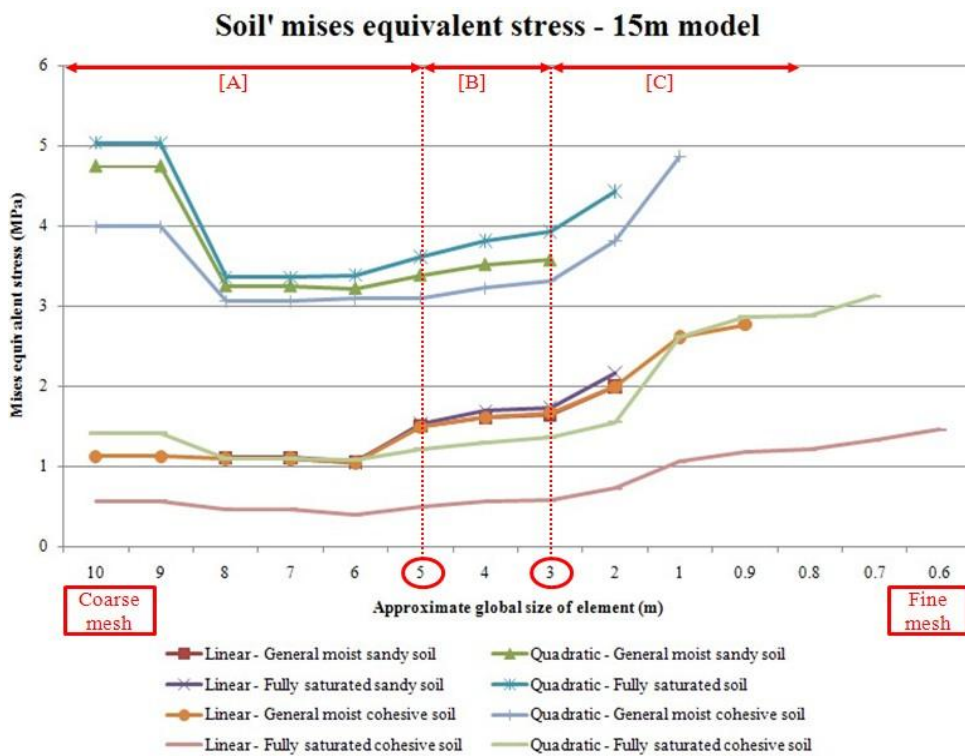
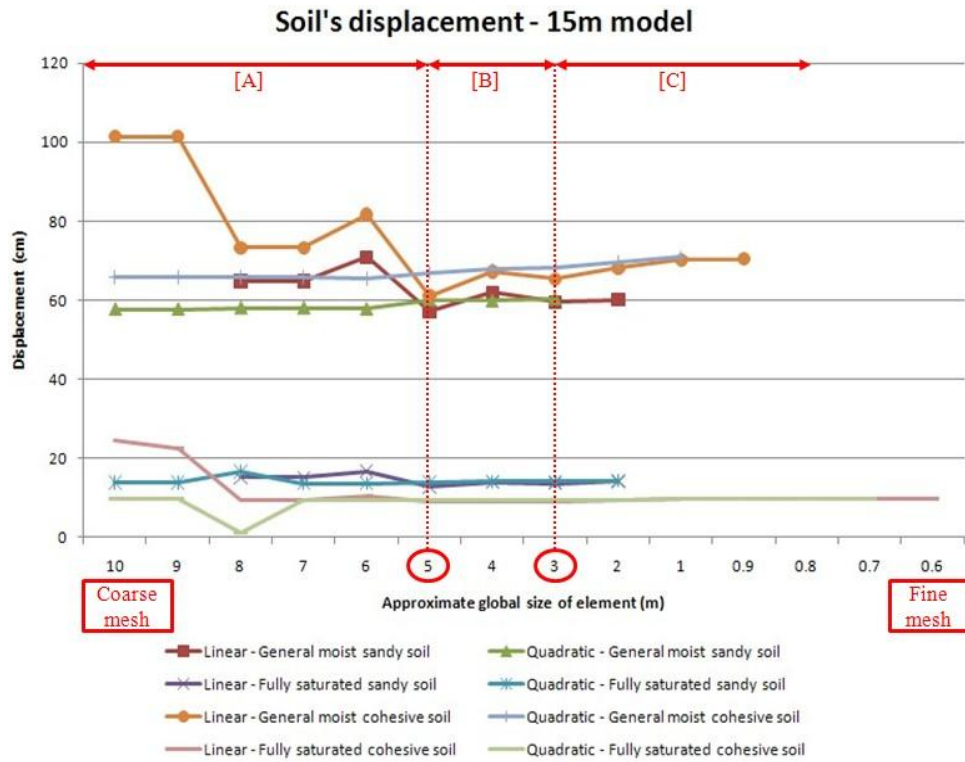
Appendix D. 3. Computed 50m soil model results according to different type and number of element

50 m model - pipeline



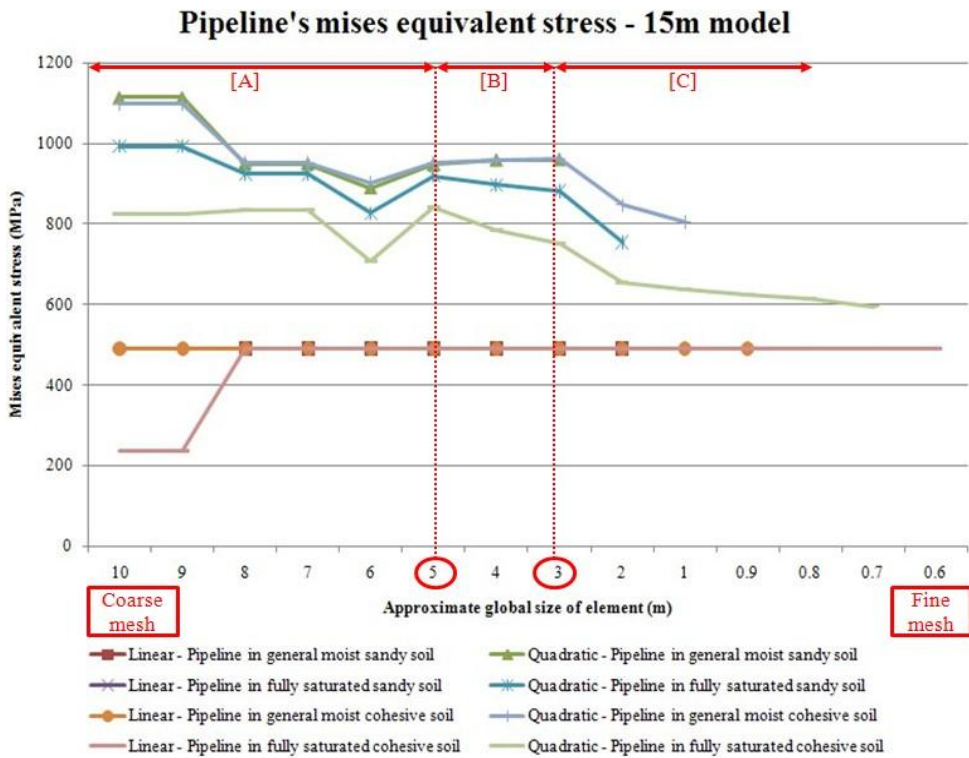
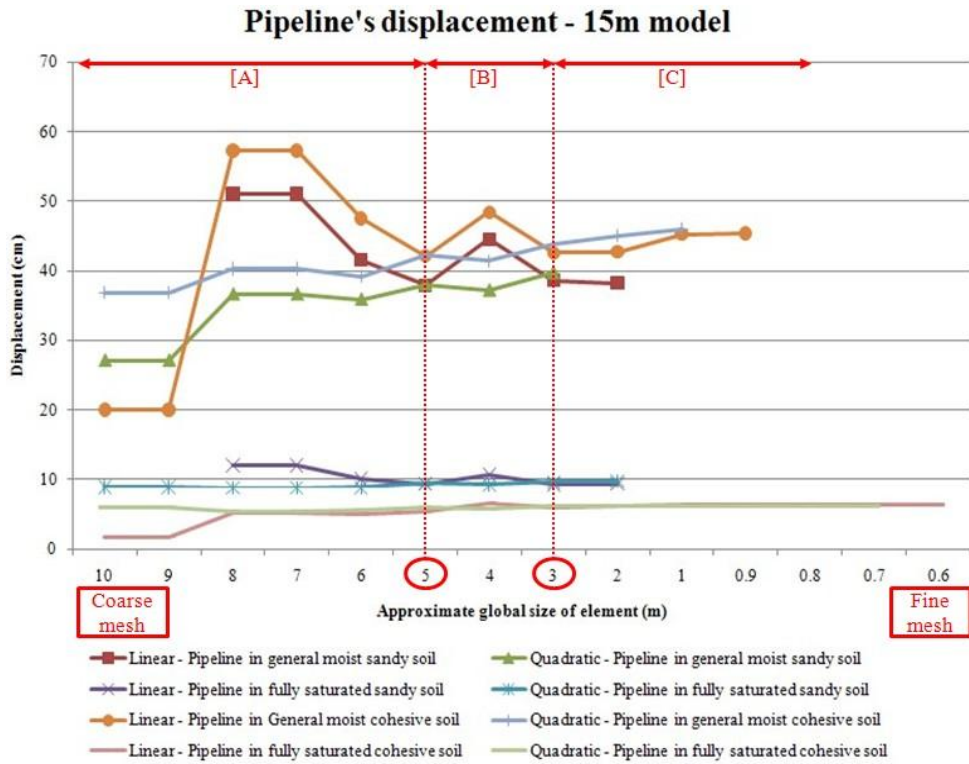
Appendix D. 4. Computed 50m pipeline model results according to different type and number of element

15 m model - soil



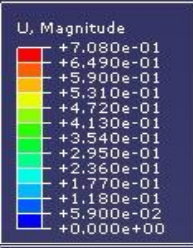
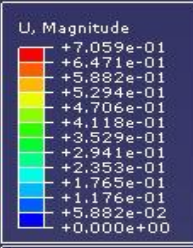
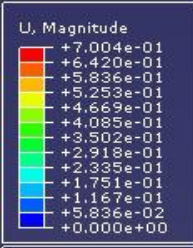
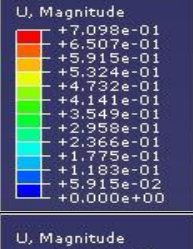
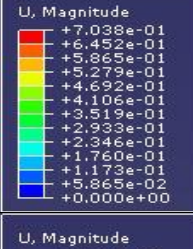
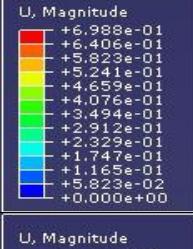
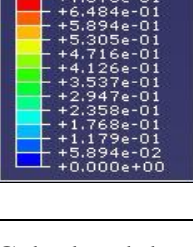

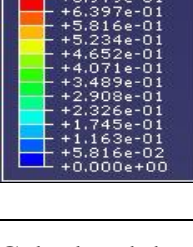
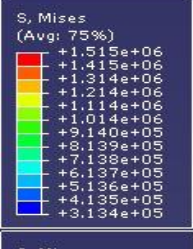
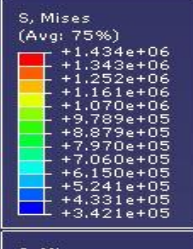
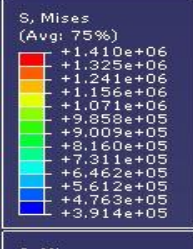
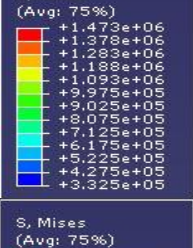
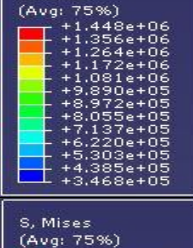
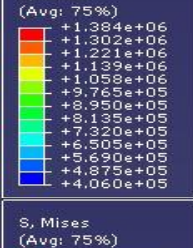
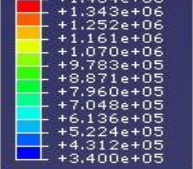
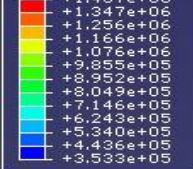
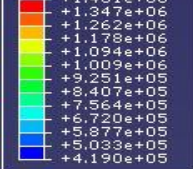
Appendix D. 5. Computed 15m soil model results according to different type and number of element

15 m model - pipeline

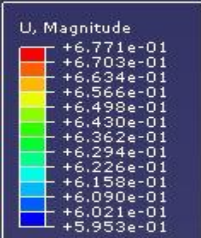
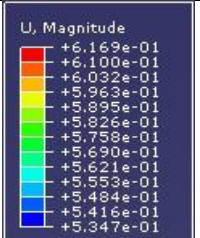
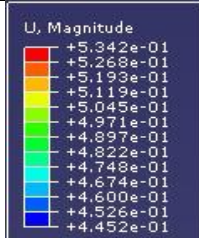
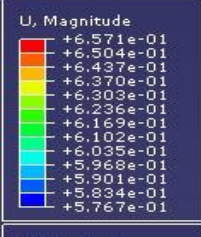
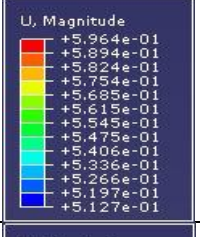
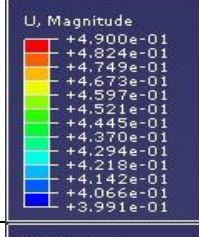
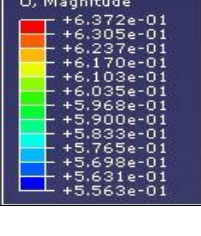
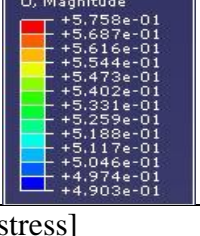
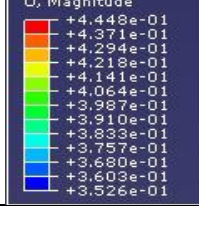

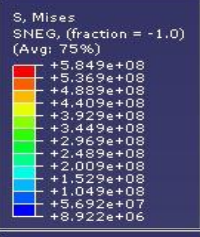
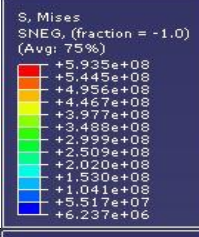
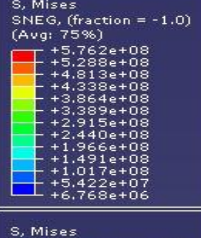
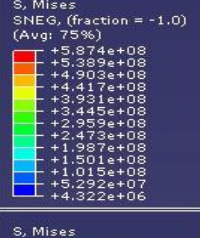
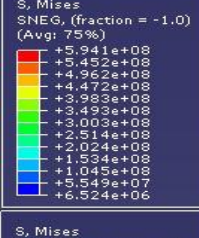
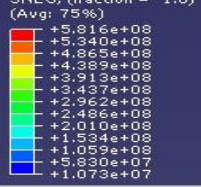
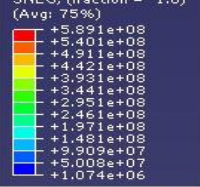
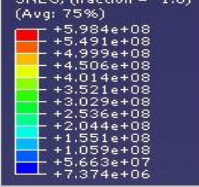


Appendix D. 6. Computed 15m pipeline model results according to different type and number of element


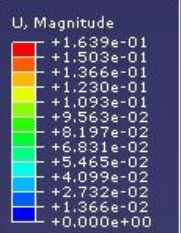
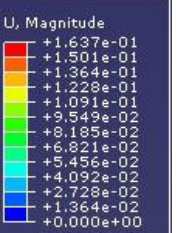
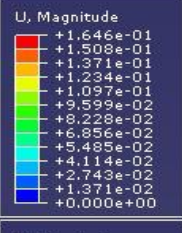
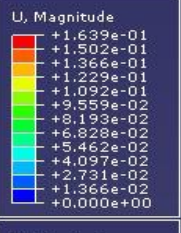
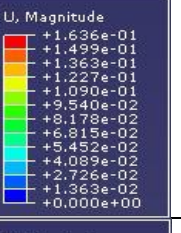
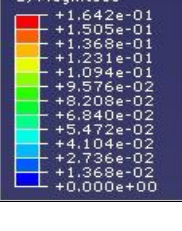
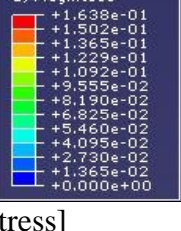
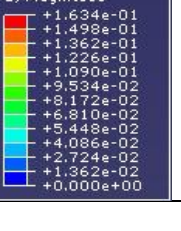
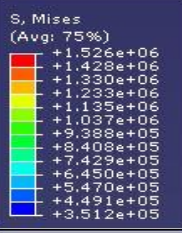
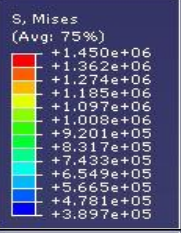
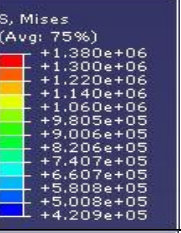
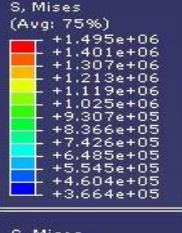

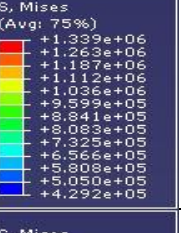
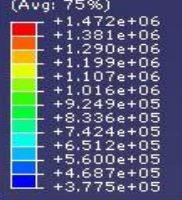
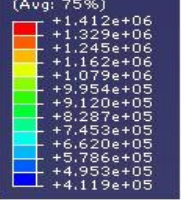
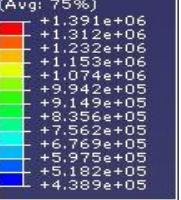
Appendix E – the calculated data for static analysis

[Displacement]					
Buried depth	Calculated data	Buried depth	Calculated data	Buried depth	Calculated data
0.5m	 <p>U, Magnitude</p> <ul style="list-style-type: none"> +7.080e-01 +6.490e-01 +5.900e-01 +5.310e-01 +4.720e-01 +4.130e-01 +3.540e-01 +2.950e-01 +2.360e-01 +1.770e-01 +1.180e-01 +5.900e-02 +0.000e+00 	2.0m	 <p>U, Magnitude</p> <ul style="list-style-type: none"> +7.059e-01 +6.471e-01 +5.882e-01 +5.294e-01 +4.706e-01 +4.118e-01 +3.529e-01 +2.941e-01 +2.353e-01 +1.765e-01 +1.176e-01 +5.882e-02 +0.000e+00 	4.0m	 <p>U, Magnitude</p> <ul style="list-style-type: none"> +7.004e-01 +6.420e-01 +5.836e-01 +5.253e-01 +4.669e-01 +4.085e-01 +3.502e-01 +2.918e-01 +2.335e-01 +1.751e-01 +1.167e-01 +5.836e-02 +0.000e+00
1.0m	 <p>U, Magnitude</p> <ul style="list-style-type: none"> +7.098e-01 +6.507e-01 +5.915e-01 +5.324e-01 +4.732e-01 +4.141e-01 +3.549e-01 +2.958e-01 +2.366e-01 +1.775e-01 +1.183e-01 +5.915e-02 +0.000e+00 	2.5m	 <p>U, Magnitude</p> <ul style="list-style-type: none"> +7.038e-01 +6.452e-01 +5.865e-01 +5.279e-01 +4.692e-01 +4.106e-01 +3.519e-01 +2.933e-01 +2.346e-01 +1.760e-01 +1.173e-01 +5.865e-02 +0.000e+00 	5.0m	 <p>U, Magnitude</p> <ul style="list-style-type: none"> +6.988e-01 +6.406e-01 +5.823e-01 +5.241e-01 +4.659e-01 +4.076e-01 +3.494e-01 +2.912e-01 +2.329e-01 +1.747e-01 +1.165e-01 +5.823e-02 +0.000e+00
1.5m	 <p>U, Magnitude</p> <ul style="list-style-type: none"> +7.073e-01 +6.484e-01 +5.894e-01 +5.305e-01 +4.716e-01 +4.126e-01 +3.537e-01 +2.947e-01 +2.358e-01 +1.768e-01 +1.179e-01 +5.894e-02 +0.000e+00 	3.0m	 <p>U, Magnitude</p> <ul style="list-style-type: none"> +7.018e-01 +6.433e-01 +5.848e-01 +5.263e-01 +4.679e-01 +4.094e-01 +3.509e-01 +2.924e-01 +2.339e-01 +1.754e-01 +1.170e-01 +5.848e-02 +0.000e+00 	6.0m	 <p>U, Magnitude</p> <ul style="list-style-type: none"> +6.979e-01 +6.397e-01 +5.816e-01 +5.234e-01 +4.652e-01 +4.071e-01 +3.489e-01 +2.908e-01 +2.326e-01 +1.745e-01 +1.163e-01 +5.816e-02 +0.000e+00
[stress]					
Buried depth	Calculated data	Buried depth	Calculated data	Buried depth	Calculated data
0.5m	 <p>S, Mises (Avg: 75%)</p> <ul style="list-style-type: none"> +1.515e+06 +1.415e+06 +1.314e+06 +1.214e+06 +1.114e+06 +1.014e+06 +9.140e+05 +8.139e+05 +7.138e+05 +6.137e+05 +5.136e+05 +4.135e+05 +3.134e+05 	2.0m	 <p>S, Mises (Avg: 75%)</p> <ul style="list-style-type: none"> +1.434e+06 +1.343e+06 +1.252e+06 +1.161e+06 +1.070e+06 +9.789e+05 +8.879e+05 +7.970e+05 +7.060e+05 +6.150e+05 +5.241e+05 +4.331e+05 +3.421e+05 	4.0m	 <p>S, Mises (Avg: 75%)</p> <ul style="list-style-type: none"> +1.410e+06 +1.325e+06 +1.241e+06 +1.156e+06 +1.071e+06 +9.85e+05 +9.009e+05 +8.160e+05 +7.311e+05 +6.462e+05 +5.612e+05 +4.763e+05 +3.914e+05
1.0m	 <p>S, Mises (Avg: 75%)</p> <ul style="list-style-type: none"> +1.473e+06 +1.378e+06 +1.283e+06 +1.188e+06 +1.093e+06 +9.975e+05 +9.025e+05 +8.075e+05 +7.125e+05 +6.175e+05 +5.225e+05 +4.275e+05 +3.325e+05 	2.5m	 <p>S, Mises (Avg: 75%)</p> <ul style="list-style-type: none"> +1.448e+06 +1.356e+06 +1.264e+06 +1.172e+06 +1.081e+06 +9.890e+05 +8.972e+05 +8.055e+05 +7.137e+05 +6.220e+05 +5.303e+05 +4.385e+05 +3.468e+05 	5.0m	 <p>S, Mises (Avg: 75%)</p> <ul style="list-style-type: none"> +1.384e+06 +1.302e+06 +1.221e+06 +1.139e+06 +1.058e+06 +9.765e+05 +8.950e+05 +8.135e+05 +7.320e+05 +6.505e+05 +5.690e+05 +4.875e+05 +4.060e+05
1.5m	 <p>S, Mises (Avg: 75%)</p> <ul style="list-style-type: none"> +1.434e+06 +1.343e+06 +1.252e+06 +1.161e+06 +1.070e+06 +9.783e+05 +8.871e+05 +7.960e+05 +7.048e+05 +6.136e+05 +5.224e+05 +4.312e+05 +3.400e+05 	3.0m	 <p>S, Mises (Avg: 75%)</p> <ul style="list-style-type: none"> +1.437e+06 +1.347e+06 +1.256e+06 +1.166e+06 +1.076e+06 +9.855e+05 +8.952e+05 +8.049e+05 +7.146e+05 +6.243e+05 +5.340e+05 +4.436e+05 +3.533e+05 	6.0m	 <p>S, Mises (Avg: 75%)</p> <ul style="list-style-type: none"> +1.431e+06 +1.347e+06 +1.262e+06 +1.178e+06 +1.094e+06 +1.009e+06 +9.251e+05 +8.407e+05 +7.564e+05 +6.720e+05 +5.877e+05 +5.033e+05 +4.190e+05

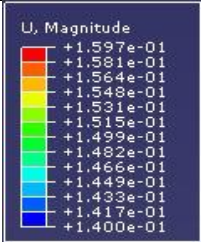
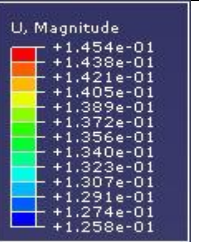
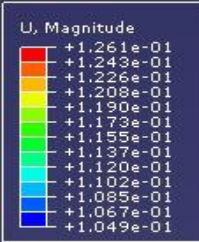
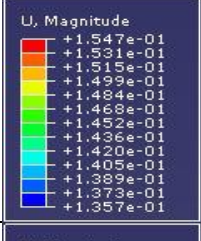
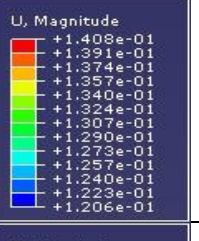
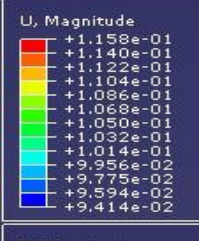
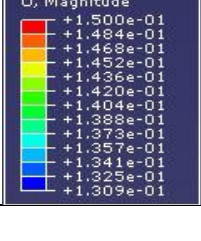
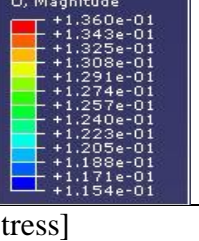
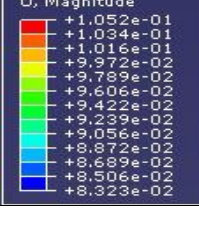
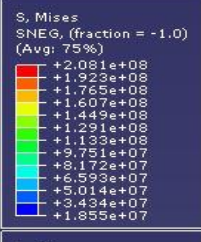
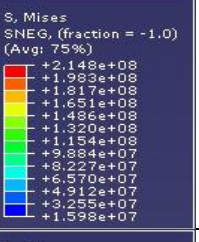
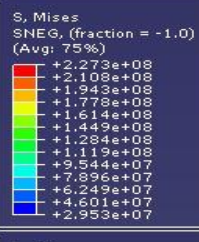
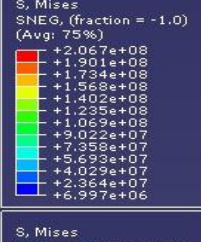
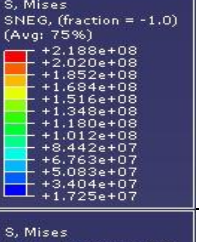
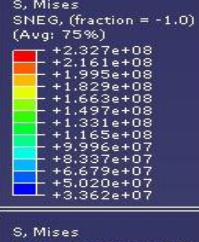
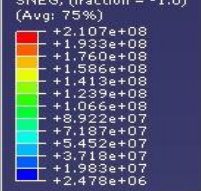
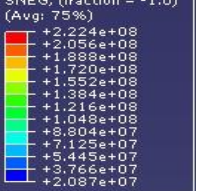
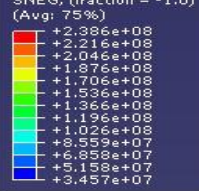
Appendix E. 1. Calculated static analysis results by ABAQUS for general moist sandy soil

[Displacement]					
Buried depth	Calculated data	Buried depth	Calculated data	Buried depth	Calculated data
0.5m	 <p>U, Magnitude</p> <ul style="list-style-type: none"> +6.771e-01 +6.703e-01 +6.634e-01 +6.566e-01 +6.498e-01 +6.430e-01 +6.362e-01 +6.294e-01 +6.226e-01 +6.158e-01 +6.090e-01 +6.021e-01 +5.953e-01 	2.0m	 <p>U, Magnitude</p> <ul style="list-style-type: none"> +6.169e-01 +6.100e-01 +6.032e-01 +5.963e-01 +5.895e-01 +5.826e-01 +5.758e-01 +5.690e-01 +5.621e-01 +5.553e-01 +5.484e-01 +5.416e-01 +5.347e-01 	4.0m	 <p>U, Magnitude</p> <ul style="list-style-type: none"> +5.342e-01 +5.268e-01 +5.193e-01 +5.119e-01 +5.045e-01 +4.971e-01 +4.897e-01 +4.822e-01 +4.748e-01 +4.674e-01 +4.600e-01 +4.526e-01 +4.452e-01
1.0m	 <p>U, Magnitude</p> <ul style="list-style-type: none"> +6.571e-01 +6.504e-01 +6.437e-01 +6.370e-01 +6.303e-01 +6.236e-01 +6.169e-01 +6.102e-01 +6.035e-01 +5.968e-01 +5.901e-01 +5.834e-01 +5.767e-01 	2.5m	 <p>U, Magnitude</p> <ul style="list-style-type: none"> +5.964e-01 +5.894e-01 +5.824e-01 +5.754e-01 +5.685e-01 +5.615e-01 +5.545e-01 +5.475e-01 +5.405e-01 +5.336e-01 +5.266e-01 +5.197e-01 +5.127e-01 	5.0m	 <p>U, Magnitude</p> <ul style="list-style-type: none"> +4.900e-01 +4.824e-01 +4.749e-01 +4.673e-01 +4.597e-01 +4.521e-01 +4.445e-01 +4.370e-01 +4.294e-01 +4.218e-01 +4.142e-01 +4.066e-01 +3.991e-01
1.5m	 <p>U, Magnitude</p> <ul style="list-style-type: none"> +6.372e-01 +6.305e-01 +6.237e-01 +6.170e-01 +6.103e-01 +6.035e-01 +5.968e-01 +5.900e-01 +5.833e-01 +5.765e-01 +5.698e-01 +5.631e-01 +5.563e-01 	3.0m	 <p>U, Magnitude</p> <ul style="list-style-type: none"> +5.758e-01 +5.687e-01 +5.616e-01 +5.544e-01 +5.473e-01 +5.402e-01 +5.331e-01 +5.259e-01 +5.188e-01 +5.117e-01 +5.046e-01 +4.974e-01 +4.903e-01 	6.0m	 <p>U, Magnitude</p> <ul style="list-style-type: none"> +4.448e-01 +4.371e-01 +4.294e-01 +4.218e-01 +4.141e-01 +4.064e-01 +3.987e-01 +3.910e-01 +3.833e-01 +3.757e-01 +3.680e-01 +3.603e-01 +3.526e-01
[stress]					
Buried depth	Calculated data	Buried depth	Calculated data	Buried depth	Calculated data
0.5m	 <p>S, Mises SNEG, (fraction = -1.0) (Avg: 75%)</p> <ul style="list-style-type: none"> +5.659e+08 +5.199e+08 +4.718e+08 +4.248e+08 +3.777e+08 +3.307e+08 +2.836e+08 +2.366e+08 +1.895e+08 +1.425e+08 +9.542e+07 +4.836e+07 +1.313e+06 	2.0m	 <p>S, Mises SNEG, (fraction = -1.0) (Avg: 75%)</p> <ul style="list-style-type: none"> +5.849e+08 +5.369e+08 +4.890e+08 +4.409e+08 +3.929e+08 +3.449e+08 +2.969e+08 +2.489e+08 +2.009e+08 +1.529e+08 +1.049e+08 +5.692e+07 +8.922e+06 	4.0m	 <p>S, Mises SNEG, (fraction = -1.0) (Avg: 75%)</p> <ul style="list-style-type: none"> +5.935e+08 +5.445e+08 +4.956e+08 +4.467e+08 +3.977e+08 +3.488e+08 +2.999e+08 +2.509e+08 +2.020e+08 +1.530e+08 +1.041e+08 +5.517e+07 +6.237e+06
1.0m	 <p>S, Mises SNEG, (fraction = -1.0) (Avg: 75%)</p> <ul style="list-style-type: none"> +5.762e+08 +5.288e+08 +4.813e+08 +4.338e+08 +3.864e+08 +3.389e+08 +2.915e+08 +2.440e+08 +1.966e+08 +1.491e+08 +1.017e+08 +5.422e+07 +6.768e+06 	2.5m	 <p>S, Mises SNEG, (fraction = -1.0) (Avg: 75%)</p> <ul style="list-style-type: none"> +5.874e+08 +5.389e+08 +4.903e+08 +4.417e+08 +3.931e+08 +3.445e+08 +2.959e+08 +2.473e+08 +1.987e+08 +1.501e+08 +1.015e+08 +5.292e+07 +4.322e+06 	5.0m	 <p>S, Mises SNEG, (fraction = -1.0) (Avg: 75%)</p> <ul style="list-style-type: none"> +5.941e+08 +5.452e+08 +4.962e+08 +4.472e+08 +3.983e+08 +3.493e+08 +3.003e+08 +2.513e+08 +2.024e+08 +1.534e+08 +1.045e+08 +5.549e+07 +6.324e+06
1.5m	 <p>S, Mises SNEG, (fraction = -1.0) (Avg: 75%)</p> <ul style="list-style-type: none"> +5.816e+08 +5.340e+08 +4.865e+08 +4.389e+08 +3.913e+08 +3.437e+08 +2.962e+08 +2.486e+08 +2.010e+08 +1.534e+08 +1.059e+08 +5.830e+07 +1.073e+07 	3.0m	 <p>S, Mises SNEG, (fraction = -1.0) (Avg: 75%)</p> <ul style="list-style-type: none"> +5.891e+08 +5.401e+08 +4.911e+08 +4.421e+08 +3.931e+08 +3.441e+08 +2.951e+08 +2.461e+08 +1.971e+08 +1.481e+08 +9.909e+07 +5.008e+07 +1.074e+06 	6.0m	 <p>S, Mises SNEG, (fraction = -1.0) (Avg: 75%)</p> <ul style="list-style-type: none"> +5.984e+08 +5.491e+08 +4.999e+08 +4.506e+08 +4.014e+08 +3.521e+08 +3.029e+08 +2.536e+08 +2.044e+08 +1.551e+08 +1.059e+08 +5.663e+07 +7.374e+06

Appendix E. 2. Calculated static analysis results by ABAQUS for the pipeline in general moist sandy soil

[Displacement]					
Buried depth	Calculated data	Buried depth	Calculated data	Buried depth	Calculated data
0.5m	 <p>U, Magnitude</p> <ul style="list-style-type: none"> +1.652e-01 +1.314e-01 +1.377e-01 +1.239e-01 +1.101e-01 +9.637e-02 +8.260e-02 +6.884e-02 +5.507e-02 +4.130e-02 +2.753e-02 +1.377e-02 +0.000e+00 	2.0m	 <p>U, Magnitude</p> <ul style="list-style-type: none"> +1.639e-01 +1.503e-01 +1.366e-01 +1.230e-01 +1.093e-01 +9.563e-02 +8.197e-02 +6.831e-02 +5.465e-02 +4.099e-02 +2.732e-02 +1.366e-02 +0.000e+00 	4.0m	 <p>U, Magnitude</p> <ul style="list-style-type: none"> +1.637e-01 +1.501e-01 +1.364e-01 +1.228e-01 +1.091e-01 +9.549e-02 +8.185e-02 +6.821e-02 +5.456e-02 +4.092e-02 +2.728e-02 +1.364e-02 +0.000e+00
1.0m	 <p>U, Magnitude</p> <ul style="list-style-type: none"> +1.646e-01 +1.508e-01 +1.371e-01 +1.234e-01 +1.097e-01 +9.599e-02 +8.228e-02 +6.856e-02 +5.485e-02 +4.114e-02 +2.743e-02 +1.371e-02 +0.000e+00 	2.5m	 <p>U, Magnitude</p> <ul style="list-style-type: none"> +1.639e-01 +1.502e-01 +1.366e-01 +1.229e-01 +1.092e-01 +9.559e-02 +8.193e-02 +6.828e-02 +5.462e-02 +4.097e-02 +2.731e-02 +1.366e-02 +0.000e+00 	5.0m	 <p>U, Magnitude</p> <ul style="list-style-type: none"> +1.636e-01 +1.499e-01 +1.363e-01 +1.227e-01 +1.090e-01 +9.540e-02 +8.178e-02 +6.815e-02 +5.452e-02 +4.089e-02 +2.726e-02 +1.363e-02 +0.000e+00
1.5m	 <p>U, Magnitude</p> <ul style="list-style-type: none"> +1.642e-01 +1.505e-01 +1.368e-01 +1.231e-01 +1.094e-01 +9.576e-02 +8.208e-02 +6.840e-02 +5.472e-02 +4.104e-02 +2.736e-02 +1.368e-02 +0.000e+00 	3.0m	 <p>U, Magnitude</p> <ul style="list-style-type: none"> +1.638e-01 +1.502e-01 +1.365e-01 +1.229e-01 +1.092e-01 +9.555e-02 +8.190e-02 +6.825e-02 +5.460e-02 +4.095e-02 +2.730e-02 +1.365e-02 +0.000e+00 	6.0m	 <p>U, Magnitude</p> <ul style="list-style-type: none"> +1.634e-01 +1.498e-01 +1.362e-01 +1.226e-01 +1.090e-01 +9.534e-02 +8.172e-02 +6.810e-02 +5.448e-02 +4.086e-02 +2.724e-02 +1.362e-02 +0.000e+00
[stress]					
Buried depth	Calculated data	Buried depth	Calculated data	Buried depth	Calculated data
0.5m	 <p>S, Mises (Avg: 75%)</p> <ul style="list-style-type: none"> +1.526e+06 +1.428e+06 +1.330e+06 +1.233e+06 +1.135e+06 +1.037e+06 +9.388e+05 +8.408e+05 +7.429e+05 +6.450e+05 +5.470e+05 +4.491e+05 +3.512e+05 	2.0m	 <p>S, Mises (Avg: 75%)</p> <ul style="list-style-type: none"> +1.450e+06 +1.362e+06 +1.274e+06 +1.185e+06 +1.097e+06 +1.008e+06 +9.201e+05 +8.317e+05 +7.433e+05 +6.549e+05 +5.665e+05 +4.781e+05 +3.897e+05 	4.0m	 <p>S, Mises (Avg: 75%)</p> <ul style="list-style-type: none"> +1.380e+06 +1.300e+06 +1.220e+06 +1.140e+06 +1.060e+06 +9.805e+05 +9.006e+05 +8.206e+05 +7.407e+05 +6.607e+05 +5.808e+05 +5.008e+05 +4.209e+05
1.0m	 <p>S, Mises (Avg: 75%)</p> <ul style="list-style-type: none"> +1.495e+06 +1.401e+06 +1.307e+06 +1.213e+06 +1.119e+06 +1.025e+06 +9.307e+05 +8.366e+05 +7.426e+05 +6.485e+05 +5.545e+05 +4.604e+05 +3.664e+05 	2.5m	 <p>S, Mises (Avg: 75%)</p> <ul style="list-style-type: none"> +1.423e+06 +1.343e+06 +1.258e+06 +1.172e+06 +1.086e+06 +1.001e+06 +9.152e+05 +8.295e+05 +7.439e+05 +6.582e+05 +5.726e+05 +4.870e+05 +4.013e+05 	5.0m	 <p>S, Mises (Avg: 75%)</p> <ul style="list-style-type: none"> +1.339e+06 +1.263e+06 +1.187e+06 +1.112e+06 +1.036e+06 +9.599e+05 +8.841e+05 +8.083e+05 +7.325e+05 +6.566e+05 +5.808e+05 +5.050e+05 +4.292e+05
1.5m	 <p>S, Mises (Avg: 75%)</p> <ul style="list-style-type: none"> +1.472e+06 +1.381e+06 +1.290e+06 +1.199e+06 +1.107e+06 +1.016e+06 +9.249e+05 +8.336e+05 +7.424e+05 +6.512e+05 +5.600e+05 +4.687e+05 +3.775e+05 	3.0m	 <p>S, Mises (Avg: 75%)</p> <ul style="list-style-type: none"> +1.412e+06 +1.329e+06 +1.245e+06 +1.162e+06 +1.079e+06 +9.954e+05 +9.120e+05 +8.287e+05 +7.453e+05 +6.620e+05 +5.786e+05 +4.953e+05 +4.119e+05 	6.0m	 <p>S, Mises (Avg: 75%)</p> <ul style="list-style-type: none"> +1.391e+06 +1.312e+06 +1.232e+06 +1.153e+06 +1.074e+06 +9.942e+05 +9.149e+05 +8.356e+05 +7.562e+05 +6.769e+05 +5.976e+05 +5.182e+05 +4.389e+05

Appendix E. 3. Calculated static analysis results by ABAQUS for fully saturated sandy soil

[Displacement]					
Buried depth	Calculated data	Buried depth	Calculated data	Buried depth	Calculated data
0.5m	 <p>U, Magnitude</p> <ul style="list-style-type: none"> +1.597e-01 +1.531e-01 +1.524e-01 +1.548e-01 +1.531e-01 +1.515e-01 +1.499e-01 +1.482e-01 +1.466e-01 +1.449e-01 +1.433e-01 +1.417e-01 +1.400e-01 	2.0m	 <p>U, Magnitude</p> <ul style="list-style-type: none"> +1.454e-01 +1.438e-01 +1.421e-01 +1.405e-01 +1.389e-01 +1.372e-01 +1.356e-01 +1.340e-01 +1.323e-01 +1.307e-01 +1.291e-01 +1.274e-01 +1.258e-01 	4.0m	 <p>U, Magnitude</p> <ul style="list-style-type: none"> +1.261e-01 +1.223e-01 +1.208e-01 +1.190e-01 +1.173e-01 +1.155e-01 +1.137e-01 +1.120e-01 +1.102e-01 +1.085e-01 +1.067e-01 +1.049e-01
1.0m	 <p>U, Magnitude</p> <ul style="list-style-type: none"> +1.547e-01 +1.531e-01 +1.515e-01 +1.499e-01 +1.484e-01 +1.468e-01 +1.452e-01 +1.436e-01 +1.420e-01 +1.405e-01 +1.389e-01 +1.373e-01 +1.357e-01 	2.5m	 <p>U, Magnitude</p> <ul style="list-style-type: none"> +1.408e-01 +1.391e-01 +1.374e-01 +1.357e-01 +1.340e-01 +1.324e-01 +1.307e-01 +1.290e-01 +1.273e-01 +1.257e-01 +1.240e-01 +1.223e-01 +1.206e-01 	5.0m	 <p>U, Magnitude</p> <ul style="list-style-type: none"> +1.158e-01 +1.140e-01 +1.122e-01 +1.104e-01 +1.086e-01 +1.068e-01 +1.050e-01 +1.032e-01 +1.014e-01 +9.956e-02 +9.775e-02 +9.594e-02 +9.414e-02
1.5m	 <p>U, Magnitude</p> <ul style="list-style-type: none"> +1.500e-01 +1.484e-01 +1.468e-01 +1.452e-01 +1.436e-01 +1.420e-01 +1.388e-01 +1.373e-01 +1.357e-01 +1.341e-01 +1.325e-01 +1.309e-01 	3.0m	 <p>U, Magnitude</p> <ul style="list-style-type: none"> +1.360e-01 +1.343e-01 +1.325e-01 +1.308e-01 +1.291e-01 +1.274e-01 +1.257e-01 +1.240e-01 +1.223e-01 +1.205e-01 +1.188e-01 +1.171e-01 +1.154e-01 	6.0m	 <p>U, Magnitude</p> <ul style="list-style-type: none"> +1.052e-01 +1.034e-01 +1.016e-01 +9.972e-02 +9.789e-02 +9.606e-02 +9.422e-02 +9.239e-02 +9.056e-02 +8.872e-02 +8.689e-02 +8.506e-02 +8.323e-02
[stress]					
Buried depth	Calculated data	Buried depth	Calculated data	Buried depth	Calculated data
0.5m	 <p>S, Mises SNEG, (fraction = -1.0) (Avg: 75%)</p> <ul style="list-style-type: none"> +2.081e+08 +1.923e+08 +1.765e+08 +1.607e+08 +1.449e+08 +1.291e+08 +1.133e+08 +9.751e+07 +8.172e+07 +6.593e+07 +5.014e+07 +3.434e+07 +1.855e+07 	2.0m	 <p>S, Mises SNEG, (fraction = -1.0) (Avg: 75%)</p> <ul style="list-style-type: none"> +2.148e+08 +1.983e+08 +1.819e+08 +1.651e+08 +1.486e+08 +1.320e+08 +1.154e+08 +9.884e+07 +8.227e+07 +6.570e+07 +4.912e+07 +3.255e+07 +1.598e+07 	4.0m	 <p>S, Mises SNEG, (fraction = -1.0) (Avg: 75%)</p> <ul style="list-style-type: none"> +2.273e+08 +2.108e+08 +1.943e+08 +1.778e+08 +1.614e+08 +1.449e+08 +1.284e+08 +1.119e+08 +9.544e+07 +7.896e+07 +6.249e+07 +4.601e+07 +2.953e+07
1.0m	 <p>S, Mises SNEG, (fraction = -1.0) (Avg: 75%)</p> <ul style="list-style-type: none"> +2.067e+08 +1.901e+08 +1.734e+08 +1.568e+08 +1.402e+08 +1.235e+08 +1.069e+08 +9.022e+07 +7.358e+07 +5.693e+07 +4.029e+07 +2.364e+07 +6.997e+06 	2.5m	 <p>S, Mises SNEG, (fraction = -1.0) (Avg: 75%)</p> <ul style="list-style-type: none"> +2.188e+08 +2.020e+08 +1.852e+08 +1.684e+08 +1.516e+08 +1.348e+08 +1.180e+08 +1.012e+08 +8.442e+07 +6.763e+07 +5.083e+07 +3.404e+07 +1.725e+07 	5.0m	 <p>S, Mises SNEG, (fraction = -1.0) (Avg: 75%)</p> <ul style="list-style-type: none"> +2.327e+08 +2.161e+08 +1.995e+08 +1.829e+08 +1.663e+08 +1.497e+08 +1.331e+08 +1.165e+08 +9.996e+07 +8.337e+07 +6.679e+07 +5.020e+07 +3.362e+07
1.5m	 <p>S, Mises SNEG, (fraction = -1.0) (Avg: 75%)</p> <ul style="list-style-type: none"> +2.107e+08 +1.933e+08 +1.760e+08 +1.586e+08 +1.413e+08 +1.239e+08 +1.066e+08 +8.922e+07 +7.187e+07 +5.452e+07 +3.718e+07 +1.983e+07 +2.478e+06 	3.0m	 <p>S, Mises SNEG, (fraction = -1.0) (Avg: 75%)</p> <ul style="list-style-type: none"> +2.224e+08 +2.056e+08 +1.888e+08 +1.720e+08 +1.552e+08 +1.384e+08 +1.216e+08 +1.048e+08 +8.804e+07 +7.125e+07 +5.446e+07 +3.766e+07 +2.087e+07 	6.0m	 <p>S, Mises SNEG, (fraction = -1.0) (Avg: 75%)</p> <ul style="list-style-type: none"> +2.386e+08 +2.218e+08 +2.046e+08 +1.876e+08 +1.706e+08 +1.536e+08 +1.366e+08 +1.196e+08 +1.026e+08 +8.559e+07 +6.858e+07 +5.158e+07 +3.457e+07

Appendix E. 4. Calculated static analysis results by ABAQUS for the pipeline in fully saturated sandy soil

[Displacement]					
Buried depth	Calculated data	Buried depth	Calculated data	Buried depth	Calculated data
0.5m		2.0m		4.0m	
1.0m		2.5m		5.0m	
1.5m		3.0m		6.0m	
[stress]					
Buried depth	Calculated data	Buried depth	Calculated data	Buried depth	Calculated data
0.5m		2.0m		4.0m	
1.0m		2.5m		5.0m	
1.5m		3.0m		6.0m	

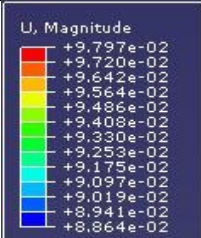
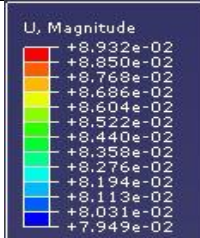
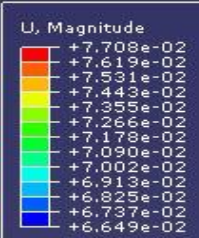
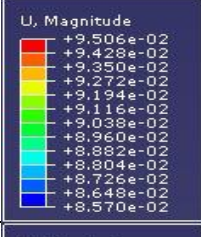
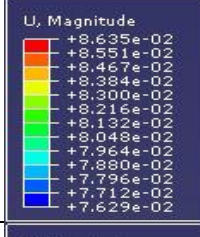
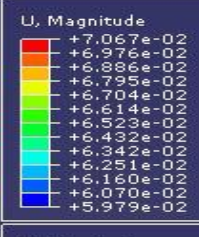
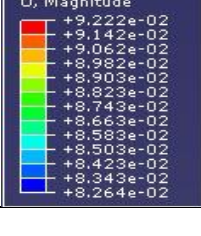
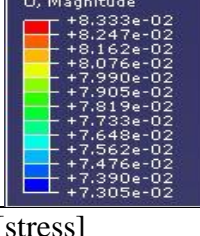
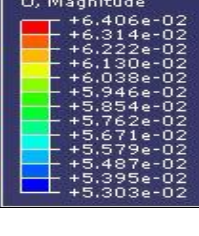
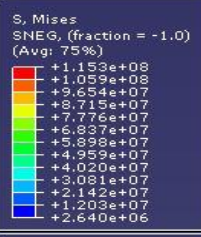
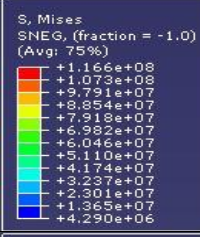
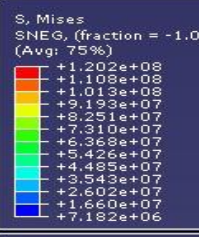
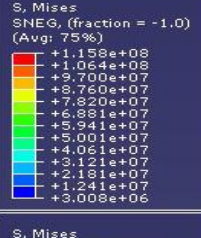

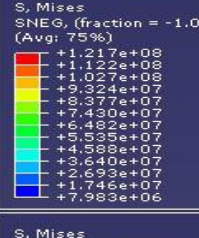
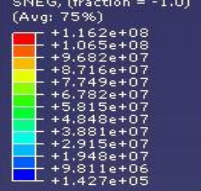
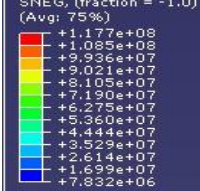
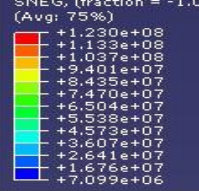
Appendix E. 5. Calculated static analysis results by ABAQUS for general moist cohesive soil

[Displacement]					
Buried depth	Calculated data	Buried depth	Calculated data	Buried depth	Calculated data
0.5m		2.0m		4.0m	
1.0m		2.5m		5.0m	
1.5m		3.0m		6.0m	
[stress]					
Buried depth	Calculated data	Buried depth	Calculated data	Buried depth	Calculated data
0.5m		2.0m		4.0m	
1.0m		2.5m		5.0m	
1.5m		3.0m		6.0m	

Appendix E. 6. Calculated static analysis results by ABAQUS for the pipeline in general moist cohesive soil

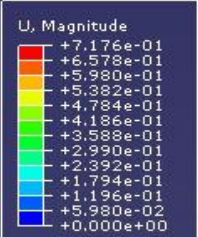
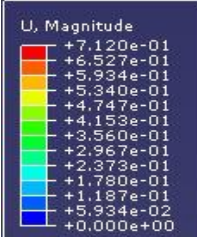
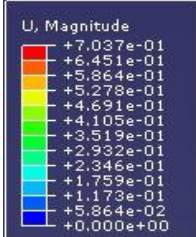
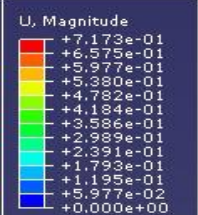
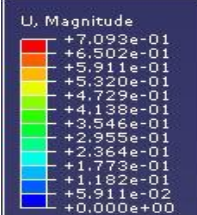
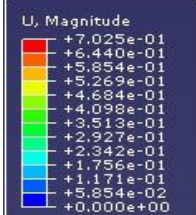
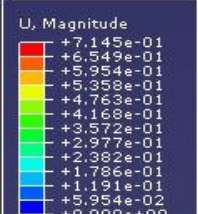
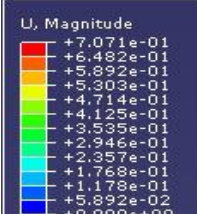
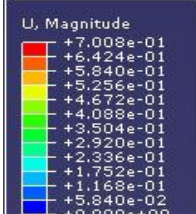
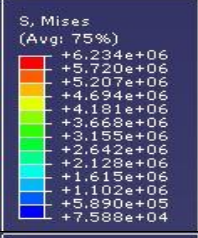
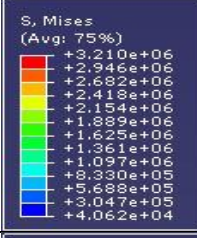
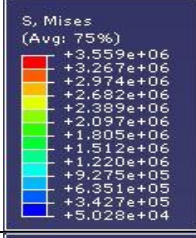
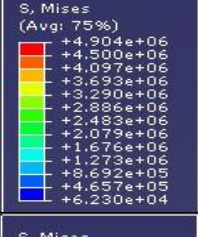
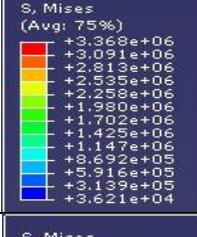
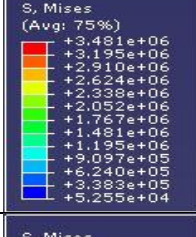
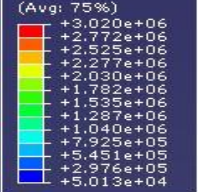
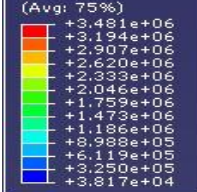
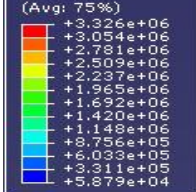
[Displacement]					
Buried depth	Calculated data	Buried depth	Calculated data	Buried depth	Calculated data
0.5m		2.0m		4.0m	
1.0m		2.5m		5.0m	
1.5m		3.0m		6.0m	
[stress]					
Buried depth	Calculated data	Buried depth	Calculated data	Buried depth	Calculated data
0.5m		2.0m		4.0m	
1.0m		2.5m		5.0m	
1.5m		3.0m		6.0m	

Appendix E. 7. Calculated static analysis results by ABAQUS for fully saturated cohesive soil

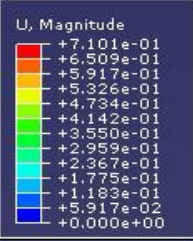
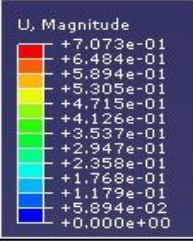
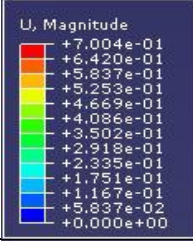
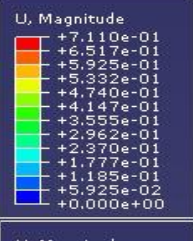
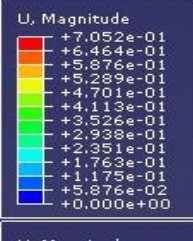
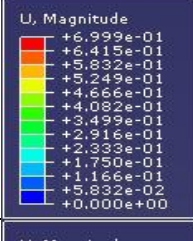
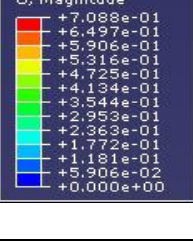
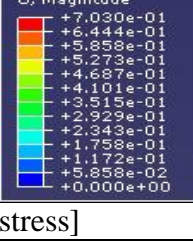
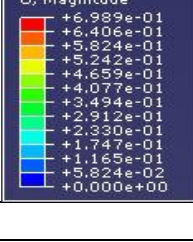
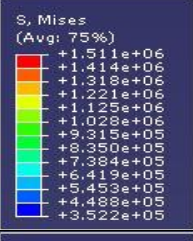
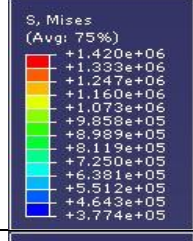
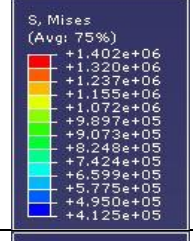
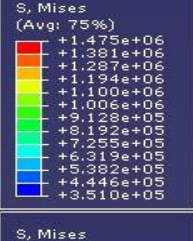
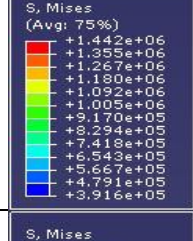
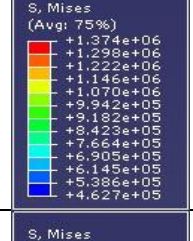
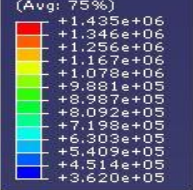
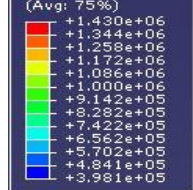
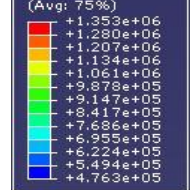
[Displacement]					
Buried depth	Calculated data	Buried depth	Calculated data	Buried depth	Calculated data
0.5m	 <p>U, Magnitude</p> <ul style="list-style-type: none"> +9.797e-02 +9.720e-02 +9.642e-02 +9.564e-02 +9.486e-02 +9.408e-02 +9.330e-02 +9.253e-02 +9.175e-02 +9.097e-02 +9.019e-02 +8.941e-02 +8.864e-02 	2.0m	 <p>U, Magnitude</p> <ul style="list-style-type: none"> +8.932e-02 +8.850e-02 +8.768e-02 +8.686e-02 +8.604e-02 +8.522e-02 +8.440e-02 +8.358e-02 +8.276e-02 +8.194e-02 +8.113e-02 +8.031e-02 +7.949e-02 	4.0m	 <p>U, Magnitude</p> <ul style="list-style-type: none"> +7.708e-02 +7.619e-02 +7.531e-02 +7.443e-02 +7.355e-02 +7.266e-02 +7.178e-02 +7.090e-02 +7.002e-02 +6.913e-02 +6.825e-02 +6.737e-02 +6.649e-02
1.0m	 <p>U, Magnitude</p> <ul style="list-style-type: none"> +9.506e-02 +9.428e-02 +9.350e-02 +9.272e-02 +9.194e-02 +9.116e-02 +9.038e-02 +8.960e-02 +8.882e-02 +8.804e-02 +8.726e-02 +8.648e-02 +8.570e-02 	2.5m	 <p>U, Magnitude</p> <ul style="list-style-type: none"> +8.635e-02 +8.551e-02 +8.467e-02 +8.384e-02 +8.300e-02 +8.216e-02 +8.132e-02 +8.048e-02 +7.964e-02 +7.880e-02 +7.796e-02 +7.712e-02 +7.629e-02 	5.0m	 <p>U, Magnitude</p> <ul style="list-style-type: none"> +7.067e-02 +6.976e-02 +6.886e-02 +6.795e-02 +6.704e-02 +6.614e-02 +6.523e-02 +6.432e-02 +6.342e-02 +6.251e-02 +6.160e-02 +6.070e-02 +5.979e-02
1.5m	 <p>U, Magnitude</p> <ul style="list-style-type: none"> +9.222e-02 +9.142e-02 +9.062e-02 +8.982e-02 +8.903e-02 +8.823e-02 +8.743e-02 +8.663e-02 +8.583e-02 +8.503e-02 +8.423e-02 +8.343e-02 +8.264e-02 	3.0m	 <p>U, Magnitude</p> <ul style="list-style-type: none"> +8.333e-02 +8.247e-02 +8.162e-02 +8.076e-02 +7.990e-02 +7.905e-02 +7.819e-02 +7.733e-02 +7.648e-02 +7.562e-02 +7.476e-02 +7.390e-02 +7.305e-02 	6.0m	 <p>U, Magnitude</p> <ul style="list-style-type: none"> +6.406e-02 +6.314e-02 +6.222e-02 +6.130e-02 +6.038e-02 +5.946e-02 +5.854e-02 +5.762e-02 +5.671e-02 +5.579e-02 +5.487e-02 +5.395e-02 +5.303e-02
[stress]					
Buried depth	Calculated data	Buried depth	Calculated data	Buried depth	Calculated data
0.5m	 <p>S, Mises SNEG, (fraction = -1.0) (Avg: 75%)</p> <ul style="list-style-type: none"> +1.153e+08 +1.059e+08 +9.644e+07 +8.715e+07 +7.776e+07 +6.837e+07 +5.898e+07 +4.959e+07 +4.020e+07 +3.081e+07 +2.142e+07 +1.203e+07 +2.640e+06 	2.0m	 <p>S, Mises SNEG, (fraction = -1.0) (Avg: 75%)</p> <ul style="list-style-type: none"> +1.166e+08 +1.073e+08 +9.791e+07 +8.854e+07 +7.918e+07 +6.982e+07 +6.046e+07 +5.110e+07 +4.174e+07 +3.237e+07 +2.301e+07 +1.365e+07 +4.290e+06 	4.0m	 <p>S, Mises SNEG, (fraction = -1.0) (Avg: 75%)</p> <ul style="list-style-type: none"> +1.202e+08 +1.108e+08 +1.013e+08 +9.193e+07 +8.251e+07 +7.310e+07 +6.368e+07 +5.426e+07 +4.485e+07 +3.543e+07 +2.602e+07 +1.660e+07 +7.182e+06
1.0m	 <p>S, Mises SNEG, (fraction = -1.0) (Avg: 75%)</p> <ul style="list-style-type: none"> +1.158e+08 +1.064e+08 +9.700e+07 +8.760e+07 +7.820e+07 +6.881e+07 +5.941e+07 +5.001e+07 +4.061e+07 +3.121e+07 +2.181e+07 +1.241e+07 +3.008e+06 	2.5m	 <p>S, Mises SNEG, (fraction = -1.0) (Avg: 75%)</p> <ul style="list-style-type: none"> +1.172e+08 +1.080e+08 +9.877e+07 +8.959e+07 +8.040e+07 +7.121e+07 +6.202e+07 +5.283e+07 +4.364e+07 +3.446e+07 +2.527e+07 +1.608e+07 +6.890e+06 	5.0m	 <p>S, Mises SNEG, (fraction = -1.0) (Avg: 75%)</p> <ul style="list-style-type: none"> +1.217e+08 +1.122e+08 +1.027e+08 +9.324e+07 +8.377e+07 +7.430e+07 +6.482e+07 +5.535e+07 +4.588e+07 +3.640e+07 +2.693e+07 +1.746e+07 +7.933e+06
1.5m	 <p>S, Mises SNEG, (fraction = -1.0) (Avg: 75%)</p> <ul style="list-style-type: none"> +1.162e+08 +1.065e+08 +9.682e+07 +8.716e+07 +7.749e+07 +6.782e+07 +5.815e+07 +4.848e+07 +3.881e+07 +2.915e+07 +1.949e+07 +9.811e+06 +1.427e+05 	3.0m	 <p>S, Mises SNEG, (fraction = -1.0) (Avg: 75%)</p> <ul style="list-style-type: none"> +1.177e+08 +1.085e+08 +9.936e+07 +9.021e+07 +8.105e+07 +7.190e+07 +6.275e+07 +5.360e+07 +4.444e+07 +3.529e+07 +2.614e+07 +1.699e+07 +7.832e+06 	6.0m	 <p>S, Mises SNEG, (fraction = -1.0) (Avg: 75%)</p> <ul style="list-style-type: none"> +1.230e+08 +1.133e+08 +1.037e+08 +9.401e+07 +8.435e+07 +7.470e+07 +6.504e+07 +5.538e+07 +4.573e+07 +3.607e+07 +2.641e+07 +1.676e+07 +7.099e+06

Appendix E. 8. Calculated static analysis results by ABAQUS for the pipeline in fully saturated cohesive soil

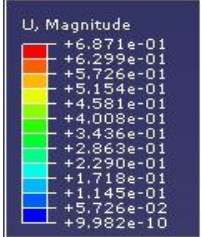
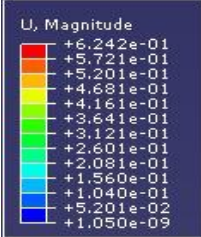
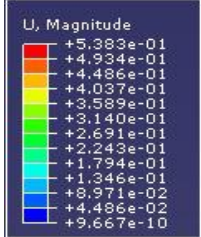
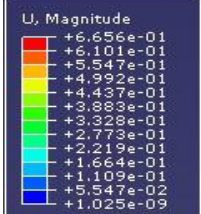
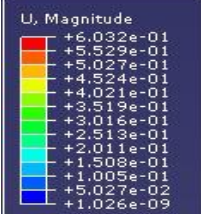
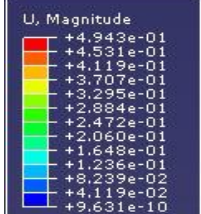
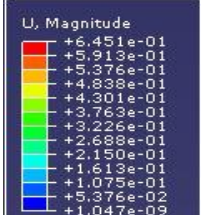
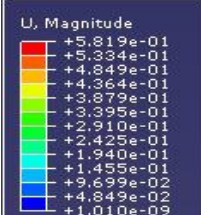
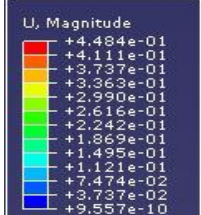
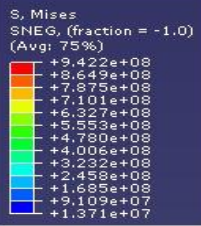
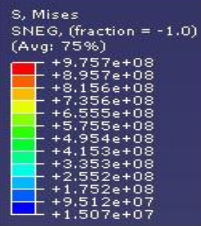
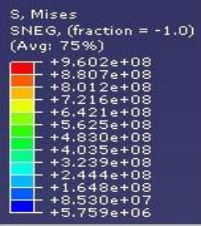
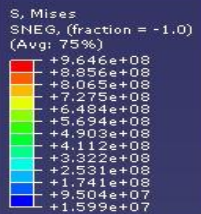
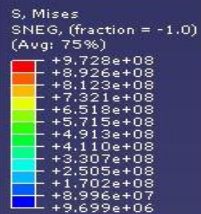
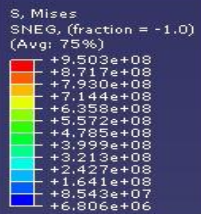
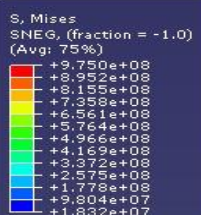
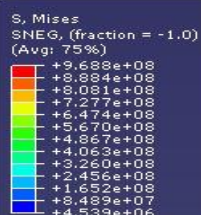
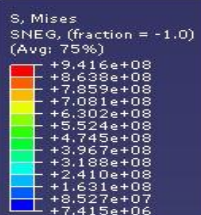
Appendix F – the calculated data for boundary condition effect

[Displacement]					
Buried depth	Calculated data	Buried depth	Calculated data	Buried depth	Calculated data
0.5m	 <p>U, Magnitude</p> <ul style="list-style-type: none"> +7.176e-01 +6.578e-01 +5.980e-01 +5.382e-01 +4.784e-01 +4.186e-01 +3.588e-01 +2.990e-01 +2.392e-01 +1.794e-01 +1.196e-01 +5.980e-02 +0.000e+00 	2.0m	 <p>U, Magnitude</p> <ul style="list-style-type: none"> +7.120e-01 +6.527e-01 +5.934e-01 +5.340e-01 +4.747e-01 +4.153e-01 +3.560e-01 +2.967e-01 +2.373e-01 +1.780e-01 +1.187e-01 +5.934e-02 +0.000e+00 	4.0m	 <p>U, Magnitude</p> <ul style="list-style-type: none"> +7.037e-01 +6.451e-01 +5.864e-01 +5.278e-01 +4.691e-01 +4.105e-01 +3.519e-01 +2.932e-01 +2.346e-01 +1.759e-01 +1.173e-01 +5.864e-02 +0.000e+00
1.0m	 <p>U, Magnitude</p> <ul style="list-style-type: none"> +7.173e-01 +6.575e-01 +5.977e-01 +5.379e-01 +4.782e-01 +4.184e-01 +3.586e-01 +2.989e-01 +2.391e-01 +1.793e-01 +1.195e-01 +5.977e-02 +0.000e+00 	2.5m	 <p>U, Magnitude</p> <ul style="list-style-type: none"> +7.093e-01 +6.502e-01 +5.911e-01 +5.320e-01 +4.729e-01 +4.138e-01 +3.546e-01 +2.955e-01 +2.364e-01 +1.773e-01 +1.182e-01 +5.911e-02 +0.000e+00 	5.0m	 <p>U, Magnitude</p> <ul style="list-style-type: none"> +7.025e-01 +6.440e-01 +5.854e-01 +5.269e-01 +4.684e-01 +4.098e-01 +3.513e-01 +2.927e-01 +2.342e-01 +1.756e-01 +1.171e-01 +5.854e-02 +0.000e+00
1.5m	 <p>U, Magnitude</p> <ul style="list-style-type: none"> +7.145e-01 +6.549e-01 +5.954e-01 +5.358e-01 +4.763e-01 +4.168e-01 +3.572e-01 +2.977e-01 +2.382e-01 +1.786e-01 +1.191e-01 +5.954e-02 +0.000e+00 	3.0m	 <p>U, Magnitude</p> <ul style="list-style-type: none"> +7.071e-01 +6.482e-01 +5.892e-01 +5.303e-01 +4.714e-01 +4.125e-01 +3.535e-01 +2.946e-01 +2.357e-01 +1.768e-01 +1.178e-01 +5.892e-02 +0.000e+00 	6.0m	 <p>U, Magnitude</p> <ul style="list-style-type: none"> +7.008e-01 +6.424e-01 +5.840e-01 +5.256e-01 +4.672e-01 +4.088e-01 +3.504e-01 +2.920e-01 +2.336e-01 +1.752e-01 +1.168e-01 +5.840e-02 +0.000e+00
[stress]					
Buried depth	Calculated data	Buried depth	Calculated data	Buried depth	Calculated data
0.5m	 <p>S, Mises (Avg: 75%)</p> <ul style="list-style-type: none"> +6.234e+06 +5.720e+06 +5.207e+06 +4.694e+06 +4.181e+06 +3.668e+06 +3.155e+06 +2.642e+06 +2.128e+06 +1.615e+06 +1.102e+06 +5.890e+05 +7.588e+04 	2.0m	 <p>S, Mises (Avg: 75%)</p> <ul style="list-style-type: none"> +3.210e+06 +2.946e+06 +2.682e+06 +2.418e+06 +2.154e+06 +1.889e+06 +1.625e+06 +1.361e+06 +1.097e+06 +8.330e+05 +5.688e+05 +3.047e+05 +4.062e+04 	4.0m	 <p>S, Mises (Avg: 75%)</p> <ul style="list-style-type: none"> +3.559e+06 +3.267e+06 +2.974e+06 +2.682e+06 +2.389e+06 +2.097e+06 +1.805e+06 +1.512e+06 +1.220e+06 +9.275e+05 +6.351e+05 +3.427e+05 +5.028e+04
1.0m	 <p>S, Mises (Avg: 75%)</p> <ul style="list-style-type: none"> +4.904e+06 +4.500e+06 +4.097e+06 +3.693e+06 +3.290e+06 +2.886e+06 +2.483e+06 +2.079e+06 +1.676e+06 +1.273e+06 +8.692e+05 +4.657e+05 +6.230e+04 	2.5m	 <p>S, Mises (Avg: 75%)</p> <ul style="list-style-type: none"> +3.368e+06 +3.091e+06 +2.813e+06 +2.535e+06 +2.258e+06 +1.980e+06 +1.702e+06 +1.425e+06 +1.147e+06 +8.692e+05 +5.916e+05 +3.139e+05 +3.621e+04 	5.0m	 <p>S, Mises (Avg: 75%)</p> <ul style="list-style-type: none"> +3.481e+06 +3.195e+06 +2.910e+06 +2.624e+06 +2.338e+06 +2.052e+06 +1.767e+06 +1.481e+06 +1.195e+06 +9.097e+05 +6.240e+05 +3.383e+05 +5.255e+04
1.5m	 <p>S, Mises (Avg: 75%)</p> <ul style="list-style-type: none"> +3.020e+06 +2.772e+06 +2.525e+06 +2.277e+06 +2.030e+06 +1.782e+06 +1.535e+06 +1.287e+06 +1.040e+06 +7.925e+05 +5.451e+05 +2.976e+05 +5.013e+04 	3.0m	 <p>S, Mises (Avg: 75%)</p> <ul style="list-style-type: none"> +3.481e+06 +3.194e+06 +2.907e+06 +2.620e+06 +2.333e+06 +2.046e+06 +1.759e+06 +1.473e+06 +1.186e+06 +8.988e+05 +6.119e+05 +3.250e+05 +3.817e+04 	6.0m	 <p>S, Mises (Avg: 75%)</p> <ul style="list-style-type: none"> +3.326e+06 +3.054e+06 +2.781e+06 +2.509e+06 +2.237e+06 +1.965e+06 +1.692e+06 +1.420e+06 +1.148e+06 +8.756e+05 +6.033e+05 +3.311e+05 +5.879e+04

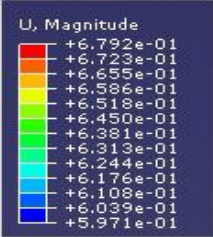
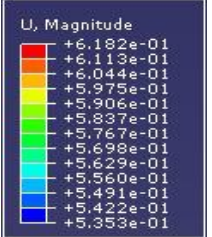
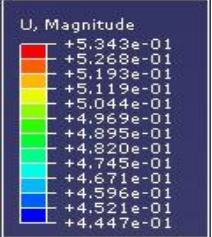
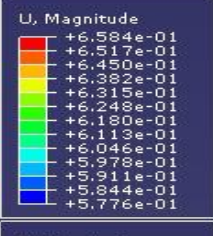
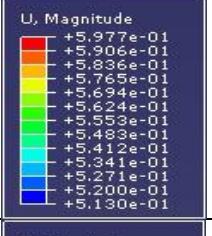
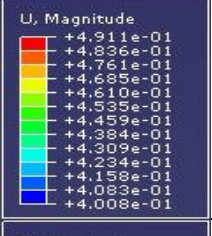
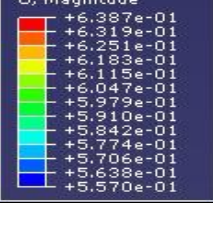
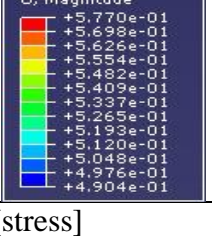
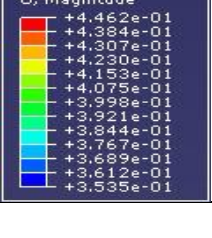
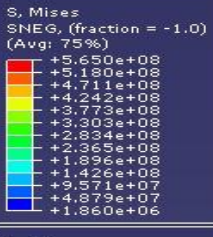
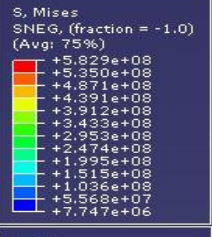
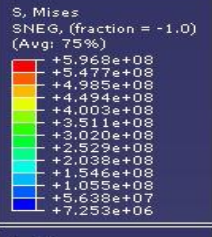
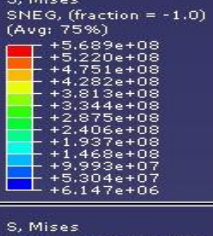
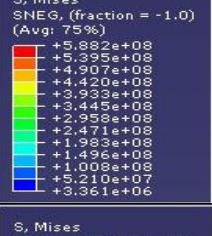
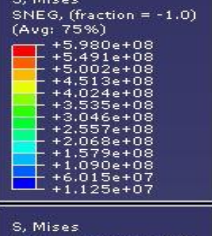
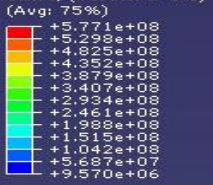
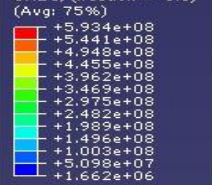
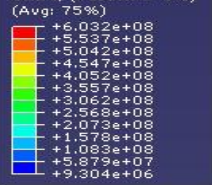
Appendix F. 1. Calculated static analysis results by ABAQUS for general moist sandy soil with hinge boundary condition at pipeline ends

[Displacement]					
Buried depth	Calculated data	Buried depth	Calculated data	Buried depth	Calculated data
0.5m	 <p>U, Magnitude</p> <ul style="list-style-type: none"> +7.101e-01 +6.509e-01 +5.917e-01 +5.326e-01 +4.734e-01 +4.142e-01 +3.550e-01 +2.959e-01 +2.367e-01 +1.775e-01 +1.183e-01 +5.917e-02 +0.000e+00 	2.0m	 <p>U, Magnitude</p> <ul style="list-style-type: none"> +7.073e-01 +6.484e-01 +5.894e-01 +5.305e-01 +4.715e-01 +4.126e-01 +3.537e-01 +2.947e-01 +2.358e-01 +1.768e-01 +1.179e-01 +5.894e-02 +0.000e+00 	4.0m	 <p>U, Magnitude</p> <ul style="list-style-type: none"> +7.004e-01 +6.420e-01 +5.837e-01 +5.253e-01 +4.669e-01 +4.086e-01 +3.502e-01 +2.918e-01 +2.335e-01 +1.751e-01 +1.167e-01 +5.837e-02 +0.000e+00
1.0m	 <p>U, Magnitude</p> <ul style="list-style-type: none"> +7.110e-01 +6.517e-01 +5.925e-01 +5.332e-01 +4.740e-01 +4.147e-01 +3.555e-01 +2.962e-01 +2.370e-01 +1.777e-01 +1.185e-01 +5.925e-02 +0.000e+00 	2.5m	 <p>U, Magnitude</p> <ul style="list-style-type: none"> +7.052e-01 +6.464e-01 +5.876e-01 +5.289e-01 +4.701e-01 +4.113e-01 +3.526e-01 +2.938e-01 +2.351e-01 +1.763e-01 +1.175e-01 +5.876e-02 +0.000e+00 	5.0m	 <p>U, Magnitude</p> <ul style="list-style-type: none"> +6.999e-01 +6.415e-01 +5.832e-01 +5.249e-01 +4.666e-01 +4.082e-01 +3.499e-01 +2.916e-01 +2.333e-01 +1.750e-01 +1.166e-01 +5.832e-02 +0.000e+00
1.5m	 <p>U, Magnitude</p> <ul style="list-style-type: none"> +7.088e-01 +6.497e-01 +5.906e-01 +5.316e-01 +4.725e-01 +4.134e-01 +3.544e-01 +2.953e-01 +2.363e-01 +1.772e-01 +1.181e-01 +5.906e-02 +0.000e+00 	3.0m	 <p>U, Magnitude</p> <ul style="list-style-type: none"> +7.030e-01 +6.444e-01 +5.858e-01 +5.273e-01 +4.687e-01 +4.101e-01 +3.515e-01 +2.929e-01 +2.343e-01 +1.758e-01 +1.172e-01 +5.858e-02 +0.000e+00 	6.0m	 <p>U, Magnitude</p> <ul style="list-style-type: none"> +6.989e-01 +6.406e-01 +5.824e-01 +5.242e-01 +4.659e-01 +4.077e-01 +3.494e-01 +2.912e-01 +2.330e-01 +1.747e-01 +1.165e-01 +5.824e-02 +0.000e+00
[stress]					
Buried depth	Calculated data	Buried depth	Calculated data	Buried depth	Calculated data
0.5m	 <p>S, Mises (Avg: 75%)</p> <ul style="list-style-type: none"> +1.511e+06 +1.414e+06 +1.318e+06 +1.221e+06 +1.125e+06 +1.028e+06 +9.315e+05 +8.350e+05 +7.384e+05 +6.419e+05 +5.453e+05 +4.488e+05 +3.522e+05 	2.0m	 <p>S, Mises (Avg: 75%)</p> <ul style="list-style-type: none"> +1.420e+06 +1.333e+06 +1.247e+06 +1.160e+06 +1.073e+06 +9.858e+05 +8.989e+05 +8.119e+05 +7.250e+05 +6.381e+05 +5.512e+05 +4.643e+05 +3.774e+05 	4.0m	 <p>S, Mises (Avg: 75%)</p> <ul style="list-style-type: none"> +1.402e+06 +1.320e+06 +1.237e+06 +1.155e+06 +1.072e+06 +9.897e+05 +9.073e+05 +8.248e+05 +7.424e+05 +6.599e+05 +5.775e+05 +4.950e+05 +4.125e+05
1.0m	 <p>S, Mises (Avg: 75%)</p> <ul style="list-style-type: none"> +1.475e+06 +1.381e+06 +1.287e+06 +1.194e+06 +1.100e+06 +1.006e+06 +9.128e+05 +8.192e+05 +7.255e+05 +6.319e+05 +5.382e+05 +4.446e+05 +3.510e+05 	2.5m	 <p>S, Mises (Avg: 75%)</p> <ul style="list-style-type: none"> +1.442e+06 +1.355e+06 +1.267e+06 +1.180e+06 +1.092e+06 +1.005e+06 +9.170e+05 +8.294e+05 +7.418e+05 +6.543e+05 +5.667e+05 +4.791e+05 +3.916e+05 	5.0m	 <p>S, Mises (Avg: 75%)</p> <ul style="list-style-type: none"> +1.374e+06 +1.298e+06 +1.222e+06 +1.146e+06 +1.070e+06 +9.942e+05 +9.182e+05 +8.423e+05 +7.664e+05 +6.905e+05 +6.145e+05 +5.386e+05 +4.627e+05
1.5m	 <p>S, Mises (Avg: 75%)</p> <ul style="list-style-type: none"> +1.435e+06 +1.346e+06 +1.256e+06 +1.167e+06 +1.078e+06 +9.881e+05 +8.987e+05 +8.092e+05 +7.198e+05 +6.303e+05 +5.409e+05 +4.514e+05 +3.620e+05 	3.0m	 <p>S, Mises (Avg: 75%)</p> <ul style="list-style-type: none"> +1.430e+06 +1.344e+06 +1.258e+06 +1.172e+06 +1.086e+06 +1.000e+06 +9.142e+05 +8.282e+05 +7.422e+05 +6.562e+05 +5.702e+05 +4.841e+05 +3.981e+05 	6.0m	 <p>S, Mises (Avg: 75%)</p> <ul style="list-style-type: none"> +1.353e+06 +1.280e+06 +1.207e+06 +1.134e+06 +1.061e+06 +9.879e+05 +9.147e+05 +8.417e+05 +7.686e+05 +6.955e+05 +6.224e+05 +5.494e+05 +4.763e+05

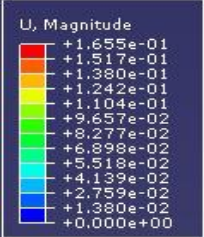
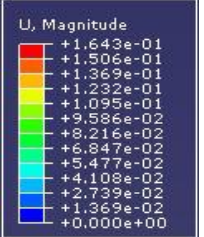
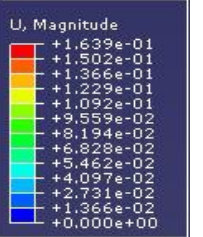
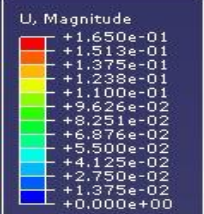
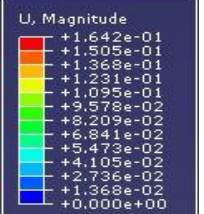
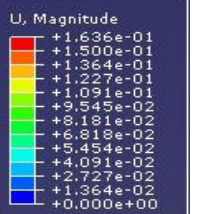
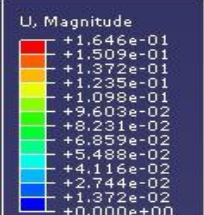
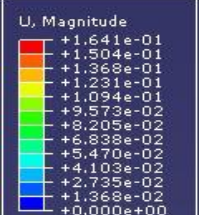
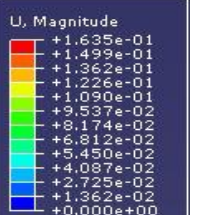
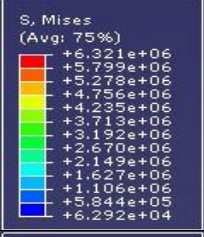
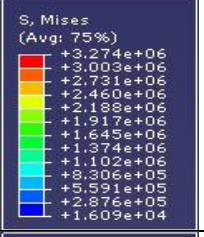
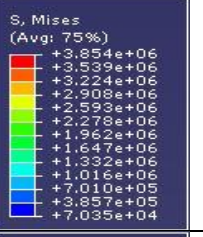
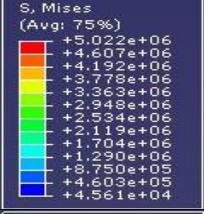
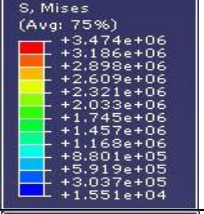
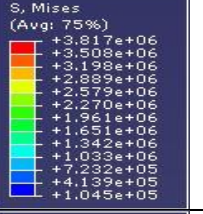
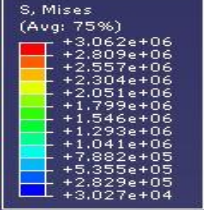
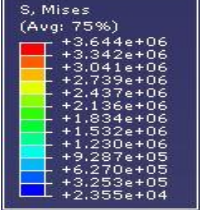
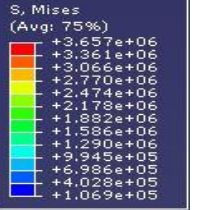
Appendix F. 2. Calculated static analysis results by ABAQUS for general moist sandy soil with roller boundary condition at pipeline ends

[Displacement]					
Buried depth	Calculated data	Buried depth	Calculated data	Buried depth	Calculated data
0.5m	 <p>U, Magnitude</p> <ul style="list-style-type: none"> +6.871e-01 +5.999e-01 +5.726e-01 +5.154e-01 +4.581e-01 +4.008e-01 +3.436e-01 +2.863e-01 +2.290e-01 +1.718e-01 +1.145e-01 +5.726e-02 +9.982e-10 	2.0m	 <p>U, Magnitude</p> <ul style="list-style-type: none"> +6.242e-01 +5.721e-01 +5.201e-01 +4.681e-01 +4.161e-01 +3.641e-01 +3.121e-01 +2.601e-01 +2.081e-01 +1.560e-01 +1.040e-01 +5.201e-02 +1.050e-09 	4.0m	 <p>U, Magnitude</p> <ul style="list-style-type: none"> +5.383e-01 +4.934e-01 +4.486e-01 +4.037e-01 +3.589e-01 +3.140e-01 +2.691e-01 +2.243e-01 +1.794e-01 +1.346e-01 +8.971e-02 +4.486e-02 +9.667e-10
1.0m	 <p>U, Magnitude</p> <ul style="list-style-type: none"> +6.656e-01 +6.101e-01 +5.547e-01 +4.992e-01 +4.437e-01 +3.883e-01 +3.328e-01 +2.773e-01 +2.219e-01 +1.664e-01 +1.109e-01 +5.547e-02 +1.025e-09 	2.5m	 <p>U, Magnitude</p> <ul style="list-style-type: none"> +6.032e-01 +5.529e-01 +5.027e-01 +4.524e-01 +4.021e-01 +3.519e-01 +3.016e-01 +2.513e-01 +2.011e-01 +1.508e-01 +1.005e-01 +5.027e-02 +1.026e-09 	5.0m	 <p>U, Magnitude</p> <ul style="list-style-type: none"> +4.943e-01 +4.531e-01 +4.119e-01 +3.707e-01 +3.295e-01 +2.884e-01 +2.472e-01 +2.060e-01 +1.648e-01 +1.236e-01 +8.239e-02 +4.119e-02 +9.631e-10
1.5m	 <p>U, Magnitude</p> <ul style="list-style-type: none"> +6.451e-01 +5.913e-01 +5.376e-01 +4.838e-01 +4.301e-01 +3.763e-01 +3.226e-01 +2.688e-01 +2.150e-01 +1.613e-01 +1.075e-01 +5.376e-02 +1.047e-09 	3.0m	 <p>U, Magnitude</p> <ul style="list-style-type: none"> +5.819e-01 +5.334e-01 +4.849e-01 +4.364e-01 +3.879e-01 +3.395e-01 +2.910e-01 +2.425e-01 +1.940e-01 +1.455e-01 +9.699e-02 +4.849e-02 +1.010e-09 	6.0m	 <p>U, Magnitude</p> <ul style="list-style-type: none"> +4.484e-01 +4.111e-01 +3.737e-01 +3.363e-01 +2.990e-01 +2.616e-01 +2.242e-01 +1.869e-01 +1.495e-01 +1.121e-01 +7.474e-02 +3.737e-02 +9.557e-10
[stress]					
Buried depth	Calculated data	Buried depth	Calculated data	Buried depth	Calculated data
0.5m	 <p>S, Mises SNEG, (fraction = -1.0) (Avg: 75%)</p> <ul style="list-style-type: none"> +9.422e+08 +8.449e+08 +7.875e+08 +7.101e+08 +6.327e+08 +5.553e+08 +4.779e+08 +4.006e+08 +3.232e+08 +2.458e+08 +1.685e+08 +9.109e+07 +1.371e+07 	2.0m	 <p>S, Mises SNEG, (fraction = -1.0) (Avg: 75%)</p> <ul style="list-style-type: none"> +9.757e+08 +8.957e+08 +8.156e+08 +7.356e+08 +6.555e+08 +5.755e+08 +4.954e+08 +4.153e+08 +3.353e+08 +2.552e+08 +1.752e+08 +9.512e+07 +1.507e+07 	4.0m	 <p>S, Mises SNEG, (fraction = -1.0) (Avg: 75%)</p> <ul style="list-style-type: none"> +9.602e+08 +8.907e+08 +8.012e+08 +7.216e+08 +6.421e+08 +5.625e+08 +4.830e+08 +4.035e+08 +3.239e+08 +2.444e+08 +1.643e+08 +8.530e+07 +5.759e+06
1.0m	 <p>S, Mises SNEG, (fraction = -1.0) (Avg: 75%)</p> <ul style="list-style-type: none"> +9.646e+08 +8.856e+08 +8.065e+08 +7.275e+08 +6.484e+08 +5.694e+08 +4.903e+08 +4.112e+08 +3.322e+08 +2.531e+08 +1.741e+08 +9.504e+07 +1.599e+07 	2.5m	 <p>S, Mises SNEG, (fraction = -1.0) (Avg: 75%)</p> <ul style="list-style-type: none"> +9.728e+08 +8.926e+08 +8.123e+08 +7.321e+08 +6.518e+08 +5.715e+08 +4.913e+08 +4.110e+08 +3.307e+08 +2.505e+08 +1.702e+08 +8.996e+07 +9.699e+06 	5.0m	 <p>S, Mises SNEG, (fraction = -1.0) (Avg: 75%)</p> <ul style="list-style-type: none"> +9.503e+08 +8.717e+08 +7.930e+08 +7.144e+08 +6.358e+08 +5.572e+08 +4.785e+08 +3.999e+08 +3.213e+08 +2.427e+08 +1.641e+08 +8.543e+07 +6.806e+06
1.5m	 <p>S, Mises SNEG, (fraction = -1.0) (Avg: 75%)</p> <ul style="list-style-type: none"> +9.750e+08 +8.952e+08 +8.155e+08 +7.358e+08 +6.561e+08 +5.764e+08 +4.966e+08 +4.169e+08 +3.372e+08 +2.575e+08 +1.778e+08 +9.804e+07 +1.832e+07 	3.0m	 <p>S, Mises SNEG, (fraction = -1.0) (Avg: 75%)</p> <ul style="list-style-type: none"> +9.688e+08 +8.884e+08 +8.081e+08 +7.277e+08 +6.474e+08 +5.670e+08 +4.867e+08 +4.063e+08 +3.260e+08 +2.456e+08 +1.652e+08 +8.489e+07 +4.539e+06 	6.0m	 <p>S, Mises SNEG, (fraction = -1.0) (Avg: 75%)</p> <ul style="list-style-type: none"> +9.416e+08 +8.638e+08 +7.859e+08 +7.081e+08 +6.302e+08 +5.524e+08 +4.745e+08 +3.967e+08 +3.188e+08 +2.410e+08 +1.631e+08 +8.527e+07 +7.415e+06

Appendix F. 3. Calculated static analysis results by ABAQUS for the pipeline in general moist sandy soil with hinge boundary condition at pipeline ends

[Displacement]					
Buried depth	Calculated data	Buried depth	Calculated data	Buried depth	Calculated data
0.5m	 <p>U, Magnitude</p> <ul style="list-style-type: none"> +6.792e-01 +6.723e-01 +6.655e-01 +6.586e-01 +6.518e-01 +6.450e-01 +6.381e-01 +6.313e-01 +6.244e-01 +6.176e-01 +6.108e-01 +6.039e-01 +5.971e-01 	2.0m	 <p>U, Magnitude</p> <ul style="list-style-type: none"> +6.182e-01 +6.113e-01 +6.044e-01 +5.975e-01 +5.906e-01 +5.837e-01 +5.767e-01 +5.698e-01 +5.629e-01 +5.560e-01 +5.491e-01 +5.422e-01 +5.353e-01 	4.0m	 <p>U, Magnitude</p> <ul style="list-style-type: none"> +5.342e-01 +5.268e-01 +5.193e-01 +5.119e-01 +5.044e-01 +4.969e-01 +4.895e-01 +4.820e-01 +4.745e-01 +4.671e-01 +4.596e-01 +4.521e-01 +4.447e-01
1.0m	 <p>U, Magnitude</p> <ul style="list-style-type: none"> +6.584e-01 +6.517e-01 +6.450e-01 +6.382e-01 +6.315e-01 +6.248e-01 +6.180e-01 +6.113e-01 +6.046e-01 +5.978e-01 +5.911e-01 +5.844e-01 +5.776e-01 	2.5m	 <p>U, Magnitude</p> <ul style="list-style-type: none"> +5.977e-01 +5.906e-01 +5.836e-01 +5.765e-01 +5.694e-01 +5.624e-01 +5.553e-01 +5.483e-01 +5.412e-01 +5.341e-01 +5.271e-01 +5.200e-01 +5.130e-01 	5.0m	 <p>U, Magnitude</p> <ul style="list-style-type: none"> +4.911e-01 +4.836e-01 +4.761e-01 +4.685e-01 +4.610e-01 +4.535e-01 +4.459e-01 +4.384e-01 +4.309e-01 +4.234e-01 +4.158e-01 +4.083e-01 +4.008e-01
1.5m	 <p>U, Magnitude</p> <ul style="list-style-type: none"> +6.387e-01 +6.319e-01 +6.251e-01 +6.183e-01 +6.115e-01 +6.047e-01 +5.979e-01 +5.910e-01 +5.842e-01 +5.774e-01 +5.706e-01 +5.638e-01 +5.570e-01 	3.0m	 <p>U, Magnitude</p> <ul style="list-style-type: none"> +5.770e-01 +5.698e-01 +5.626e-01 +5.554e-01 +5.482e-01 +5.409e-01 +5.337e-01 +5.265e-01 +5.193e-01 +5.120e-01 +5.048e-01 +4.976e-01 +4.904e-01 	6.0m	 <p>U, Magnitude</p> <ul style="list-style-type: none"> +4.462e-01 +4.387e-01 +4.312e-01 +4.237e-01 +4.162e-01 +4.087e-01 +3.998e-01 +3.921e-01 +3.844e-01 +3.767e-01 +3.689e-01 +3.612e-01 +3.535e-01
[stress]					
Buried depth	Calculated data	Buried depth	Calculated data	Buried depth	Calculated data
0.5m	 <p>S, Mises SNEG, (fraction = -1.0) (Avg: 75%)</p> <ul style="list-style-type: none"> +5.650e+08 +5.180e+08 +4.711e+08 +4.242e+08 +3.773e+08 +3.303e+08 +2.834e+08 +2.365e+08 +1.896e+08 +1.426e+08 +9.571e+07 +4.879e+07 +1.860e+06 	2.0m	 <p>S, Mises SNEG, (fraction = -1.0) (Avg: 75%)</p> <ul style="list-style-type: none"> +5.922e+08 +5.350e+08 +4.771e+08 +4.191e+08 +3.612e+08 +3.033e+08 +2.454e+08 +1.875e+08 +1.296e+08 +7.171e+07 +1.036e+08 +5.568e+07 +7.747e+06 	4.0m	 <p>S, Mises SNEG, (fraction = -1.0) (Avg: 75%)</p> <ul style="list-style-type: none"> +5.968e+08 +5.396e+08 +4.817e+08 +4.238e+08 +3.659e+08 +3.080e+08 +2.501e+08 +1.922e+08 +1.343e+08 +7.64e+07 +1.055e+08 +5.638e+07 +7.253e+06
1.0m	 <p>S, Mises SNEG, (fraction = -1.0) (Avg: 75%)</p> <ul style="list-style-type: none"> +5.689e+08 +5.220e+08 +4.751e+08 +4.282e+08 +3.813e+08 +3.344e+08 +2.875e+08 +2.406e+08 +1.937e+08 +1.468e+08 +9.99e+07 +5.304e+07 +6.147e+06 	2.5m	 <p>S, Mises SNEG, (fraction = -1.0) (Avg: 75%)</p> <ul style="list-style-type: none"> +5.882e+08 +5.395e+08 +4.907e+08 +4.420e+08 +3.933e+08 +3.445e+08 +2.958e+08 +2.471e+08 +1.983e+08 +1.496e+08 +1.008e+08 +5.210e+07 +3.361e+06 	5.0m	 <p>S, Mises SNEG, (fraction = -1.0) (Avg: 75%)</p> <ul style="list-style-type: none"> +5.980e+08 +5.491e+08 +5.002e+08 +4.513e+08 +4.024e+08 +3.535e+08 +3.046e+08 +2.557e+08 +2.068e+08 +1.579e+08 +1.090e+08 +6.015e+07 +1.125e+07
1.5m	 <p>S, Mises SNEG, (fraction = -1.0) (Avg: 75%)</p> <ul style="list-style-type: none"> +5.771e+08 +5.298e+08 +4.825e+08 +4.352e+08 +3.879e+08 +3.407e+08 +2.934e+08 +2.461e+08 +1.989e+08 +1.515e+08 +1.042e+08 +5.687e+07 +9.570e+06 	3.0m	 <p>S, Mises SNEG, (fraction = -1.0) (Avg: 75%)</p> <ul style="list-style-type: none"> +5.934e+08 +5.441e+08 +4.948e+08 +4.455e+08 +3.962e+08 +3.469e+08 +2.975e+08 +2.482e+08 +1.989e+08 +1.496e+08 +1.003e+08 +5.098e+07 +1.662e+06 	6.0m	 <p>S, Mises SNEG, (fraction = -1.0) (Avg: 75%)</p> <ul style="list-style-type: none"> +6.032e+08 +5.537e+08 +5.042e+08 +4.547e+08 +4.052e+08 +3.557e+08 +3.062e+08 +2.568e+08 +2.073e+08 +1.578e+08 +1.083e+08 +5.879e+07 +9.304e+06

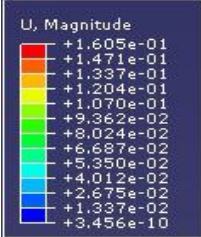
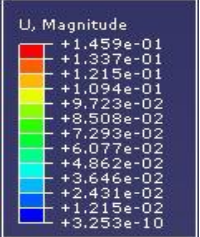
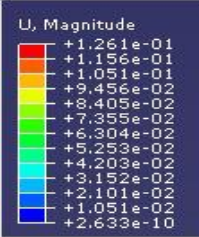
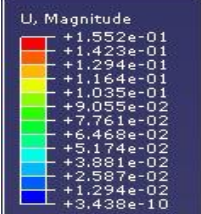
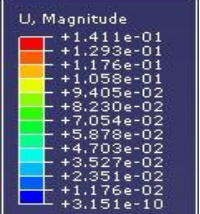
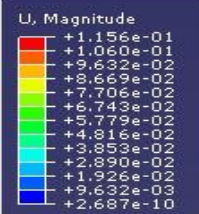
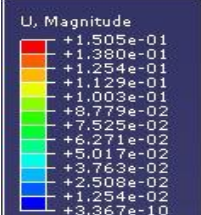
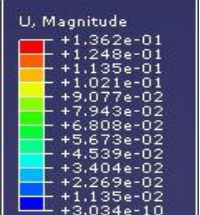
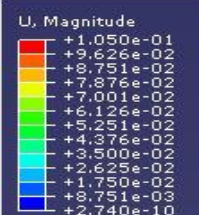
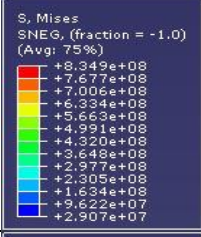
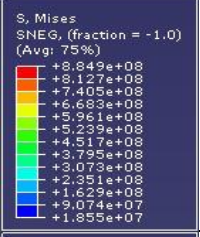
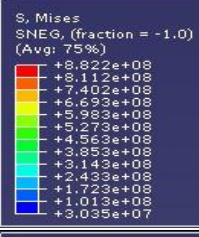
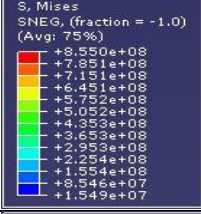
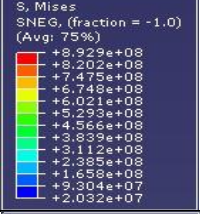
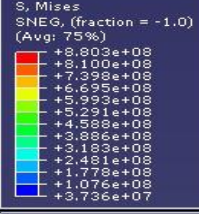
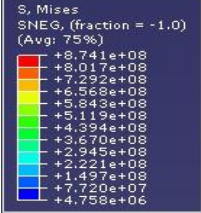
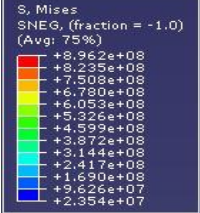
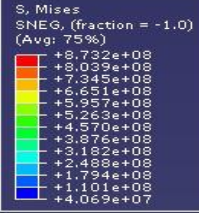
Appendix F. 4. Calculated static analysis results by ABAQUS for the pipeline in general moist sandy soil with roller boundary condition at pipeline ends

[Displacement]					
Buried depth	Calculated data	Buried depth	Calculated data	Buried depth	Calculated data
0.5m	 <p>U, Magnitude</p> <ul style="list-style-type: none"> +1.655e-01 +1.517e-01 +1.380e-01 +1.242e-01 +1.104e-01 +9.657e-02 +8.277e-02 +6.898e-02 +5.518e-02 +4.139e-02 +2.759e-02 +1.380e-02 +0.000e+00 	2.0m	 <p>U, Magnitude</p> <ul style="list-style-type: none"> +1.643e-01 +1.506e-01 +1.369e-01 +1.232e-01 +1.095e-01 +9.586e-02 +8.216e-02 +6.847e-02 +5.477e-02 +4.108e-02 +2.739e-02 +1.369e-02 +0.000e+00 	4.0m	 <p>U, Magnitude</p> <ul style="list-style-type: none"> +1.639e-01 +1.502e-01 +1.366e-01 +1.229e-01 +1.092e-01 +9.559e-02 +8.194e-02 +6.828e-02 +5.462e-02 +4.097e-02 +2.731e-02 +1.366e-02 +0.000e+00
1.0m	 <p>U, Magnitude</p> <ul style="list-style-type: none"> +1.650e-01 +1.513e-01 +1.375e-01 +1.238e-01 +1.100e-01 +9.626e-02 +8.251e-02 +6.876e-02 +5.500e-02 +4.125e-02 +2.750e-02 +1.375e-02 +0.000e+00 	2.5m	 <p>U, Magnitude</p> <ul style="list-style-type: none"> +1.642e-01 +1.505e-01 +1.368e-01 +1.231e-01 +1.095e-01 +9.578e-02 +8.209e-02 +6.841e-02 +5.473e-02 +4.105e-02 +2.736e-02 +1.368e-02 +0.000e+00 	5.0m	 <p>U, Magnitude</p> <ul style="list-style-type: none"> +1.636e-01 +1.500e-01 +1.364e-01 +1.227e-01 +1.091e-01 +9.545e-02 +8.181e-02 +6.819e-02 +5.454e-02 +4.091e-02 +2.727e-02 +1.364e-02 +0.000e+00
1.5m	 <p>U, Magnitude</p> <ul style="list-style-type: none"> +1.646e-01 +1.509e-01 +1.372e-01 +1.235e-01 +1.098e-01 +9.603e-02 +8.231e-02 +6.859e-02 +5.488e-02 +4.116e-02 +2.744e-02 +1.372e-02 +0.000e+00 	3.0m	 <p>U, Magnitude</p> <ul style="list-style-type: none"> +1.641e-01 +1.504e-01 +1.368e-01 +1.231e-01 +1.094e-01 +9.573e-02 +8.205e-02 +6.838e-02 +5.470e-02 +4.103e-02 +2.735e-02 +1.368e-02 +0.000e+00 	6.0m	 <p>U, Magnitude</p> <ul style="list-style-type: none"> +1.635e-01 +1.499e-01 +1.362e-01 +1.226e-01 +1.090e-01 +9.537e-02 +8.174e-02 +6.812e-02 +5.450e-02 +4.087e-02 +2.725e-02 +1.362e-02 +0.000e+00
[stress]					
Buried depth	Calculated data	Buried depth	Calculated data	Buried depth	Calculated data
0.5m	 <p>S, Mises (Avg: 75%)</p> <ul style="list-style-type: none"> +6.321e+06 +5.799e+06 +5.278e+06 +4.756e+06 +4.235e+06 +3.713e+06 +3.192e+06 +2.670e+06 +2.149e+06 +1.627e+06 +1.106e+06 +5.844e+05 +6.292e+04 	2.0m	 <p>S, Mises (Avg: 75%)</p> <ul style="list-style-type: none"> +3.274e+06 +3.003e+06 +2.731e+06 +2.460e+06 +2.188e+06 +1.917e+06 +1.645e+06 +1.374e+06 +1.102e+06 +8306e+05 +5591e+05 +2.876e+05 +1.609e+04 	4.0m	 <p>S, Mises (Avg: 75%)</p> <ul style="list-style-type: none"> +3.854e+06 +3.539e+06 +3.224e+06 +2.909e+06 +2.593e+06 +2.278e+06 +1.962e+06 +1.647e+06 +1.332e+06 +1.016e+06 +7.010e+05 +3.857e+05 +7.035e+04
1.0m	 <p>S, Mises (Avg: 75%)</p> <ul style="list-style-type: none"> +5.022e+06 +4.607e+06 +4.192e+06 +3.778e+06 +3.363e+06 +2.948e+06 +2.534e+06 +2.119e+06 +1.704e+06 +1.290e+06 +8750e+05 +4.603e+05 +4.561e+04 	2.5m	 <p>S, Mises (Avg: 75%)</p> <ul style="list-style-type: none"> +3.474e+06 +3.186e+06 +2.898e+06 +2.609e+06 +2.321e+06 +2.033e+06 +1.745e+06 +1.457e+06 +1.168e+06 +8.801e+05 +5.919e+05 +3.037e+05 +1.551e+04 	5.0m	 <p>S, Mises (Avg: 75%)</p> <ul style="list-style-type: none"> +3.817e+06 +3.508e+06 +3.198e+06 +2.889e+06 +2.579e+06 +2.270e+06 +1.961e+06 +1.651e+06 +1.342e+06 +1.033e+06 +7.232e+05 +4.139e+05 +1.045e+05
1.5m	 <p>S, Mises (Avg: 75%)</p> <ul style="list-style-type: none"> +3.062e+06 +2.809e+06 +2.557e+06 +2.304e+06 +2.051e+06 +1.799e+06 +1.546e+06 +1.293e+06 +1.041e+06 +7.882e+05 +5.355e+05 +2.829e+05 +3.027e+04 	3.0m	 <p>S, Mises (Avg: 75%)</p> <ul style="list-style-type: none"> +3.644e+06 +3.342e+06 +3.041e+06 +2.739e+06 +2.437e+06 +2.136e+06 +1.834e+06 +1.532e+06 +1.230e+06 +9.287e+05 +6.270e+05 +3.253e+05 +2.355e+04 	6.0m	 <p>S, Mises (Avg: 75%)</p> <ul style="list-style-type: none"> +3.657e+06 +3.361e+06 +3.066e+06 +2.770e+06 +2.474e+06 +2.178e+06 +1.882e+06 +1.586e+06 +1.290e+06 +9.345e+05 +6.328e+05 +3.311e+05 +1.069e+05

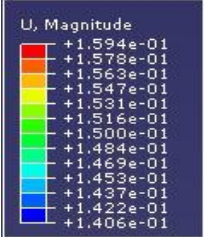
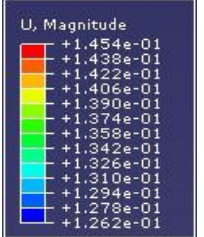
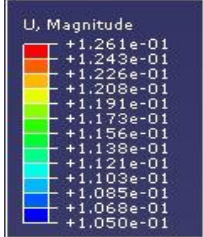
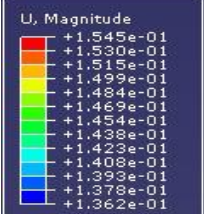
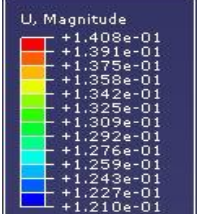
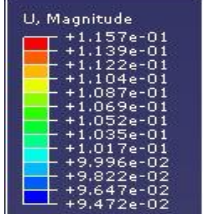
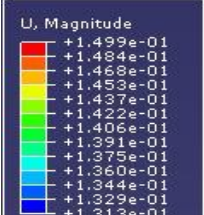
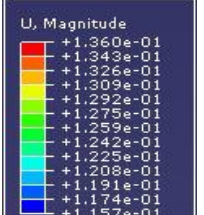
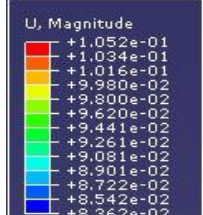
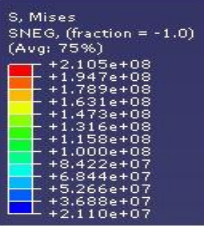
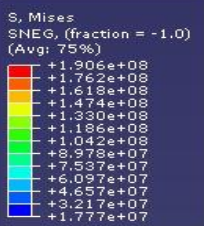
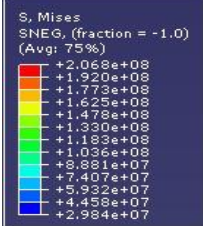
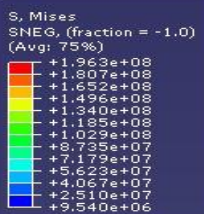
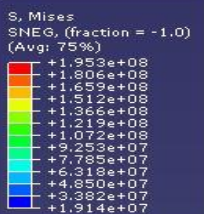
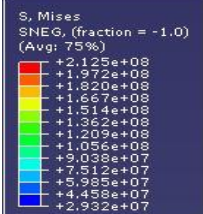
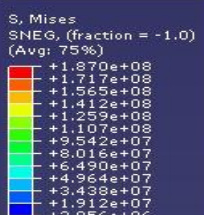
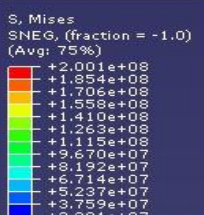
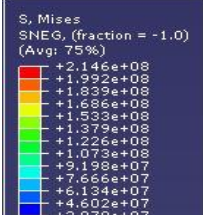
Appendix F. 5. Calculated static analysis results by ABAQUS for fully saturated sandy soil with hinge boundary condition at pipeline ends

[Displacement]					
Buried depth	Calculated data	Buried depth	Calculated data	Buried depth	Calculated data
0.5m		2.0m		4.0m	
1.0m		2.5m		5.0m	
1.5m		3.0m		6.0m	
[stress]					
Buried depth	Calculated data	Buried depth	Calculated data	Buried depth	Calculated data
0.5m		2.0m		4.0m	
1.0m		2.5m		5.0m	
1.5m		3.0m		6.0m	

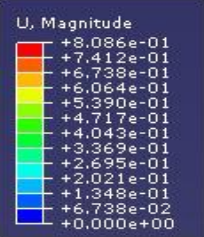
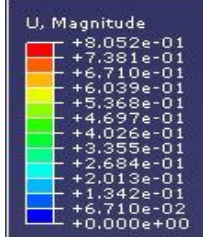
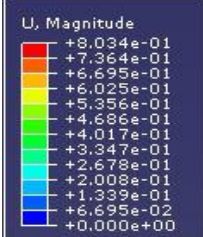
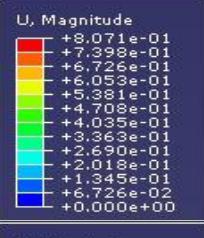
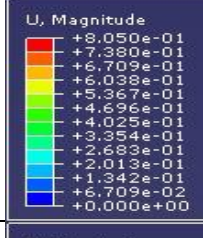
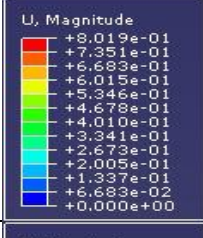
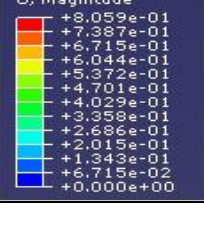
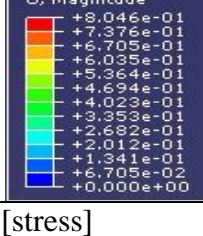
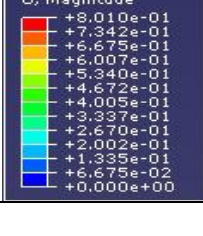
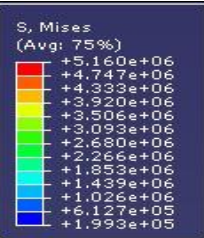
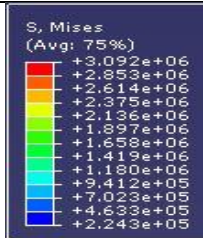
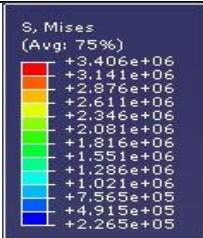
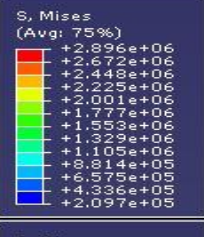
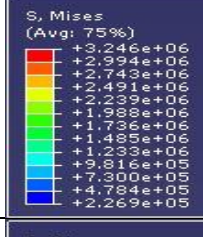
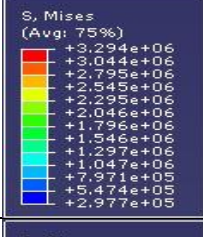
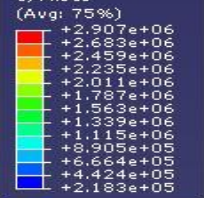
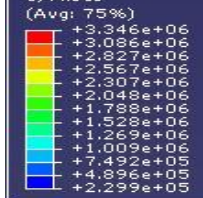
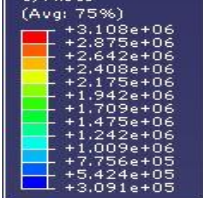
Appendix F. 6. Calculated static analysis results by ABAQUS for fully saturated sandy soil with roller boundary condition at pipeline ends

[Displacement]					
Buried depth	Calculated data	Buried depth	Calculated data	Buried depth	Calculated data
0.5m	 <p>U, Magnitude</p> <ul style="list-style-type: none"> +1.605e-01 +1.471e-01 +1.337e-01 +1.204e-01 +1.070e-01 +9.362e-02 +8.024e-02 +6.687e-02 +5.350e-02 +4.012e-02 +2.675e-02 +1.337e-02 +3.456e-10 	2.0m	 <p>U, Magnitude</p> <ul style="list-style-type: none"> +1.459e-01 +1.337e-01 +1.215e-01 +1.094e-01 +9.723e-02 +8.508e-02 +7.293e-02 +6.077e-02 +4.862e-02 +3.646e-02 +2.431e-02 +1.215e-02 +3.253e-10 	4.0m	 <p>U, Magnitude</p> <ul style="list-style-type: none"> +1.261e-01 +1.156e-01 +1.051e-01 +9.456e-02 +8.405e-02 +7.355e-02 +6.304e-02 +5.253e-02 +4.203e-02 +3.152e-02 +2.101e-02 +1.051e-02 +2.633e-10
1.0m	 <p>U, Magnitude</p> <ul style="list-style-type: none"> +1.552e-01 +1.423e-01 +1.294e-01 +1.164e-01 +1.035e-01 +9.055e-02 +7.761e-02 +6.468e-02 +5.174e-02 +3.881e-02 +2.587e-02 +1.294e-02 +3.438e-10 	2.5m	 <p>U, Magnitude</p> <ul style="list-style-type: none"> +1.411e-01 +1.293e-01 +1.176e-01 +1.058e-01 +9.405e-02 +8.230e-02 +7.054e-02 +5.873e-02 +4.703e-02 +3.527e-02 +2.351e-02 +1.176e-02 +3.151e-10 	5.0m	 <p>U, Magnitude</p> <ul style="list-style-type: none"> +1.156e-01 +1.060e-01 +9.632e-02 +8.669e-02 +7.706e-02 +6.743e-02 +5.779e-02 +4.816e-02 +3.853e-02 +2.890e-02 +1.926e-02 +9.632e-03 +2.687e-10
1.5m	 <p>U, Magnitude</p> <ul style="list-style-type: none"> +1.505e-01 +1.390e-01 +1.254e-01 +1.129e-01 +1.003e-01 +8.779e-02 +7.525e-02 +6.271e-02 +5.017e-02 +3.763e-02 +2.508e-02 +1.254e-02 +3.367e-10 	3.0m	 <p>U, Magnitude</p> <ul style="list-style-type: none"> +1.362e-01 +1.249e-01 +1.135e-01 +1.021e-01 +9.077e-02 +7.943e-02 +6.808e-02 +5.673e-02 +4.539e-02 +3.404e-02 +2.269e-02 +1.135e-02 +3.034e-10 	6.0m	 <p>U, Magnitude</p> <ul style="list-style-type: none"> +1.050e-01 +8.751e-02 +7.875e-02 +7.001e-02 +6.126e-02 +5.251e-02 +4.376e-02 +3.500e-02 +2.625e-02 +1.750e-02 +8.751e-03 +2.740e-10
[stress]					
Buried depth	Calculated data	Buried depth	Calculated data	Buried depth	Calculated data
0.5m	 <p>S, Mises SNEG, (fraction = -1.0) (Avg: 75%)</p> <ul style="list-style-type: none"> +8.349e+08 +7.677e+08 +7.006e+08 +6.334e+08 +5.663e+08 +4.991e+08 +4.320e+08 +3.648e+08 +2.977e+08 +2.305e+08 +1.634e+08 +9.622e+07 +2.907e+07 	2.0m	 <p>S, Mises SNEG, (fraction = -1.0) (Avg: 75%)</p> <ul style="list-style-type: none"> +8.849e+08 +8.171e+08 +7.405e+08 +6.633e+08 +5.961e+08 +5.239e+08 +4.517e+08 +3.795e+08 +3.073e+08 +2.351e+08 +1.629e+08 +9.074e+07 +1.855e+07 	4.0m	 <p>S, Mises SNEG, (fraction = -1.0) (Avg: 75%)</p> <ul style="list-style-type: none"> +8.822e+08 +8.121e+08 +7.402e+08 +6.693e+08 +5.983e+08 +5.273e+08 +4.563e+08 +3.853e+08 +3.143e+08 +2.433e+08 +1.723e+08 +1.013e+08 +3.035e+07
1.0m	 <p>S, Mises SNEG, (fraction = -1.0) (Avg: 75%)</p> <ul style="list-style-type: none"> +8.550e+08 +7.851e+08 +7.151e+08 +6.451e+08 +5.752e+08 +5.052e+08 +4.353e+08 +3.653e+08 +2.953e+08 +2.254e+08 +1.554e+08 +8.546e+07 +1.549e+07 	2.5m	 <p>S, Mises SNEG, (fraction = -1.0) (Avg: 75%)</p> <ul style="list-style-type: none"> +8.929e+08 +8.202e+08 +7.475e+08 +6.748e+08 +6.021e+08 +5.293e+08 +4.566e+08 +3.839e+08 +3.112e+08 +2.385e+08 +1.658e+08 +9.304e+07 +2.052e+07 	5.0m	 <p>S, Mises SNEG, (fraction = -1.0) (Avg: 75%)</p> <ul style="list-style-type: none"> +8.803e+08 +8.100e+08 +7.398e+08 +6.695e+08 +5.993e+08 +5.291e+08 +4.588e+08 +3.886e+08 +3.183e+08 +2.481e+08 +1.778e+08 +1.076e+08 +3.736e+07
1.5m	 <p>S, Mises SNEG, (fraction = -1.0) (Avg: 75%)</p> <ul style="list-style-type: none"> +8.741e+08 +8.017e+08 +7.292e+08 +6.568e+08 +5.843e+08 +5.119e+08 +4.394e+08 +3.670e+08 +2.945e+08 +2.221e+08 +1.497e+08 +7.720e+07 +4.758e+06 	3.0m	 <p>S, Mises SNEG, (fraction = -1.0) (Avg: 75%)</p> <ul style="list-style-type: none"> +8.962e+08 +8.235e+08 +7.508e+08 +6.780e+08 +6.053e+08 +5.326e+08 +4.599e+08 +3.872e+08 +3.144e+08 +2.417e+08 +1.690e+08 +9.626e+07 +2.354e+07 	6.0m	 <p>S, Mises SNEG, (fraction = -1.0) (Avg: 75%)</p> <ul style="list-style-type: none"> +8.732e+08 +8.039e+08 +7.345e+08 +6.651e+08 +5.957e+08 +5.263e+08 +4.570e+08 +3.876e+08 +3.182e+08 +2.488e+08 +1.794e+08 +1.101e+08 +4.069e+07

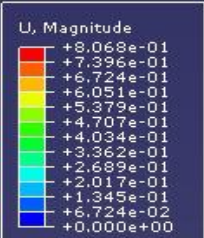
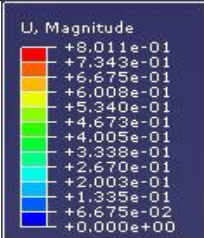
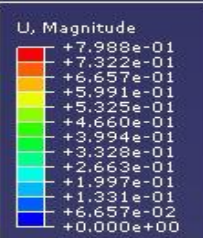
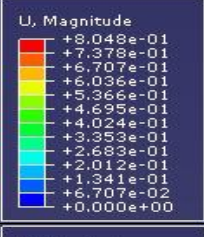
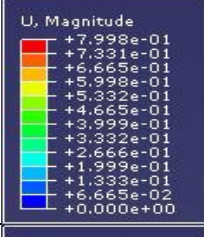
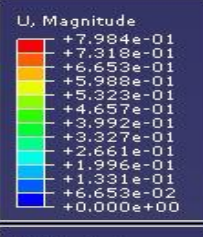
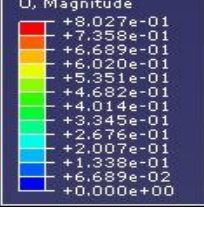
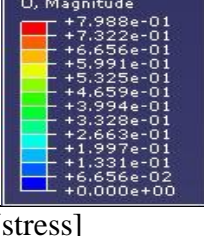
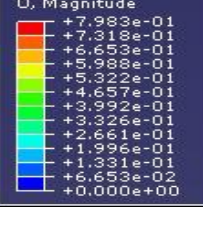
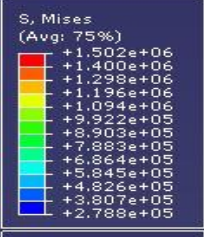
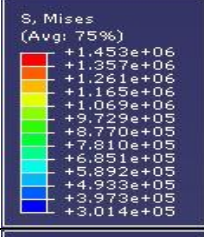
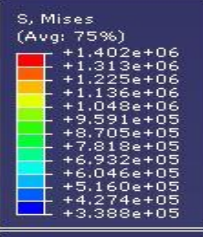
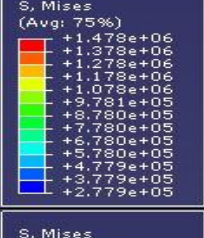
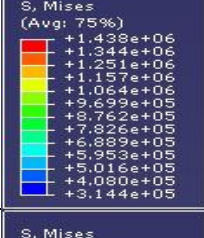
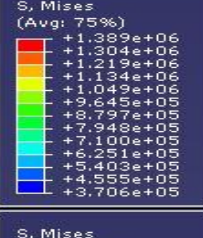
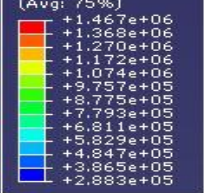
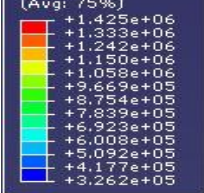
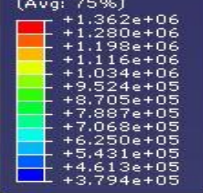
Appendix F. 7. Calculated static analysis results by ABAQUS for the pipeline in fully saturated sandy soil with hinge boundary condition at pipeline ends

[Displacement]					
Buried depth	Calculated data	Buried depth	Calculated data	Buried depth	Calculated data
0.5m	 <p>U, Magnitude</p> <ul style="list-style-type: none"> +1.594e-01 +1.578e-01 +1.563e-01 +1.547e-01 +1.531e-01 +1.516e-01 +1.500e-01 +1.484e-01 +1.469e-01 +1.453e-01 +1.437e-01 +1.422e-01 +1.406e-01 	2.0m	 <p>U, Magnitude</p> <ul style="list-style-type: none"> +1.454e-01 +1.438e-01 +1.422e-01 +1.406e-01 +1.390e-01 +1.374e-01 +1.358e-01 +1.342e-01 +1.326e-01 +1.310e-01 +1.294e-01 +1.278e-01 +1.262e-01 	4.0m	 <p>U, Magnitude</p> <ul style="list-style-type: none"> +1.261e-01 +1.243e-01 +1.226e-01 +1.208e-01 +1.191e-01 +1.173e-01 +1.156e-01 +1.138e-01 +1.121e-01 +1.103e-01 +1.085e-01 +1.068e-01 +1.050e-01
1.0m	 <p>U, Magnitude</p> <ul style="list-style-type: none"> +1.545e-01 +1.530e-01 +1.515e-01 +1.499e-01 +1.484e-01 +1.469e-01 +1.454e-01 +1.438e-01 +1.423e-01 +1.408e-01 +1.393e-01 +1.378e-01 +1.362e-01 	2.5m	 <p>U, Magnitude</p> <ul style="list-style-type: none"> +1.408e-01 +1.391e-01 +1.375e-01 +1.358e-01 +1.342e-01 +1.325e-01 +1.309e-01 +1.292e-01 +1.276e-01 +1.259e-01 +1.243e-01 +1.227e-01 +1.210e-01 	5.0m	 <p>U, Magnitude</p> <ul style="list-style-type: none"> +1.157e-01 +1.139e-01 +1.122e-01 +1.104e-01 +1.087e-01 +1.069e-01 +1.052e-01 +1.035e-01 +1.017e-01 +9.996e-02 +9.822e-02 +9.647e-02 +9.472e-02
1.5m	 <p>U, Magnitude</p> <ul style="list-style-type: none"> +1.499e-01 +1.484e-01 +1.469e-01 +1.453e-01 +1.437e-01 +1.422e-01 +1.406e-01 +1.391e-01 +1.375e-01 +1.360e-01 +1.344e-01 +1.329e-01 +1.313e-01 	3.0m	 <p>U, Magnitude</p> <ul style="list-style-type: none"> +1.360e-01 +1.343e-01 +1.326e-01 +1.309e-01 +1.292e-01 +1.275e-01 +1.259e-01 +1.242e-01 +1.225e-01 +1.208e-01 +1.191e-01 +1.174e-01 +1.157e-01 	6.0m	 <p>U, Magnitude</p> <ul style="list-style-type: none"> +1.052e-01 +1.034e-01 +1.016e-01 +9.980e-02 +9.800e-02 +9.620e-02 +9.441e-02 +9.261e-02 +9.081e-02 +8.901e-02 +8.722e-02 +8.542e-02 +8.362e-02
[stress]					
Buried depth	Calculated data	Buried depth	Calculated data	Buried depth	Calculated data
0.5m	 <p>S, Mises SNEG, (fraction = -1.0) (Avg: 75%)</p> <ul style="list-style-type: none"> +2.105e+08 +1.947e+08 +1.799e+08 +1.631e+08 +1.473e+08 +1.316e+08 +1.158e+08 +1.000e+08 +8.422e+07 +6.844e+07 +5.266e+07 +3.688e+07 +2.110e+07 	2.0m	 <p>S, Mises SNEG, (fraction = -1.0) (Avg: 75%)</p> <ul style="list-style-type: none"> +1.906e+08 +1.762e+08 +1.617e+08 +1.474e+08 +1.330e+08 +1.186e+08 +1.042e+08 +8.978e+07 +7.537e+07 +6.097e+07 +4.657e+07 +3.217e+07 +1.777e+07 	4.0m	 <p>S, Mises SNEG, (fraction = -1.0) (Avg: 75%)</p> <ul style="list-style-type: none"> +2.068e+08 +1.920e+08 +1.779e+08 +1.625e+08 +1.478e+08 +1.330e+08 +1.183e+08 +1.036e+08 +8.881e+07 +7.407e+07 +5.932e+07 +4.458e+07 +2.984e+07
1.0m	 <p>S, Mises SNEG, (fraction = -1.0) (Avg: 75%)</p> <ul style="list-style-type: none"> +1.963e+08 +1.807e+08 +1.652e+08 +1.496e+08 +1.340e+08 +1.185e+08 +1.029e+08 +8.735e+07 +7.179e+07 +5.623e+07 +4.067e+07 +2.510e+07 +9.540e+06 	2.5m	 <p>S, Mises SNEG, (fraction = -1.0) (Avg: 75%)</p> <ul style="list-style-type: none"> +1.953e+08 +1.806e+08 +1.659e+08 +1.512e+08 +1.366e+08 +1.219e+08 +1.072e+08 +9.253e+07 +7.785e+07 +6.318e+07 +4.850e+07 +3.382e+07 +1.914e+07 	5.0m	 <p>S, Mises SNEG, (fraction = -1.0) (Avg: 75%)</p> <ul style="list-style-type: none"> +2.125e+08 +1.972e+08 +1.820e+08 +1.667e+08 +1.514e+08 +1.362e+08 +1.209e+08 +1.056e+08 +9.038e+07 +7.512e+07 +5.985e+07 +4.458e+07 +2.932e+07
1.5m	 <p>S, Mises SNEG, (fraction = -1.0) (Avg: 75%)</p> <ul style="list-style-type: none"> +1.870e+08 +1.717e+08 +1.565e+08 +1.412e+08 +1.259e+08 +1.107e+08 +9.542e+07 +8.016e+07 +6.490e+07 +4.964e+07 +3.438e+07 +1.912e+07 +3.856e+06 	3.0m	 <p>S, Mises SNEG, (fraction = -1.0) (Avg: 75%)</p> <ul style="list-style-type: none"> +2.001e+08 +1.854e+08 +1.706e+08 +1.558e+08 +1.410e+08 +1.263e+08 +1.115e+08 +9.670e+07 +8.192e+07 +6.714e+07 +5.237e+07 +3.759e+07 +2.281e+07 	6.0m	 <p>S, Mises SNEG, (fraction = -1.0) (Avg: 75%)</p> <ul style="list-style-type: none"> +2.146e+08 +1.992e+08 +1.839e+08 +1.686e+08 +1.533e+08 +1.379e+08 +1.226e+08 +1.073e+08 +9.198e+07 +7.666e+07 +6.134e+07 +4.602e+07 +3.070e+07

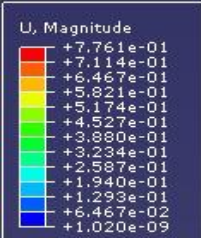
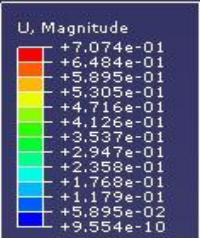
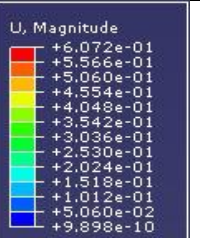
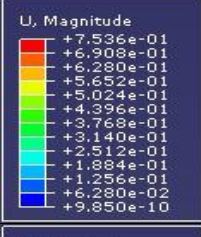
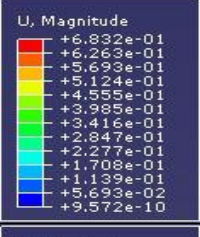
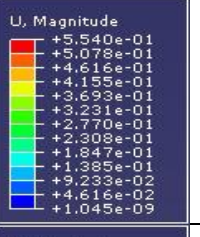
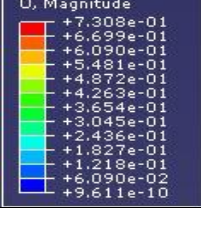
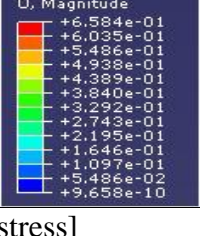
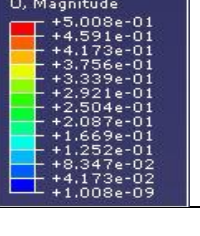
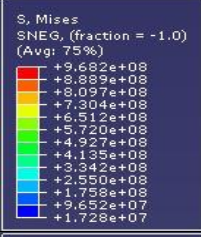
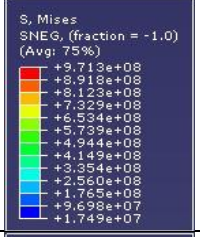
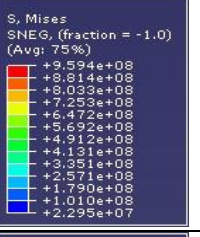
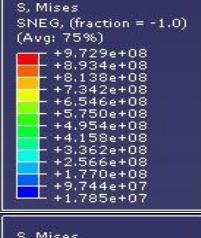
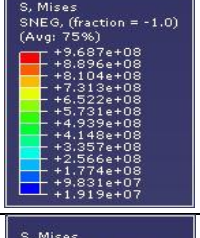
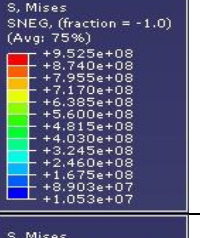
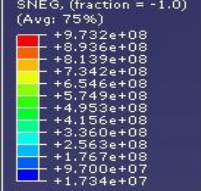
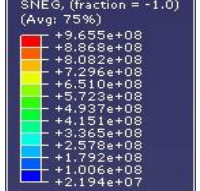
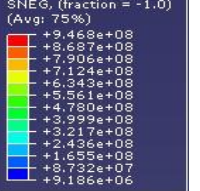
Appendix F. 8. Calculated static analysis results by ABAQUS for the pipeline in fully saturated sandy soil with roller boundary condition at pipeline ends

[Displacement]					
Buried depth	Calculated data	Buried depth	Calculated data	Buried depth	Calculated data
0.5m	 <p>U, Magnitude</p> <ul style="list-style-type: none"> +8.086e-01 +7.412e-01 +6.738e-01 +6.064e-01 +5.390e-01 +4.717e-01 +4.043e-01 +3.369e-01 +2.695e-01 +2.021e-01 +1.348e-01 +6.738e-02 +0.000e+00 	2.0m	 <p>U, Magnitude</p> <ul style="list-style-type: none"> +8.052e-01 +7.381e-01 +6.710e-01 +6.039e-01 +5.368e-01 +4.697e-01 +4.026e-01 +3.355e-01 +2.684e-01 +2.013e-01 +1.342e-01 +6.710e-02 +0.000e+00 	4.0m	 <p>U, Magnitude</p> <ul style="list-style-type: none"> +8.034e-01 +7.364e-01 +6.695e-01 +6.025e-01 +5.355e-01 +4.686e-01 +4.017e-01 +3.347e-01 +2.678e-01 +2.008e-01 +1.339e-01 +6.695e-02 +0.000e+00
1.0m	 <p>U, Magnitude</p> <ul style="list-style-type: none"> +8.071e-01 +7.398e-01 +6.726e-01 +6.053e-01 +5.381e-01 +4.708e-01 +4.035e-01 +3.363e-01 +2.690e-01 +2.018e-01 +1.345e-01 +6.726e-02 +0.000e+00 	2.5m	 <p>U, Magnitude</p> <ul style="list-style-type: none"> +8.050e-01 +7.380e-01 +6.709e-01 +6.038e-01 +5.367e-01 +4.696e-01 +4.025e-01 +3.354e-01 +2.683e-01 +2.013e-01 +1.342e-01 +6.709e-02 +0.000e+00 	5.0m	 <p>U, Magnitude</p> <ul style="list-style-type: none"> +8.019e-01 +7.351e-01 +6.683e-01 +6.015e-01 +5.346e-01 +4.678e-01 +4.010e-01 +3.341e-01 +2.673e-01 +2.005e-01 +1.337e-01 +6.683e-02 +0.000e+00
1.5m	 <p>U, Magnitude</p> <ul style="list-style-type: none"> +8.059e-01 +7.387e-01 +6.715e-01 +6.044e-01 +5.372e-01 +4.701e-01 +4.029e-01 +3.358e-01 +2.686e-01 +2.015e-01 +1.343e-01 +6.715e-02 +0.000e+00 	3.0m	 <p>U, Magnitude</p> <ul style="list-style-type: none"> +8.046e-01 +7.376e-01 +6.705e-01 +6.035e-01 +5.364e-01 +4.694e-01 +4.023e-01 +3.353e-01 +2.682e-01 +2.012e-01 +1.341e-01 +6.705e-02 +0.000e+00 	6.0m	 <p>U, Magnitude</p> <ul style="list-style-type: none"> +8.010e-01 +7.342e-01 +6.675e-01 +6.007e-01 +5.340e-01 +4.672e-01 +4.005e-01 +3.337e-01 +2.670e-01 +2.002e-01 +1.335e-01 +6.675e-02 +0.000e+00
[stress]					
Buried depth	Calculated data	Buried depth	Calculated data	Buried depth	Calculated data
0.5m	 <p>S, Mises (Avg: 75%)</p> <ul style="list-style-type: none"> +5.160e+06 +4.747e+06 +4.333e+06 +3.920e+06 +3.506e+06 +3.093e+06 +2.680e+06 +2.266e+06 +1.853e+06 +1.439e+06 +1.026e+06 +6.127e+05 +1.993e+05 	2.0m	 <p>S, Mises (Avg: 75%)</p> <ul style="list-style-type: none"> +3.092e+06 +2.853e+06 +2.614e+06 +2.375e+06 +2.136e+06 +1.897e+06 +1.658e+06 +1.419e+06 +1.180e+06 +9.412e+05 +7.033e+05 +4.633e+05 +2.243e+05 	4.0m	 <p>S, Mises (Avg: 75%)</p> <ul style="list-style-type: none"> +3.406e+06 +3.141e+06 +2.876e+06 +2.611e+06 +2.346e+06 +2.081e+06 +1.816e+06 +1.551e+06 +1.286e+06 +1.021e+06 +7.55e+05 +4.915e+05 +2.265e+05
1.0m	 <p>S, Mises (Avg: 75%)</p> <ul style="list-style-type: none"> +2.896e+06 +2.672e+06 +2.448e+06 +2.225e+06 +2.001e+06 +1.777e+06 +1.553e+06 +1.329e+06 +1.105e+06 +8.814e+05 +6.575e+05 +4.336e+05 +2.097e+05 	2.5m	 <p>S, Mises (Avg: 75%)</p> <ul style="list-style-type: none"> +3.246e+06 +2.946e+06 +2.743e+06 +2.491e+06 +2.239e+06 +1.988e+06 +1.736e+06 +1.485e+06 +1.233e+06 +9.816e+05 +7.300e+05 +4.784e+05 +2.269e+05 	5.0m	 <p>S, Mises (Avg: 75%)</p> <ul style="list-style-type: none"> +3.294e+06 +3.044e+06 +2.795e+06 +2.545e+06 +2.295e+06 +2.046e+06 +1.796e+06 +1.546e+06 +1.297e+06 +1.047e+06 +7.971e+05 +5.474e+05 +2.977e+05
1.5m	 <p>S, Mises (Avg: 75%)</p> <ul style="list-style-type: none"> +2.907e+06 +2.683e+06 +2.459e+06 +2.235e+06 +2.011e+06 +1.787e+06 +1.563e+06 +1.339e+06 +1.115e+06 +8.905e+05 +6.664e+05 +4.424e+05 +2.183e+05 	3.0m	 <p>S, Mises (Avg: 75%)</p> <ul style="list-style-type: none"> +3.346e+06 +3.086e+06 +2.827e+06 +2.567e+06 +2.307e+06 +2.048e+06 +1.788e+06 +1.529e+06 +1.269e+06 +1.009e+06 +7.492e+05 +4.896e+05 +2.299e+05 	6.0m	 <p>S, Mises (Avg: 75%)</p> <ul style="list-style-type: none"> +3.108e+06 +2.875e+06 +2.642e+06 +2.408e+06 +2.175e+06 +1.942e+06 +1.709e+06 +1.475e+06 +1.242e+06 +1.009e+06 +7.756e+05 +5.424e+05 +3.091e+05

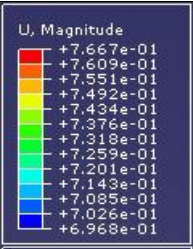
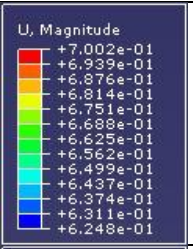
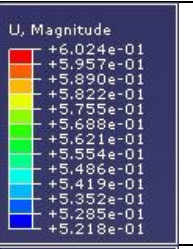
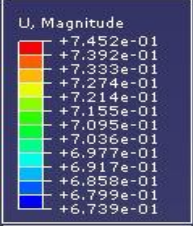
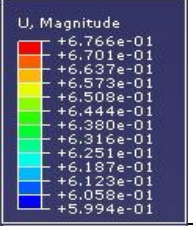
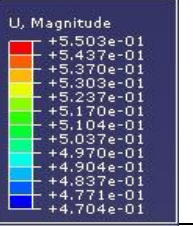
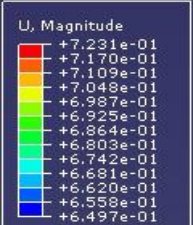
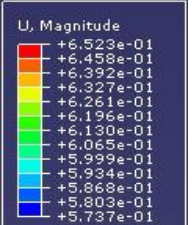
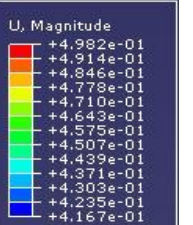
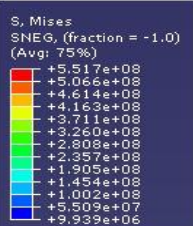
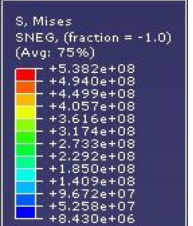
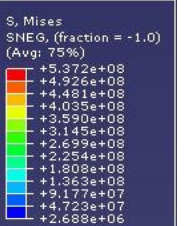
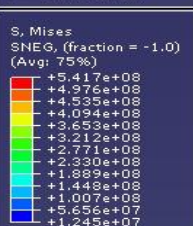
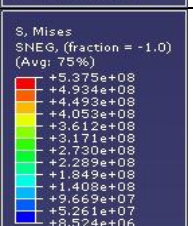
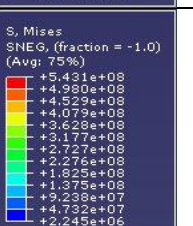
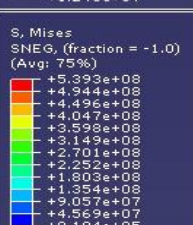
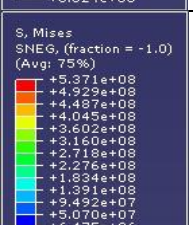
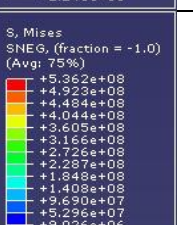
Appendix F. 9. Calculated static analysis results by ABAQUS for general moist cohesive soil with hinge boundary condition at pipeline ends

[Displacement]					
Buried depth	Calculated data	Buried depth	Calculated data	Buried depth	Calculated data
0.5m	 <p>U, Magnitude</p> <ul style="list-style-type: none"> +8.068e-01 +7.392e-01 +6.724e-01 +6.051e-01 +5.379e-01 +4.707e-01 +4.034e-01 +3.362e-01 +2.689e-01 +2.017e-01 +1.345e-01 +6.724e-02 +0.000e+00 	2.0m	 <p>U, Magnitude</p> <ul style="list-style-type: none"> +8.011e-01 +7.343e-01 +6.675e-01 +6.008e-01 +5.340e-01 +4.673e-01 +4.005e-01 +3.338e-01 +2.670e-01 +2.003e-01 +1.335e-01 +6.675e-02 +0.000e+00 	4.0m	 <p>U, Magnitude</p> <ul style="list-style-type: none"> +7.988e-01 +7.322e-01 +6.657e-01 +5.991e-01 +5.325e-01 +4.660e-01 +3.994e-01 +3.328e-01 +2.663e-01 +1.997e-01 +1.331e-01 +6.657e-02 +0.000e+00
1.0m	 <p>U, Magnitude</p> <ul style="list-style-type: none"> +8.048e-01 +7.378e-01 +6.707e-01 +6.036e-01 +5.366e-01 +4.695e-01 +4.024e-01 +3.353e-01 +2.683e-01 +2.012e-01 +1.341e-01 +6.707e-02 +0.000e+00 	2.5m	 <p>U, Magnitude</p> <ul style="list-style-type: none"> +7.998e-01 +7.331e-01 +6.665e-01 +5.998e-01 +5.332e-01 +4.665e-01 +3.999e-01 +3.332e-01 +2.666e-01 +1.999e-01 +1.333e-01 +6.665e-02 +0.000e+00 	5.0m	 <p>U, Magnitude</p> <ul style="list-style-type: none"> +7.984e-01 +7.318e-01 +6.653e-01 +5.988e-01 +5.322e-01 +4.657e-01 +3.992e-01 +3.327e-01 +2.661e-01 +1.995e-01 +1.331e-01 +6.653e-02 +0.000e+00
1.5m	 <p>U, Magnitude</p> <ul style="list-style-type: none"> +8.027e-01 +7.358e-01 +6.689e-01 +6.020e-01 +5.351e-01 +4.682e-01 +4.014e-01 +3.345e-01 +2.676e-01 +2.007e-01 +1.338e-01 +6.689e-02 +0.000e+00 	3.0m	 <p>U, Magnitude</p> <ul style="list-style-type: none"> +7.988e-01 +7.322e-01 +6.656e-01 +5.991e-01 +5.325e-01 +4.659e-01 +3.994e-01 +3.328e-01 +2.663e-01 +1.997e-01 +1.331e-01 +6.656e-02 +0.000e+00 	6.0m	 <p>U, Magnitude</p> <ul style="list-style-type: none"> +7.983e-01 +7.318e-01 +6.653e-01 +5.988e-01 +5.322e-01 +4.657e-01 +3.992e-01 +3.326e-01 +2.661e-01 +1.996e-01 +1.331e-01 +6.653e-02 +0.000e+00
[stress]					
Buried depth	Calculated data	Buried depth	Calculated data	Buried depth	Calculated data
0.5m	 <p>S, Mises (Avg: 75%)</p> <ul style="list-style-type: none"> +1.502e+06 +1.400e+06 +1.298e+06 +1.196e+06 +1.094e+06 +9.922e+05 +8.903e+05 +7.883e+05 +6.864e+05 +5.845e+05 +4.826e+05 +3.807e+05 +2.788e+05 	2.0m	 <p>S, Mises (Avg: 75%)</p> <ul style="list-style-type: none"> +1.453e+06 +1.357e+06 +1.261e+06 +1.165e+06 +1.069e+06 +9.729e+05 +8.770e+05 +7.810e+05 +6.851e+05 +5.892e+05 +4.933e+05 +3.973e+05 +3.014e+05 	4.0m	 <p>S, Mises (Avg: 75%)</p> <ul style="list-style-type: none"> +1.402e+06 +1.313e+06 +1.225e+06 +1.136e+06 +1.048e+06 +9.531e+05 +8.705e+05 +7.818e+05 +6.932e+05 +6.046e+05 +5.160e+05 +4.274e+05 +3.388e+05
1.0m	 <p>S, Mises (Avg: 75%)</p> <ul style="list-style-type: none"> +1.478e+06 +1.378e+06 +1.278e+06 +1.178e+06 +1.078e+06 +9.781e+05 +8.780e+05 +7.780e+05 +6.780e+05 +5.780e+05 +4.779e+05 +3.779e+05 +2.779e+05 	2.5m	 <p>S, Mises (Avg: 75%)</p> <ul style="list-style-type: none"> +1.438e+06 +1.344e+06 +1.251e+06 +1.157e+06 +1.064e+06 +9.699e+05 +8.762e+05 +7.826e+05 +6.889e+05 +5.953e+05 +5.016e+05 +4.080e+05 +3.144e+05 	5.0m	 <p>S, Mises (Avg: 75%)</p> <ul style="list-style-type: none"> +1.389e+06 +1.304e+06 +1.219e+06 +1.134e+06 +1.049e+06 +9.645e+05 +8.797e+05 +7.948e+05 +7.100e+05 +6.251e+05 +5.403e+05 +4.555e+05 +3.706e+05
1.5m	 <p>S, Mises (Avg: 75%)</p> <ul style="list-style-type: none"> +1.467e+06 +1.368e+06 +1.270e+06 +1.172e+06 +1.074e+06 +9.757e+05 +8.775e+05 +7.793e+05 +6.811e+05 +5.829e+05 +4.847e+05 +3.865e+05 +2.883e+05 	3.0m	 <p>S, Mises (Avg: 75%)</p> <ul style="list-style-type: none"> +1.425e+06 +1.333e+06 +1.242e+06 +1.150e+06 +1.058e+06 +9.669e+05 +8.754e+05 +7.839e+05 +6.923e+05 +6.008e+05 +5.092e+05 +4.177e+05 +3.262e+05 	6.0m	 <p>S, Mises (Avg: 75%)</p> <ul style="list-style-type: none"> +1.362e+06 +1.280e+06 +1.198e+06 +1.116e+06 +1.034e+06 +9.524e+05 +8.705e+05 +7.887e+05 +7.069e+05 +6.250e+05 +5.431e+05 +4.613e+05 +3.794e+05

Appendix F. 10. Calculated static analysis results by ABAQUS for general moist cohesive soil with roller boundary condition at pipeline ends

[Displacement]					
Buried depth	Calculated data	Buried depth	Calculated data	Buried depth	Calculated data
0.5m	 <p>U, Magnitude</p> <ul style="list-style-type: none"> +7.761e-01 +7.414e-01 +7.467e-01 +5.821e-01 +5.174e-01 +4.527e-01 +3.880e-01 +3.234e-01 +2.587e-01 +1.940e-01 +1.293e-01 +6.467e-02 +1.020e-09 	2.0m	 <p>U, Magnitude</p> <ul style="list-style-type: none"> +7.074e-01 +6.484e-01 +5.895e-01 +5.305e-01 +4.716e-01 +4.126e-01 +3.537e-01 +2.947e-01 +2.358e-01 +1.768e-01 +1.179e-01 +5.895e-02 +9.554e-10 	4.0m	 <p>U, Magnitude</p> <ul style="list-style-type: none"> +6.072e-01 +5.586e-01 +5.060e-01 +4.554e-01 +4.048e-01 +3.542e-01 +3.036e-01 +2.530e-01 +2.024e-01 +1.518e-01 +1.012e-01 +5.060e-02 +9.898e-10
1.0m	 <p>U, Magnitude</p> <ul style="list-style-type: none"> +7.536e-01 +6.908e-01 +6.280e-01 +5.652e-01 +5.024e-01 +4.396e-01 +3.768e-01 +3.140e-01 +2.512e-01 +1.884e-01 +1.256e-01 +6.280e-02 +9.850e-10 	2.5m	 <p>U, Magnitude</p> <ul style="list-style-type: none"> +6.832e-01 +6.263e-01 +5.693e-01 +5.124e-01 +4.555e-01 +3.985e-01 +3.416e-01 +2.847e-01 +2.277e-01 +1.708e-01 +1.139e-01 +5.693e-02 +9.572e-10 	5.0m	 <p>U, Magnitude</p> <ul style="list-style-type: none"> +5.540e-01 +5.078e-01 +4.616e-01 +4.155e-01 +3.693e-01 +3.231e-01 +2.770e-01 +2.308e-01 +1.847e-01 +1.385e-01 +9.233e-02 +4.616e-02 +1.045e-09
1.5m	 <p>U, Magnitude</p> <ul style="list-style-type: none"> +7.308e-01 +6.699e-01 +6.090e-01 +5.481e-01 +4.872e-01 +4.263e-01 +3.654e-01 +3.045e-01 +2.436e-01 +1.827e-01 +1.218e-01 +6.090e-02 +9.611e-10 	3.0m	 <p>U, Magnitude</p> <ul style="list-style-type: none"> +6.584e-01 +6.035e-01 +5.486e-01 +4.938e-01 +4.389e-01 +3.840e-01 +3.292e-01 +2.743e-01 +2.195e-01 +1.646e-01 +1.097e-01 +5.486e-02 +9.658e-10 	6.0m	 <p>U, Magnitude</p> <ul style="list-style-type: none"> +5.008e-01 +4.591e-01 +4.173e-01 +3.755e-01 +3.339e-01 +2.921e-01 +2.504e-01 +2.087e-01 +1.669e-01 +1.252e-01 +8.347e-02 +4.173e-02 +1.008e-09
[stress]					
Buried depth	Calculated data	Buried depth	Calculated data	Buried depth	Calculated data
0.5m	 <p>S, Mises SNEG, (fraction = -1.0) (Avg: 75%)</p> <ul style="list-style-type: none"> +9.682e+08 +8.889e+08 +8.097e+08 +7.304e+08 +6.512e+08 +5.720e+08 +4.927e+08 +4.135e+08 +3.342e+08 +2.550e+08 +1.758e+08 +9.652e+07 +1.728e+07 	2.0m	 <p>S, Mises SNEG, (fraction = -1.0) (Avg: 75%)</p> <ul style="list-style-type: none"> +9.713e+08 +8.918e+08 +8.123e+08 +7.329e+08 +6.534e+08 +5.739e+08 +4.944e+08 +4.149e+08 +3.354e+08 +2.560e+08 +1.765e+08 +9.698e+07 +1.749e+07 	4.0m	 <p>S, Mises SNEG, (fraction = -1.0) (Avg: 75%)</p> <ul style="list-style-type: none"> +9.594e+08 +8.814e+08 +8.034e+08 +7.253e+08 +6.472e+08 +5.692e+08 +4.912e+08 +4.131e+08 +3.351e+08 +2.571e+08 +1.790e+08 +1.010e+08 +2.295e+07
1.0m	 <p>S, Mises SNEG, (fraction = -1.0) (Avg: 75%)</p> <ul style="list-style-type: none"> +9.729e+08 +8.934e+08 +8.138e+08 +7.342e+08 +6.546e+08 +5.750e+08 +4.954e+08 +4.158e+08 +3.362e+08 +2.566e+08 +1.770e+08 +9.744e+07 +1.785e+07 	2.5m	 <p>S, Mises SNEG, (fraction = -1.0) (Avg: 75%)</p> <ul style="list-style-type: none"> +9.687e+08 +8.896e+08 +8.104e+08 +7.313e+08 +6.522e+08 +5.731e+08 +4.939e+08 +4.148e+08 +3.357e+08 +2.566e+08 +1.774e+08 +9.831e+07 +1.919e+07 	5.0m	 <p>S, Mises SNEG, (fraction = -1.0) (Avg: 75%)</p> <ul style="list-style-type: none"> +9.525e+08 +8.740e+08 +7.955e+08 +7.170e+08 +6.385e+08 +5.600e+08 +4.815e+08 +4.030e+08 +3.245e+08 +2.460e+08 +1.675e+08 +8.903e+07 +1.053e+07
1.5m	 <p>S, Mises SNEG, (fraction = -1.0) (Avg: 75%)</p> <ul style="list-style-type: none"> +9.732e+08 +8.936e+08 +8.139e+08 +7.342e+08 +6.546e+08 +5.749e+08 +4.953e+08 +4.156e+08 +3.360e+08 +2.563e+08 +1.767e+08 +9.700e+07 +1.734e+07 	3.0m	 <p>S, Mises SNEG, (fraction = -1.0) (Avg: 75%)</p> <ul style="list-style-type: none"> +9.695e+08 +8.888e+08 +8.082e+08 +7.296e+08 +6.510e+08 +5.723e+08 +4.937e+08 +4.151e+08 +3.365e+08 +2.578e+08 +1.792e+08 +1.006e+08 +2.194e+07 	6.0m	 <p>S, Mises SNEG, (fraction = -1.0) (Avg: 75%)</p> <ul style="list-style-type: none"> +9.468e+08 +8.687e+08 +7.905e+08 +7.124e+08 +6.343e+08 +5.561e+08 +4.780e+08 +3.999e+08 +3.217e+08 +2.436e+08 +1.655e+08 +8.732e+07 +9.186e+06

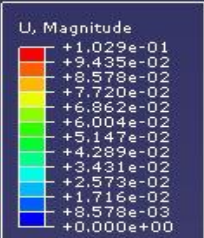
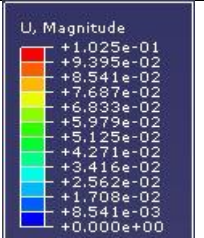
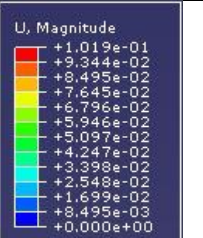
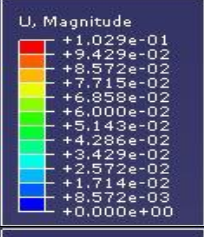
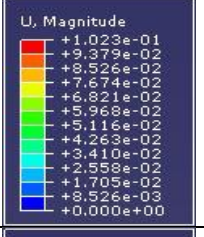
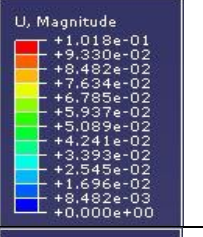
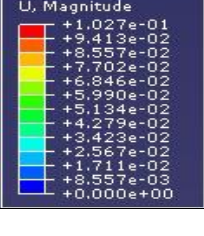
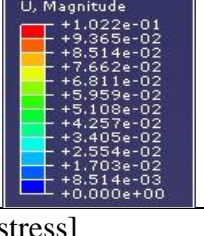
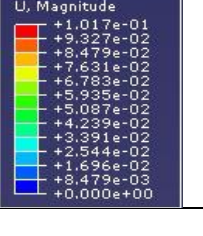
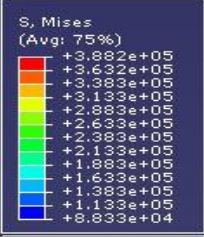
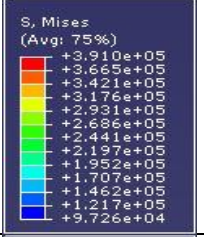
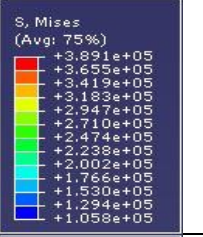
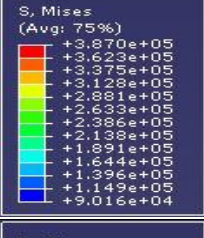
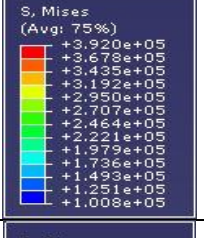
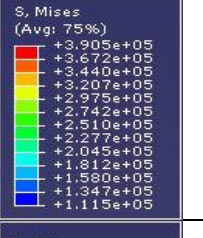
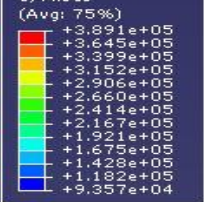
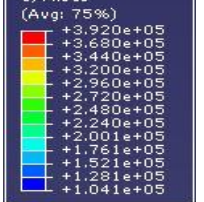
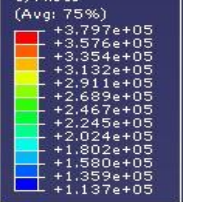
Appendix F. 11. Calculated static analysis results by ABAQUS for the pipeline in general moist cohesive soil with hinge boundary condition at pipeline ends

[Displacement]					
Buried depth	Calculated data	Buried depth	Calculated data	Buried depth	Calculated data
0.5m	 <p>U, Magnitude</p> <ul style="list-style-type: none"> +7.667e-01 +7.649e-01 +7.551e-01 +7.492e-01 +7.434e-01 +7.376e-01 +7.318e-01 +7.259e-01 +7.201e-01 +7.143e-01 +7.085e-01 +7.026e-01 +6.968e-01 	2.0m	 <p>U, Magnitude</p> <ul style="list-style-type: none"> +7.002e-01 +6.933e-01 +6.876e-01 +6.814e-01 +6.751e-01 +6.688e-01 +6.625e-01 +6.562e-01 +6.499e-01 +6.437e-01 +6.374e-01 +6.311e-01 +6.248e-01 	4.0m	 <p>U, Magnitude</p> <ul style="list-style-type: none"> +6.024e-01 +5.957e-01 +5.890e-01 +5.822e-01 +5.755e-01 +5.688e-01 +5.621e-01 +5.554e-01 +5.486e-01 +5.419e-01 +5.352e-01 +5.285e-01 +5.218e-01
1.0m	 <p>U, Magnitude</p> <ul style="list-style-type: none"> +7.452e-01 +7.392e-01 +7.333e-01 +7.274e-01 +7.214e-01 +7.155e-01 +7.095e-01 +7.036e-01 +6.977e-01 +6.917e-01 +6.858e-01 +6.799e-01 +6.739e-01 	2.5m	 <p>U, Magnitude</p> <ul style="list-style-type: none"> +6.766e-01 +6.701e-01 +6.637e-01 +6.573e-01 +6.508e-01 +6.444e-01 +6.380e-01 +6.316e-01 +6.251e-01 +6.187e-01 +6.123e-01 +6.058e-01 +5.994e-01 	5.0m	 <p>U, Magnitude</p> <ul style="list-style-type: none"> +5.503e-01 +5.437e-01 +5.370e-01 +5.303e-01 +5.237e-01 +5.170e-01 +5.104e-01 +5.037e-01 +4.970e-01 +4.904e-01 +4.837e-01 +4.771e-01 +4.704e-01
1.5m	 <p>U, Magnitude</p> <ul style="list-style-type: none"> +7.231e-01 +7.170e-01 +7.109e-01 +7.048e-01 +6.987e-01 +6.925e-01 +6.864e-01 +6.803e-01 +6.742e-01 +6.681e-01 +6.620e-01 +6.558e-01 +6.497e-01 	3.0m	 <p>U, Magnitude</p> <ul style="list-style-type: none"> +6.523e-01 +6.458e-01 +6.392e-01 +6.327e-01 +6.261e-01 +6.196e-01 +6.130e-01 +6.065e-01 +5.999e-01 +5.934e-01 +5.868e-01 +5.803e-01 +5.737e-01 	6.0m	 <p>U, Magnitude</p> <ul style="list-style-type: none"> +4.982e-01 +4.914e-01 +4.846e-01 +4.778e-01 +4.710e-01 +4.643e-01 +4.575e-01 +4.507e-01 +4.439e-01 +4.371e-01 +4.303e-01 +4.235e-01 +4.167e-01
[stress]					
Buried depth	Calculated data	Buried depth	Calculated data	Buried depth	Calculated data
0.5m	 <p>S, Mises SNEG, (fraction = -1.0) (Avg: 75%)</p> <ul style="list-style-type: none"> +5.517e+08 +5.066e+08 +4.614e+08 +4.163e+08 +3.711e+08 +3.260e+08 +2.809e+08 +2.357e+08 +1.905e+08 +1.454e+08 +1.002e+08 +5.509e+07 +9.939e+06 	2.0m	 <p>S, Mises SNEG, (fraction = -1.0) (Avg: 75%)</p> <ul style="list-style-type: none"> +5.382e+08 +4.940e+08 +4.499e+08 +4.057e+08 +3.616e+08 +3.174e+08 +2.733e+08 +2.292e+08 +1.850e+08 +1.409e+08 +9.672e+07 +5.258e+07 +8.430e+06 	4.0m	 <p>S, Mises SNEG, (fraction = -1.0) (Avg: 75%)</p> <ul style="list-style-type: none"> +5.372e+08 +4.926e+08 +4.481e+08 +4.035e+08 +3.590e+08 +3.145e+08 +2.699e+08 +2.254e+08 +1.808e+08 +1.363e+08 +9.177e+07 +4.723e+07 +2.688e+06
1.0m	 <p>S, Mises SNEG, (fraction = -1.0) (Avg: 75%)</p> <ul style="list-style-type: none"> +5.417e+08 +4.976e+08 +4.535e+08 +4.094e+08 +3.653e+08 +3.212e+08 +2.771e+08 +2.330e+08 +1.889e+08 +1.448e+08 +1.007e+08 +5.656e+07 +1.245e+07 	2.5m	 <p>S, Mises SNEG, (fraction = -1.0) (Avg: 75%)</p> <ul style="list-style-type: none"> +5.375e+08 +4.934e+08 +4.493e+08 +4.053e+08 +3.612e+08 +3.171e+08 +2.730e+08 +2.289e+08 +1.848e+08 +1.408e+08 +9.669e+07 +5.261e+07 +8.524e+06 	5.0m	 <p>S, Mises SNEG, (fraction = -1.0) (Avg: 75%)</p> <ul style="list-style-type: none"> +5.431e+08 +4.980e+08 +4.529e+08 +4.079e+08 +3.628e+08 +3.177e+08 +2.727e+08 +2.276e+08 +1.825e+08 +1.375e+08 +9.238e+07 +4.732e+07 +2.245e+06
1.5m	 <p>S, Mises SNEG, (fraction = -1.0) (Avg: 75%)</p> <ul style="list-style-type: none"> +5.393e+08 +4.944e+08 +4.496e+08 +4.047e+08 +3.598e+08 +3.149e+08 +2.701e+08 +2.252e+08 +1.803e+08 +1.354e+08 +9.057e+07 +4.569e+07 +8.184e+05 	3.0m	 <p>S, Mises SNEG, (fraction = -1.0) (Avg: 75%)</p> <ul style="list-style-type: none"> +5.371e+08 +4.929e+08 +4.487e+08 +4.045e+08 +3.602e+08 +3.160e+08 +2.718e+08 +2.276e+08 +1.834e+08 +1.391e+08 +9.492e+07 +5.070e+07 +6.475e+06 	6.0m	 <p>S, Mises SNEG, (fraction = -1.0) (Avg: 75%)</p> <ul style="list-style-type: none"> +5.352e+08 +4.903e+08 +4.484e+08 +4.044e+08 +3.605e+08 +3.165e+08 +2.726e+08 +2.287e+08 +1.848e+08 +1.409e+08 +9.690e+07 +5.296e+07 +9.026e+06

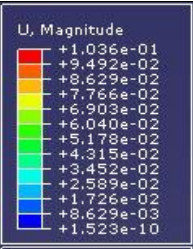
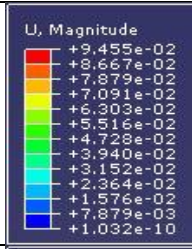
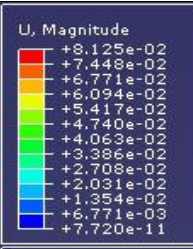
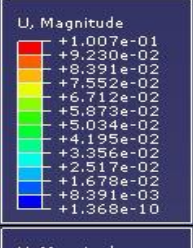
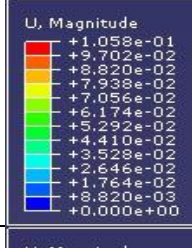
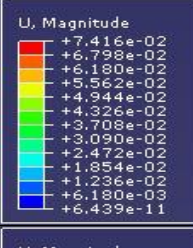

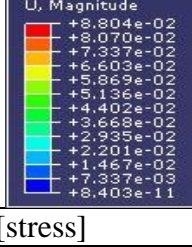
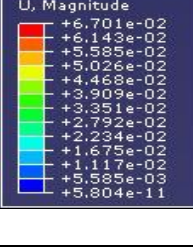
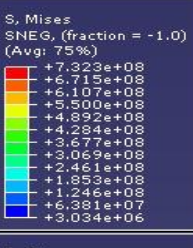
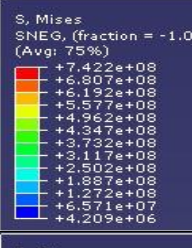

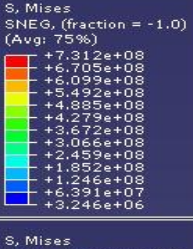
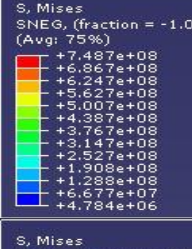
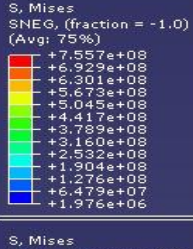
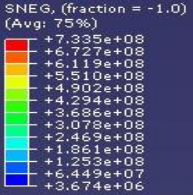


Appendix F. 12. Calculated static analysis results by ABAQUS for the pipeline in general moist cohesive soil with roller boundary condition at pipeline ends

[Displacement]					
Buried depth	Calculated data	Buried depth	Calculated data	Buried depth	Calculated data
0.5m		2.0m		4.0m	
1.0m		2.5m		5.0m	
1.5m		3.0m		6.0m	
[stress]					
Buried depth	Calculated data	Buried depth	Calculated data	Buried depth	Calculated data
0.5m		2.0m		4.0m	
1.0m		2.5m		5.0m	
1.5m		3.0m		6.0m	

Appendix F. 13. Calculated static analysis results by ABAQUS for fully saturated cohesive soil with hinge boundary condition at pipeline ends

[Displacement]					
Buried depth	Calculated data	Buried depth	Calculated data	Buried depth	Calculated data
0.5m	 <p>U, Magnitude</p> <ul style="list-style-type: none"> +1.029e-01 +9.435e-02 +8.378e-02 +7.720e-02 +6.862e-02 +6.004e-02 +5.147e-02 +4.289e-02 +3.431e-02 +2.573e-02 +1.716e-02 +8.578e-03 +0.000e+00 	2.0m	 <p>U, Magnitude</p> <ul style="list-style-type: none"> +1.025e-01 +9.395e-02 +8.541e-02 +7.687e-02 +6.833e-02 +5.979e-02 +5.125e-02 +4.271e-02 +3.416e-02 +2.562e-02 +1.708e-02 +8.541e-03 +0.000e+00 	4.0m	 <p>U, Magnitude</p> <ul style="list-style-type: none"> +1.019e-01 +9.344e-02 +8.495e-02 +7.645e-02 +6.796e-02 +5.946e-02 +5.097e-02 +4.247e-02 +3.398e-02 +2.548e-02 +1.699e-02 +8.495e-03 +0.000e+00
1.0m	 <p>U, Magnitude</p> <ul style="list-style-type: none"> +1.029e-01 +9.429e-02 +8.572e-02 +7.715e-02 +6.858e-02 +6.000e-02 +5.143e-02 +4.286e-02 +3.429e-02 +2.572e-02 +1.714e-02 +8.572e-03 +0.000e+00 	2.5m	 <p>U, Magnitude</p> <ul style="list-style-type: none"> +1.023e-01 +9.379e-02 +8.526e-02 +7.674e-02 +6.821e-02 +5.968e-02 +5.116e-02 +4.263e-02 +3.410e-02 +2.558e-02 +1.705e-02 +8.526e-03 +0.000e+00 	5.0m	 <p>U, Magnitude</p> <ul style="list-style-type: none"> +1.018e-01 +9.330e-02 +8.482e-02 +7.634e-02 +6.785e-02 +5.937e-02 +5.089e-02 +4.241e-02 +3.393e-02 +2.545e-02 +1.696e-02 +8.482e-03 +0.000e+00
1.5m	 <p>U, Magnitude</p> <ul style="list-style-type: none"> +1.027e-01 +9.413e-02 +8.557e-02 +7.702e-02 +6.846e-02 +5.990e-02 +5.134e-02 +4.279e-02 +3.423e-02 +2.567e-02 +1.711e-02 +8.557e-03 +0.000e+00 	3.0m	 <p>U, Magnitude</p> <ul style="list-style-type: none"> +1.022e-01 +9.365e-02 +8.514e-02 +7.662e-02 +6.811e-02 +5.959e-02 +5.108e-02 +4.257e-02 +3.405e-02 +2.554e-02 +1.703e-02 +8.514e-03 +0.000e+00 	6.0m	 <p>U, Magnitude</p> <ul style="list-style-type: none"> +1.017e-01 +9.327e-02 +8.479e-02 +7.631e-02 +6.783e-02 +5.935e-02 +5.087e-02 +4.239e-02 +3.391e-02 +2.544e-02 +1.696e-02 +8.479e-03 +0.000e+00
[stress]					
Buried depth	Calculated data	Buried depth	Calculated data	Buried depth	Calculated data
0.5m	 <p>S, Mises (Avg: 75%)</p> <ul style="list-style-type: none"> +3.882e+05 +3.632e+05 +3.383e+05 +3.133e+05 +2.883e+05 +2.633e+05 +2.383e+05 +2.133e+05 +1.883e+05 +1.633e+05 +1.383e+05 +1.133e+05 +8.833e+04 	2.0m	 <p>S, Mises (Avg: 75%)</p> <ul style="list-style-type: none"> +3.910e+05 +3.665e+05 +3.421e+05 +3.176e+05 +2.931e+05 +2.686e+05 +2.441e+05 +2.197e+05 +1.952e+05 +1.707e+05 +1.462e+05 +1.217e+05 +9.726e+04 	4.0m	 <p>S, Mises (Avg: 75%)</p> <ul style="list-style-type: none"> +3.891e+05 +3.655e+05 +3.419e+05 +3.183e+05 +2.947e+05 +2.710e+05 +2.474e+05 +2.238e+05 +2.002e+05 +1.766e+05 +1.530e+05 +1.294e+05 +1.058e+05
1.0m	 <p>S, Mises (Avg: 75%)</p> <ul style="list-style-type: none"> +3.870e+05 +3.623e+05 +3.375e+05 +3.128e+05 +2.881e+05 +2.633e+05 +2.386e+05 +2.139e+05 +1.891e+05 +1.644e+05 +1.396e+05 +1.149e+05 +9.016e+04 	2.5m	 <p>S, Mises (Avg: 75%)</p> <ul style="list-style-type: none"> +3.920e+05 +3.678e+05 +3.435e+05 +3.192e+05 +2.950e+05 +2.707e+05 +2.464e+05 +2.221e+05 +1.979e+05 +1.736e+05 +1.493e+05 +1.251e+05 +1.008e+05 	5.0m	 <p>S, Mises (Avg: 75%)</p> <ul style="list-style-type: none"> +3.905e+05 +3.672e+05 +3.440e+05 +3.207e+05 +2.975e+05 +2.742e+05 +2.510e+05 +2.277e+05 +2.045e+05 +1.812e+05 +1.580e+05 +1.347e+05 +1.115e+05
1.5m	 <p>S, Mises (Avg: 75%)</p> <ul style="list-style-type: none"> +3.891e+05 +3.645e+05 +3.399e+05 +3.152e+05 +2.906e+05 +2.660e+05 +2.414e+05 +2.167e+05 +1.921e+05 +1.675e+05 +1.428e+05 +1.182e+05 +9.357e+04 	3.0m	 <p>S, Mises (Avg: 75%)</p> <ul style="list-style-type: none"> +3.920e+05 +3.680e+05 +3.440e+05 +3.200e+05 +2.960e+05 +2.720e+05 +2.480e+05 +2.240e+05 +2.001e+05 +1.761e+05 +1.521e+05 +1.281e+05 +1.041e+05 	6.0m	 <p>S, Mises (Avg: 75%)</p> <ul style="list-style-type: none"> +3.797e+05 +3.576e+05 +3.354e+05 +3.132e+05 +2.911e+05 +2.689e+05 +2.467e+05 +2.245e+05 +2.024e+05 +1.802e+05 +1.580e+05 +1.359e+05 +1.137e+05

Appendix F. 14. Calculated static analysis results by ABAQUS for fully saturated cohesive soil with roller boundary condition at pipeline ends

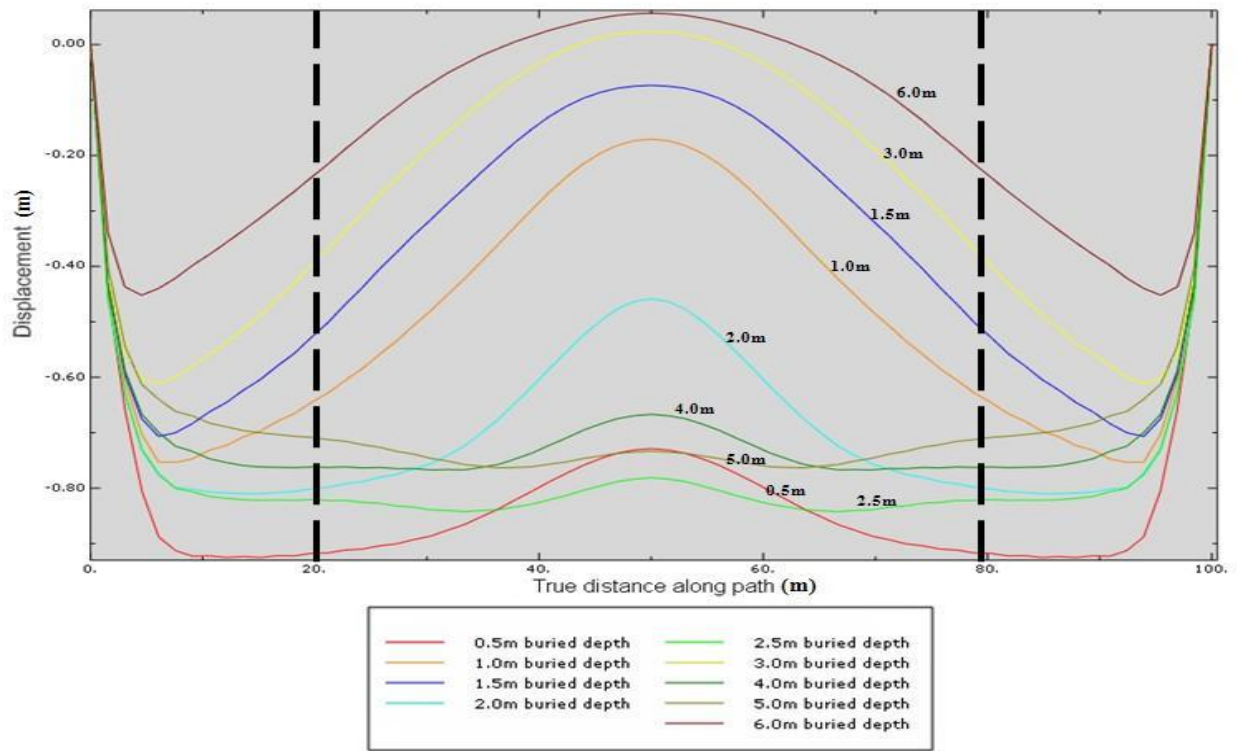
[Displacement]					
Buried depth	Calculated data	Buried depth	Calculated data	Buried depth	Calculated data
0.5m	 <p>U, Magnitude</p> <ul style="list-style-type: none"> +1.036e-01 +9.322e-02 +8.629e-02 +7.766e-02 +6.903e-02 +6.040e-02 +5.178e-02 +4.315e-02 +3.452e-02 +2.589e-02 +1.726e-02 +8.629e-03 +1.523e-10 	2.0m	 <p>U, Magnitude</p> <ul style="list-style-type: none"> +9.455e-02 +8.687e-02 +7.879e-02 +7.091e-02 +6.303e-02 +5.516e-02 +4.728e-02 +3.940e-02 +3.152e-02 +2.364e-02 +1.576e-02 +7.879e-03 +1.032e-10 	4.0m	 <p>U, Magnitude</p> <ul style="list-style-type: none"> +8.125e-02 +7.448e-02 +6.771e-02 +6.094e-02 +5.417e-02 +4.740e-02 +4.063e-02 +3.386e-02 +2.708e-02 +2.031e-02 +1.354e-02 +6.771e-03 +7.720e-11
1.0m	 <p>U, Magnitude</p> <ul style="list-style-type: none"> +1.007e-01 +9.230e-02 +8.391e-02 +7.552e-02 +6.712e-02 +5.873e-02 +5.034e-02 +4.195e-02 +3.356e-02 +2.517e-02 +1.678e-02 +8.391e-03 +1.368e-10 	2.5m	 <p>U, Magnitude</p> <ul style="list-style-type: none"> +1.058e-01 +9.702e-02 +8.820e-02 +7.938e-02 +7.056e-02 +6.174e-02 +5.292e-02 +4.410e-02 +3.528e-02 +2.646e-02 +1.764e-02 +8.820e-03 +0.000e+00 	5.0m	 <p>U, Magnitude</p> <ul style="list-style-type: none"> +7.416e-02 +6.798e-02 +6.180e-02 +5.562e-02 +4.944e-02 +4.326e-02 +3.708e-02 +3.090e-02 +2.472e-02 +1.854e-02 +1.236e-02 +6.180e-03 +6.439e-11
1.5m	 <p>U, Magnitude</p> <ul style="list-style-type: none"> +9.768e-02 +8.954e-02 +8.140e-02 +7.326e-02 +6.512e-02 +5.698e-02 +4.884e-02 +4.070e-02 +3.256e-02 +2.442e-02 +1.628e-02 +8.140e-03 +1.197e-10 	3.0m	 <p>U, Magnitude</p> <ul style="list-style-type: none"> +8.804e-02 +8.070e-02 +7.337e-02 +6.603e-02 +5.869e-02 +5.136e-02 +4.402e-02 +3.668e-02 +2.935e-02 +2.201e-02 +1.467e-02 +7.337e-03 +6.403e-11 	6.0m	 <p>U, Magnitude</p> <ul style="list-style-type: none"> +6.701e-02 +6.143e-02 +5.585e-02 +5.027e-02 +4.468e-02 +3.909e-02 +3.351e-02 +2.792e-02 +2.234e-02 +1.675e-02 +1.117e-02 +5.585e-03 +5.804e-11
[stress]					
Buried depth	Calculated data	Buried depth	Calculated data	Buried depth	Calculated data
0.5m	 <p>S, Mises SNEG, (fraction = -1.0) (Avg: 75%)</p> <ul style="list-style-type: none"> +7.323e+08 +6.715e+08 +6.107e+08 +5.500e+08 +4.892e+08 +4.284e+08 +3.677e+08 +3.069e+08 +2.461e+08 +1.853e+08 +1.246e+08 +6.391e+07 +3.034e+06 	2.0m	 <p>S, Mises SNEG, (fraction = -1.0) (Avg: 75%)</p> <ul style="list-style-type: none"> +7.422e+08 +6.807e+08 +6.192e+08 +5.577e+08 +4.962e+08 +4.347e+08 +3.732e+08 +3.117e+08 +2.502e+08 +1.887e+08 +1.272e+08 +6.571e+07 +4.209e+06 	4.0m	 <p>S, Mises SNEG, (fraction = -1.0) (Avg: 75%)</p> <ul style="list-style-type: none"> +7.571e+08 +6.945e+08 +6.320e+08 +5.694e+08 +5.069e+08 +4.443e+08 +3.818e+08 +3.192e+08 +2.567e+08 +1.941e+08 +1.316e+08 +6.901e+07 +6.458e+06
1.0m	 <p>S, Mises SNEG, (fraction = -1.0) (Avg: 75%)</p> <ul style="list-style-type: none"> +7.312e+08 +6.705e+08 +6.099e+08 +5.492e+08 +4.885e+08 +4.279e+08 +3.672e+08 +3.066e+08 +2.459e+08 +1.852e+08 +1.246e+08 +6.391e+07 +3.246e+06 	2.5m	 <p>S, Mises SNEG, (fraction = -1.0) (Avg: 75%)</p> <ul style="list-style-type: none"> +7.487e+08 +6.867e+08 +6.247e+08 +5.627e+08 +5.007e+08 +4.387e+08 +3.767e+08 +3.147e+08 +2.527e+08 +1.908e+08 +1.288e+08 +6.677e+07 +4.784e+06 	5.0m	 <p>S, Mises SNEG, (fraction = -1.0) (Avg: 75%)</p> <ul style="list-style-type: none"> +7.557e+08 +6.929e+08 +6.301e+08 +5.673e+08 +5.045e+08 +4.417e+08 +3.789e+08 +3.160e+08 +2.532e+08 +1.904e+08 +1.276e+08 +6.479e+07 +1.976e+06
1.5m	 <p>S, Mises SNEG, (fraction = -1.0) (Avg: 75%)</p> <ul style="list-style-type: none"> +7.335e+08 +6.727e+08 +6.119e+08 +5.510e+08 +4.902e+08 +4.294e+08 +3.686e+08 +3.078e+08 +2.469e+08 +1.861e+08 +1.253e+08 +6.449e+07 +3.674e+06 	3.0m	 <p>S, Mises SNEG, (fraction = -1.0) (Avg: 75%)</p> <ul style="list-style-type: none"> +7.532e+08 +6.908e+08 +6.285e+08 +5.662e+08 +5.039e+08 +4.416e+08 +3.793e+08 +3.169e+08 +2.546e+08 +1.923e+08 +1.300e+08 +6.768e+07 +5.364e+06 	6.0m	 <p>S, Mises SNEG, (fraction = -1.0) (Avg: 75%)</p> <ul style="list-style-type: none"> +7.511e+08 +6.889e+08 +6.266e+08 +5.644e+08 +5.021e+08 +4.399e+08 +3.776e+08 +3.154e+08 +2.531e+08 +1.909e+08 +1.287e+08 +6.641e+07 +4.167e+06

Appendix F. 15. Calculated static analysis results by ABAQUS for the pipeline in fully saturated cohesive soil with hinge boundary condition at pipeline ends

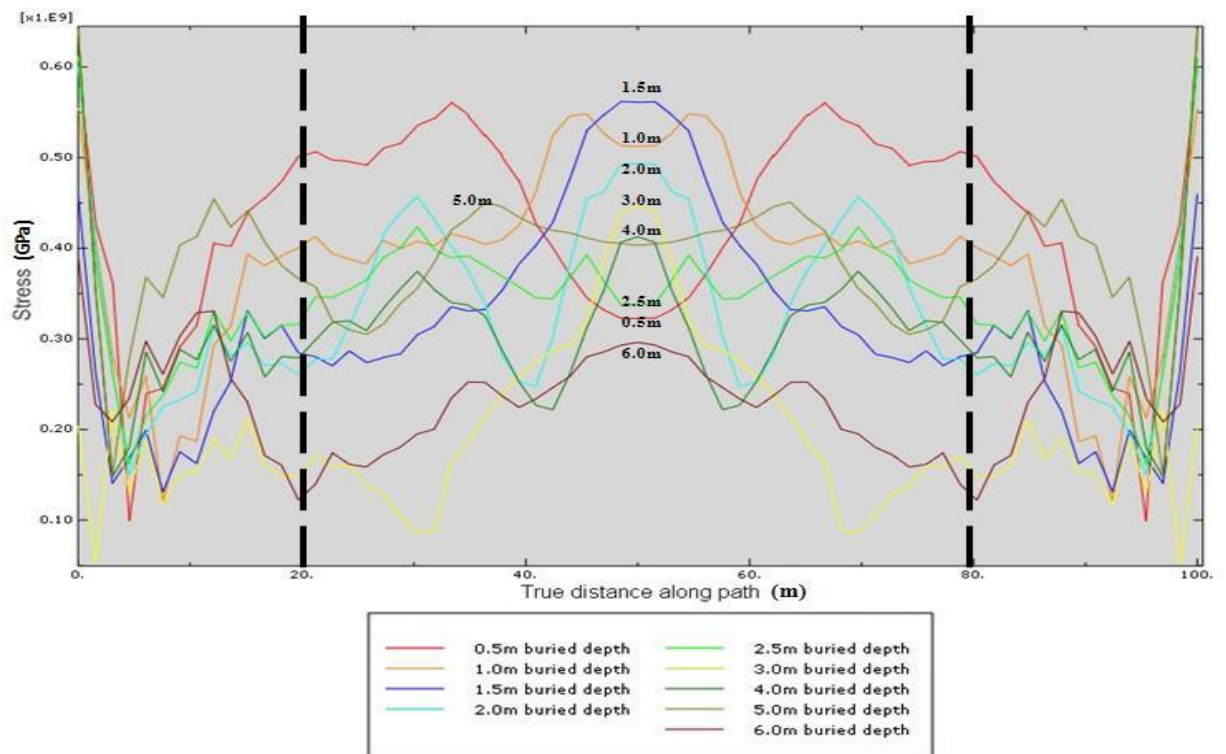
[Displacement]					
Buried depth	Calculated data	Buried depth	Calculated data	Buried depth	Calculated data
0.5m		2.0m		4.0m	
1.0m		2.5m		5.0m	
1.5m		3.0m		6.0m	
[stress]					
Buried depth	Calculated data	Buried depth	Calculated data	Buried depth	Calculated data
0.5m		2.0m		4.0m	
1.0m		2.5m		5.0m	
1.5m		3.0m		6.0m	

Appendix F. 16. Calculated static analysis results by ABAQUS for the pipeline in fully saturated cohesive soil with roller boundary condition at pipeline ends

Appendix G – the enlarged graphs for seismic analysis

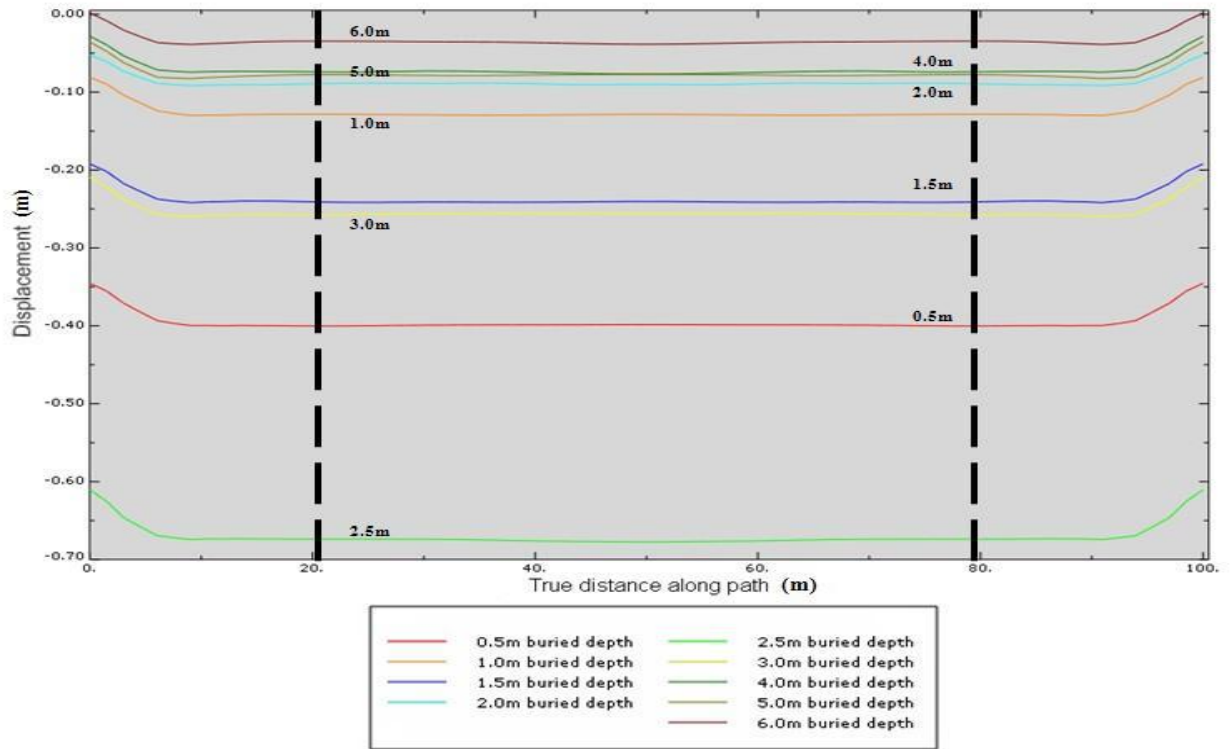


[Displacement]

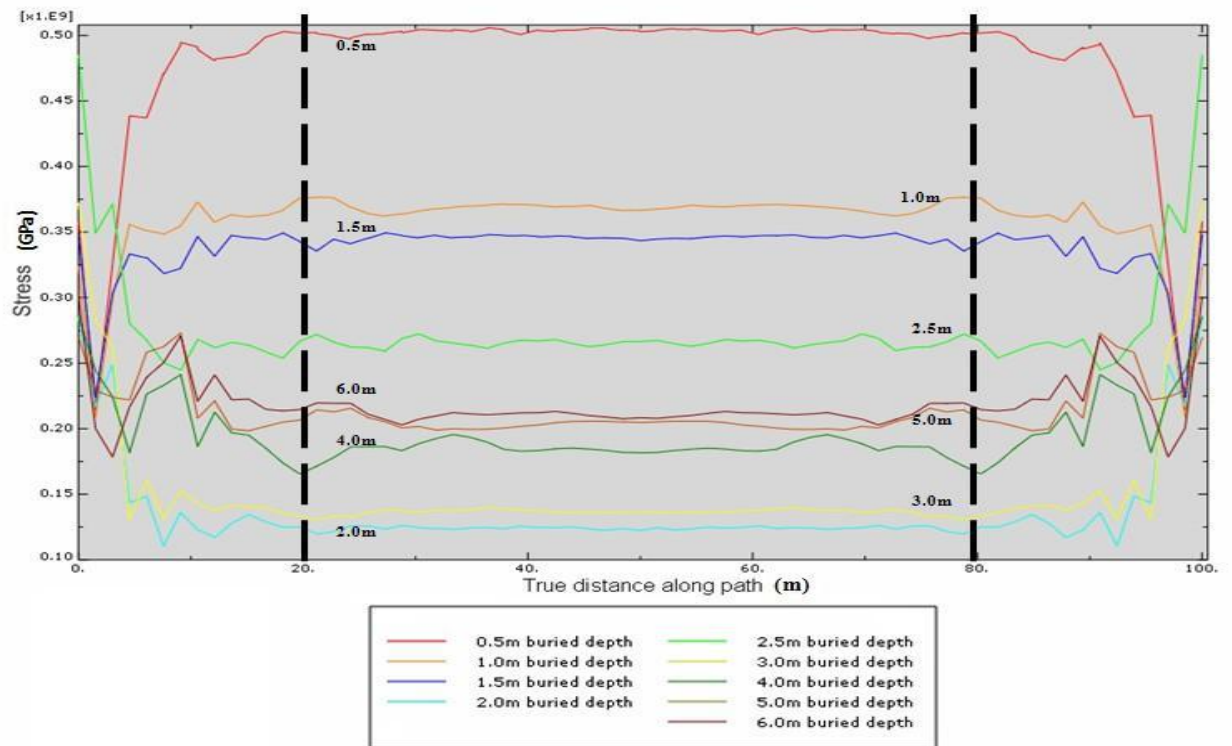


[Stress]

Appendix G 1: Diagrams for general moist sandy soil with hinge boundary at pipeline ends

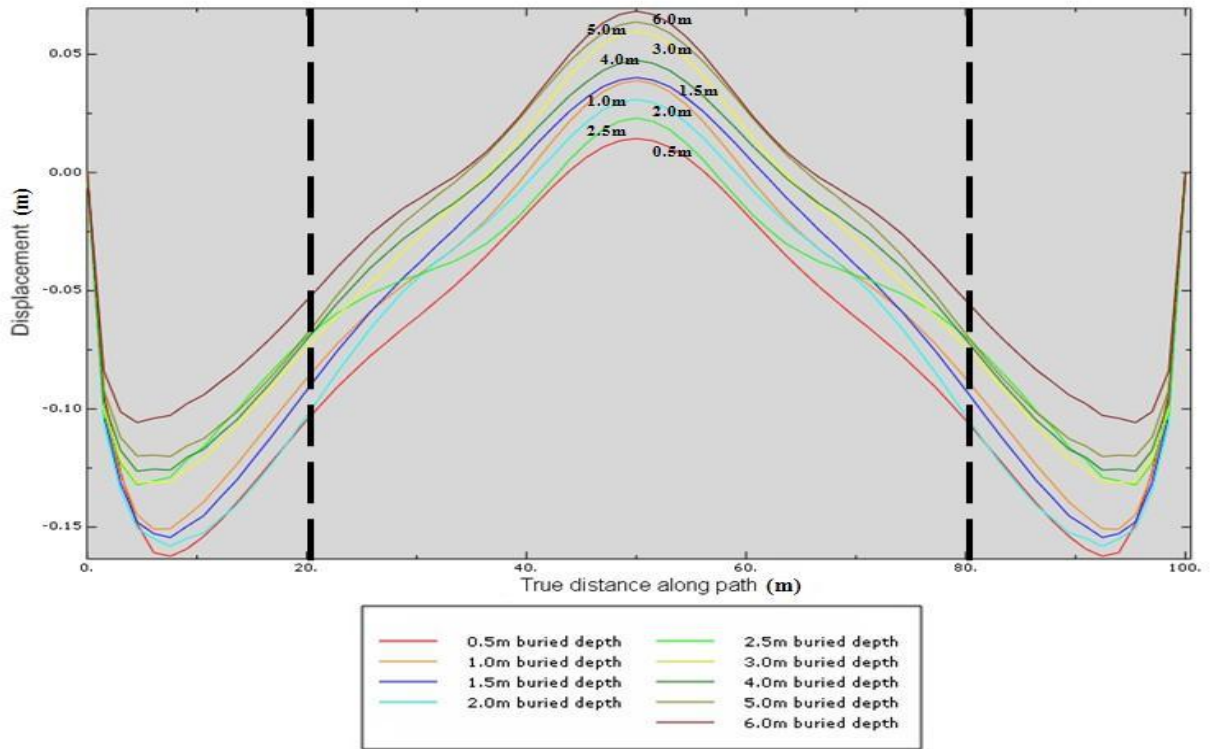


[Displacement]

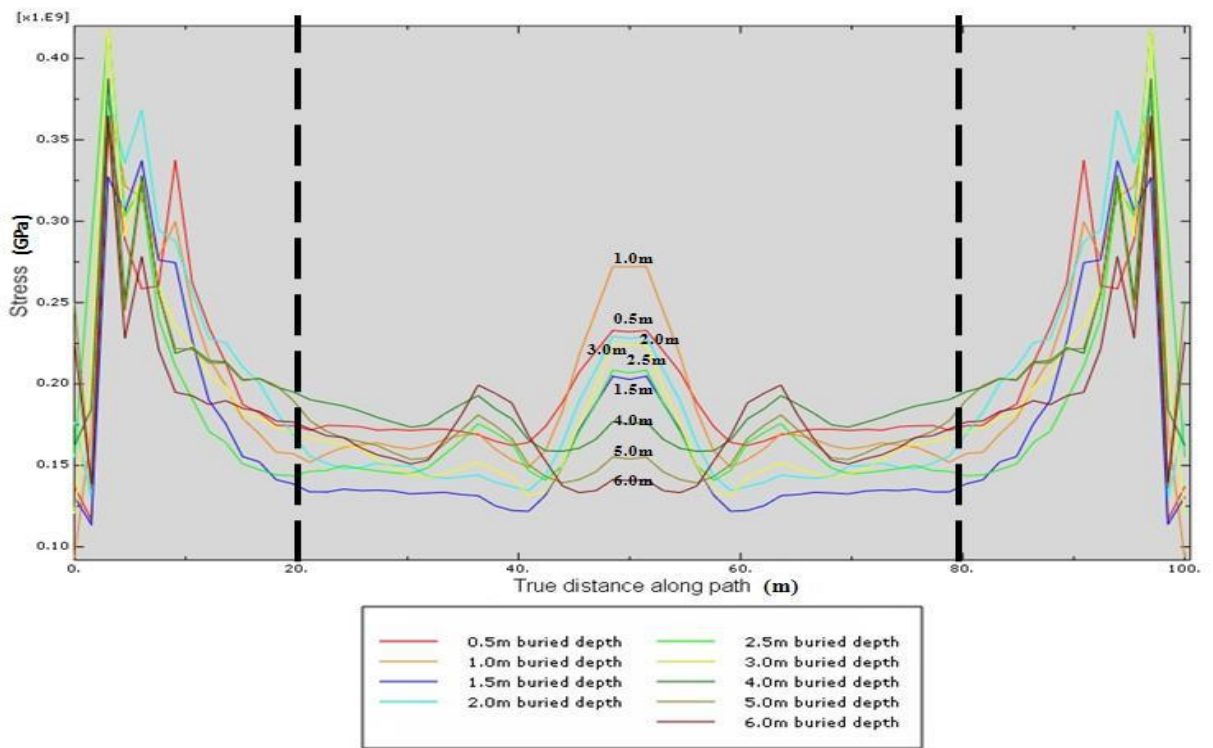


[Stress]

Appendix G 2: Diagrams for general moist sandy soil with roller boundary at pipeline ends

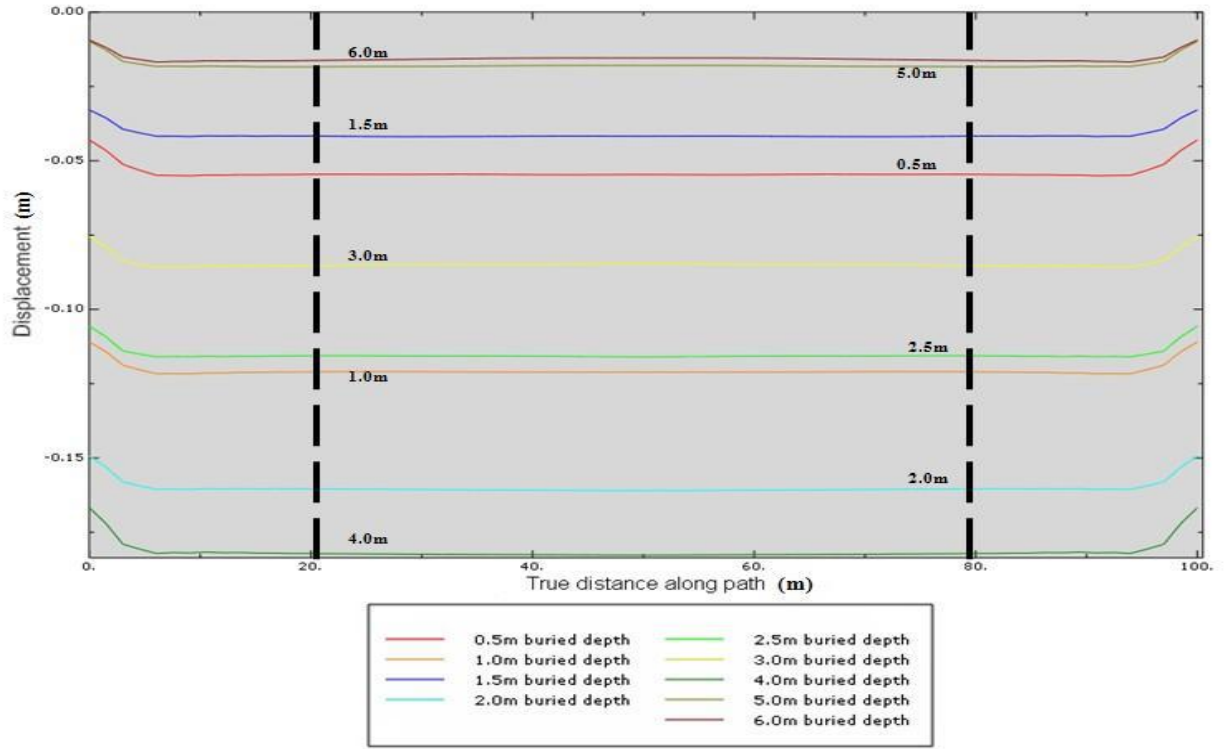


[Displacement]

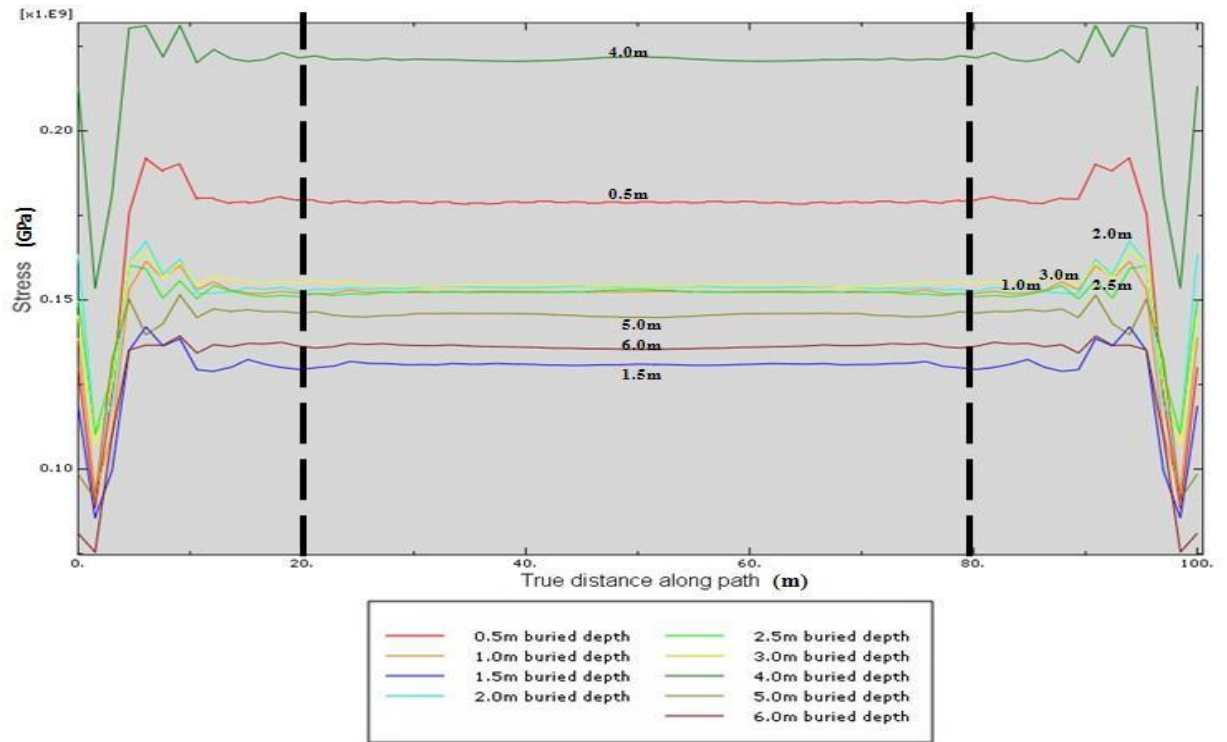


[Stress]

Appendix G 3: Diagrams for fully saturated sandy soil with hinge boundary at pipeline ends

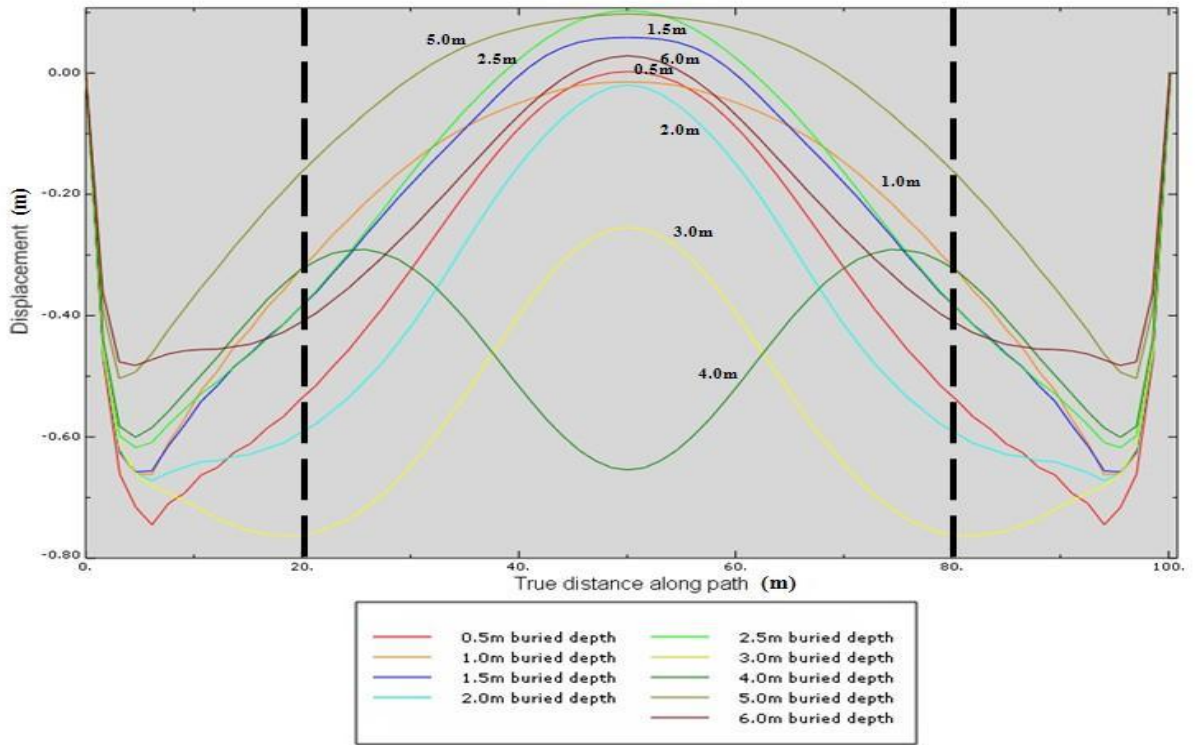


[Displacement]

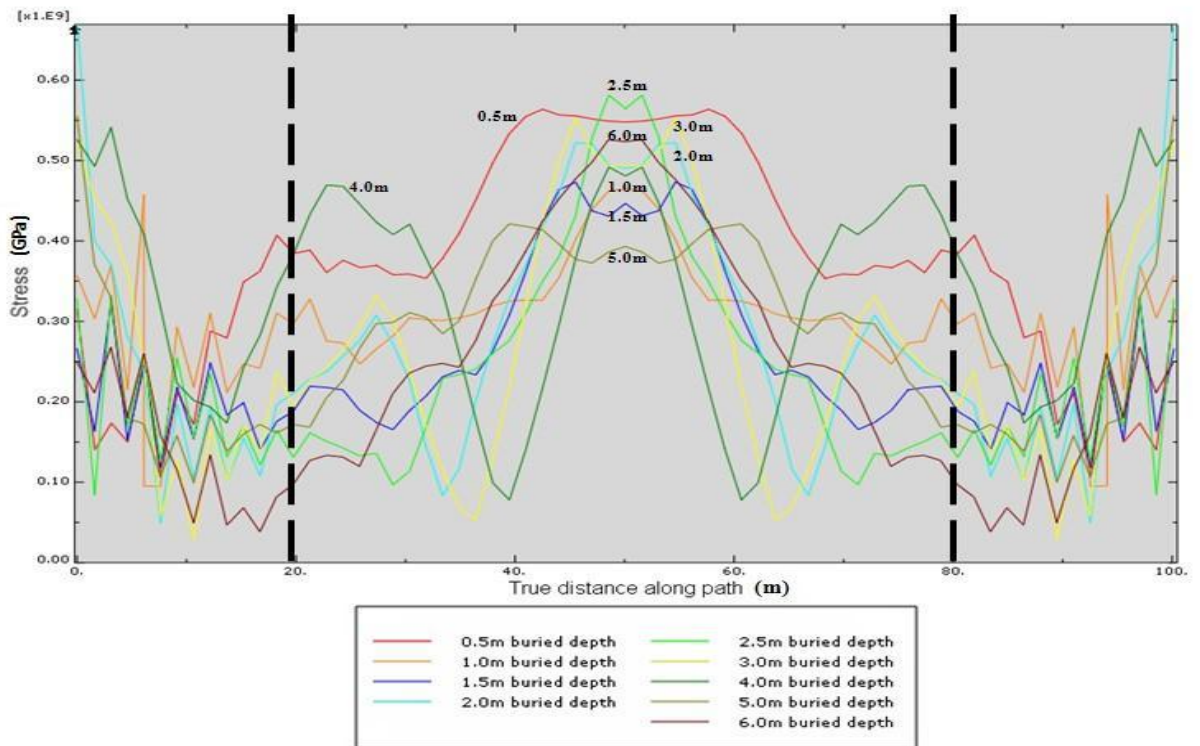


[Stress]

Appendix G 4: Diagrams for fully saturated sandy soil with roller boundary at pipeline ends

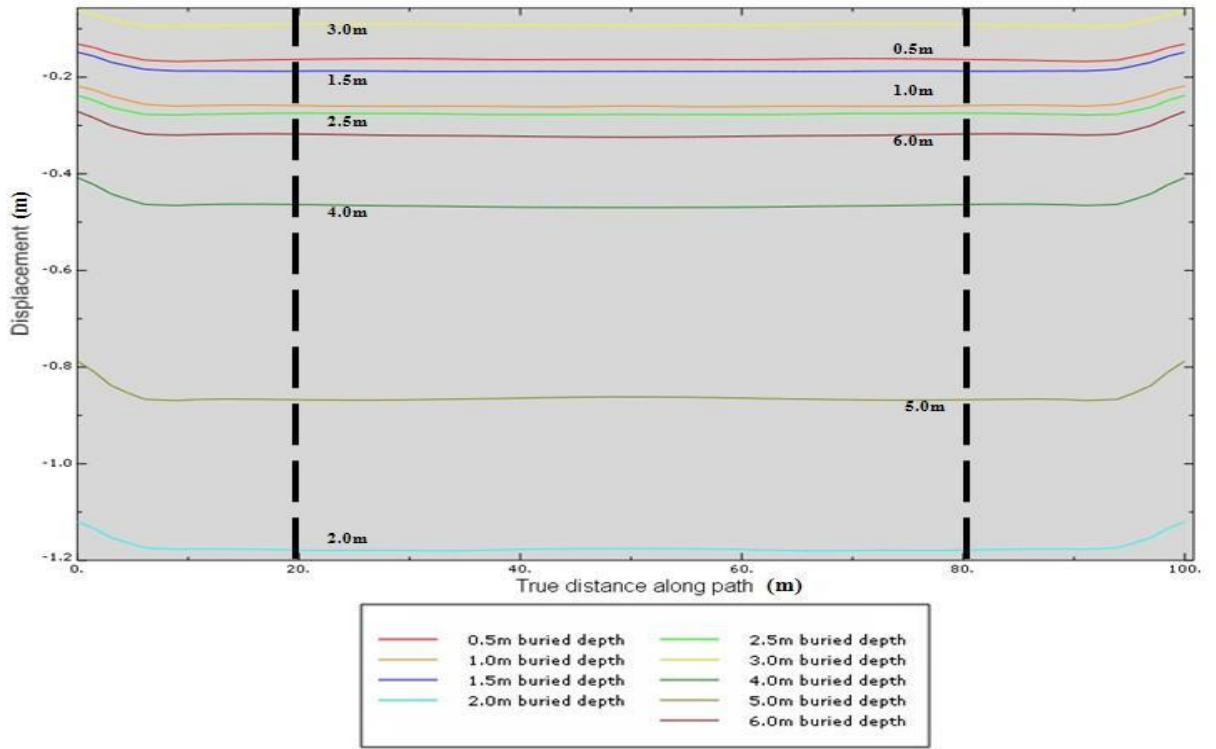


[Displacement]

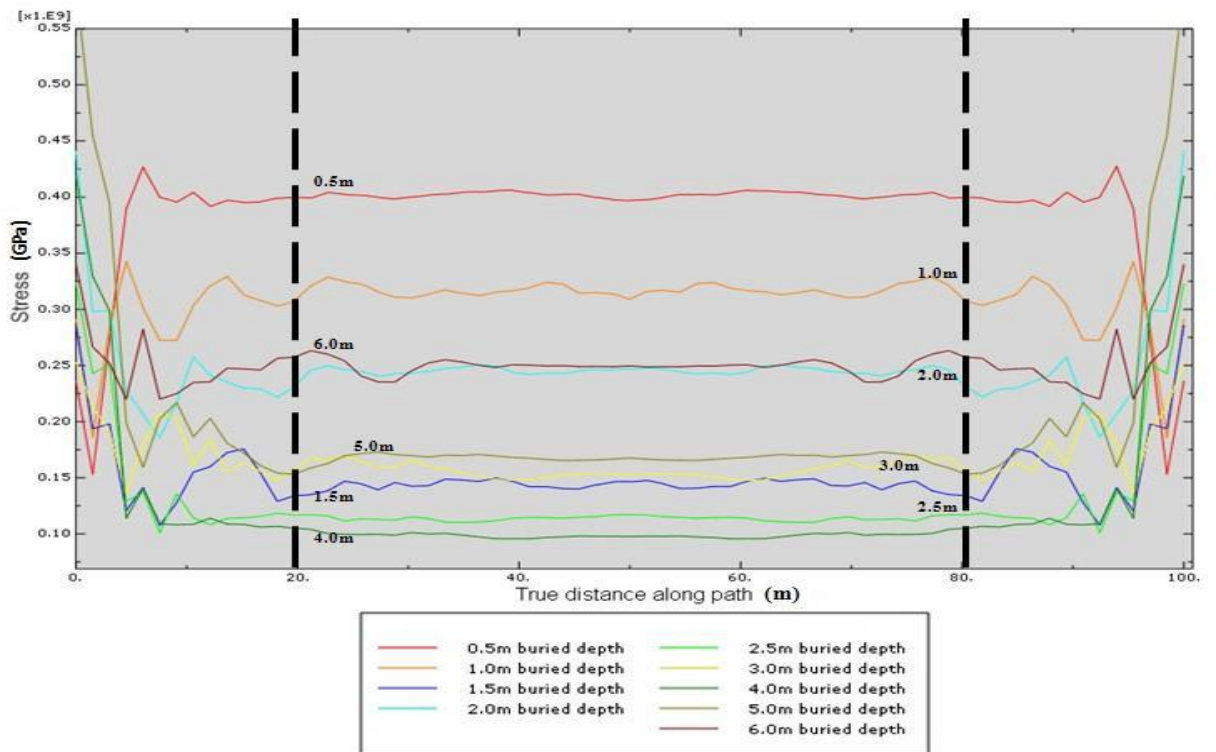


[Stress]

Appendix G 5: Diagrams for general moist cohesive soil with hinge boundary at pipeline ends

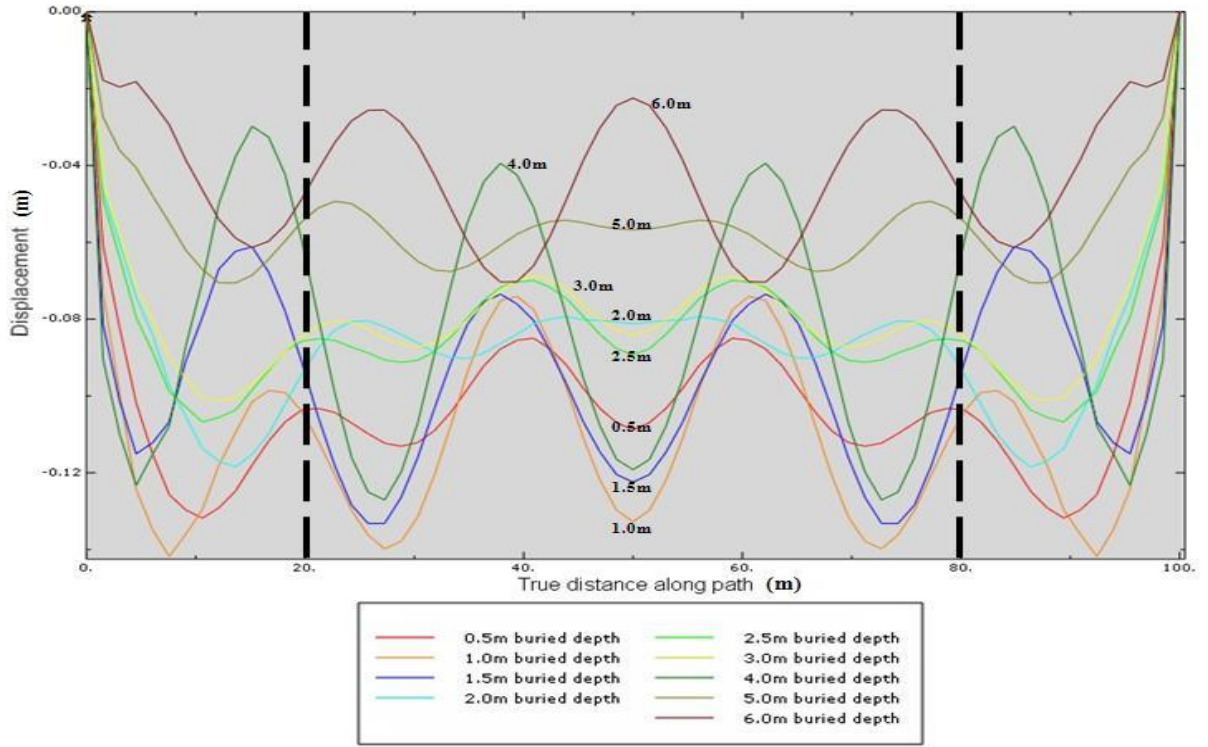


[Displacement]

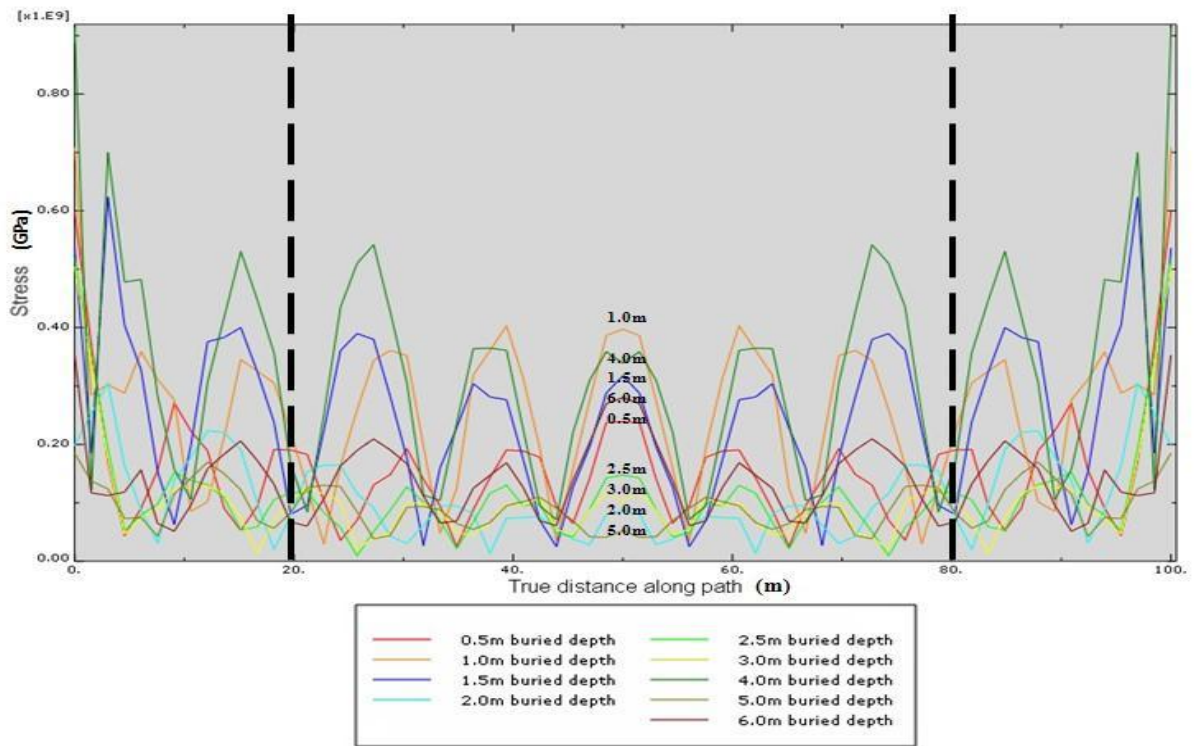


[Stress]

Appendix G 6: Diagrams for general moist cohesive soil with roller boundary at pipeline ends

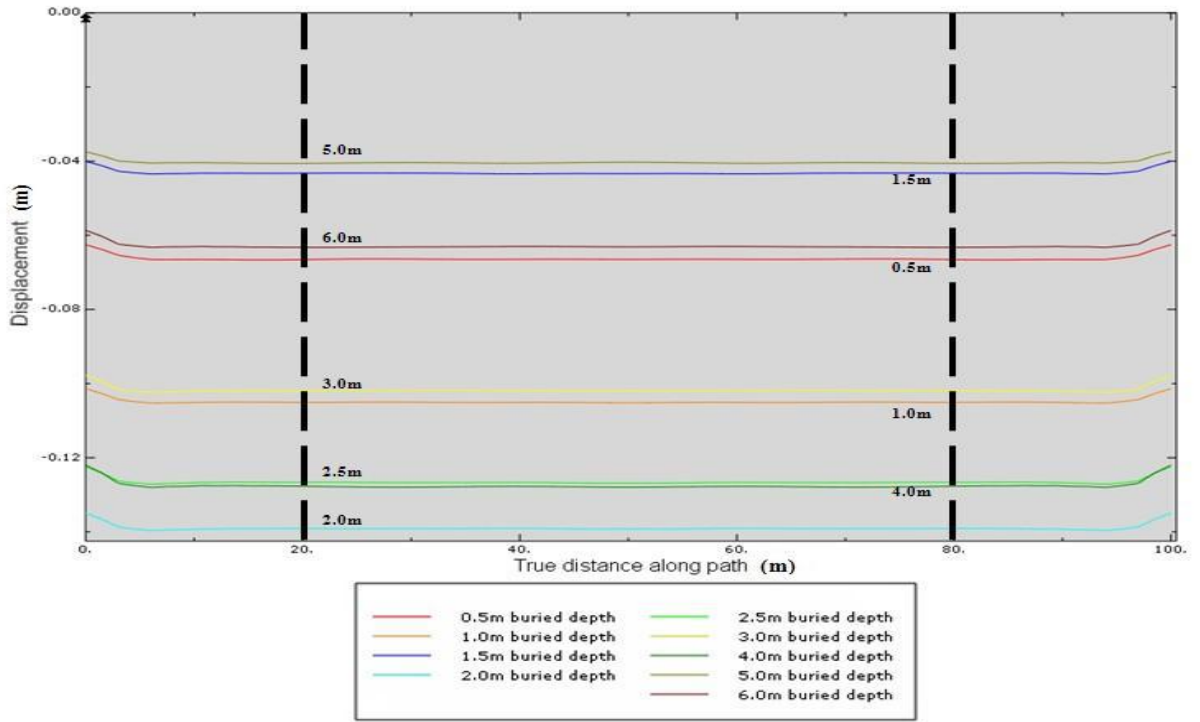


[Displacement]

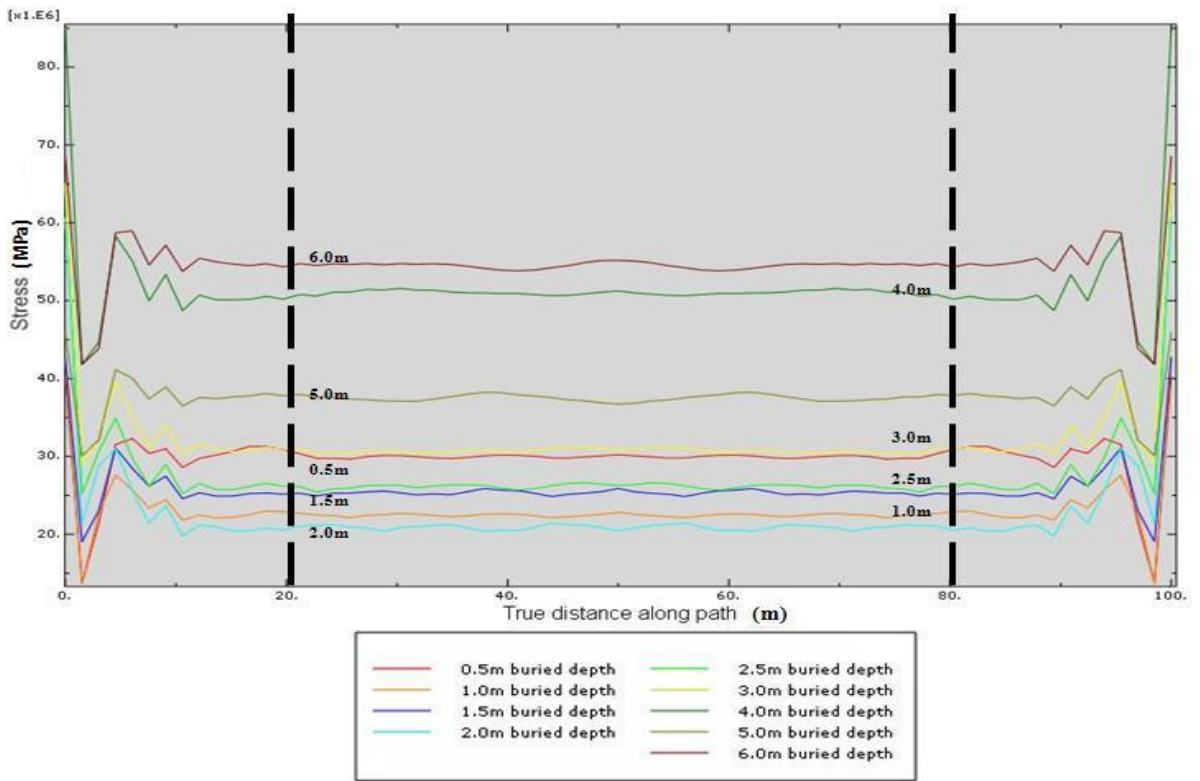


[Stress]

Appendix G 7: Diagrams for fully saturated cohesive soil with hinge boundary at pipeline ends



[Displacement]



[Stress]

Appendix G 8: Diagrams for fully saturated cohesive soil with roller boundary at pipeline ends

Appendix H – Tutorial

[ABAQUS/CAE Tutorial]

Once the simulation has been completed and the stresses, displacements or other fundamental variables have been calculated by ABAQUS, the results can be evaluated. The evaluation by ABAQUS is generally executed by using the visualization module of ABAQUS/CAE. The ABAQUS/CAE is the Complete Abaqus Environment that offers a simple interface for creating models, monitoring created models and evaluating results. In this section of dissertation, the processes related to creating models will be explained and the following tasks will be performed.


- Creating the three-dimensional geometry and parts representing the created models
- Applying the material properties to created models
- Assembling models
- Configuring the analysis procedures
- Defining boundary conditions and loads
- Meshing the created models
- Creating and submitting the jobs for analysis



All information related to considered models, such as material properties, physical dimensions of models, loads and boundary conditions, is based on chapter 1, 2 and 3 in this dissertation.

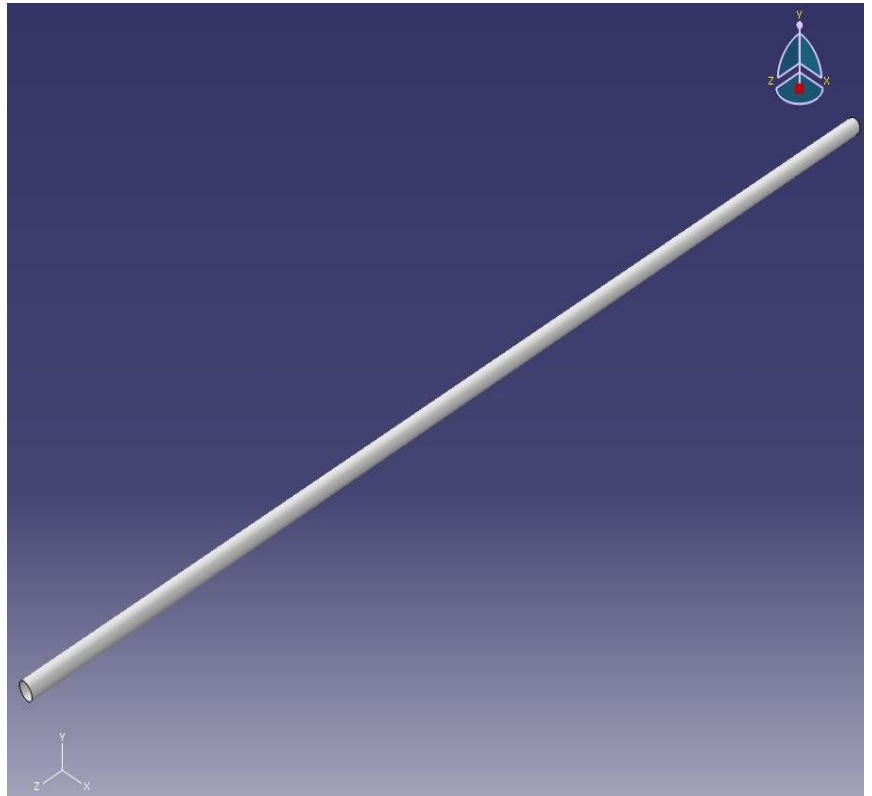
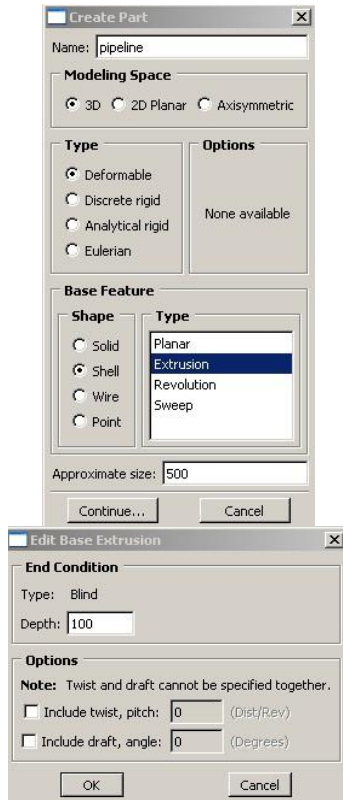
1) Modelling both soil and pipeline


The [part](#) module allows ABAQUS/CAE to create individual parts by sketching their geometry directly. The pipeline and soil model is generated by the part module in ABAQUS/CAE.

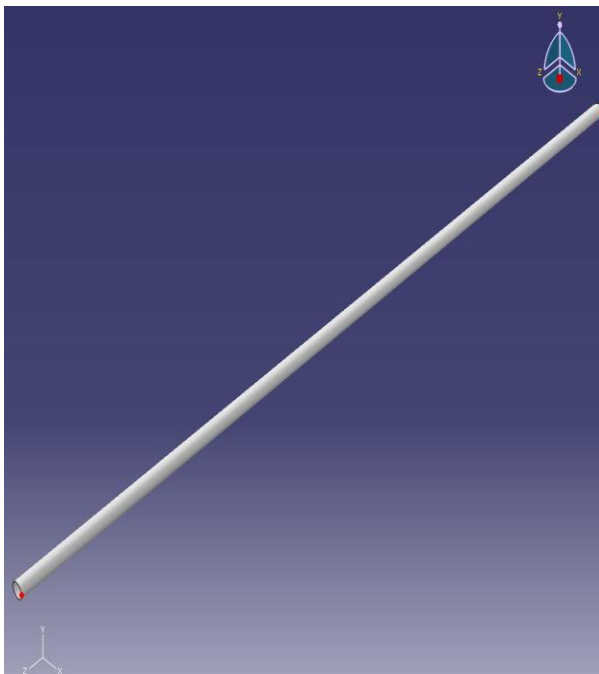
First of all, the pipeline is created by shell model because the thickness of pipeline is thin. The physical and mechanical characteristics are followed as shown Figure 1.1 in section 1.2.4. In order to create pipeline in ABAQUS/CAE, shell model of pipeline should be drawn by part manager.

Click on [Create part](#) tool, . When the [create part](#) dialog box appears, name the part *pipeline*. Accept the default setting of a [three-dimensional, deformable body](#) and a [shell, extruded](#) base feature. In the [Approximate size](#) text field which decides the size of drawing space, type 500 in order to ensure enough drawing space. Click [Continue](#) to exit [create part](#) dialog box.


To sketch the profile of pipeline, there is need to select [Create circle](#) drawing tool, . Draw circle and input the radius of pipeline in metres, which is $1.524/2$ by using [Add dimension](#) tool, . Then click [Done](#) in the bottom prompt area. ABAQUS/CAE displays [Edit base extrusion](#) dialogue because pipeline is created by an extruded part. In depth field, type a value of 100 which means 100m lengths. Click [OK](#) to accept this value. ABAQUS/CAE displays an isometric view of shell model of pipeline as shown below.

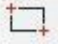



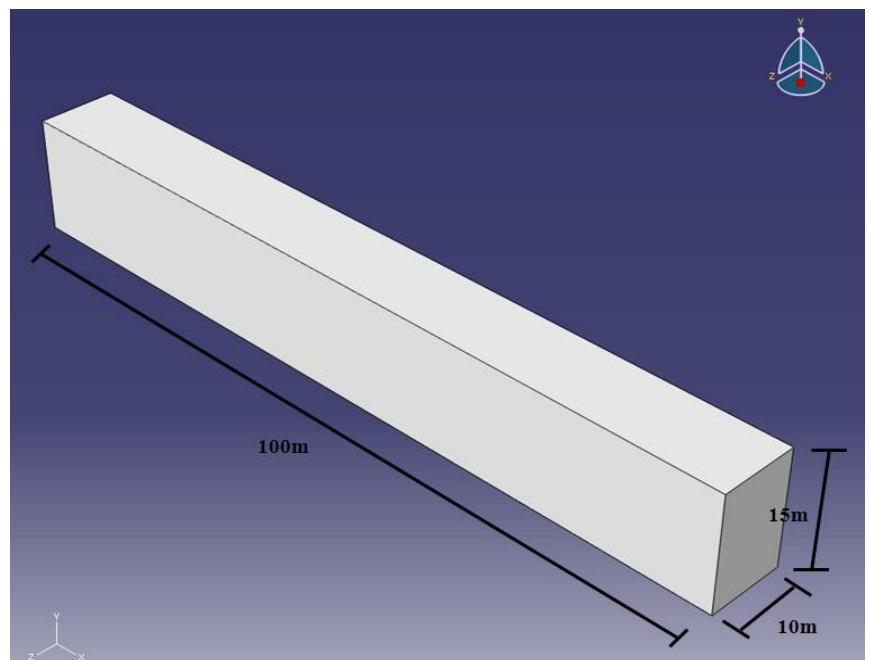
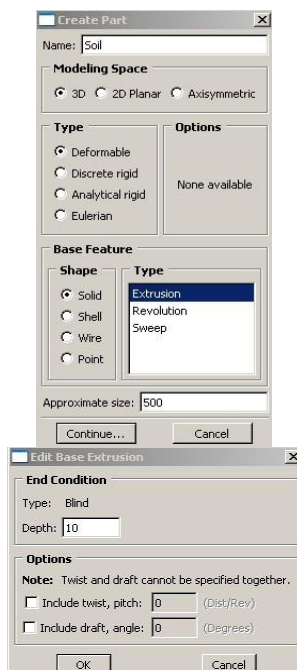
The pipeline model created has to be partitioned for making the model do the mesh uniformly. In order to partition the pipeline model created, there is need to select [Partition face – use shortest path between two points](#) tool, . Divide into four parts as shown below.







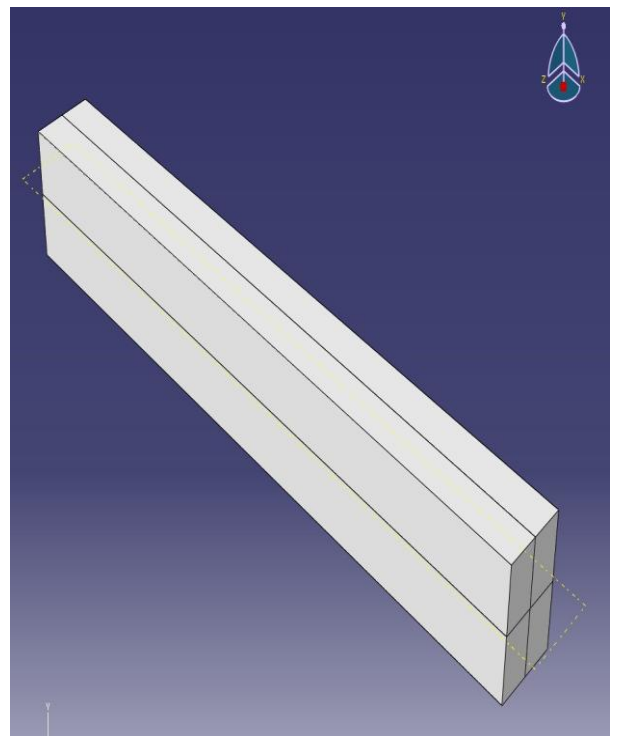
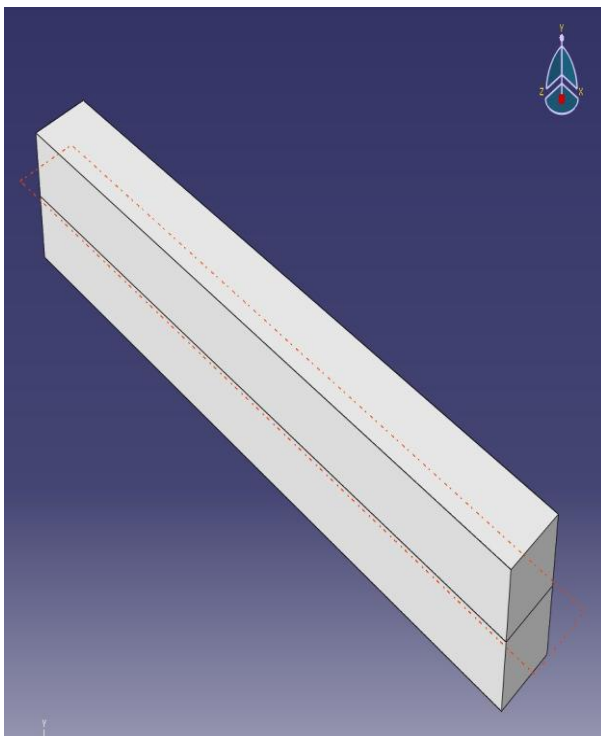
Secondly, the soil model is created as a cuboid. The physical and mechanical characteristics are followed as shown Figure 1.2 in section 1.2.4. In order to generate soil model in ABAQUS/CAE, solid model for soil should be also drawn by part manager.





Click on **Create part** tool, . When the **Created part** dialog box appears, name the part *soil*. Accept the default setting of a **three-dimensional, deformable body** and **solid, extruded** base feature. In the **Approximate size** text field, type 500. Click **Continue** to exit the Create part dialog box.

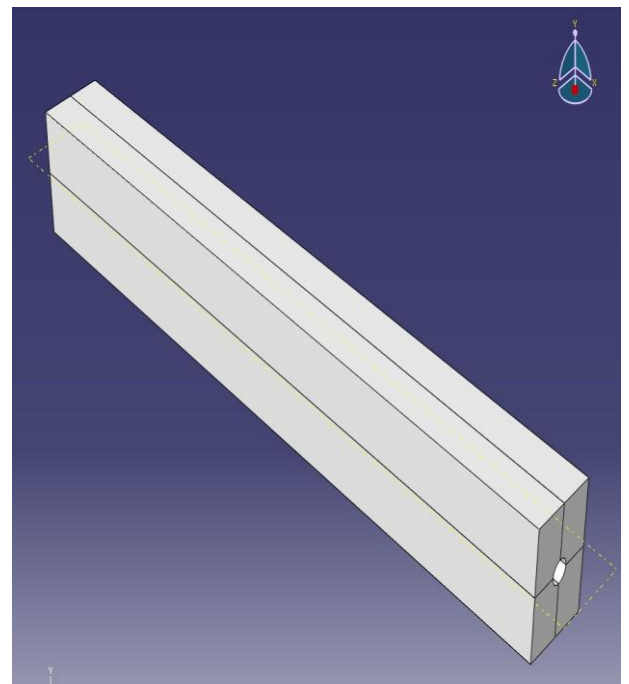
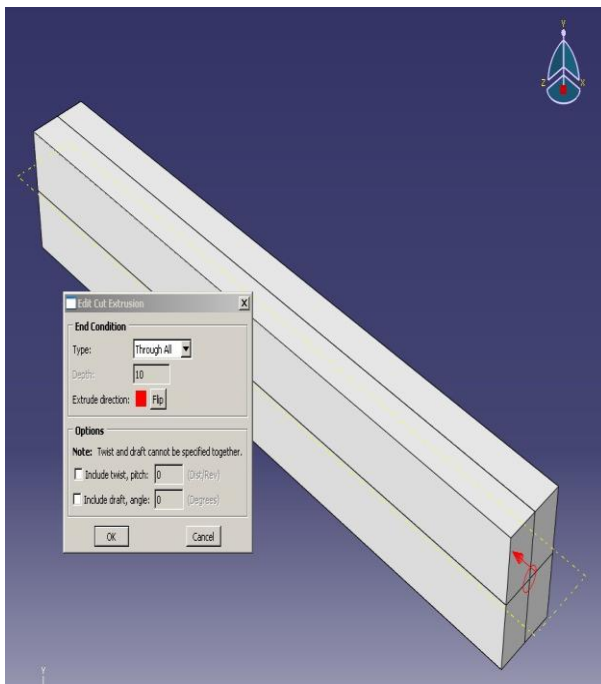
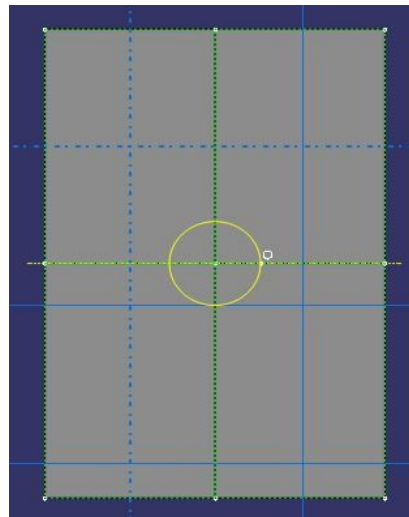
To sketch the profile of the soil, there is need to select **Create lines** tool, . Draw the rectangle and regulate the size of soil, which is 100m 15m, by using **Add dimension** tool, . Click **Done** in the bottom prompt area. ABAQUS/CAE displays **Edit base extrusion** dialog box for us to regulate the size of soil model's width because the solid model of soil is also created by an extruded part. In the depth field, type a value of 10 which means 10m of soil model's width. Click **OK** to accept this value. ABAQUS/CAE displays an isometric view of the soil model part as shown below.



The created solid model for soil must also be partitioned for ensuring uniform mesh. Before partitioning horizontal direction of model, datum plane should be created by [Create datum plane – offset from plane](#) tool,  because created datum plane helps to create the mesh effectively and makes the position of the pipeline model, which will be embedded in solid model of soil, change the location of pipeline model automatically in accordance with the consideration of buried depth of pipeline. Click [Created datum plane – offset from plane](#) tool, , with accepting upper surface of soil model. Click [Enter value](#) in the bottom prompt area and click [Flip](#) once. When offset blank area appears, type 7.5 in offset area which means offset 7.5m from upper surface of solid model. Click [OK](#) in the bottom prompt area. It is possible to partition the solid model of soil in horizontal direction by [Partition cell – use datum plane](#) tool, , after selecting created datum plane. In order to partition vertical direction of solid model, [Partition cell – define cutting plane](#) tool, , makes the solid model possible to partition vertical direction of the model as shown below.



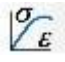
In order to embed the shell model of pipeline, the position of the shell model has to be created in the datum plane by **Create cut – extrude** tool, . Circle is drawn by **Create circle** tool, , in the solid model's plane selected by **Create cut – extrude** tool, . Type the radius of the circle by using **Add dimension** tool, . The value of the circle radius is $1.524/2$ because the diameter of circle is the outer diameter of pipeline. Click **Done** in the bottom prompt area and accept the cutting type of **through all**. ABAQUS/CAE displays an isometric view of the solid model, which creates the hole, as shown below.

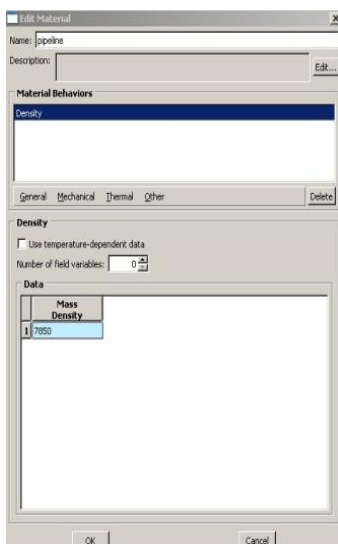


2) Application of mechanical properties

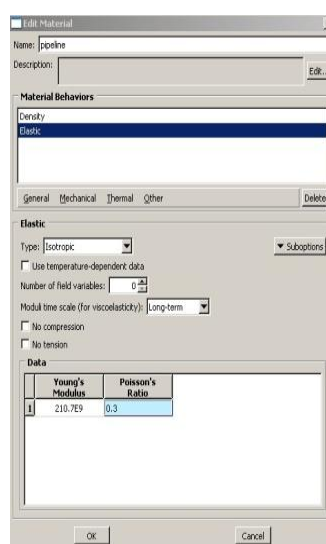
The second step is the application of mechanical properties related to each created model. This step is quite important because the accuracy of material properties decides the quality of analysis. Even though all of processes are accomplished accurately, inaccurate material properties spoil the quality of results. A section definition contains information about the properties of a part or the region of a part, such as a region's associated material definition and cross-sectional geometry. In the property module, section and material definition can be created and these two can be assigned into regions of parts.

First of all, pipeline and soil mechanical properties should be created by material manager. The mechanical properties of both pipeline and soil model are based on Table 1 and Table 2 in section 1.2.4.

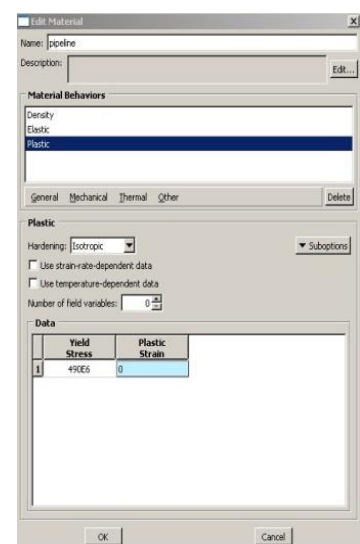
In the module list, choose **Property** and click on **Create material** tool, . When the **Edit material** dialog box appears, name the material *pipeline*. From the material editor's menu bar, select **General** -> **Density**, **Mechanical** -> **Elasticity** -> **Elastic** and **Mechanical** -> **Plasticity** -> **Plastic**. ABAQUS/CAE displays the density, elastic and plastic data form. Type the values based on Table 1 in section 1.2.4 as shown below.



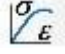
Mass Density
1 7850

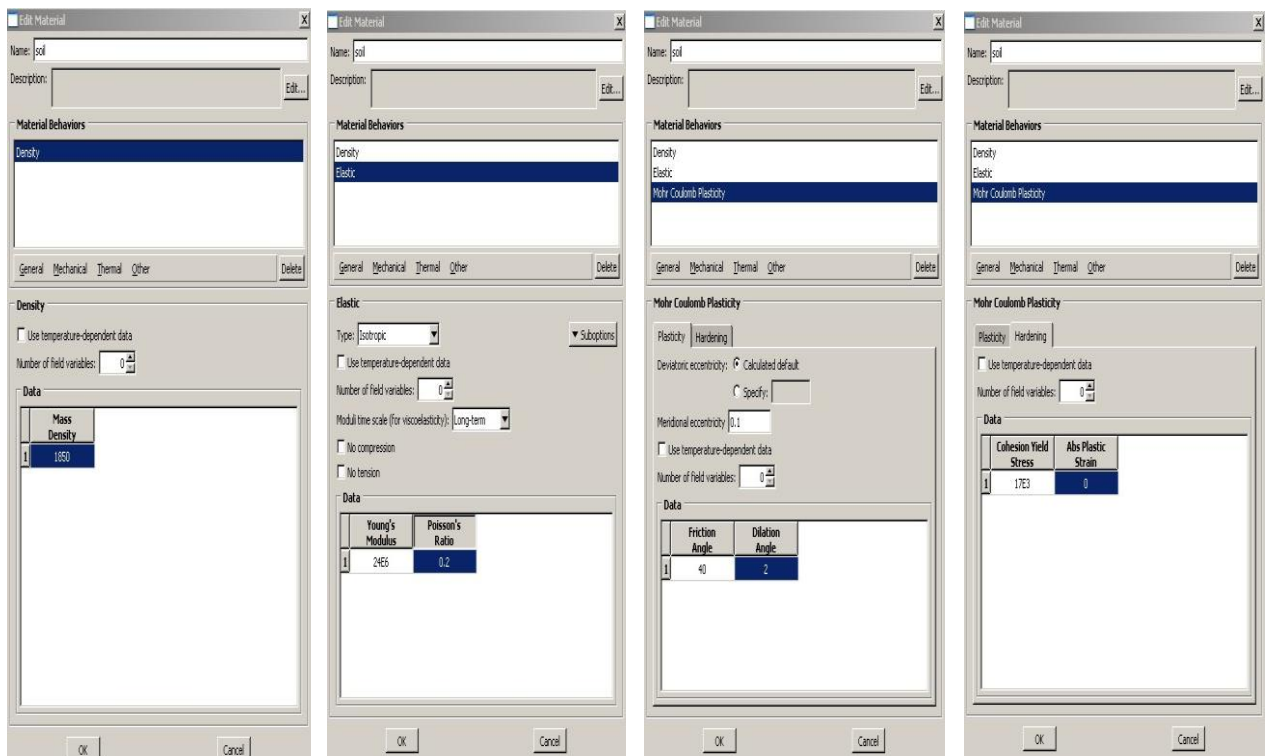



Young's Modulus	Poisson's Ratio
1 210.769	0.3




Yield Stress	Plastic Strain
1 45005	0

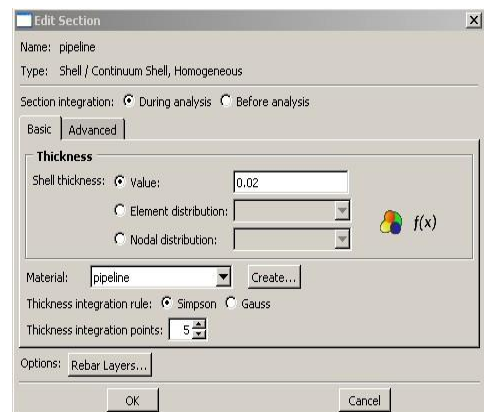
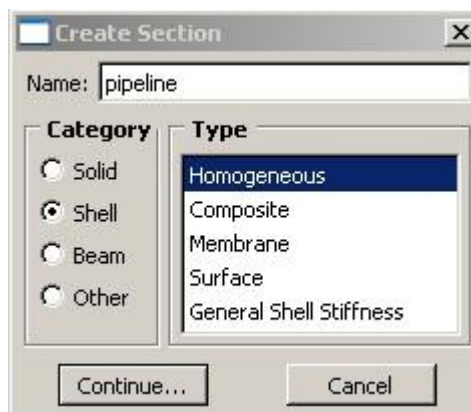
In the module list, choose **Property** and click on **Create material** tool, . When the **Edit material** dialog box appears, name the material *soil*. From the material editor's menu bar, select **General** -> **Density**, **Mechanical** -> **Elasticity** -> **Elastic** and **Mechanical** -> **Plasticity** -> **Mohr Coulomb Plasticity**. ABAQUS/CAE displays the density, elastic and plastic data form. Type the values based on Table 2 in section 1.2.4 as shown below.



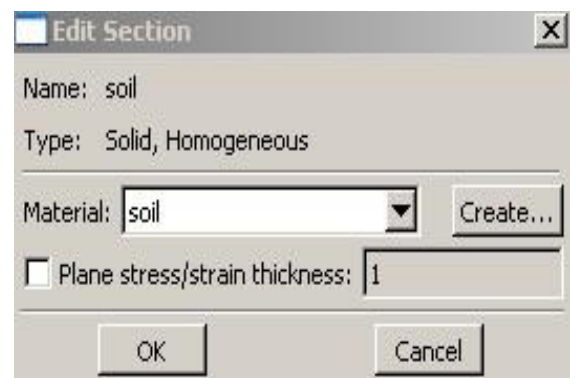
Secondly, creating section, which is involved in information related to mechanical properties, is needed before assigning material's mechanical properties by section manager. Especially, the thickness of pipeline can be designated by creating pipeline section. Click on **Create section** tool, . When the **Created section** dialog box appears, Name the section *pipeline*; in the **Category** list, accept **Shell** as the default category selection; in **Type** list, accept **Homogeneous** as the default type section. Click **Continue**. The **Edit section** dialog box appears. In the dialog box, accept the default selection of pipeline for the material associated with the section; type the shell thickness as 0.02 which means the thickness of 0.02m. Click **OK**.

The process of soil for creating section is also similar to the above process of pipeline. Click on **Create section** tool, . The **Create section** dialog box appears. In the **Create section** dialog box, name the section *soil*; in the **Category** list, accept **Solid** as the default category selection; in **Type** list, accept **Homogeneous** as the default type selection. Click **Continue**. The **Edit section** dialog box appears. In the dialog box, accept the default selection of soil for the material associated with the selection; accept the default value of 1 for the **Plane stress/strain thickness**. Click **OK**. The above two processes can be shown as below.


Pipeline:



Soil:



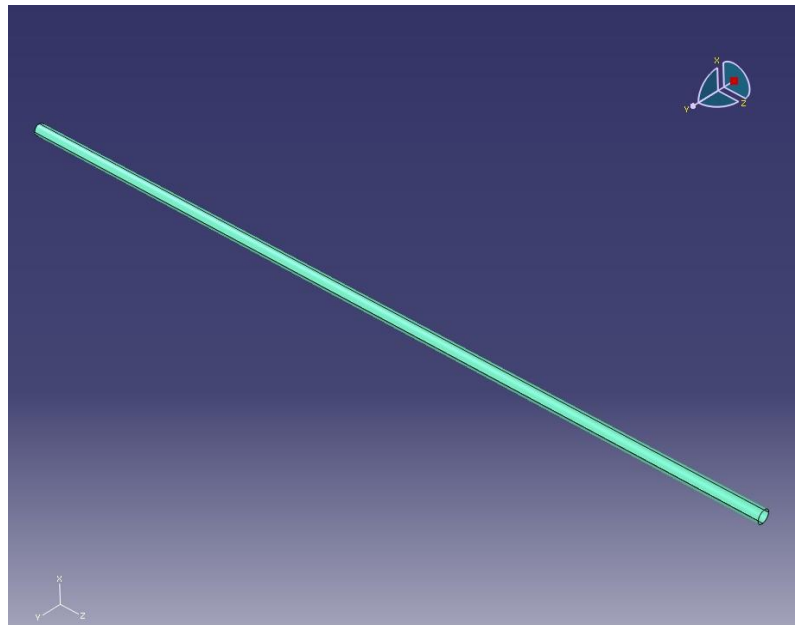
Finally, the last step is the assigning mechanical properties to both soil and pipeline. That is, created sections, which are involved in information related to each model's mechanical property, are assigned to each created model.

In the case of pipeline, click on **Assign section** tool, . ABAQUS/CAE displays *'selection the region to be assigned a section'* in the bottom prompt area. Drag whole of the

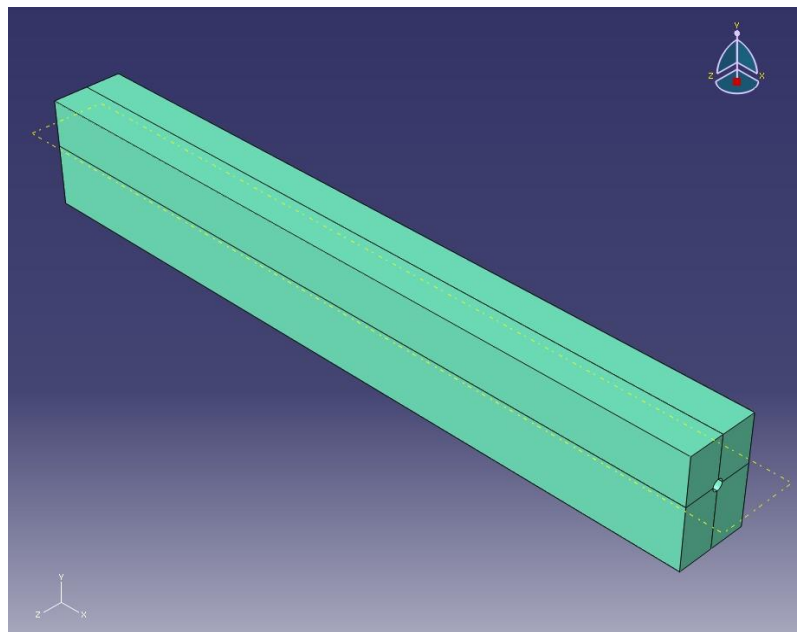
pipeline to select the region to which the selection will be applied. ABAQUS/CAE highlights the entire pipeline model. Click **Done** in the bottom prompt area to accept the selected geometry. The **Edit section assignment dialog** box appears. Accept the default selection of pipeline as the selection, and click **OK**.

In the case of soil model, the process of assignment is almost the same. The applied mechanical property in each model is shown with green colour like below.

Pipeline:




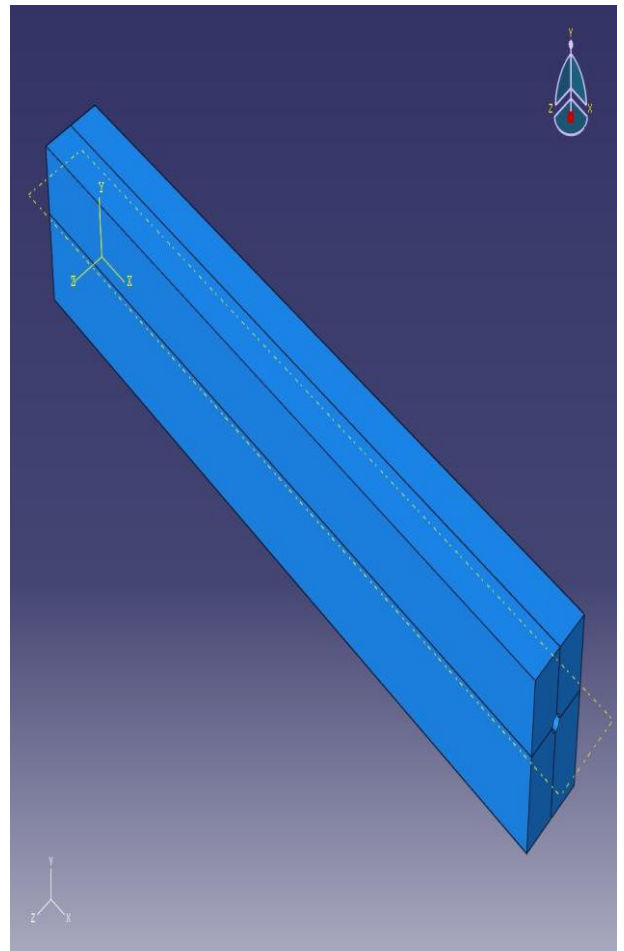
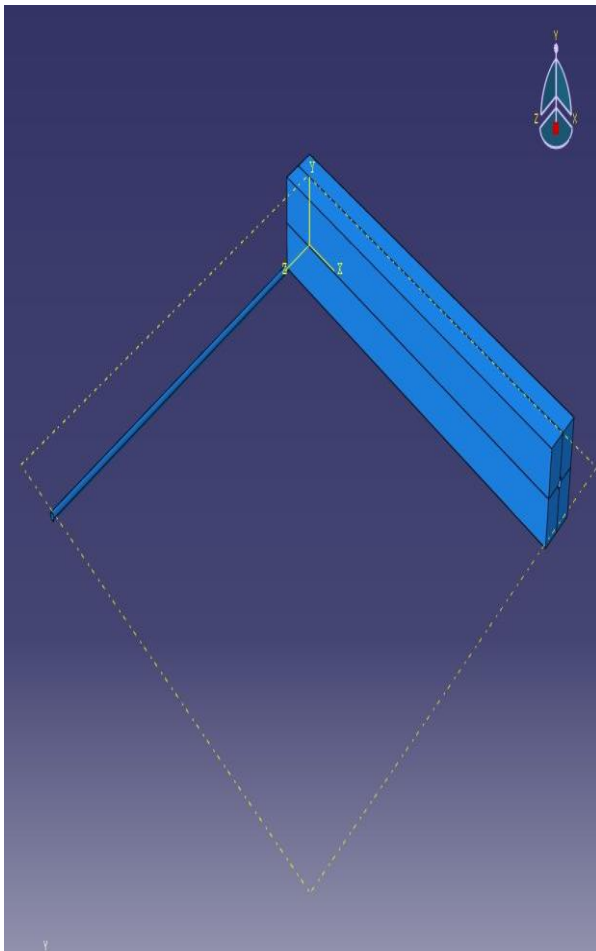
Soil:



3) Defining the assembly

Each created part is oriented in its own coordinate system and is independent of the other parts in the model. Although a model may contain many parts, it must contain only one assembly. It is possible to define the geometry of the assembly by creating instance of a part and position the instance relative to each other in a global coordinate system.

In this step, created models which were involved in all of material properties have to couple together because soil and pipeline are made separately in different part. In the module list, choose **Assembly** and click on **Instance part** tool, . **Create instance** dialog box appears. In the dialog box, select pipeline and soil simultaneously and accept **Independent - mesh on instance**. Click **OK**.




4) Configuring analysis

The [step](#) module is used to create and to configure simulation steps and associated output requests. The step sequence provides a convenient way to capture changes in a model such as loading and boundary condition changes; output requests can vary as necessary between steps. The analysis for interaction between soil and pipeline consists of three steps.

- An initial step, in which a boundary condition will be applied.
- A general, static analysis step, in which a pressure load to the top surface of soil, gravity to the whole of two models and an internal pressure to inner surface of pipeline will be applied.
- A dynamic, implicit analysis step, in which a body force to the whole of two models will be applied.

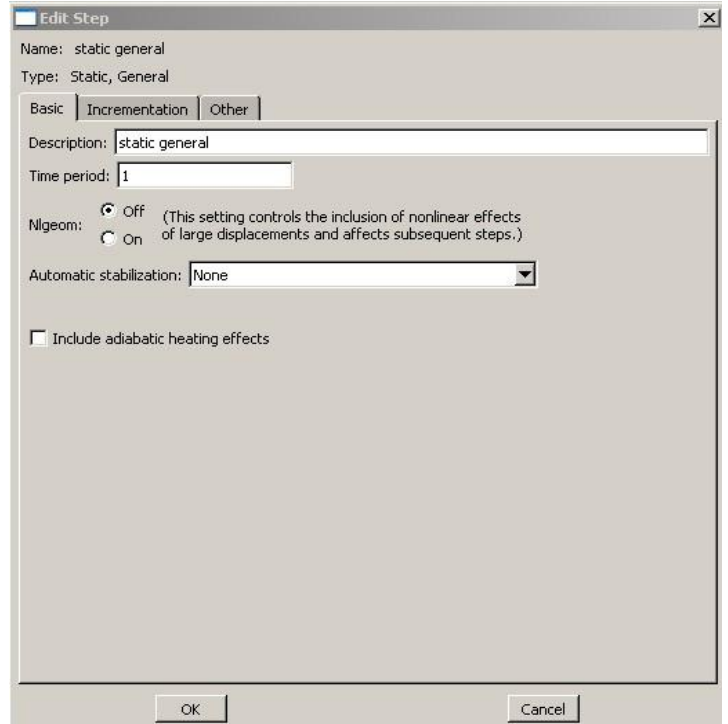
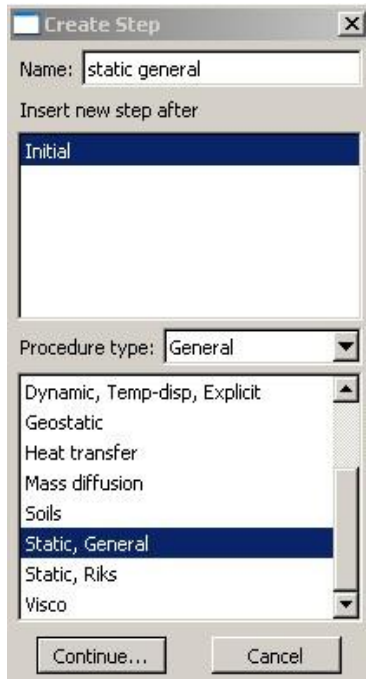
ABAQUS/CAE generates the initial step automatically, but the analysis step should be created in accordance with adaptable analysis related to the type of load.

In the module list, choose [Step](#) and click on [Create step](#), . The [Create step](#) dialog box appears with a list of all the general procedures and a default step name of *step-1*. General procedures are those that can be used to analyze linear or nonlinear response. Name the step *static general*; from the list of available general procedures in the [Create step](#) dialog box, select [Static, General](#) if it is not already selected and click [Continue](#). [Edit step](#) dialog box appears with the default settings for a static, general step. [Basic](#) tab is selected by default. In [Description](#) field, type *static, general*. Click [OK](#) to accept the step and to exit the [Edit step](#) dialog box.

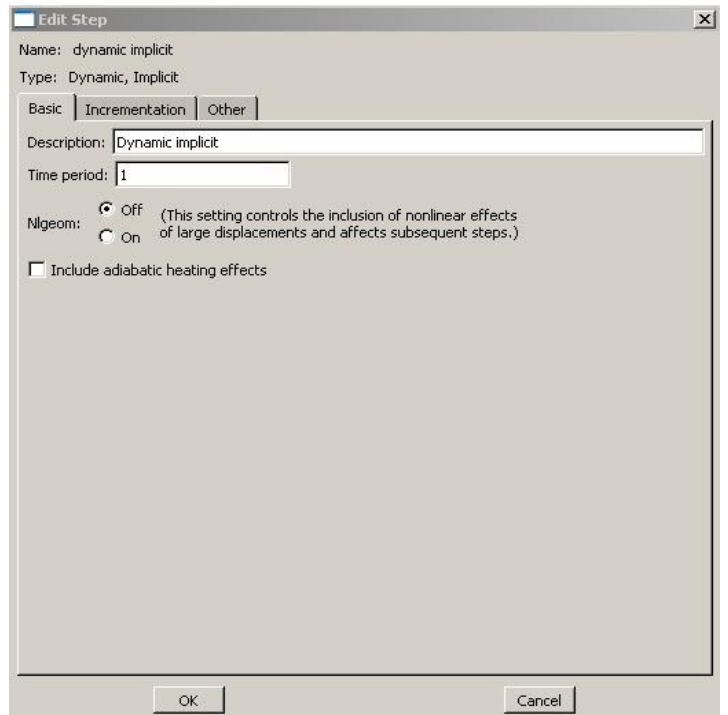
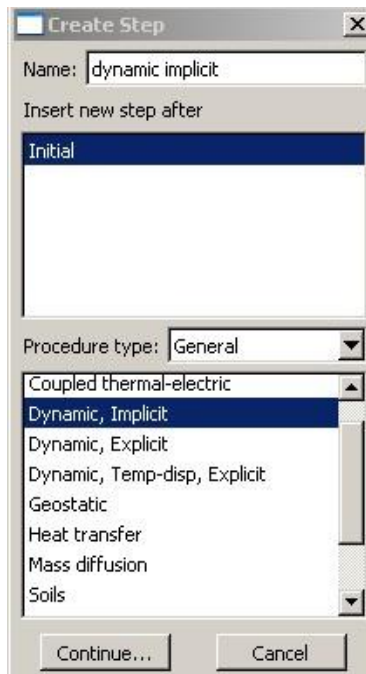
In the case of dynamic implicit step for seismic load, the process of configuring analysis step is almost the same.

The created dialog boxes in [Step](#) module are shown like below.

Static,
general:




Dynamic,
implicit:

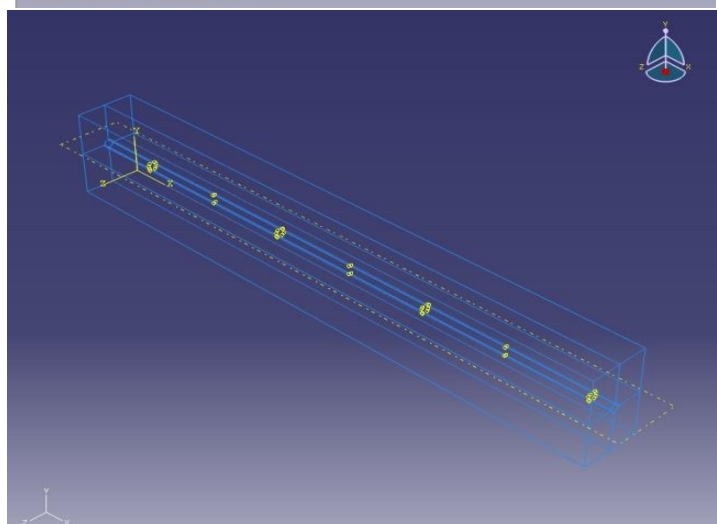
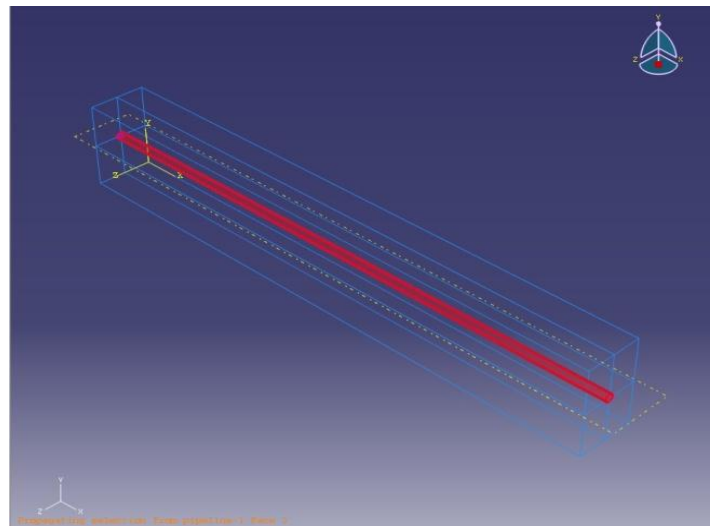
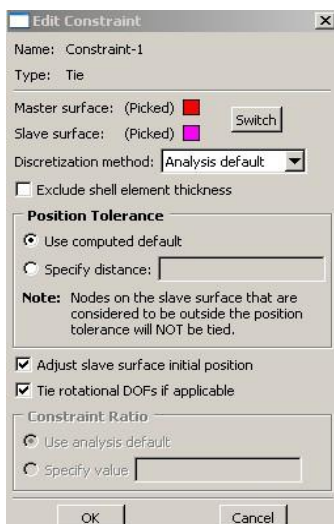
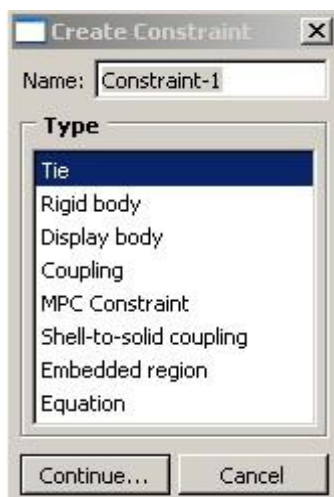


5) Defining interaction of two created models

In **interaction** module, it is possible to specify mechanical interaction of regions which are contacted with each other. In this step, it is necessary to consider a contact surface between soil and pipeline model as a tie with each other.

In the module list, choose **Interaction** and click on **Create constraints** tool, . When the **Create constraints** dialog box appears, select **Tie** and click **Continue**. Accept the contacted surface between soil and pipeline. When **Edit constraints** dialog box appears, click **OK**.

The created dialog boxes and applied interaction condition between soil and pipeline model are shown like below.





6) Applying loads and boundary conditions to the assembled model

The **load** module allows ABAQUS/CAE to specify loads and boundary conditions of predefined models.

① Applying loads on models

Whereas Self-weights of both soil and pipeline and two types of pressure load, which are traffic surface pressure load and internal pressure load of pipeline, are considered as static loads. Body force for seismic load on the assembled model is considered as a dynamic load based on Table 3 in section 1.3.3.

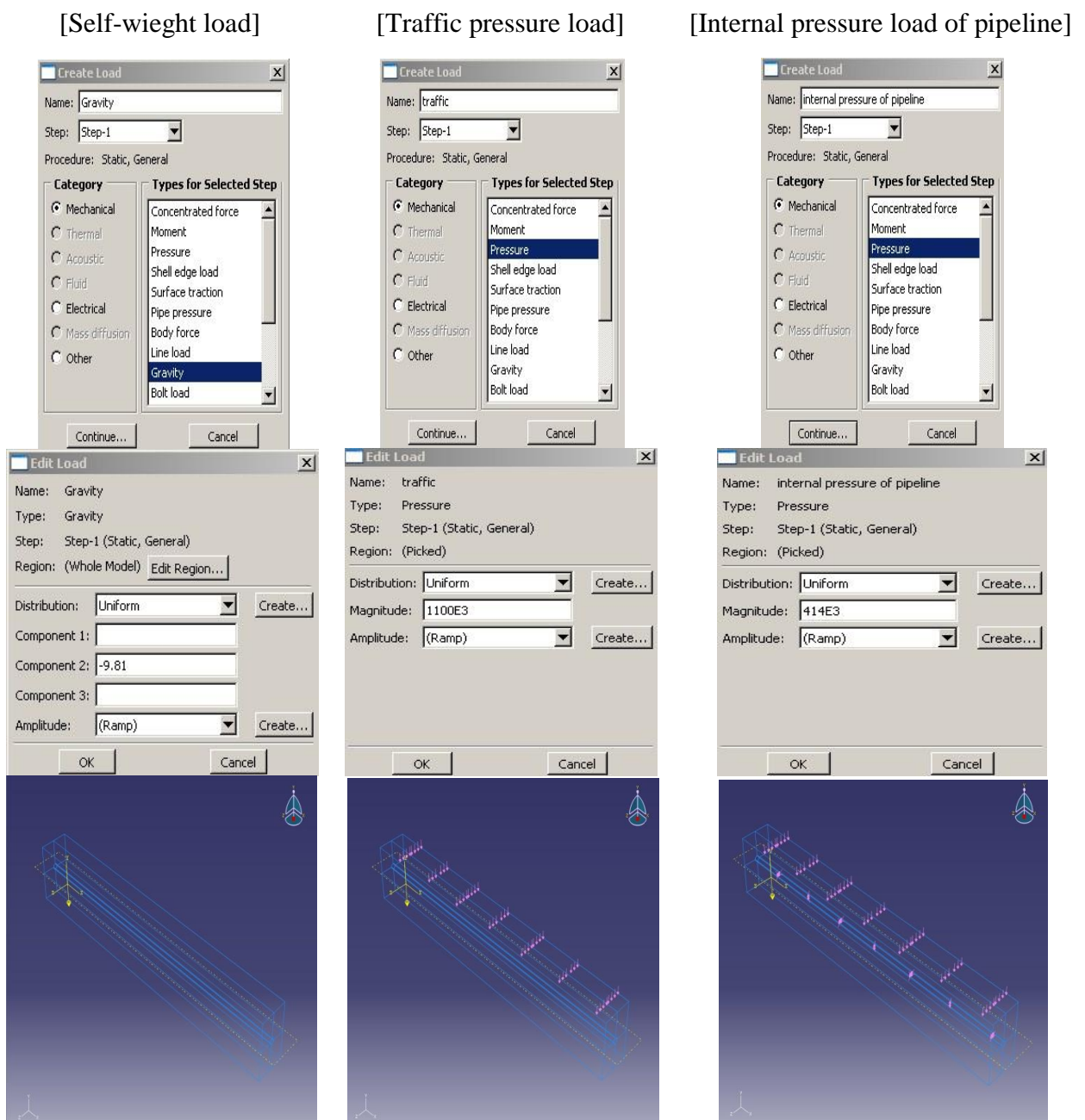
First of all, click on **Create load** tool, , for creating self weight load in whole models. The **Create load** dialog box appears. In the dialog box, name the load *Gravity*; from the list of steps, select **Static analysis** as the step in which the load will be applied; in the **Category** list, accept **Mechanical** as the default category selection; in the **Types for selected step** list, select **Gravity** and Click **Continue**. When click **Done** in the prompt area, **Edit dialog** box appears. In the dialog box, enter a magnitude of -9.81 in the component 2 area, which means 9.81 N in Y direction toward the underneath; Click **OK** to create the load and to close the dialog box.


Secondly, click also on **Create load**, , for creating traffic surface pressure load onto the soil model. The **Create load** dialog box appears. In the dialog box, name the load *Traffic*; from the list of steps, select **static analysis** as the step in which the load will be applied; in the **Category** list, accept **Mechanical** as the default category selection; in the **Types for selected step** list, select **Pressure** and click **Continue**. When ABAQUS/CAE displays a prompt 'select surfaces pressure for load' in the bottom prompt area, choose the top surface of the soil model as the surface to which the considered load will be applied. The desired surface is shown by the red gridded one. When click **Done** in the bottom prompt area, **Edit load** dialog box appears. In the

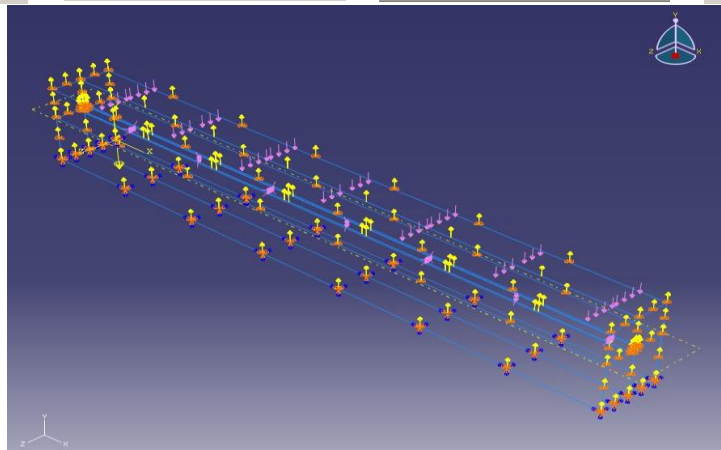
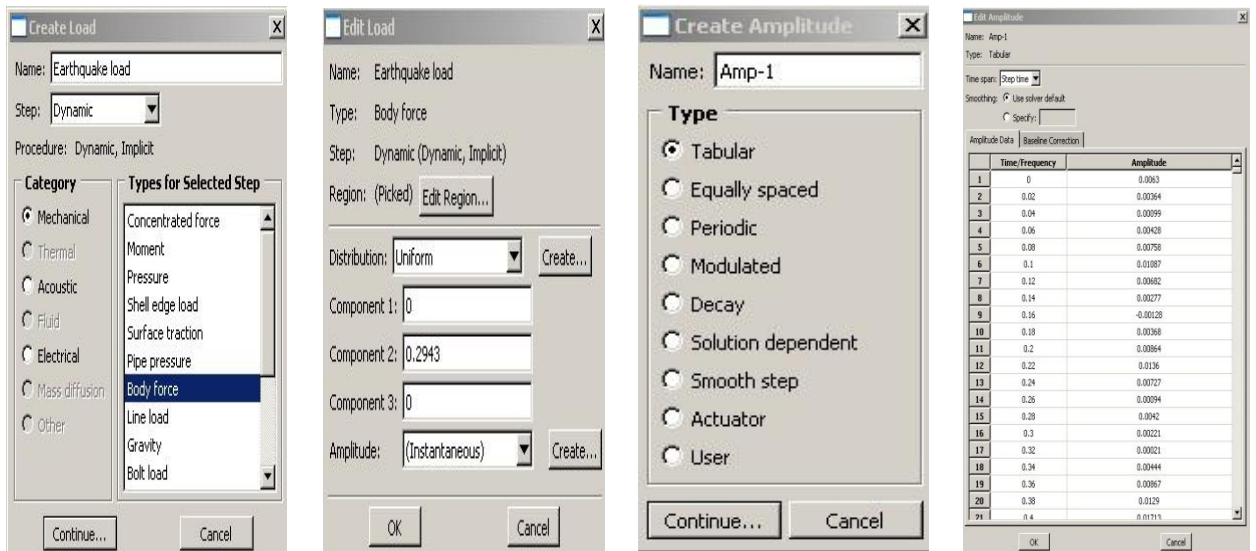
dialog box, enter a magnitude of 1100E3 which means 1100 kPa. ABAQUS/CAE will apply the pressure load uniformly over the desired surface; accept the default Amplitude selection the dialog box; Click **OK** to create the load and to close the dialog box.

Additionally, the process for creating internal pressure load in pipeline is almost the same with above process of creating traffic surface pressure load.

The created dialog boxes and applied loads in model are shown like below.

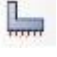


Finally, Click on **Create load** tool, , for creating seismic load in whole model. The **Create load** dialog box appears. In the dialog box, name the load *Earthquake load*; from the list of steps, select **dynamic analysis** as the step in which the load will be applied; in the **Category** list, accept **Mechanical** as the default category selection; in the **Types for the selected step** list, select **Body force** and click **Continue**. When ABAQUS/CAE displays a prompt ‘select surfaces for the load’ in the prompt area, drag whole model to which the load will be applied. When click **Done** in the prompt area, the **Edit load** dialog box appears. In the dialog box, enter a magnitude of 0.2943 in the component 2 area, which means $0.2943 \text{ N}\cdot\text{m}/\text{sec}^2$ in Y direction; accept **Amplitude** selection in the dialog box, create amplitude of an earthquake load and type the each value of amplitude in accordance with time dependence after selecting **Tabular** in the **Type** dialog box; click **OK** to create the load and to close the dialog box.



② Defining boundary conditions of models

Four boundary conditions are considered based on section 3.3; all beside surfaces of soil model, bottom surface of soil model, two cases of end surfaces of pipeline; roller and hinge.

Firstly, all beside surfaces of soil model delineated as cuboid are considered as a roller boundary condition. In the module list, choose **Load** and click on **Created boundary condition** tool, . When the **Create boundary condition** dialog box appears, name the boundary condition *beside surface of soil* in the dialog box; from the list of **step**, select **static analysis** as the step in which the boundary condition will be activated; in the **Category** list, accept **Mechanical** as the default category selection; in the **Types for the selected step** list, choose **Displacement/Rotation** as the default type selection and click **OK**. When ABAQUS/CAE displays a prompt in the prompt 'select regions for the boundary condition' in the prompt bottom area, select all surrounding surfaces of the soil model, check both U1 and U3 in **Edit boundary condition** dialog box and click **OK**.

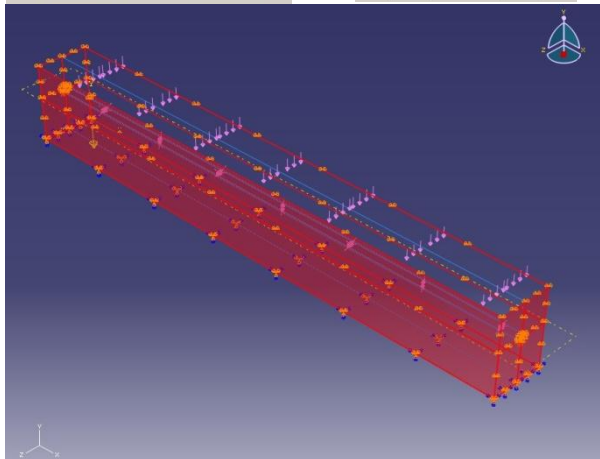
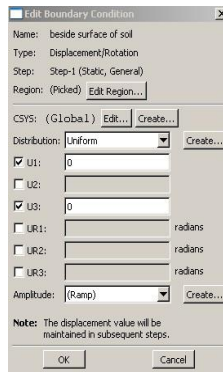
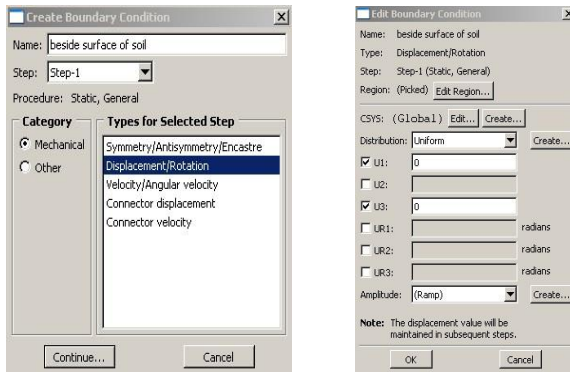
Secondly, all above processes are almost the same in the case of bottom surface of soil model. However, it is necessary to check all selections from U1 to UR3 in **Edit boundary condition** dialog box because the boundary condition of soil model's bottom surface is considered as whole fixed boundary condition.

Finally, two cases of boundary condition related to end surfaces of pipe are also similar to above processes. When the end surfaces of pipeline consider the boundary condition as hinge, check U1, U2 and U3 in **Edit boundary condition** dialog box. On the contrary, when the end surfaces of pipeline consider the boundary condition as roller, check U1 to U3 in **Edit boundary condition** dialog box.

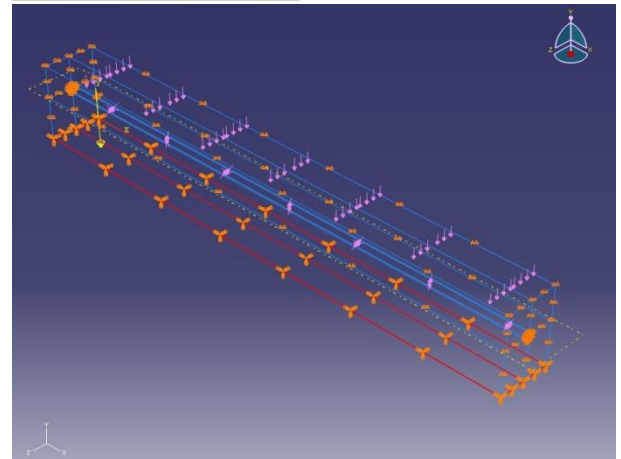
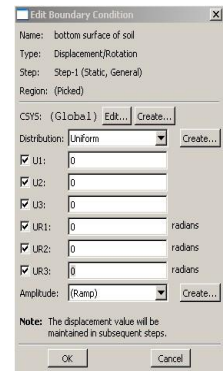
All considered boundary conditions in ABAQUS/CAE are shown as below.

[Boundary conditions for soil model]

Beside surfaces of soil model

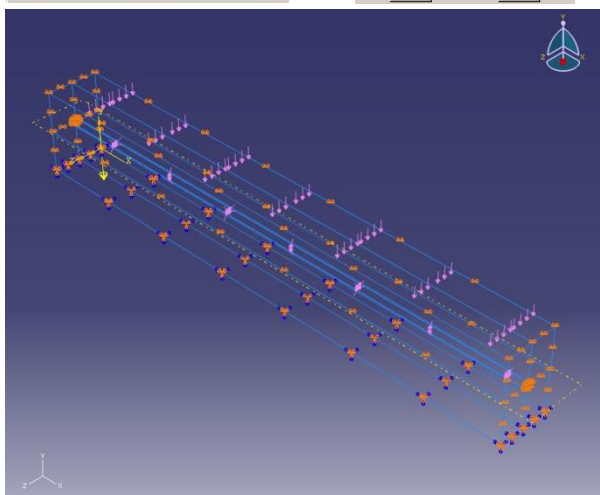
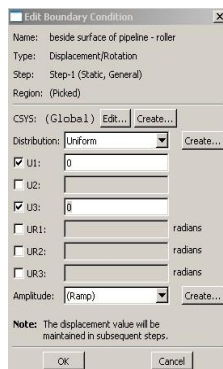
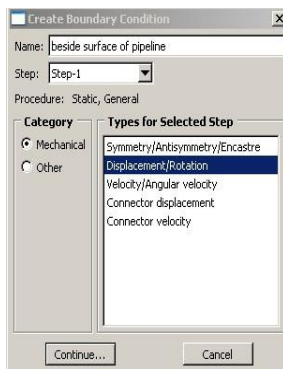


Bottom surface of soil model

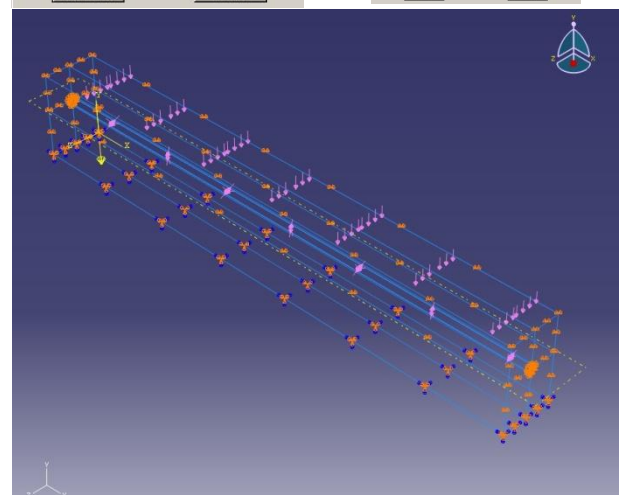
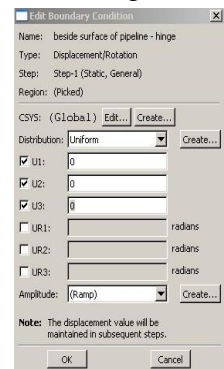
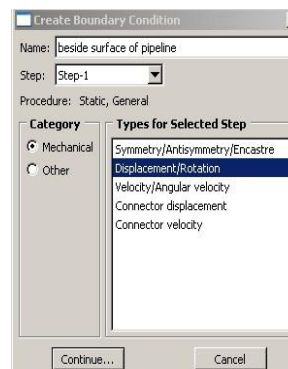


[Boundary conditions for pipeline model]

End surface of pipeline - Roller








End surface of pipeline - Hinge



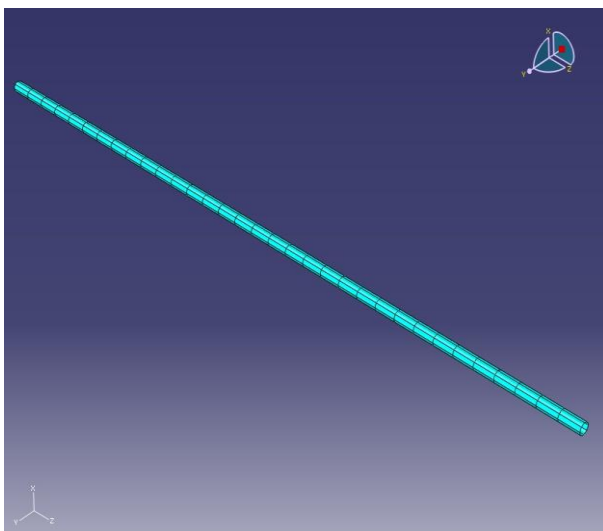
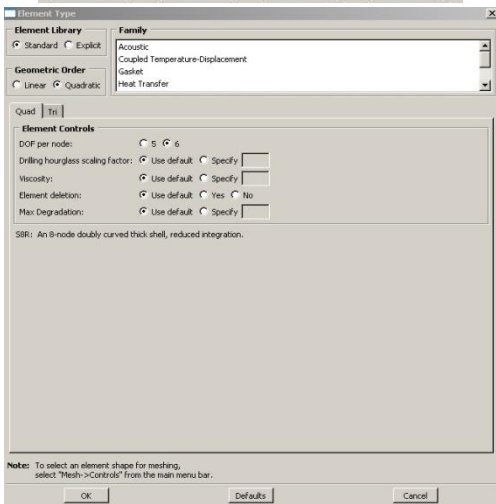
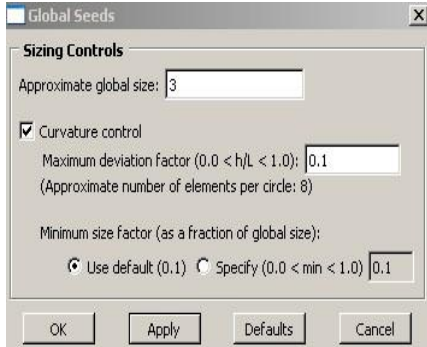
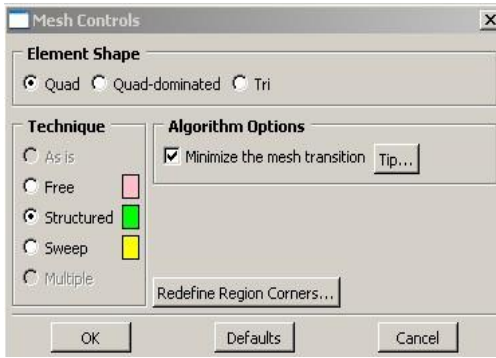
7) Meshing both soil and pipeline model

The [mesh](#) module contains tool that allow ABAQUS/CAE to generate a finite element mesh on created models. Various levels of automation and control are available so that a mesh is produced. The mesh is the step related to dividing the models into lots of small parts. These divided 3D small meshed elements in models play an important role to offer suitable results in accordance with chosen number of elements and type of element. The type of meshed element and the number of elements in model are generated in this step based on section 3.4.

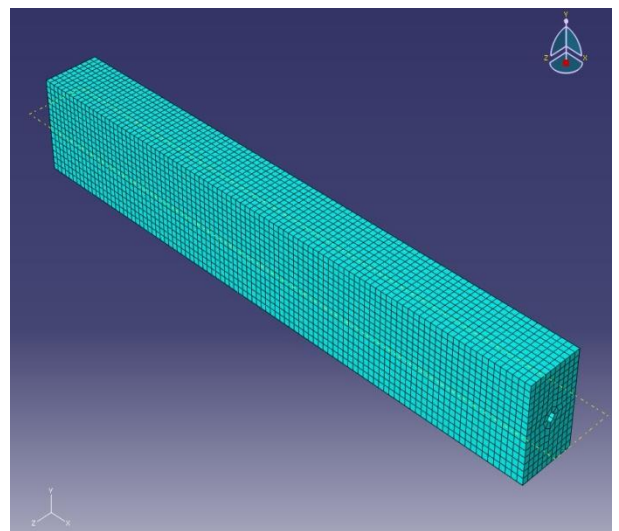
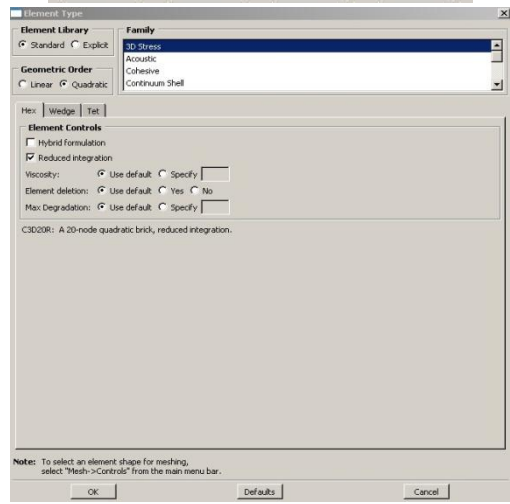
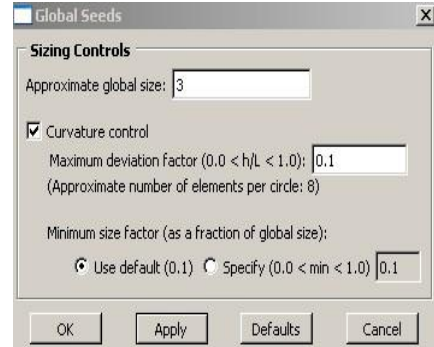
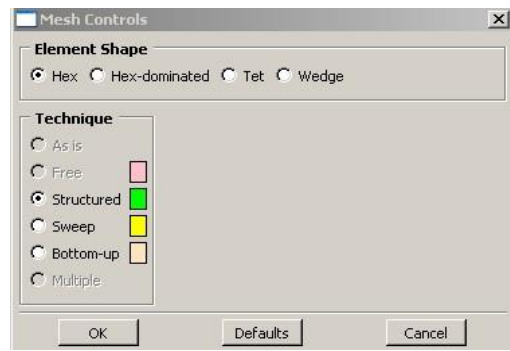
Firstly, in the module list, choose [Mesh](#). Click on [Assign mesh control](#) tool, , for meshing pipeline model. Drag whole of pipeline model and click [Done](#) in the bottom prompt area. When [Mesh control](#) dialog box appears, accept [Quad](#) as the default [Element shape](#) section; accept [Structured](#) as the default [Technique](#); click [OK](#) to assign the mesh controls and to close the dialog box. Click on [Assign element type](#) tool, , for designating element type of mesh. When the [Element type](#) dialog box appears, accept [Quadratic](#) as the default [Geometric order](#) section. Click on [Seed part](#) tool, , for assigning number of elements in pipeline model. The [global seeds](#) dialog box appears. In the dialog box, enter an approximate global size of 3 and click [OK](#). Click on [Mesh parts](#) tool, , for meshing the part instance. Click [Yes](#) from the bottom prompt area in order to confirm that ABAQUS/CAE let the pipeline model do mesh.

Additionally, Click on [Assign mesh control](#) tool, , for meshing soil model. Drag whole of soil model and click [Done](#) in the bottom prompt area. When [Mesh control](#) dialog box appears, accept [Hex](#) as the default [Element shape](#) section; accept [Structured](#) as the default [Technique](#) section; click [OK](#) to assign the mesh controls and to close the dialog box. The following processes for assigning number of elements and element type related to soil model are almost the same.

[Mesh in pipeline model]




[Mesh in soil model]



8) Creating an analysis job

Once all of the tasks involved in defining model are finished, it is necessary to use **job** module for analysing created model. The **job** module allows ABAQUS/CAE to interactively submit a job for analysis and monitor its progress.

In the module list, choose **Job**. Click on **Create job** tool, . When the **Create job** dialog box appears, Name the job available name according to the type of analysis and click **Continue** to create job. When the **Edit job** dialog box appears, type available name of analysis in **Description** field. Click **OK** to accept all the default job setting and to close the dialog box. When **Job manager** dialog box appears, click **Submit** the created job for analysis.